Geology and Origin of the Century Zinc Deposit

Thesis submitted by
Graeme Charles BROADBENT BSc *Vic*
in 1999

Volume 1. Text.

For the degree of Doctor of Philosophy
in the Department of Earth Sciences
James Cook University of North Queensland

STATEMENT OF ACCESS

I, the undersigned, the author of this thesis, understand that James Cook University of North Queensland will make it available for use within the University Library and, by microfilm or other means, allow access to users in other approved libraries. All users consulting this thesis will have to sign the following statement:

> In consulting this thesis I agree not to copy or closely paraphrase it whole or in part without the written consent of the author; and to make proper public written acknowledgement for any assistance which I have obtained from it.

Beyond this, I do not wish to place any restriction on access to this thesis.

(30/4/99)

(.....)

Abstract

The Century deposit represents an important new genetic variation of the style of sediment-hosted Zn-Pb-Ag mineralisation that is so well represented in the Mount Isa Inlier and McArthur Basin of north-eastern Australia. The deposit is hosted by shale and siltstone of the Mesoproterozoic age Lawn Hill Formation. Mineralisation comprises fine-grained sphalerite with minor galena and pyrite. Most sulphides (80-90%) occur as delicate replacive lamellae in black shale units, separated by siderite-rich siltstone marker horizons. The remainder are present as stratabound progressively coarser grained and more discordant fracture filling forms. The position of the highest grade mineralisation migrates upward within the mineralised sequence from southeast to northwest. Despite systematic lateral variation in grades from 3-5% zinc to greater than 25% zinc in individual units, this grade variation occurs without concomitant changes in thickness of the host shale, suggesting that the mineralisation is dominantly of replacement origin. The host sedimentary rocks show no lateral chemical or textural changes suggestive of exhalative facies.

Two dominant textural varieties of stratabound sphalerite are recognised: "porous", which has a high pyrobitumen content and "non-porous", which has a relatively low pyrobitumen content. These varieties appear to be co-genetic and almost co-abundant. They are respectively interpreted to represent the products of oil- and gas- mediated thermochemical sulphate reduction (TSR) and sulphide deposition from a metal-and sulphate-rich fluid. A paleo *source-reservoir* type hydrocarbon- reservoir model is invoked to explain the onset of TSR, the cross-stratigraphic migration of the mineralisation and the zoning of the "porous" and "non-porous" sphalerite types.

Sulphur isotope values of mineralisation appear to evolve with time to progressively heavier values. Paragenetically early stratabound sulphides have $\delta^{34}S$ values of between 5 and 10 ‰CDT, while the later transgressive and fracture filling styles evolve to values of between 10 and 20 ‰CDT. This isotopic evolution appears to follow through into more widespread syn-deformational vein-style lodes in the 100-200 km^2 area surrounding the deposit. In the regional lodes, early sphalerite has a sulphur composition of 20-25 ‰CDT while later sphalerite generations have progressively heavier values, reaching a maximum of 25-30 ‰CDT in the final stages of vein mineralisation. This progressive enrichment in ^{34}S suggests that the total mineralising fluid system was a large closed-system reservoir in the latter stages of the deformation and mineralisation event.

Migration of the mineralising fluids at regional scale was triggered by the early stages of basin inversion and regional deformation, continuing through into the development of gentle north-south trending folds. In the early stages of the fluid flow system, gravity-driven recharge from the developing Mt Isa Orogen to the south and east of the Lawn Hill district possibly helped maintain the regional hydrodynamic regime. As regional deformation proceeded, faults progressively developed or were reactivated, modifying and redistributing fluid flow. The closure of the district-scale fluid system is attributed to this progressive tectonically driven fragmentation of the regional scale fluid system. These changes were manifested initially by the development of a stratabound network of hairline fractures throughout the Century orebody, which were mineralised with progressively more discordant sphalerite, galena and siderite. As tectonism continued, vein-style lode deposits were emplaced into district-scale faults. The process culminated in the reactivation of major regional structures such as the Termite Range Fault and preservation of the orebody in an extensional fault duplex parasitic to the Termite Range Fault.

STATEMENT ON SOURCES

DECLARATION

I declare that this thesis is my own work and has not been submitted in any form for another degree or diploma at any other university or other institution of tertiary education. Information derived from the published or unpublished work of others has been acknowledged in the text and a list of references is given.

Graeme Broadbent
(30/4/99)

(.....)

Table of Contents

Chapter 6 continued...

List of Figures

List of Figures, cont...

List of Figures, cont...

List of Figures, cont...

List of Tables

List of Plates

List of Appendices

List of Enclosures

Acknowledgments

The management of Rio Tinto Exploration is especially thanked for conceiving the concept of the project, by way of inaugurating the Haddon King Research Scholarship. In particular Jacob Rebek and John Main have acted as guides and mentors, not only for this project, but for much of my exploration career.

The patience and knowledge of Russell Myers are gratefully acknowledged for discussing so many of the issues with me at length and suggesting the remedies for many problems. Following his departure from JCU, Nick Oliver has assumed the role of long-suffering supervisor and devils advocate. Thanks Nick.

Much of the work presented here was foreshadowed and prompted by the extensive contributions made by John Wright over the period from 1986 to the present. Every effort has been made to cite directly his contributions as presented in RTE unpublished reports and memoranda, but this does not include the immense value of the many conversations that we have had over the past few years.

Discussions with Roger Taylor, David Johnson, Bob Henderson, Andrew Waltho, Steve Andrews, Dave Fielding, Gregg Morrison, Neil Herriman, Marjorie Muir and Steven Allnutt have kept many of my flights of fancy in check. Lots of other people helped, on subjects ranging from technical discussions to isotope analysis. Their names are: Anita Andrew, Graham Carr, Sharon Ness, Alan Chappell, Tim Bell, Scott Szulc, Hugh Bresser, Helen Cutler, Ken Lawrie, Bruce McConachie, Steve Newbury, Rod Page, Peter Aberline, Marty Hooper, Jamie Wilkinson, Joe Cartwright, Rob Raiswell, Stewart Burley, Shelagh Baines, Charles Curtis, Alex Maltman, Miryam Glikson and Stafford McKnight. David Splatt, Greg O'Connell, Adrian Perry, Teresa Coxon, Lindsay Hooker and Ian Hubbard have from time to time given their special talents to drafting or modification of diagrams.

Finally, special thanks for my wife Debbie, for encouragement and support always.

Chapter 1
Introduction

The Century zinc deposit is located in far north-western Queensland, Australia, at approximate latitude 18 44'S and longitude 138 36'E (Fig. 1-1). The current geological resource estimate for the deposit is 118 million metric tonnes of material grading 10.2% zinc, 1.5% lead and 36 g/t silver (Waltho et al., 1993). The deposit was discovered in April, 1990 (Broadbent, 1995) by Rio Tinto Exploration Pty Ltd (RTE). In 1997, Century was sold to another company, Pasminco Ltd, and is presently being developed as an open cut mine.

The author's involvement with the project commenced in 1991 during the course of early evaluation drilling of the deposit. At the end of 1991, RTE provided a twelve-month scholarship, the Haddon King Research Scholarship, to commence a comprehensive study of the geology of the mineralisation. The scholarship was in honour of the memory of the late Haddon F. King, a former director of exploration for Rio Tinto Exploration, who exerted a profound, pioneering, influence on theories of ore genesis for several decades, particularly with respect to sediment-hosted base metal mineralisation.

Objectives of the study were as follows:

- To assemble base descriptive data for the mineralisation, most particularly the deposit stratigraphy, structural evolution and ore textures, together with the distribution of metal zones with respect to these. Preliminary geochemical and isotopic data on selected mineralisation species were also obtained.

- To review available literature on present theories of formation for these types of deposit; to decide which features of Century are congruent with these, and to thereby produce a preliminary genetic hypothesis for the mineralisation.

The study was based at James Cook University, and initially formed the subject of an MSc level project by the author. This was subsequently converted into a PhD level investigation. Additionally, in 1992, three Honours level projects by JCU students were conducted in and around the deposit on separate but related topics, viz;

Discordant lodes of the Lawn Hill region (Bresser, 1992)
Stratigraphy of limestones overlying the Century zinc deposit (Szulc, 1992)
Paleo-weathering profile development over the Century zinc deposit (Cutler, 1992)

These projects were intended as stand alone projects, and have produced useful information to supplement this thesis, and for subsequent work by Rio Tinto Exploration Pty Ltd.

This thesis is divided into eight chapters. Following this introduction, the regional geological and tectonic setting is described in Chapter 2. Chapter 3 describes the detailed stratigraphy and sedimentology of the Century deposit, and is followed by an analysis of the structure of the deposit in Chapter 4. Mineralisation textures, metal zoning and the paragenesis and timing of the deposit are presented in Chapter 5, followed by carbonate and isotope geochemistry in Chapter 6. Chapter 7 discusses wider scale implications of postulated mineralisation processes within the deposit. Chapter 8 summarises the major findings of the study. Research methods employed in the study are described at the appropriate junctures throughout the thesis.

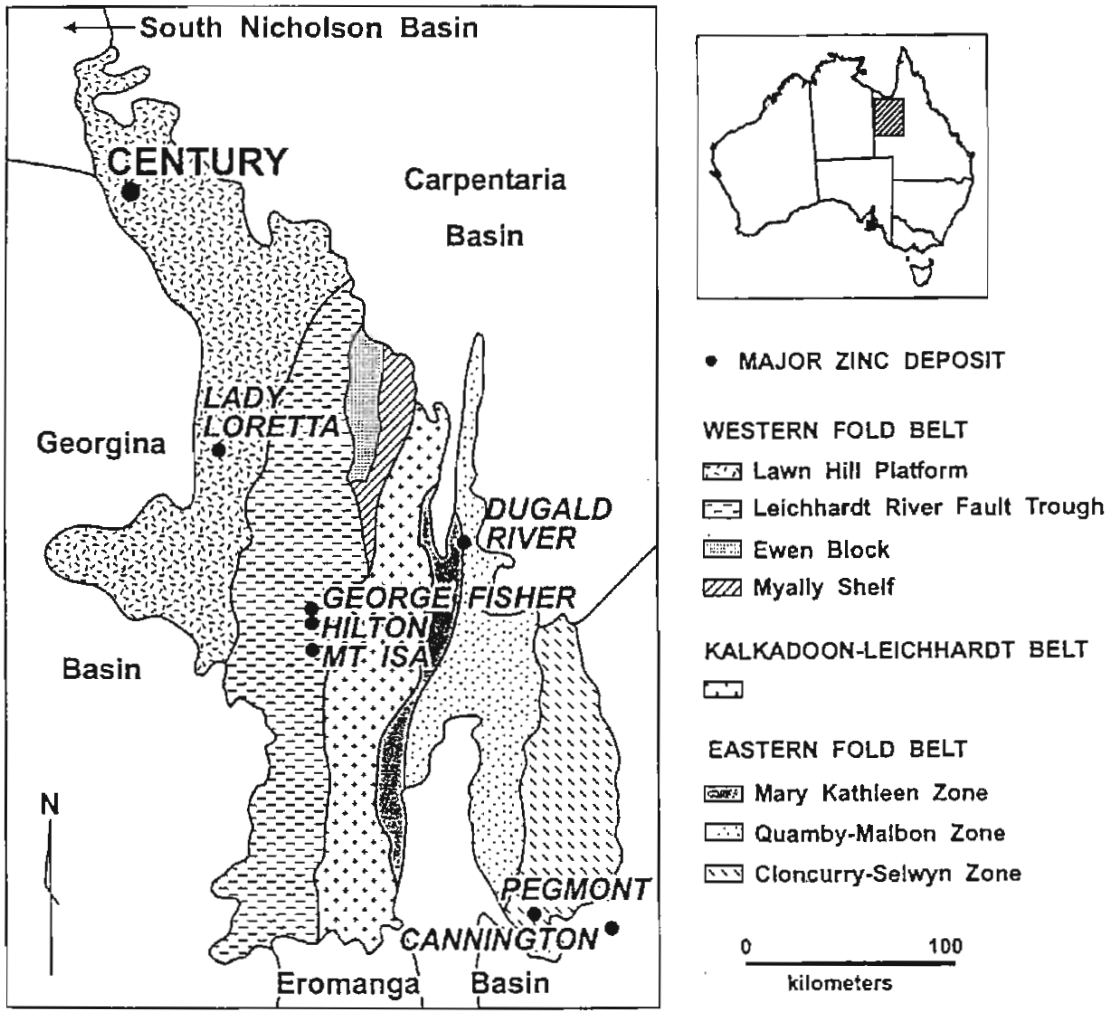

Figure 1.1 Century deposit location, and regional subdivisions of the Mt Isa Province (after Blake, 1987).

Chapter 2
Geological Setting

2.1 Introduction

The Century deposit is hosted by mid-Proterozoic age sedimentary rocks of the Lawn Hill Formation. It lies within the Mount Isa Inlier, which occupies an area of more than 50,000 sq km in northwestern Queensland. In this chapter aspects of the regional and local geological setting are briefly (and admittedly selectively) summarised, as an introduction to the discussions of various aspects of Century made in subsequent sections. Most of the chapter therefore consists of a synthesis of previous work, to provide context for new descriptions, results and interpretations from this PhD study, as presented in later chapters. Various aspects of the regional geology have been the subject of considerable debate and many fundamental questions remain unresolved. A full discussion of regional geology of the Mt Isa Inlier is outside the scope of this thesis: the reader is referred to the publications by Blake (1987) and Stewart and Blake (1992), for the best compilations available at present. Recent geochronology data are reported by Page (1993), Page et al. (1994), Page (1995), Page and Sweet (1996) and Connors and Page (1996).

2.2 Regional Geological and Tectonic Setting

The Mt Isa Inlier was divided by Blake (1987) into three broad tectonic units, termed the Western and Eastern Fold Belts, separated by the Kalkadoon- Leichhardt Belt. The Western Fold Belt is further subdivided into the Lawn Hill Platform, Leichardt River Fault Trough, Ewen Block and Myally Shelf. The Eastern Fold Belt is subdivided into the Mary Kathleen, Quamby-Malbon and Cloncurry-Selwyn zones. The location of Century relative to these broad tectonic divisions is shown on Figure 1.1.

Within the Mt Isa Block, four major Proterozoic sequences are present (Blake, 1987). The oldest, designated basement, was deformed and metamorphosed at about 1870 Ma. The three younger sequences are designated Cover Sequences 1 to 3 (Blake, 1987;

Stewart and Blake, 1992). Despite some problems of detailed local correlation and timing of events between individual units, this scheme provides a useful contextual framework for the Mt Isa Inlier, including the Century area. Cover Sequence 1 consists predominantly of 1870 to 1850 Ma felsic volcanic rocks (Stewart and Blake, 1992). Cover Sequence 2 comprises sedimentary and bimodal volcanic rocks ranging in age from about 1790Ma to 1760 Ma (Stewart and Blake, 1992). Cover Sequence 3 is mainly finer grained sedimentary rocks with subordinate volcanic rocks, dated from 1670 to +1595 Ma (Page et al., 1994). The Lawn Hill Formation is near the top of Cover Sequence 3, in the uppermost portion of the major stratigraphic succession known as the McNamara Group (Fig. 2.1).

The structural evolution of the Mt Isa Inlier has been the subject of numerous studies in the past, with compilations and correlation of events being presented in Blake (1987); Blake et al., (1990) and Stewart and Blake (1992). An updated version of Blakes' correlation chart is presented as Figure 2.2.

Briefly, Cover Sequence 2 was the product of a period of crustal extension from 1790 to 1760 Ma, with early rift-phase coarse clastic sedimentary rocks and bimodal lavas deposited and erupted in restricted fault-controlled basins. These were overlain by extensive finer grained clastic and carbonate sag-phase rocks. Termination of the cycle was marked by intrusion of the Wonga Granite at ~1740Ma (Stewart and Blake, 1992). There are severe difficulties of correlation within the deformed and metamorphosed Eastern Fold Belt, and more detailed geochronology is needed.

Most workers (e.g. Loosveld, 1989; Jackson et al., 1990) consider the rifting to have been intracratonic, rather than being developed on continental margin crust. Basement structures developed during the deposition of Cover Sequence 2 probably had a strong influence on the depositional architecture of Cover Sequence 3. Rifts developed on thick stabilised crust will tend to exploit kinematically-suitable structural weaknesses established during earlier tectonic episodes (Cartwright, 1987). This 'basement template' of inherited structural directions must be considered when attempting to reconstruct geometry of later basins.

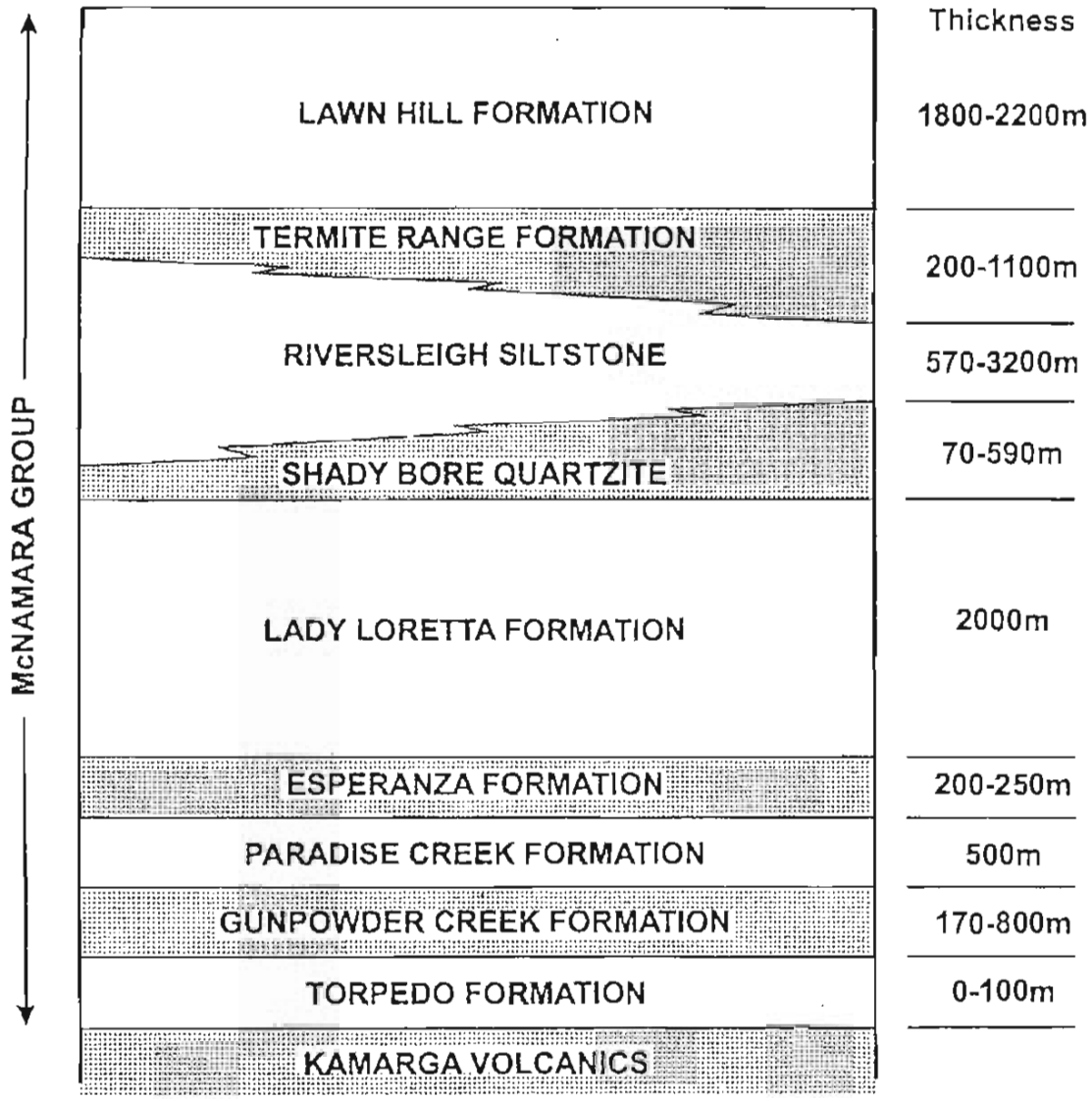

Figure 2.1. McNamara Group stratigraphy (after Waltho and Andrews, 1993).

Sedimentological studies of Cover Sequence 2 (Beardsmore et al., 1988; Eriksson and Simpson, 1990; Jackson et al., 1990) interpret east-west sediment transport directions, which suggests a strong north-south orientation to the development of underlying basement grabens. Regional geophysical data compilations (BMR, RTE, various corporate surveys) show a strong north-south grain coincident with exposed Cover Sequence 2 lithologies in the southern Mt Isa Inlier. Dominantly east-west trends are present in the Elizabeth Creek area further north of Century (McConachie et al., 1993). Century lies in a transitional zone between these domains, with prominent north-west and north-east striking structures evident on geology maps (Fig. 2.3). East-west, north-

south and north-westerly sedimentation trends are evident in various Formations at various levels of Cover Sequence 3 in the Century area (Andrews, 1998). This suggests that different, and possibly varying, regional stress directions may have been present during the deposition of Cover Sequence 3, with differently oriented basement structures activated at different times.

Several workers (Passchier, 1986; Stewart, 1989; Williams, 1989; Passchier and Williams, 1989) have recognised the existence of a regional phase of northeasterly to southwesterly directed extension that post-dates Cover Sequence 2. The extensional event is interpreted to have initiated the rift-sag phase cycle of Cover Sequence 3 (Stewart, 1989). This sequencing is congruent with present interpretations of seismic data to the north of Century (McConachie et al., 1993). Compressional deformation episodes prior to Cover Sequence 3 are poorly dated and not well correlated. The oft-cited "D1" to "D3" compressional deformation event scheme for the Mt Isa Inlier (Bell, 1983; 1991) really only applies to post-Cover Sequence 3 deformation. It is recognised that there is little flexibility to incorporate any prior events in this scheme, but the convention is used in this thesis, as pre-Cover Sequence 3 events are only discussed in passing.

Some further aspects of the stratigraphy of Cover Sequence 3 require discussion before turning to the more detailed aspects of the geology of the Lawn Hill area and the setting of Century. Century is hosted by the upper Lawn Hill Formation, which is part of the upper McNamara Group. The lower portion of the McNamara Group is the stratigraphic equivalent to the Mount Isa Group, which hosts the important Mount Isa and Hilton deposits. Published depositional ages based on SHRIMP U-Pb zircon in tuff beds for the Lower McNamara Group and Mt Isa orebody are 1653$\pm$ 7 Ma and 1652$\pm$ 7 Ma, respectively (Page and Sweet, 1996). Century is some 5000m stratigraphically higher in the McNamara Group than the Lady Loretta Formation (Fig 2.1), which is thought by most workers to be equivalent to the top of the Mt Isa Group (Blake, 1987). SHRIMP U-Pb dating of zircons from the tuffaceous marker beds immediately above the Century mineralisation sequence gives a depositional age of 1595$\pm$ 6 Ma (Page and Sweet, 1996).

The top of the Lady Loretta Formation marks an important change in the character of the McNamara Group. It is effectively the last major unit with a dominant component of evaporitic carbonate sedimentation before deposition of the thick siliciclastic units of the upper McNamara Group (Fig. 2). There appears to be little evidence for large scale development of hypersaline evaporitic facies in the Riversleigh Siltstone, the Termite Range Formation, or the Lawn Hill Formation (Wright, 1992; Andrews, 1998).

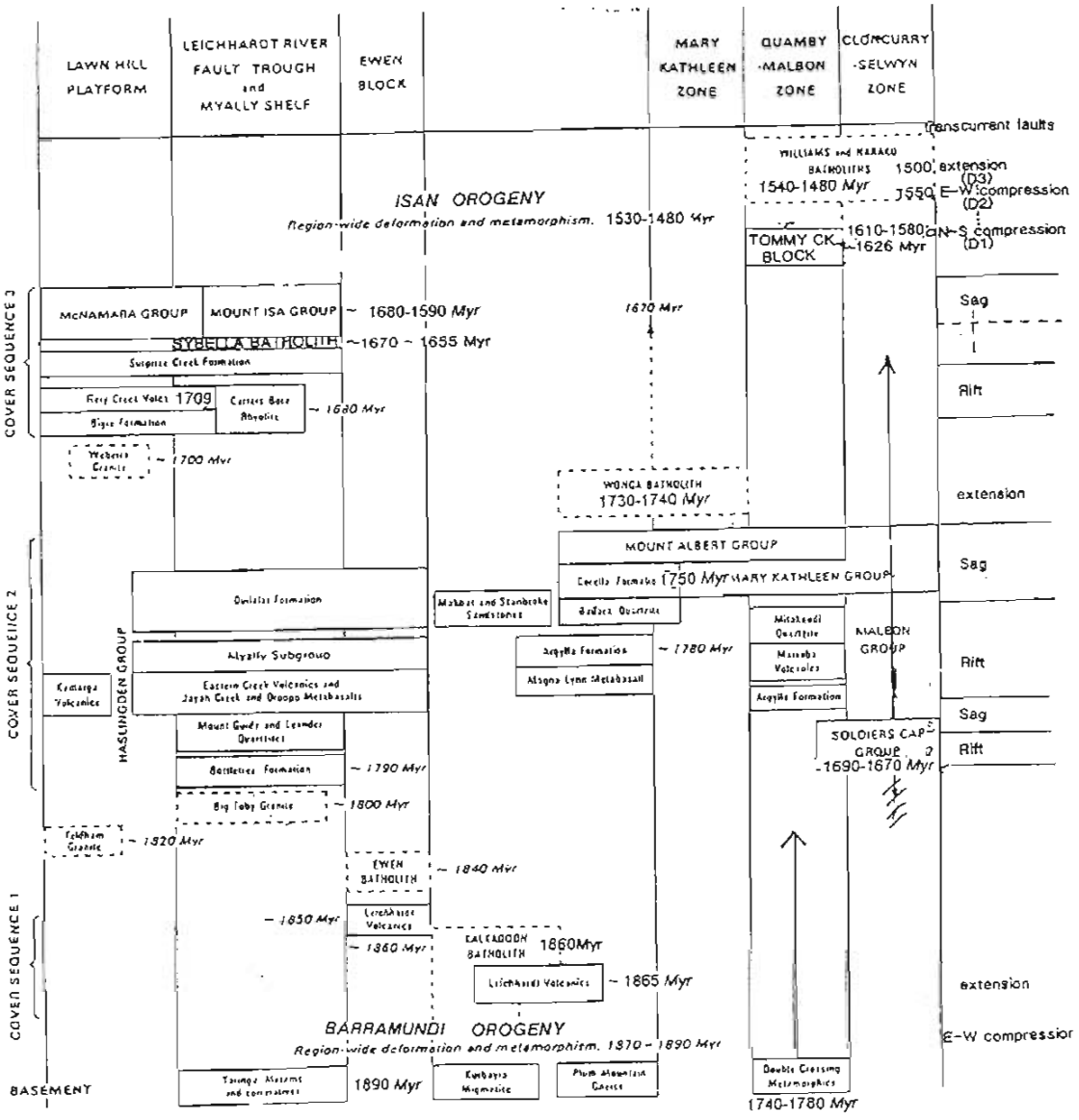

Figure 2.2. Mt Isa Inlier stratigraphic framework, showing rift and sag phase sedimentation subdivisions and tectonic events [modified from Blake (1987) and Stewart and Blake, (1992); additional SHRIMP U-Pb zircon dates from Wyborn (1992); Page (1993); Connors and Page (1995)].

A brief review of the timing and orientation of regional deformation events and the setting of major mineralisation (section 2.3) is made before moving to the local setting of Century.

The major orogeny which terminates the deposition of the McNamara Group is termed the Isan Orogeny by Blake et al. (1990). Although there is much discussion of the local effects and relative intensities of the components of this major deformational event (Bell, 1983, 1991; Page and Bell, 1986; Lister, 1990; Smith, 1991; Connors et al., 1992; Connors and Page, 1995), two main phases are generally distinguished. The first, D1, is characterised by northerly directed thrusting (Bell, 1983; Loosveld and Schreurs, 1987) and some folding about easterly trending axes; the second (D2) by a major phase of later upright folding, about north trending axes.

The D2 event was accompanied by regional thermal metamorphism and local pegmatite intrusion (see studies in the Mount Novitt area by Connors et al., 1992). The tectonic significance of this low pressure, high temperature metamorphism associated with deformation is still being debated. The exposure of the high grade metamorphic rocks in the south east of the Mt Isa Inlier may be partially reflecting a higher degree of uplift and exhumation by erosion in this area (McConachie et al., 1993).

It appears that the continuation of the D2 episode of east-west compression led to extensive later strike slip faulting on two major fault orientations, trending north-northeast and north-northwest respectively. The D3 structures of Perkins (1984), Swager et al. (1987), and Bell et al. (1988) are correlated with the main phases of this faulting. Lister (1990) argues that the east-west trending D1 folds of Bell (1983) in the Lake Julius area are actually D2 folds which have been rotated into their present position by local intense transpression on dominantly north-south trending segments of the major faults. The transpression argument has some relevance to the possible evolution of the Century deposit and the transgressive lodes in the Lawn Hill area. This is discussed further in Chapter 4.

Recent geochronological studies of the relative timing of these events in the Mt Isa area by Connors et al. (1992), Page (1993) and Connors and Page (1995) have helped

constrain their absolute ages. The D1 event is still poorly constrained. There are metamorphic zircon overgrowth ages of 1584Ma recorded in the Eastern Fold Belt (Page, 1993). These record a peak metamorphic and uplift event that just post-dates the depositional age of the Century host sequence. This event could correlate with the D1 fold deformation of the lower McNamara Group rocks in the south of the Mt Isa Inlier. Indeed, the onset of deposition of the Pmh5 sandstone unit marks a major shift in sediment provenance from the west to the south (Andrews, 1998), signifying likely major uplift in the south at this time. However, there is also evidence for early south-easterly to north-westerly directed deformation of the Lawn Hill Formation which is then re-folded by D2 folds (chapter 4). If the late stages of deposition of the McNamara Group relate to development of a contractional ("foreland") basin (McConachie et al., 1993), ongoing deformation of the sequence can be expected over a considerable time frame. The best interpretation of the D1 event is that it represents the final stages of a contractional basin, with activity extending from about 1600Ma to 1570Ma.

The best estimate for the peak of the D2 event ranges from around 1550Ma (N. Oliver, pers comm., 1999) to 1530 Ma. Dating of deformed and undeformed pegmatites in the Mount Novitt area, together with structural constraints, places the peak of metamorphism associated with, or slightly post-dating, the peak of D2 at 1532Ma (Connors and Page, 1995).

During the likely span of both the D1 and D2 events, there was a progressive change in continental motion from north-south to east-west as shown by Apparent Polar Wander Path (APWP) data (Loutit et al., 1994; Idnurm et al., 1995). The tectonic transport directions of both events are congruent with the expected change in kinematics implied by the APWP data. It is possible that the D2 event was transitional with the D1 event, both events simply reflecting aspects of a larger-scale orogenic transition. This may have relevance to possible geodynamic models for the regional setting of mineralisation (section 2.3).

Previous work by Page and Bell (1986), based on timing relationships of SHRIMP U-Pb zircon dates from tuff beds and granitoids with structural fabrics, placed a likely age

of around 1510 Ma for the D3 event. An absolute younger constraint for the age of D3 is given by a SHRIMP U-Pb on zircon date of 1480 Ma from a pegmatite that is undeformed by D3 (Connors and Page, 1995). Intrusion of major felsic plutons occurred in the south-eastern Mt Isa Inlier from 1560-1480 Ma, in particular the emplacement of the volatile-rich, high uranium, granites of the Williams and Naraku Batholiths, based on SHRIMP U-Pb dating of zircons from the granites (Wyborn, 1992). The late stages of this plutonism have been linked to the regional emplacement of numerous copper-gold and uranium deposits (Wyborn, 1992).

2.3 Ore Genesis Models

Academic debate concerning genesis of the various major bodies of base metal (zinc-lead-silver ± copper) mineralisation in the Mt Isa Inlier-McArthur Basin base metal province has historically been polarised between syngenetic and epigenetic theories.

HYC in the McArthur Basin is the least deformed and metamorphosed of the deposits known prior to the discovery of Century. It comprises a series of lenses of mineralised dolomitic black shale separated by weakly mineralised breccia beds. The major sulphide species are pyrite, sphalerite and galena although anomalous copper is also present as chalcopyrite (Eldridge et al., 1993). Early workers (e.g. Croxford and Jephcott, 1972) considered the ores to be sedimentary-exhalative into deep (below wave base) marine sediments. Williams (1978) and Williams and Logan (1986) proposed a syn-diagenetic replacement model into sabkha/lacustrine sediments. In their model, organic material in the host shale catalysed the production of reduced sulphur from pore water sulphate for metal fixation. Ore metals were supplied from hydrothermal fluids delivered by the Emu Fault system. Muir (1983) advanced a similar syn-diagenetic exhalative model, with the difference that the majority of reduced sulphur was produced by biogenically catalysed processes. Eldridge et al. (1993) argued for a syndiagenetic replacement origin, based on textural relationships and sulphur isotope systematics. Hinman (1996) argued for the mineralisation at HYC to be timed close to sedimentation, and correlated deformation textures in the ores and enclosing sedimentary rocks with differently oriented phases of syn-sedimentary

tectonic activity. A sedimentary-exhalative model for HYC is cogently argued by Large et al. (1998).

The main points of controversy rest upon differing interpretations of the host sedimentary environment (i.e. deep versus shallow water; proportion of evaporitic facies) and the significance and origin of various small-scale textural features of the ores. Little attention appears to have been paid to examining questions such as the relationships of ore grade to the stratigraphic thickness of various units. Such larger-scale relationships could provide important corroborative evidence for either replacement or exhalative origin. Curiously, the occurrence and distribution of copper in the orebody is rarely discussed or compared with other deposits such as Mt Isa. The apparent lack of silica-rich or barite-rich exhalite facies compared to, say, the Lady Loretta deposit is likewise not highlighted in discussions of metal sourcing and genesis.

Although important in defining detailed models for further exploration, from a regional scale perspective the points of controversy may not really be that significant. The models for HYC may differ in important details, but at least are united in suggesting relatively close-to-sedimentation introduction and fixation of metals. The debate at other deposits embraces radically different syn-diagenetic to epigenetic alternatives, which have much larger-scale implications.

Most models for the lead-zinc mineralisation in the giant Mt Isa group of deposits (Isamine, Hilton, George Fisher) advocate syn-sedimentary to early diagenetic "SEDEX" emplacement (Forrestal, 1990, Valenta, 1994a, 1994b). The existence of major economic copper-rich, zinc and lead-poor mineralisation in close proximity to the lead-zinc at Mount Isa is unusual in sediment-hosted "SEDEX"-type mineralisation. In particular, the remarkable segregation of metals between the two ore types (in places only separated by a few metres) is poorly explained. The Hilton zinc-lead-silver deposit 20km to the north of Mount Isa also has distinctly anomalous, albeit sub-economic, copper mineralisation which partly overlaps and is not so well separated from the zinc-lead ore lenses (Valenta, 1994a, 1994b). Some models of Mt Isa interpret the copper mineralisation as proximal "feeder zone" stockwork mineralisation

related to emplacement of syn-diagenetic zinc-lead-pyrite bodies (e.g. McGoldrick & Keays, 1989; Goodfellow et al, 1993). However, the most popularly accepted view of the genesis of the total Mt Isa system places 'silica dolomite' alteration and associated copper mineralisation as the result of later syn-tectonic fluid mobilisation. This is based on correlation of syn-mineralisation structural relationships and textures with the 'D2-D3' deformational events of the Mt Isa Inlier (Perkins, 1990; Valenta, 1994a, 1994b). Several workers have noted that the zinc-lead mineralisation at Mount Isa has small-scale textural features that are more consistent with it being of replacement origin (e.g. Swager, 1985; Swager et al., 1987; Bell et al., 1988). It has been recently proposed that the lead-zinc mineralisation may have been deposited as the more distal expression of a zoned syn-tectonic hydrothermal system that deposited the copper mineralisation (Perkins, 1997). This important alternative body of opinion has profound implications for exploration insofar as it predicts very different ore-controlling structures to the syn-diagenetic model.

Zinc-lead mineralization occurs in extremely deformed and metamorphosed rocks at Dugald River and Cannington (and on a wider scale at Broken Hill). Because of the difficulty in even recognising original lithofacies, these deposits are even more controversial. At Cannington, a syn-diagenetic model followed by remobilisation during metamorphism (Bodon, 1996) has been proposed. This is contrasted with a syn-deformational, syn-metamorphic replacement theory based on detailed textural relationships (Richmond et al., 1996).

It is not the purpose of this thesis to examine the relative merits of these arguments and pronounce judgement on appropriate models for various deposits. The author has no detailed knowledge of textures, paragenesis or relationships at any of these other deposits and is therefore not qualified to comment on the validity or otherwise of particular models. However, two observations may be made. First, from the published record of controversy on the known deposits, the significance of small-scale ore textures and timing relationships seem to offer particular difficulties of interpretation unless they are placed in a wider deposit context. Second, it may not be appropriate or even particularly helpful to try and force all deposits into dogmatic "syn-diagenetic" or "epigenetic" paradigms. Good evidence exists for significant differences in age of host

stratigraphy (Page and Sweet, 1996) and depositional environments for the major deposits in the province. Evidence for absolute timing of mineralisation emplacement is very difficult to obtain. The major deposits have quite different lead isotope signatures (Sun et al., 1996). This has been interpreted as evidence for different ages of (syn-diagenetic) formation (Sun et al., 1996). Alternative epigenetic models for ore genesis must adequately explain such data.

Ongoing work by AGSO and other researchers has begun to establish timing relationships of regional tectonic events to stratigraphic packages and the existence of possible province-wide episodic pulses of fluid migration (Loutit et al., 1994). Models of driving mechanisms for these pulses of fluid flow cover a range of conceptual possibilities, and deposit data therefore need to be integrated into the widest possible regional context. There are numerous geodynamic model alternatives with potential application to ore genesis. These could range from classic episodes of rift-related sediment/basin/basement dewatering implicit in "SEDEX"-style concepts (e.g. Sawkins, 1984; Goodfellow et al., 1993), to distal fluid expulsion driven by far-field orogenic events (e.g. Garven and Freeze, 1984a, 1984b; Oliver, 1986), to direct involvement of syn-deformational fluids associated with the Isan Orogeny (e.g. Perkins, 1997).

Given this rich tapestry of conceptual possibility, there is no necessity to believe that all deposits everywhere have formed by the same mechanisms of sulphide deposition. It is salutary that such important controversies about absolute timing of metal fluid mobilisation and mechanisms of ore metal entrapment still exist in areas such as Mt Isa, which has been mined for over 70 years. This mandates that a fairly sceptical and open-minded approach should be made to the description and interpretation of a new deposit such as Century.

2.4 Stratigraphy, Lawn Hill Region

Proterozoic and Cambrian age sedimentary rocks dominate the geology of the Lawn Hill region (Fig. 2.3). Regional stratigraphic divisions according to published government mapping are shown on Figure 2.4. Andrews (1998) has developed detailed subdivisions of this stratigraphy, with substantially revised and improved environmental interpretations, but the major published stratigraphic formations remain unchanged.

2.4.1 Cambrian Sequence

Cambrian rocks in the area of the Century deposit (Figure 2.3) comprise limestone, chert, chert breccia and phosphorite. The outlier of Cambrian limestone, which partially conceals Century, is lithologically similar to the Thorntonia Limestone of the nearby Georgina Basin (Szulc, 1992). This outlier has a distinctive and unusual annular shape about 20km in diameter. The total stratigraphic thickness of the limestone sequence within the outlier is around 200-300m, comparable to that of the normal basal Georgina Basin sequence (Szulc, 1992). Later structural disturbance of the sequence has produced drilled thicknesses of up to 400m immediately northeast of Century (RTE unpublished data). Dips and strikes of limestone in the annulus reflect chaotic folding, in marked contrast to flat-lying undeformed limestone of the Georgina Basin to the west. These observations indicate that the boundaries and internal structure of the annular feature developed after deposition and compaction of the Cambrian sequence.

Structural complexity in the Cambrian cover sequence is not reflected in the underlying Proterozoic sequence which hosts the mineralisation, apart from the presence of numerous minor high-angle faults, which displace both the limestone sequence and the underlying Proterozoic lithologies. Downward intruding neptunian carbonate breccia-dykes are commonly associated with these. These variably disrupt and truncate the Proterozoic lithologies and the mineralised sequence.

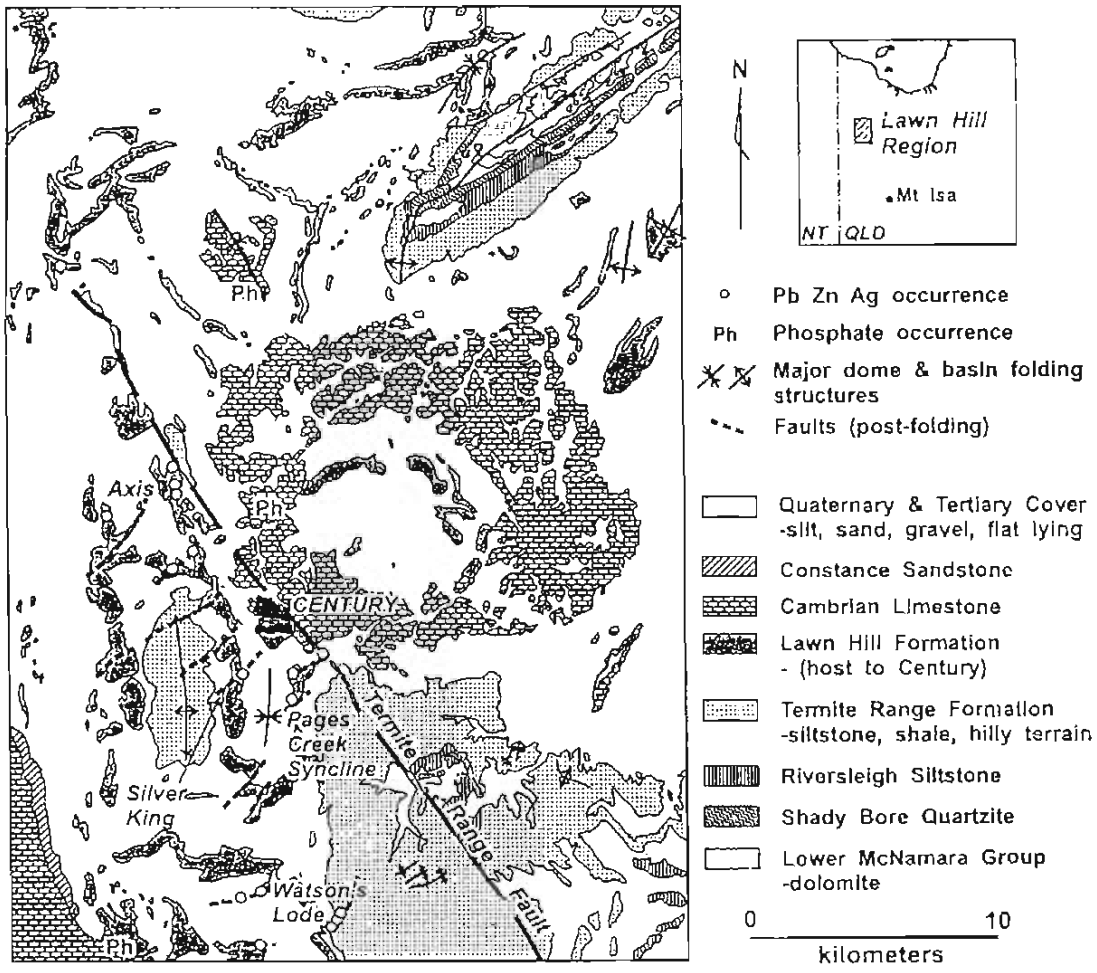

Figure 2.3 Lawn Hill region simplified geology (after Sweet and Hutton, 1982)

Some large fragments of the underlying Proterozoic sequence appear to have been incorporated into the Cambrian sequence as clasts or megabreccia blocks. One of these includes an approximate 1 million tonne slice of the Century orebody in the vicinity of the LH31-15 drillholes, to the east of the main body of mineralisation. This body appears to have been separated from the main body of the mineralisation and incorporated into the limestones. Reasons for its present location are not relevant to any genetic hypothesis for the deposit, and are therefore not discussed further.

Work on the oxidised profile beneath Century has demonstrated that the Century mineralisation was oxidised prior to the deposition of the limestone sequence (Cutler, 1992). Veins of pyrite, base metals (galena, sphalerite) and gypsum cut this oxidised surface and are considered to be related to widespread weakly disseminated trace base-

metal mineralisation known regionally to be present in the limestones (RTE unpublished data).

2.4.2 Proterozoic Sedimentary Rocks

Exposed Proterozoic age rocks in the Lawn Hill region around Century are represented by three Formations of the Upper McNamara Group. From oldest to youngest they are the Riversleigh Siltstone, Termite Range Formation and Lawn Hill Formation (Figs. 2.3, 2 4).

Only limited exposures of the Riversleigh Siltstone are present within 10 km of Century, on the eastern side of the Termite Range Fault. Lithologically the formation consists of poorly outcropping shale and siltstone, with laterally persistent packages of turbiditic sandstone lithologies which crop out as prominent strike ridges. Wright (1992) made a preliminary interpretation of the Riversleigh Siltstone. He concluded that the mudstone and siltstone of the formation were interbedded with, or transitional to, turbiditic facies. Although some evidence is present for the presence of shallow water sand bodies, the overall depositional setting was a deeper-water marine shelf environment. No evidence for substantial shallow-water evaporitic facies was noted (Wright, 1992). However, recent work by Andrews (1998) indicates there to be some thin intervals in the lower Riversleigh Siltstone that exhibit dessication textures. These are volumetrically very small and occur in the lower portion of the unit.

The Termite Range Formation semi-conformably overlies the Riversleigh Siltstone (Hutton et al., 1981; Andrews, 1998). It is exposed over a large area to the south-east of the deposit and in the cores of isolated domal folds to the west and north-west of this, along the trend of the Termite Range Fault. Lithologically, it consists of one to ten metre thick turbiditic-sandstone beds, interleaved with poorly-exposed thin black carbonaceous-shale bands up to 10m thick. Soft sediment folding and disruption features are relatively common, and shale rip-up clasts are also commonly incorporated in the sandy beds. Quite coarse-grained fresh feldspars and quartz are the dominant sand-size mineral grains, suggesting derivation from a reasonably proximal area of granitic basement.

Finely disseminated pyrite and abundant carbonaceous material are a feature of the shaly interbeds, particularly in the upper part of the formation, where it appears to grade semi-conformably into the Lawn Hill Formation. The formation thins dramatically to the east in the Archie Creek area and on the western side of the Kamarga Dome, suggesting that the Kamarga Dome area may have been a basement high during sedimentation. Andrews (1998) considers that the Termite Range Formation comprises turbiditic mass-flow facies, with likely source areas from the north and west.

The Lawn Hill Formation has been subdivided into six sub-units by BMR/GSQ mapping (Sweet and Hutton, 1982; fig 2.4). At Century, all of the sub-units except the uppermost (Pmh6) are represented within a two kilometre radius of the deposit. Stratigraphic thicknesses for the lowermost portions of the Lawn Hill Formation in the deposit area have not been estimated due to structural complications, but they appear comparable to those in the described type section area. A brief description of the units follows (from Hutton et al., 1981):

Pmh1: 250m of concretion bearing grey-weathering laminated silty shale and black carbonaceous shale (Plate 1H).

Pmh2: 80m of thin to medium bedded green tuff, siltstone and finely bedded to laminated siltstone and sandstone (Plates 1F, 1G).

Pmh3: 'Bulmung sandstone member'. 40m of lithic sandstone and intraclast conglomerate (Plates 1E, 1F, 1G), interbedded with tuffaceous siltstone and shale.

Pmh4: 850m of siltstone, laminated black shale and minor tuff with sparse sandstone lenses. The basal section of this unit has abundant greenish weathering tuffaceous beds, lithologically similar to parts of the Pmh2. The upper portion of the unit (unit "h4s" of Andrews, 1998) hosts the Century mineralisation.

Pmh5: 'Widdallion Sandstone Member'. Lithic felspathic arenite, >550m thick. In outcrop, the sandstone is friable and reddish-brown in colour. Where intersected in core, the unit is greenish grey in colour and consists of massive beds of sandstone from 1-25m thick separated by greenish grey or black siltstone and shale.

Pmh6: +80m of purplish weathering green siltstone, shale and minor sandstone.(Plates 1C, 1D).

Facies and associations of these units have been described by Andrews (1998), who concluded that only unit Pmh3 contained facies features (current lamination, hummocky cross stratification) that could be unambiguously associated with relatively shallow depositional environments. Units Pmh2/3 are best interpreted as being the product of a basin-shoaling event, with deposition of the major sand bodies between fair-weather and storm-wave base (Andrews, 1998).

From Century to the east across the Termite Range Fault, the thicknesses and character of the lower Lawn Hill Formation units (Pmh1, 2, 3) change quite substantially over a relatively short distance of a few kilometres (Andrews, 1998). Unit 1 thickens from 250m to as much as 1800m and gains large (250-300m thick) fine-grained sandy units. Unit 2 splits into two intervals separated by a recessive mudrock interval. Unit 3 becomes finer grained, thinner and eventually disappears or changes laterally into fine-grained muddy facies. These changes also take place to a more gradual extent to the north, across the east-west striking Little Range Fault system. The pattern of overlapping facies changes and changing current directions outlined by Andrews (1998) strongly suggests a series of discrete tectonically-triggered sedimentation events. Geometry of major sediment packages suggests control by repeated activation of basement structures such as the northwesterly striking Termite Range Fault and

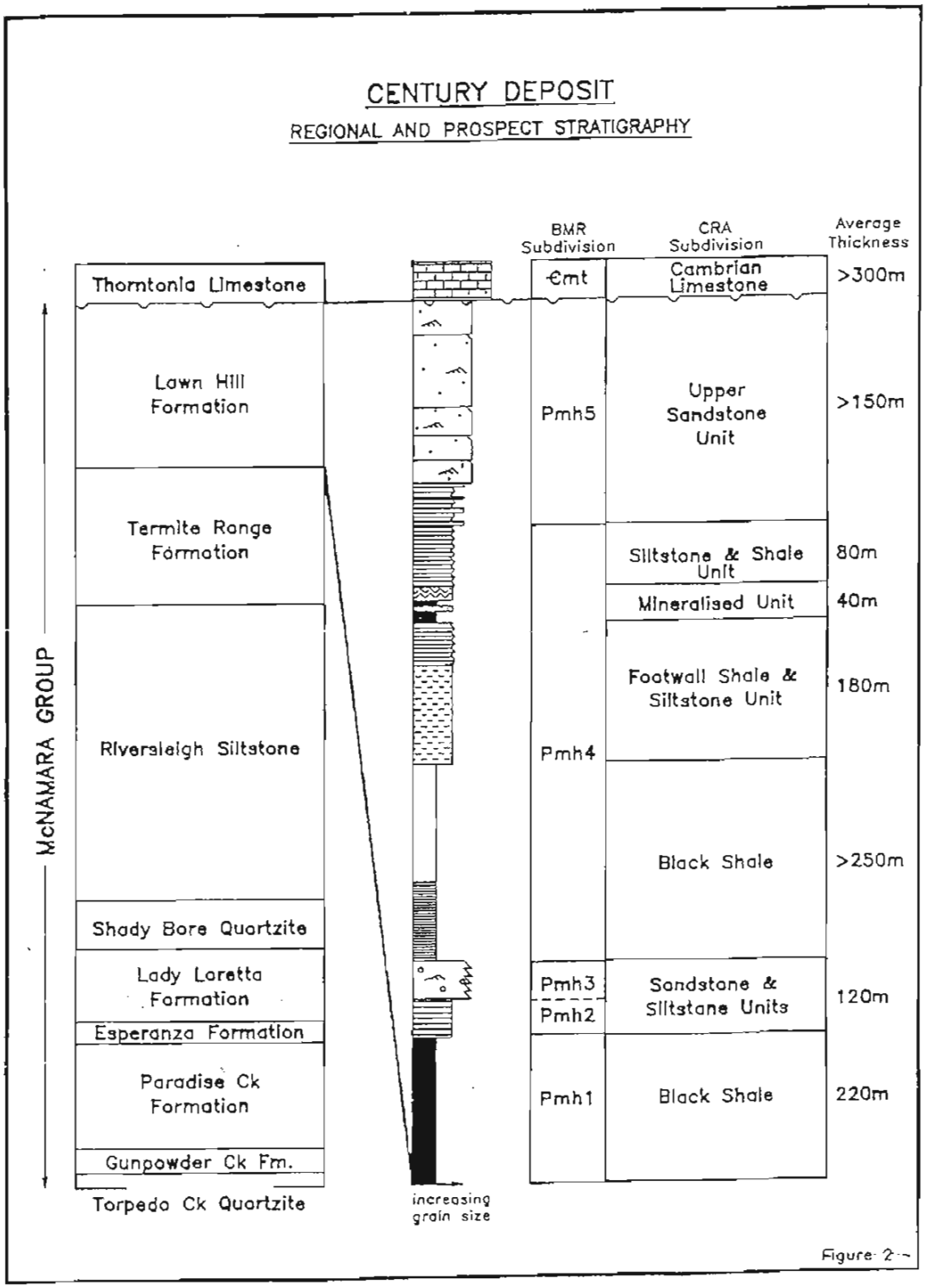

Figure 2.4 Regional and prospect stratigraphy. Lawn Hill area and Century deposit (after Waltho and Andrews, 1993).

east to northeast striking cross structures. Implications of the geometry of the sediment packages for constraining fluid flow and the influence of basement structures on mineralisation distribution are discussed in subsequent Chapters.

2.4.3 Stratigraphic Correlations, Lawn Hill Formation

The Century deposit is hosted by the uppermost portion of unit Pmh4 (unit h4s of Andrews, 1998) of the Lawn Hill Formation (Waltho et al., 1993; Fig. 2.4). This correlation is based on the similarities between the hanging-wall sandstone unit of the deposit stratigraphy to the Pmh5 sandstone regionally, a task made easier by the distinct textural and mineralogical differences between the Pmh5 and Pmh3 sandstones. The deepest unit drilled to date beneath the deposit is a major black-shale dominated package greater than 500m thick. This package is correlated with unit h4r of Andrews (1998). Overall stratigraphic thickness is consistent with the approximate 850m thickness of Pmh4 regionally, although drilling of the upper Pmh4 (h4s) stratigraphy outside the Century deposit area has revealed substantial variations in thickness. At Lilydale, 12km to the south of Century, a stratigraphic drillhole (LH 265) intersects the litho-stratigraphically equivalent h4s unit to the Century host sequence. This unit has weakly anomalous manganese and zinc (associated with weak siderite alteration; Fig. 2.5). It can be seen from Figure 2.5 that the overall thicknesses of the siltstone rich sequence at Lilydale (approximately 60m) is much less than at Century (approximately 140m), although there are similarities in the vertical pattern of shale abundances. This suggests that either:

- a thicker package of sediment was deposited at Century relative to Lilydale, or;

- the Pmh5 sandstone at Lilydale was deposited on an erosionally truncated sequence which was originally similar to that at Century

On the data available, the first alternative appears most likely. Very thin (1-2cm) tuffaceous marker units are present in the Lilydale intersection, which appear to be of similar composition to those in the hanging wall sequence at Century.

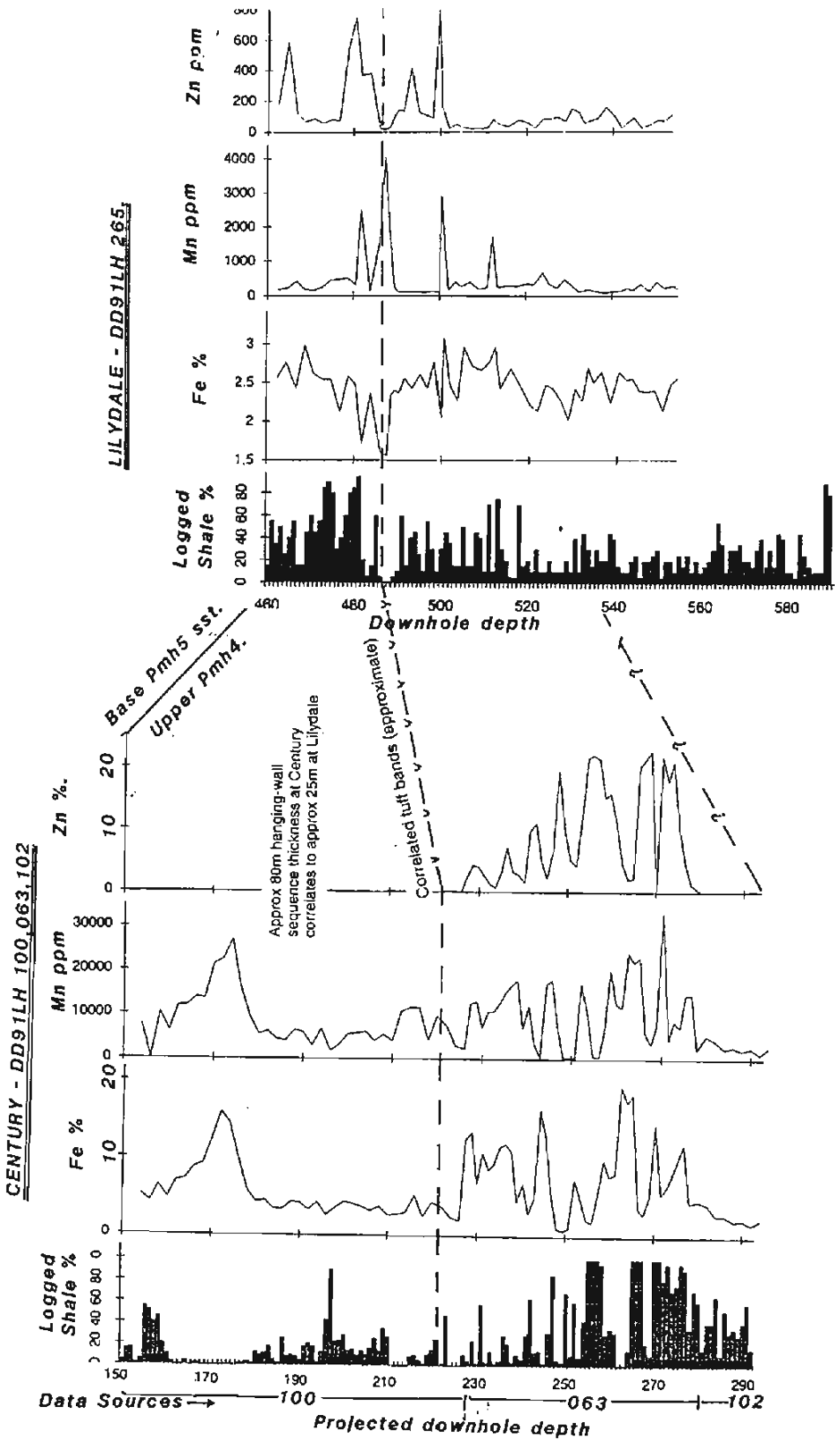

Figure 2.5 Shale percentages and Pb, Zn, Mn abundances in drillholes (LH100 and LH265) for the transition from Pmh4 to Pmh5 at Century and Lilydale. Geochemical data courtesy of Rio Tinto Exploration.

However, the tuffaceous marker beds in the Century hanging wall sequence are locally much thicker than at Lilydale. Tuffaceous beds appear to have been substantially reworked and to be of submarine mass-flow origin rather than pyroclastic derivation (refer section 3.3.5). This suggests that the immediate Century area received a greater quantity of sediment than Lilydale at any given time. Also, the Lilydale section passes downwards into massive black mudrocks, seemingly without development of the distinctive upper and lower footwall sub-units that are present at Century (section 3.5). Removal of this additional 180m thick section by erosion seems rather improbable when the lateral continuity of the upper Pmh4 for over 20km to the south of Lilydale is considered (Andrews, 1998).

The implication is that lateral thicknesses within time-equivalent mudrock-dominated sequences in the Lawn Hill Formation can effectively double or triple over lateral distances of around 10 km. Stratigraphic variation on this scale is more a feature of shelf or ramp depositional environments (including delta-fed turbidite-fan systems) than deep-basin distal-turbidite environments (Miall, 1990). Further, in upper Pmh4 time, sufficient topography must have existed on the depositional surface to explain the deposition of such different sediment thicknesses. In the regional context, it appears likely that basin topography was partly controlled by syn-depositional fault movements (Andrews, 1998, 1999). Evidence for syn-sedimentary growth faulting in the immediate Century deposit area is documented in Chapter 3.

The upper Pmh4 shows an overall coarsening-upward trend (refer section 3.3). This is interpreted to reflect a steady increase in sedimentary activity, in advance of the major rejuvenation of sediment supply represented by the Pmh5 sandstone unit (Andrews, 1998). The Pmh5 sandstone was deposited relatively rapidly on the underlying mud dominated sequence and was cemented early in its burial history (Andrews, 1998). This has implications for local development of under-compacted intervals of Pmh4 that are further discussed in Chapter 3.

2.4.4 Volcaniclastic Rich Units

The Pmh2 to lowermost Pmh4 units of the Lawn Hill Formation comprise the bulk of the outcropping expression of the Lawn Hill Formation, as the Pmh1 and Pmh4 black shale units are almost totally recessive. These units are characteristically thin-bedded, fine-grained and greenish-coloured and have a substantial component of re-worked volcaniclastic material (Sweet and Hutton, 1982; Wright, 1992; Andrews, 1998). No preserved time-equivalent volcanic edifices have been located: sedimentary provenance was from the west (Andrews, 1998).

The most striking feature of these units, apart from their anomalous volcaniclastic content, is the widespread presence of intrafolial deformation features within discrete zones (Plates 17A, 1F, 1G). Some of this deformation may have developed by slumping and possible local re-deposition of the beds during syn-depositional instability. Wright (1992) and Andrews (1998) noted the common occurrence of mudstone clast conglomerates (Plate 1G), which they interpreted as possible evidence of local mass-flow origins of many of the beds. Myrow and Hiscott (1991) documented similar mudstone-clast conglomerate textures in shallow water gravity-flow deposits, in units directly underlying hummocky-cross-stratified sandstone beds. They link the sediment failure to the cyclical wave and sediment loading associated with large storms. The widespread presence of hummocky cross stratification in the Pmh3 sandstone facies (Plate 1E) further indicates the similarities of this association.

However, there is a possibility that many of these intrafolial structures have a relationship to early tectonism, and are parasitic to larger-scale east-north-east striking early folds evident from regional map patterns (Fig. 2.3; Flottmann, 1996). Texturally similar intrafolial folds, developed during hydraulic fracturing and overpressuring events associated with dolomitisation and hydrocarbon maturation, have been documented in the Monterey Formation in California by Roehl (1981) and Redwine (1981). It is therefore uncertain how many of these structures relate to early sediment instability and how many reflect a post-depositional tectonic event. If they are developed post-sedimentation, their textures suggest that the sediments were

substantially under-compacted and/or overpressured during fold development. Systematic structural work is required to solve this problem.

There is an apparent systematic change in the thickness and separation of the two major volcaniclastic units and the intervening sandy facies (Pmh3 or h3s of Andrews, 1998) from west to east across the Lawn Hill 1:100,000 sheet (Andrews, 1998). In the west and northwest of the sheet, Pmh3 comprises massive micaceous beds with well-developed cross stratification; to the east in the Archie Creek area, sand-rich facies in the same stratigraphic position are more thinly bedded, with fine low-angle cross lamination, suggesting a lower energy depositional environment. The tuffaceous units appear to be thinner and to be more widely separated, possibly being present as a series of lenses (Andrews, 1998). These features are consistent with a ramp style setting for sedimentation on a storm-dominated clastic-shelf environment (Fig. 2.6; Sami and Desrochers, 1992).

The sedimentological changes within the Pmh2/3 unit from west to east occur in concert with the already mentioned thickness and grainsize variations within the underlying Pmh1 (Andrews, 1998; Sweet and Hutton, 1982). They are also consistent with the reconstruction made by Sweet (1985) for the Maloney Creek Inlier and the Carrara Range region further to the northwest of Lawn Hill. Sweet (1985) considered that the overall sedimentological distribution was influenced by the longstanding existence of the Murphy Tectonic Ridge as a controlling basin margin structure, coupled with a likely source of sediment from the west. The work of Andrews (1998) indicates that, in the local Century area, northwest (Termite Range Fault) and northeast structures are important local controls within this larger framework. Chapter 3 details the detailed sedimentology of the immediate Century deposit area.

2.5 Mineralisation, Lawn Hill Region

There are numerous old lead and zinc workings in the area to the west and southwest of Century and the Termite Range Fault. Regional lode mineralisation extends over a 10 by 20 km area to the west and southwest of the deposit (Fig. 2.7). These were the only known base-metal showings in the area for over one hundred years, until the discovery of Century (Broadbent, 1995).

Bresser (1992) studied the lodes in detail. They have simple mineralogy, showing repeated deposition of yellow and brown sphalerite, galena, quartz and Mg-rich siderite, with lesser pyrite and chalcopyrite. The mineralisation is mostly deposited as simple infill of fault structures which apparently cross cut the north-south "dome and basin" fold grain and are controlled by dilational stepover structures (Bresser, 1992). Most of these lodes strike north-east, with some east-west and rarely north-west trends. Repeated episodes of fault movement and fluid activity are implied by overprinting brecciation and vein infill relationships (Bresser, 1992). The most recent work on the lodes suggest that the lode development was most likely partly synchronous with the late stages of folding. There is evidence for systematic rotation of early-formed vein sets and many small-scale mineralised fractures and veins have orientations congruent with their origin as fold-related joints (D'Aigle, 1996; Flottman, 1996).

Six common paragenetic stages have been defined for both the Silver King and Watson's Lode deposits (Figure2.8; Bresser, 1992). This suggests that the entire Lawn Hill region experienced the same general history of structural movement and fluid migration during lode emplacement. Sulphur isotope and fluid inclusion data indicate that the mineralising fluids were evolved basinal brines, derived from a source that was continually undergoing sulphur isotope fractionation and producing heavier $\delta\,^{34}S$ values with time (Bresser, 1992, Bresser and Myers, 1993).

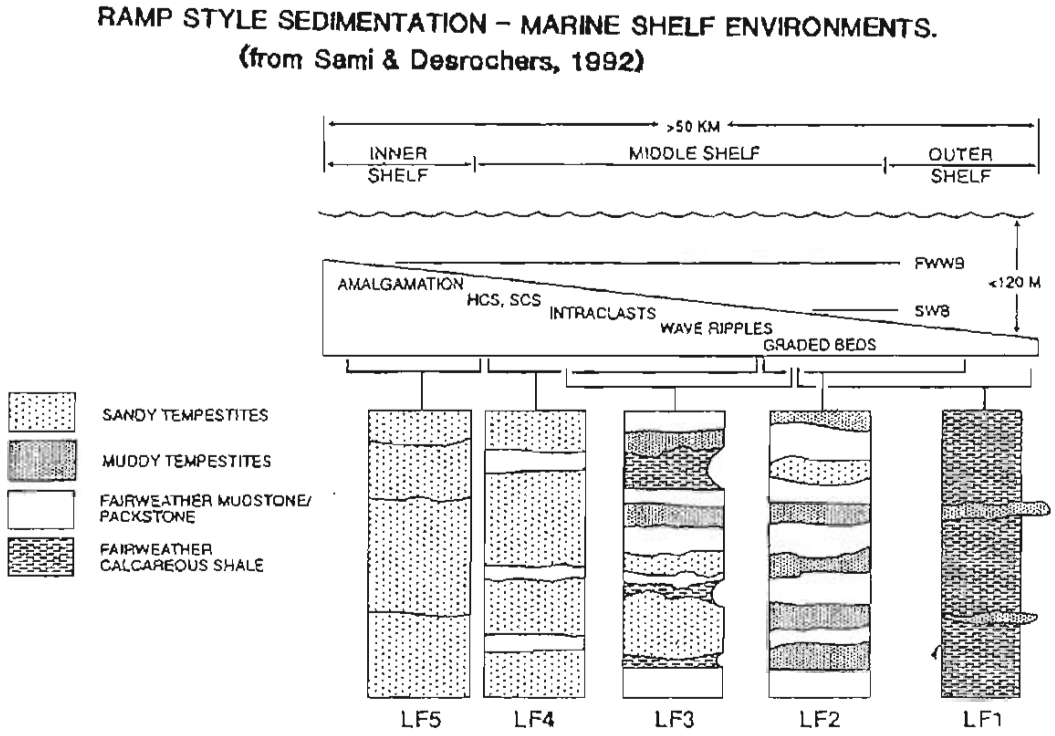

Depositional profile for the Becscie and Merrimack formations showing lateral relationships between lithofacies types. Of particular note is the overlapping of the depositional environments of LF1, LF2, LF3 and LF4 (modified from Handford, 1986). FWWB = fairweather wave base; SWB = storm wave base.

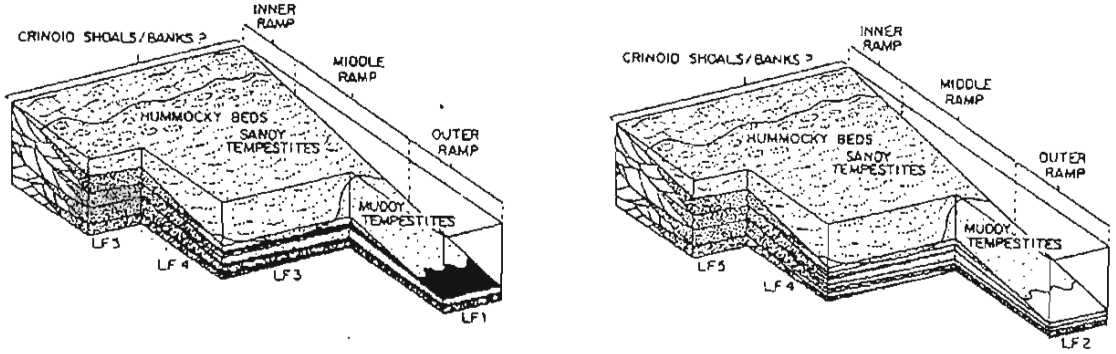

Block diagrams illustrating the inferred distribution of depositional environments and their associated lithofacies for: right a carbonate mud-dominated ramp (Becscie Formation) and left an argillaceous mud-dominated ramp (Merrimack Formation). A crinoid shoal/bank environment is inferred as a source of abundant carbonate sand in the sequence and is not preserved within the Becscie or Merrimack formations.

Figure 2.6. Block diagrams showing inferred distribution of depositional environments and associated lithofacies in a storm dominated ramp setting. The upper Pmh4 host sequence at Century is inferred to be an outer shelf environment; Pmh2/3 to be a middle to inner shelf environment. (From Sami and Desrochers, 1992).

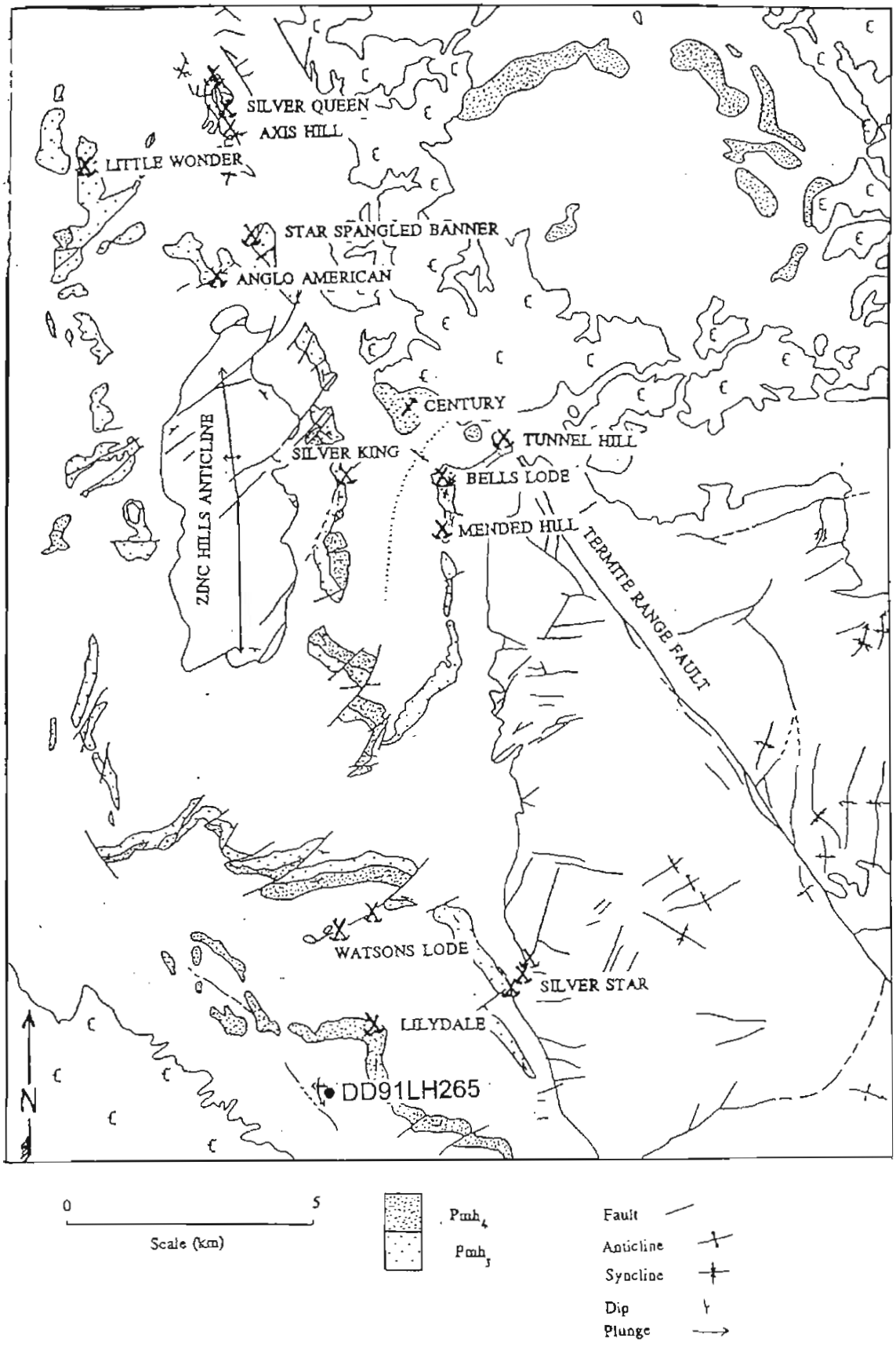

Figure 2.7. Structural map of the Lawn Hill Mineral field, taken from Bresser (1992).

A. WATSON'S LODE PARAGENESIS SUMMARY

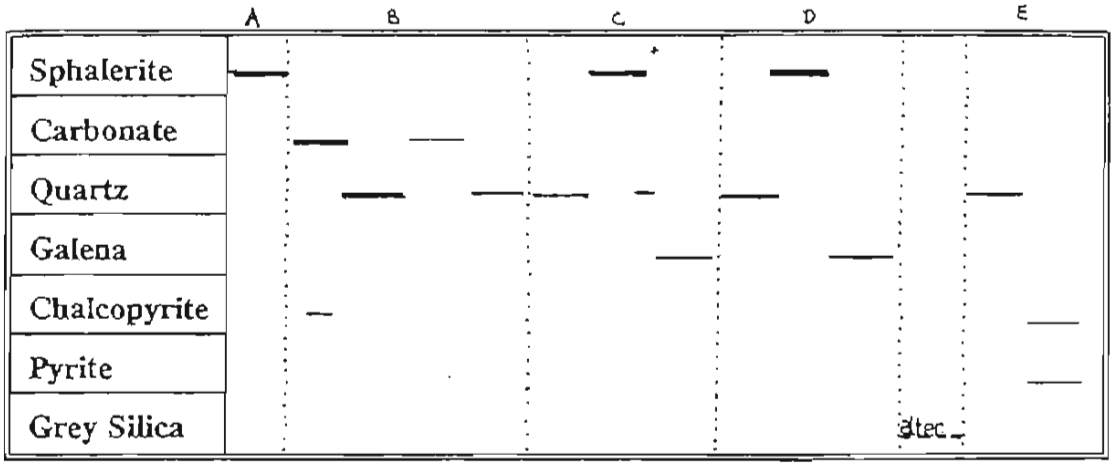

- The paragenetic summary of mineralisation at Watson's Lode. The six stages of the paragenesis are represented and their internal phases are demonstrated relative to each other. Brecciation events separating the stages are represented as dotted vertical lines. The thickness of the lines representing individual phases is representative of relative abundances.

B. SILVER KING PARAGENESIS SUMMARY

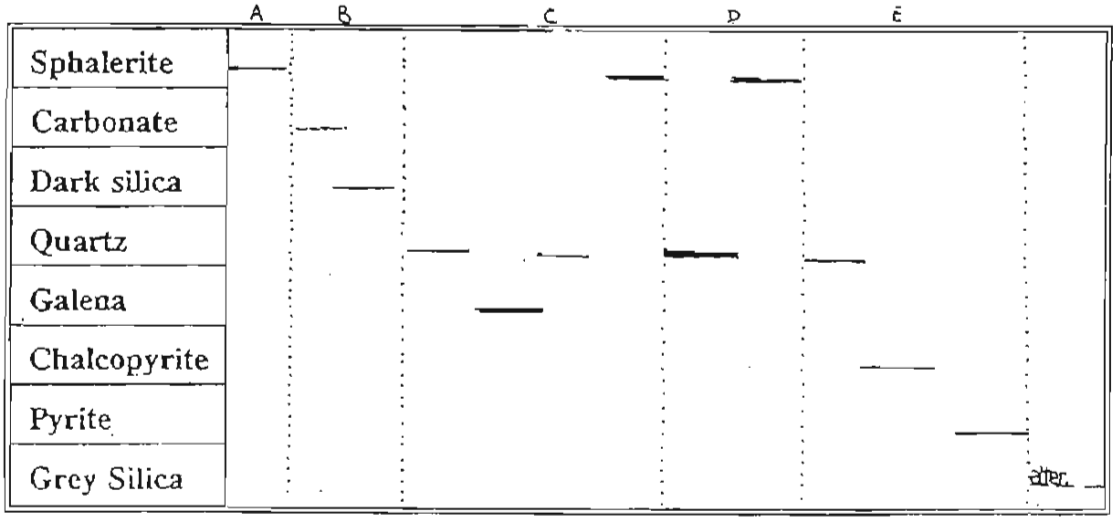

- The paragenetic summary of mineralisation at Silver King. The six stages of the paragenesis are represented and their internal phases are demonstrated relative to each other. Brecciation events separating the stages are represented as dotted vertical lines. The thickness of the lines representing individual phases is representative of relative abundances.

Figure 2.8. Paragenetic summary tables for A: Watson's Lode and B; Silver King. Stages A-E of each paragenesis are correlated on fluid inclusion, mineral assemblages and isotopic data, suggesting emplacement during the same general episodes of structuring and fluid movement. Taken from Bresser (1992).

2.6 Summary

Most current and historic models for known base-metal deposits of the Mt Isa – McArthur propose early syn-diagenetic genesis (e.g. McClay and Carlile, 1978; Williams, 1978; Neudert and Russell, 1981;Muir, 1985; Hinman, 1996; Large et al., 1998). The presence of evaporite facies has been invoked as an essential component of many models that invoke an early syn-diagenetic origin for these deposits (e.g. Williams, 1978; Muir, 1985). However, there are major controversies involving the Mt Isa deposit in particular, with a number of workers advocating syn-tectonic replacement for this and other deposits (e.g. Perkins, 1997). Century is hosted by much younger sedimentary rocks of the Upper McNamara Group, without substantial evaporite content in the host Lawn Hill Formation. Such differences, together with the very existence of major genetic controversies on deposits which have been mined for over 70 years, mandates caution in applying any of the established ore genesis models to the Century deposit.

The best interpretation of the late stages of deposition of the Upper McNamara Group is that it developed as a contractional ("foreland") basin (McConachie et al., 1993). Regional south to north compression associated with this event was manifested partly as the regional "D1" event of the lower McNamara Group in the southern Mt Isa Inlier. South- to north-directed orogenic activity probably extended from about 1600Ma to 1570Ma, in part influencing sedimentation of the upper Lawn Hill Formation and probably extending to ongoing deformation of the Lawn Hill Formation as sedimentation was terminated by basin closure.

Transgressive lode mineralisation in the vicinity of Century has dominantly north-easterly trends and has likely syn-tectonic timing with development of dome and basin fold closures. The latest stages of this deformation are correlated with the D2-D3 events of the Isan Orogeny. Available evidence constrains timing of the peak D2-D3 deformation and metamorphism events to the period 1532-1510 Ma (Connors and Page, 1995), but the early stages of the orogeny likely started considerably earlier, from 1570 Ma onwards. It is possible that the D2 event was transitional from the D1 event,

both events simply reflecting aspects of a larger-scale orogenic transition. This has relevance to possible geodynamic models for the regional setting and timing of mineralisation.

There are several geodynamic model alternatives with potential application to ore genesis. These range from classic "SEDEX"-style concepts involving episodes of rift-related sediment/basin/basement dewatering (e.g. Sawkins, 1984; Goodfellow et al., 1993); to distal fluid expulsion driven by far-field orogenic events (e.g. Garven and Freeze, 1984a, 1984b; Oliver, 1986); to direct involvement of syn-deformational fluids associated with the Isan Orogeny (e.g. Perkins, 1997).

In the context of the overall contractional basin setting of the upper McNamara Group (McConachie et al., 1993), rift-related, high heat flow, scenarios for fluid mobilisation would seem to be rather less probable than geodynamic scenarios involving compression-driven expulsion of fluids from an orogen to the south or southeast. Such fluid expulsion can extend over substantial time frames (ranging from syn-sedimentational to syn-tectonic) and long distances (Garven, 1984, Oliver, 1986). Ongoing work by AGSO and other researchers has begun to establish timing relationships of regional tectonic events to stratigraphic packages and the existence of possible province-wide episodic pulses of fluid migration (Loutit et al., 1994). These large-scale timing relationships of mineralisation to orogenic events have important conceptual implications and are further discussed in subsequent sections of this thesis.

Chapter 3
Century Deposit Stratigraphy

3.1 Introduction - Overview of Century Deposit Geometry

This chapter presents hand specimen and petrological characteristics of the various facies of the Century deposit stratigraphy, followed by an analysis of the distribution of key facies. These features are then discussed to develop an interpretation of the depositional environment of the host sedimentary rocks. The chapter concludes with a discussion of the significance of textural changes in the host strata with proximity to the mineralisation. Formation names used in this study conform to the nomenclature of Sweet and Hutton (1982) and Waltho and Andrews (1993).

Overview of Century deposit geometry and structure

A brief summary of the deposit geometry and structure is made to provide context for the detailed description and analysis of the stratigraphy. The descriptive papers by Waltho and Andrews (1993) and Waltho et al. (1993) give excellent summaries of the main features of the deposit as well as good descriptions of the macroscopic features and subdivisions of the ore zone stratigraphy.

The deposit is composed of two major blocks, termed the northern and southern blocks (Figs. 3.1, 3.2, 3.3). These represent an originally continuous body of mineralisation now separated by a major north-dipping normal fault named the Pandora's Fault. The east-west trending southern boundary of the southern block is created by the intersection of the dominantly south-dipping mineralised zone with another north-dipping low-angle normal fault named the Magazine Hill fault. The eastern and western margins of the southern block are erosional terminations. The western end (Discovery Hill area) is a present day erosional surface, with the eastern end being a Cambrian age erosional surface beneath limestone cover (Fig. 3.3).

The northern block is completely concealed by the Cambrian limestone sequence, only being known from drill intercepts. It is gently folded into a roughly north-south synclinal structure. Folding predates the deposition of the limestone sequence. The western and north-eastern margins are erosional unconformity terminations against the limestone sequence. The far north-western termination of the deposit is controlled by an east-west trending, south-dipping, normal fault named the Nikki's Fault.

The Pandora's fault has a pronounced rotational component, with a displacement of less than 30 metres at its eastern end and a displacement of around 250-300 metres at its western end. There are some indications that the Nikki's Fault has a similar westward increasing displacement. If this is true, then the northern block appears to be preserved in a rotational graben, with a hinge line close to the present eastern margin of the deposit. This point of zero displacement lies very close to the intersection of the Pandora's Fault with the Termite Range Fault structure, suggesting that the Pandora's fault may terminate against the Termite Range Fault. The only other significant body of mineralisation (the 'LH31-15 outcrop') known in the deposit area is a small (approx 1mt) body of mineralisation incorporated as a megaclast within the limestone sequence. Because of its similarities to the rest of the mineralisation and its small size, no systematic study of this body has been done.

Importantly, there appear to be no preserved "natural" terminations to the Century mineralisation - faults and/or erosional surfaces truncate it on all sides. The potentially significant relationship of the deposit to the regional Termite Range Fault has likewise been removed by later erosion. The south-western corner of the deposit (Discovery Hill area) most closely approximates a "natural" termination to the mineralisation (in the sense of an apparent primary diminution of base metal grades along the stratigraphy). The pristine body of mineralisation prior to faulting and erosional events may have been two to three times its present size.

Interpretation of the deposit stratigraphy is severely constrained by the limited areal extent of the preserved sequence. Away from the immediate deposit area, no exposures of equivalents to the Century host sequence are known for a distance of at least 15km (Lilydale area; Fig. 2.7).

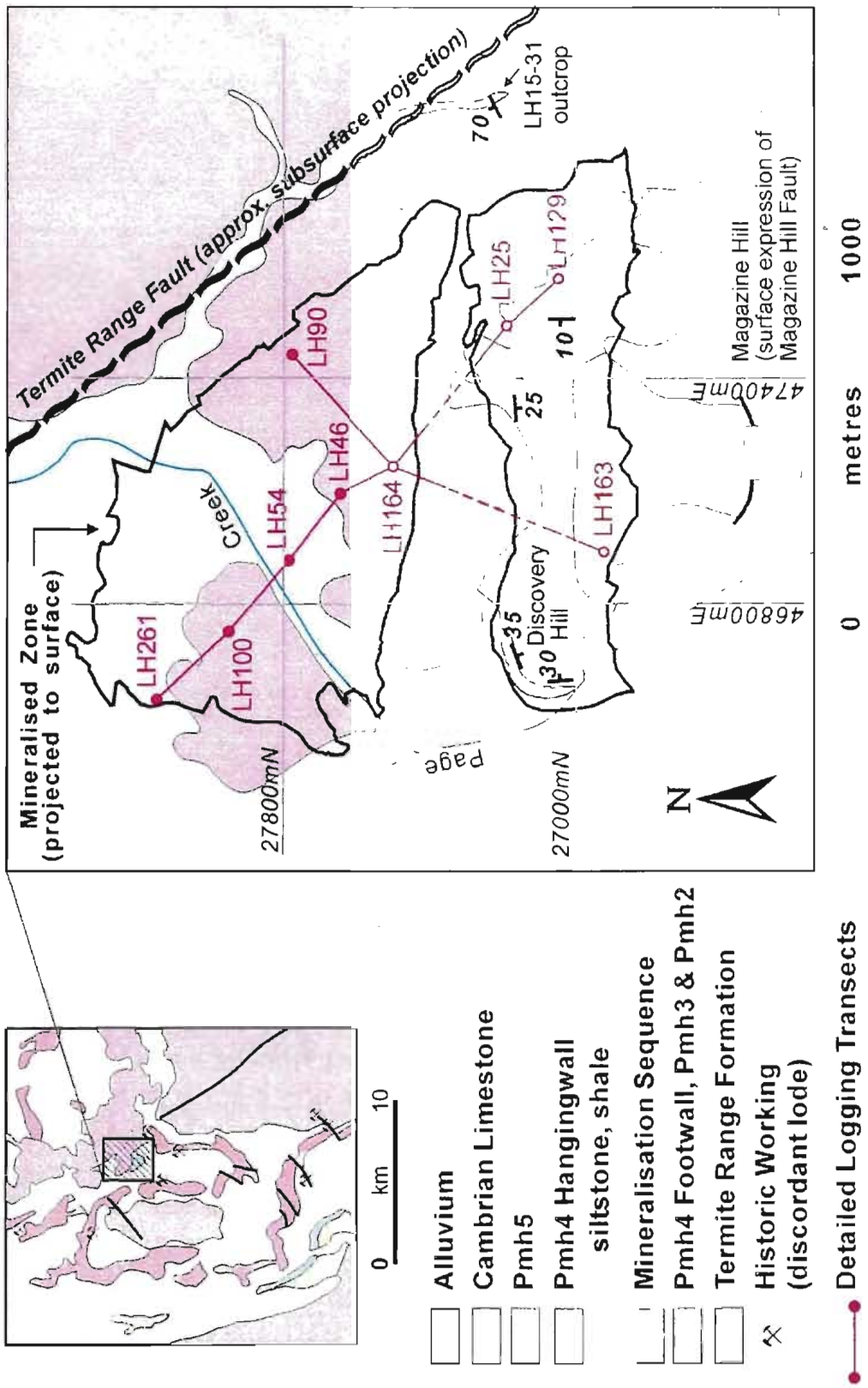

Figure 3.1 Surface geology, Century deposit. (after Waltho and Andrews, 1993).

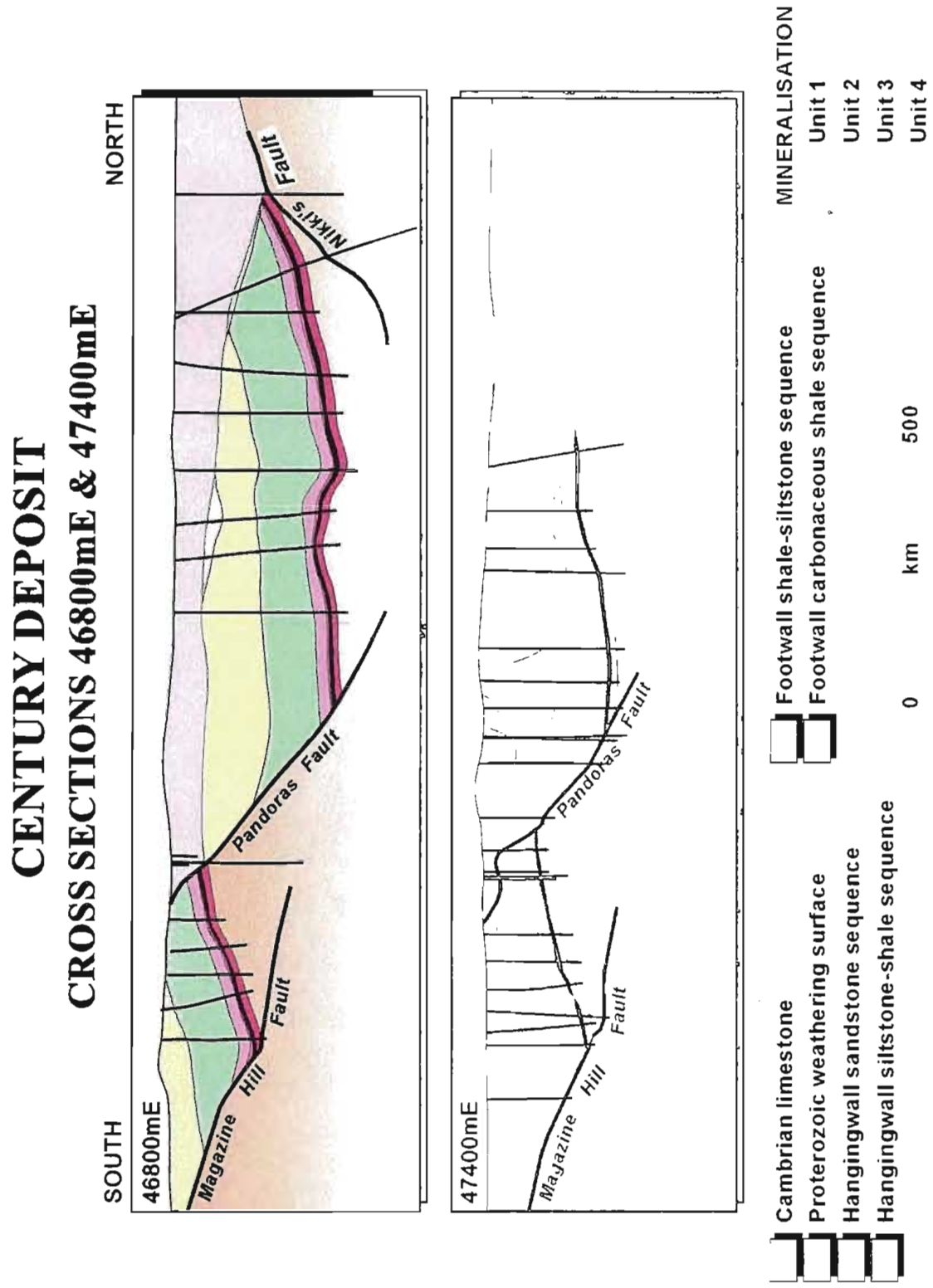

Figure 3.2 Schematic north-south cross sections, Century deposit. (after Waltho & Andrews, 1993).

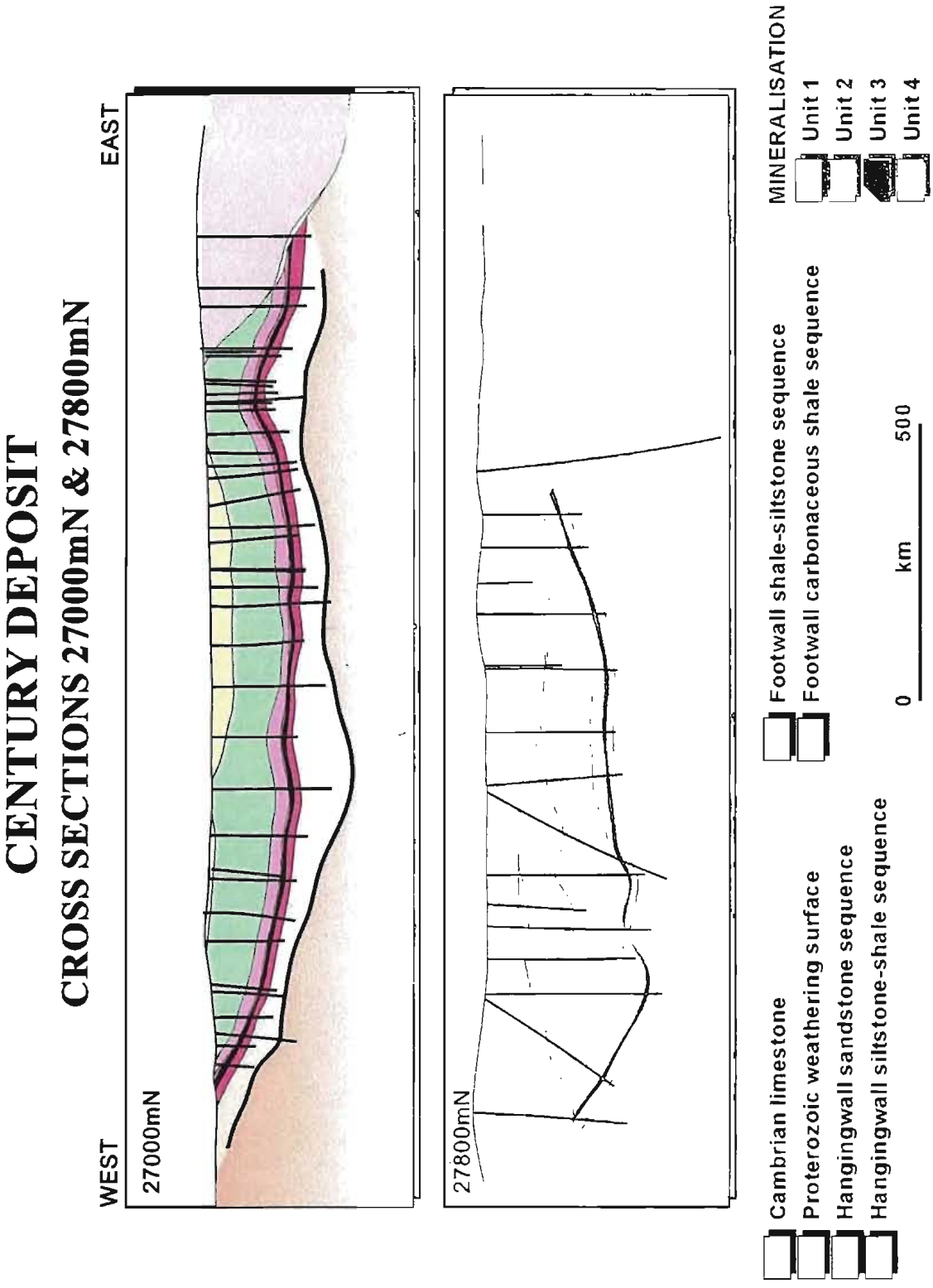

Figure 3.3 Schematic east-west cross sections, Century deposit. (after Waltho and Andrews, 1993).

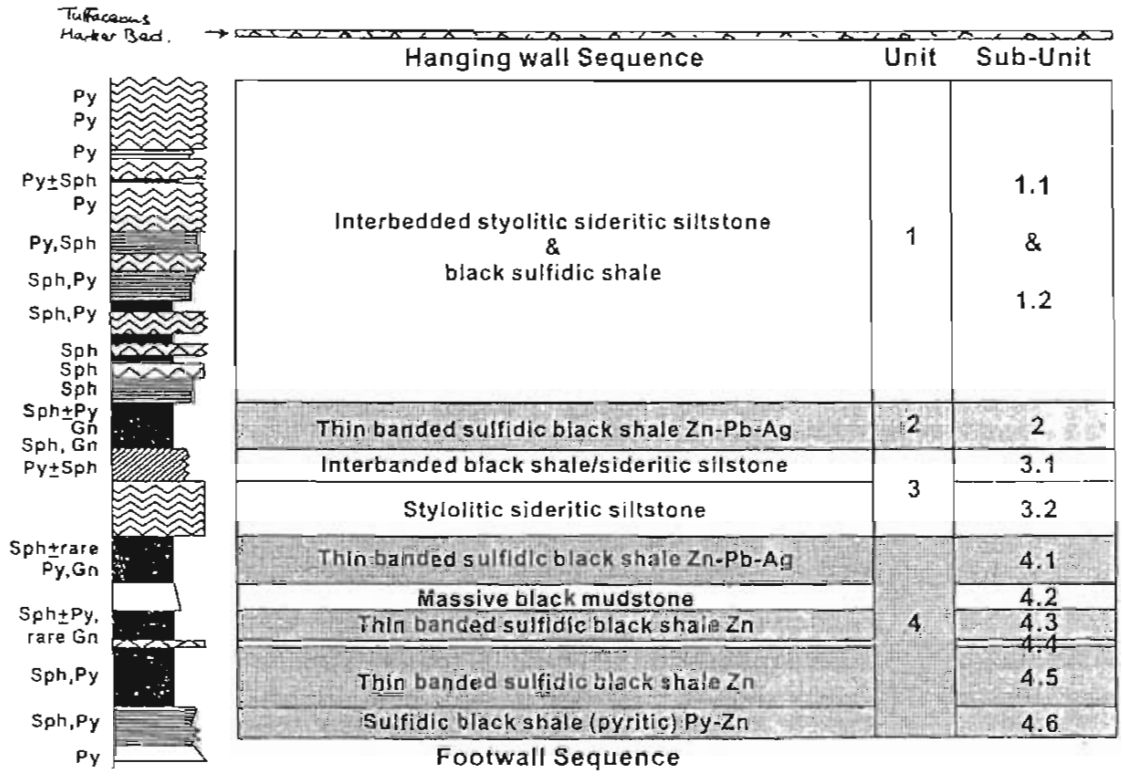

Figure 3.4 Stratigraphic subdivisions of mineralisation sequence, Century deposit (after Waltho and Andrews, 1993).

3.2 Hanging Wall Sandstone Sequence (Widallion Sandstone; Pmh5)

The Widallion Sandstone (hereafter referred to as Pmh5 in conformity with most published descriptions of the deposit) is the uppermost preserved Proterozoic unit at Century. It consists mainly of grey, massive to graded medium-grained feldspathic quartzose sandstone with minor interbedded siltstone and shale (Plates 2A, 2B). Rare mudstone clasts are present within sandstone beds. For the most part, these appear to be transported 'rip-up' clasts, but, in some of the larger shaley intervals intersected in core, they may represent remnants of sheared fine-grained interbeds.

Wright (1992) noted the presence of three facies types; grain-flow sandstone, turbidites and debris flow deposits. Grain-flow sandstone beds represent the dominant facies type. These commonly attain individual bed thicknesses of greater than 5 metres, with amalgamated bed thicknesses up to 25 metres. Abundant dewatering structures (dish structures, pillars, sand flames) indicate rapid deposition and high pore fluid pressures (Wright, 1992). The base of the unit is transitional to the underlying silt-rich sequence

(Plate 2B), with thin sandstone interbeds commonly preserved. This suggests an overall upward coarsening or progradational relationship from the underlying Pmh4 siltstone and shale.

Sweet and Hutton (1982) noted high glauconite content in the Pmh5 regionally, suggesting that laterally-equivalent shelf sands may have resided for some time in a shallow marine environment. The facies associations at Century suggest that they are likely to be channelised turbidites deposited in a deeper marine environment (Wright, 1992; Andrews, 1998). However, Sweet and Hutton (1982) observed ripple marks and cross lamination regionally, which they interpreted as representing a shallow marine environment.

A ramp or slope facies environment offers one way of reconciling these observations. Storm reworking of unstable shallow-marine sands could generate extensive submarine transport of sandy material as turbidity/density currents. If the nearshore environment is being fed by a delta type distributary system, then channelised submarine fan systems could be expected. A possible analogy is perhaps the Nile Delta, (see Miall, 1990, p. 379-382 for summary). In the offshore Nile delta, only 5% or so of the total sediment load is sand, but it is distributed as thick channel sands and turbidites in blankets up to 50 km across and up to 50 km offshore, being interleaved with mud turbidites and tempestites ('unifites': Stanley, 1981).

Petrographically, the Pmh5 sandstone comprises immature lithic arkose with high feldspar content, suggesting derivation from a granitic source terrain (Plate 3A). Regional provenance from the south has been established by Andrews (1998), but has not been established in the deposit area due to paucity of outcrop. Petrographic studies of the Pmh5 sandstone in the deposit area have revealed high clay and chlorite content in intergranular cement. This chlorite-clay assemblage appears to have been developed during early diagenesis, substantially occluding porosity and thereby preserving unstable material such as microcline from further diagenetic breakdown (Plate 3B). Chlorite-rich cement is demonstrated at the regional scale (Andrews, 1998). Feldspar destructive alteration is rare in the sandstone except where there is evidence of hydrocarbon mobility. The hydrocarbon material appears to fill secondary solution

porosity and post-dates the earlier chlorite-rich cement (Plates 6G, 6H). This has important implications for the relative timing of mineralisation and hydrocarbon mobilisation (section 3.7.4).

3.3 Hanging Wall Siltstone Sequence

Lithologically, the hanging wall sequence comprises interbedded black mudstones, grey siltstone and variably siderite-rich siltstone (Plates 2C, 2D). Minor pyrite is developed in the more carbonaceous shaly units. Other lithologies are beds termed "friable mudstones" (Wright, 1992), and there are occasional thin sandstone beds in the upper portion of the hanging wall sequence. Five distinctive facies types were recognised by Wright (1992), composed of varying mixtures of the above lithologies. Brief descriptions of these follow, with comments on their possible environmental significance.

3.3.1 Thinly Bedded Siltstone and Shale Facies

This facies consists of laminated to thinly bedded (0.2-10cm) grey siliceous siltstone interbedded with black carbonaceous (pyritic) mudstones and shale laminae (see upper two rows of Plate 2C). Shale laminae range from partings to more massive mudstone intervals up to 30cm thick. Detailed core logging suggests that coarsening-upwards cycles occur on the scale of <1m to >10m (Wright, 1992; Fig. 2.5). The regional significance of the overall coarsening-upwards trend in the hanging-wall sequence (Fig. 2.5) is discussed in Chapter 2.

The fine-scale lamellae are characteristically internally graded, as are the top few milimetres of the thicker silt beds (Plates 3E, 3F). Once individual beds exceed about 5 mm or so thickness, their basal portions become internally massive and lack convincing evidence for any small-scale current lamination or Bouma style structures as in the overlying Pmh5 sandstone. These features suggest that individual beds were deposited from single-event density flows, with final stage deposition of sediment from suspension. They have many features in common with tempestite facies described by

many authors (e.g. Scheiber, 1989, Sami and Desrochers, 1992, Myrow, 1992, Ghibaudo, 1992). This facies forms the majority of the hangingwall sequence, with sedimentary cycles defined by subtle variations in silt/shale ratio and bed thicknesses.

3.3.2 Massive Siltstone Facies

These beds are larger scale versions of the thinner siliceous siltstone beds described above. They reach thicknesses of up to 60cm, but more commonly 5-30cm (several are visible in the lower portion of Plate 2C). As noted by Wright (1992), they share many features in common with beds termed 'unifites' in the literature (Stanley, 1981). Poorly-defined parallel lamination, without internal bedding discontinuities, is common within these beds (Plates 5D, 19D). This is interpreted to be the result of fluctuations in sediment deposition from suspension during single gravity- or mass-flow events. Parallel lamination of this kind is interpreted as diagnostic of tempestite shelf facies, rather than turbidity current deposits (e.g. Myrow, 1992).

Petrographically the massive siltstone is silica- and illite-rich, with rare inclusions of carbonaceous fragments (Plate 3G). They are commonly siderite-rich as shown by the brown stain on core surfaces which have been exposed to the air for short periods (Plates 2C, 2D). This siderite is grossly replacive, showing no signs of primary deposition (Plate 4; see Chapter 5). Representative hand-specimen textures of siderite relationships relative to sedimentary fabrics are shown on Plates 5A-5D. Early diagenetic siderite is not commonly associated with marine mudrock facies except under special conditions (Mozley and Carothers., 1992). Siderite in marine shale sequences is more commonly developed during deeper burial (Curtis and Coleman, 1986). At Century, the extensive replacement of compacted fabrics in the siltstone facies is consistent with siderite deposition during relatively deep burial. This is discussed further in Chapter 5.

3.3.3 Laminated Shale Facies

Fine-grained laminated shale-rich units separate the siltstone-rich intervals. They are developed throughout the hanging wall siltstone sequence, achieving thicknesses up to 1.5m. Sub facies types in the laminated shale range from massive and laminated black carbonaceous mudstones to laminated (1-2mm scale) black shale and grey siltstone with high shale/silt ratios. Similar facies are present in other units of the Lawn Hill Formation and achieve substantial thicknesses (e.g. Pmh1; Plate 1H).

Carbonaceous matter is abundant in this facies, with total organic carbon contents as high as 10% in places (Minenco, 1990). In thin section, organic material occurs as fine brown laminae which separate micro lenses of silt- and clay-size material and as opaque films and partings of bituminous material up to 0.5 mm thick. Texturally, this latter material resembles algal mat fabrics (Scheiber, 1986, 1989). Typical thin section textures are shown in Plates 3E and 3F. Deformed and isolated fragments of carbonaceous material are present in many of the more massive units (Plate 3G). This texture resembles the 'swirl shale' facies of Scheiber (1989), interpreted to be due to reworking and resedimentation of algal mat material during storm conditions. However, in many instances, the thicker organic seams do not show evidence of compaction and are associated with base metal sulphides (see 5.2.3; 5.3.6). They are interpreted to represent the degraded residue of bedding-parallel intrusions of mobile hydrocarbons (Plates 13, 15).

Micro-lenses of silty material characteristically occur between the carbonaceous seams (Plates 3E, 3F, 4C). This texture is frequently interpreted as evidence of micro-current lamination (Wright, 1992; Scheiber, 1986), and may have partly originated in this fashion. However there is a spectrum of oriented and partly oriented fabrics which show convincing evidence for truncation of some siliceous sedimentary lenses by dissolution adjacent to carbonaceous seams (Plates 4A to 4F). The geometry of some micro-lens shaped bodies of coarser-grained silt-rich material has therefore, at least in part, been imposed during compaction. This has relevance to the significance of the stylolitic dissolution surfaces that are one of the diagnostic textural features of the mineralised zone. An explanation of this phenomenon may illuminate one of the key

mechanisms for the textural changes in the vicinity of the mineralisation (see section 3.4.1).

Pyrite is present in places as discrete nodules up to 3cm in diameter. These are surrounded by compactional fabrics in the surrounding sediment beds and are interpreted to have formed prior to the majority of compaction. Pyrite is more commonly present as fine bedding-parallel lamellae up to 1mm thick, commonly concentrated in zones from 5 to 30 cm thick. Microscopically, the lamellae are crowded with 1-2 micron euhedral crystals. Rare circular aggregates superficially resemble framboidal clusters (Plate 13G).

3.3.4 Interbedded Sandstone and Shale Facies

This facies represents the transition between the hanging wall siltstone and the Pmh5 sandstone sequence (Plate 2B). It strongly resembles the thinly bedded siltstone and shale facies, but includes sandstone beds that are texturally and mineralogically identical to the Pmh5 sandstone. The significance of this is discussed in Chapter 2; the only other feature of note is the paucity of siderite in comparison to the patchy, but generally increasing, siderite content near the mineralisation in the lower portion of the hanging wall siltstone unit.

3.3.5 Tuffaceous Marker Units and Friable Mudstones

Tuffaceous marker bands, together with the "friable mudstone facies" of Wright (1992), are an interesting feature of the hanging wall sequence. Beds with a substantial volcaniclastic component are relatively common throughout the hanging wall sequence (Plates 2C, 2D). They attain thicknesses of up to three metres, but are more commonly from 1cm to 40 cm thick. The largest and best developed of these units lies just above the mineralised sequence and has proved a useful marker horizon (Fig. 3.4). This unit thins quite substantially from north-west to south-east across the deposit area (section 3.3.6).

Many features suggest that these beds are not the product of primary pyroclastic deposition (see also Wright, 1992). These include the presence of incorporated shale clasts, changes in bed thickness in sympathy with thickness trends in the enclosing sediment beds (section 3.4.5) and fining upwards trends in grainsize within individual beds to shale-rich tops (Plates 2C, 2D). Petrographically, they contain abundant clay and siderite altered glass shards (Plate 3C), with rare well-preserved fragments of accretionary lapilli (Plate 3D). Preservation of features as delicate as these in what are interpreted as mass-flow transported sediments indicates a relatively short residence time in the sedimentary environment prior to their final deposition. There appears to be no preserved volcanic centre in the Lawn Hill region to source the volcanic material in either these beds or the thick sequence of unit Pmh2/3 (section 2.3.4).

The friable mudstone beds consist of framework-supported mud-clast conglomerates. Clasts may be compositionally varied and commonly have ragged terminations. In places the friable mudstones have a tuffaceous matrix. The tuffaceous matrix may have an oriented fabric in clay minerals at an angle to the compactional fabric (Plate 3H). The origin of these fabrics is not known, but may relate to low-angle shear during compaction and diagenesis.

The friable mudstone beds were discussed by Wright (1992), who concluded that they were problematic and required further documentation of their three dimensional geometry to properly understand their significance. This has not been attempted in the present study, but, from core logging, the facies appears to be most common in the north-western portion of the deposit, occurring in association with the thicker tuffaceous units.

The friable mudstones probably represent original zones of reworked sediment with high original tuffaceous content. Some may have been debris flows. They are intrinsically mechanically weak, and have likely been preferentially disrupted by slumping and perhaps early tectonic effects because of this. The matrix of both the friable mudstones and the tuff units has a high proportion of swelling (presumably smectite) clays derived from the breakdown of volcanic detritus. Similar intraformational bedding fabrics, (clasts are termed 'rip-down clasts') have been

described by Chough and Chun (1988). They are interpreted as the result of liquefied intrastratal flow during penecontemporaneous deformation of tuffaceous sediments.

3.3.6 Stratigraphic Analysis

This section is intended to develop an overview of the continuity and degree of lateral variation in the various facies assemblages of the hanging wall sequence. Facies, relationships and continuity of the ore zone stratigraphy at Century are discussed in detail in section 3.4, to constrain the discussion of metal and sulphide species distribution in Chapter 5. Sedimentological logging (Wright, 1992) of several widely spaced drillholes in the deposit area indicates good lateral continuity of the major packages in the hanging wall and mineralisation sequences, over distances of several hundred metres. Major shale packages, in particular, appear to have relatively uniform thickness and continuity (Wright, 1992). However, careful inspection of these logs, in combination with detailed logging of several drillholes in the present study, suggests subtle lateral changes in thicknesses of the massive siltstone units from north-west to south-east. Subjectively, the massive siltstone beds appeared on average to be slightly thicker in the north-west of the deposit.

To assess this subjective impression, estimates were made of the average thickness and abundance of siltstone beds on a widely spaced grid of drillholes across the deposit using core photographs. The hanging wall and mineralised sequences were examined on a metre by metre basis.

Twenty eight drillholes were selected to give the thickest and best preserved possible drill intersections of the hanging wall siltstone sequence, spread over the entire deposit area. In each metre of intersected sequence, the aggregate length of siltstone beds with individual thicknesses between 50mm and 100mm was measured from core photographs. Aggregate lengths of siltstone beds with individual thicknesses greater than 100mm were also compiled for the same intervals. Core to bedding angles were obtained from the deposit database on a metre by metre basis and used to dip-correct intersected lengths to true thicknesses. Raw data are presented in Appendix 8 and a graphical montage of the data as Enclosure 1.

A careful inspection of Enclosure 1 clearly shows increased abundance of "thick" (>100mm) to "thin" (<100>50mm) siltstone beds in the north-west of the deposit area.

To simplify these data further, measurements of the two thickness parameters were then aggregated for the entire length of the intervals logged, from the base of the Pmh5 sandstone to the base of the mineralised sequence. A simple ratio of the total aggregate lengths of 'thick' and 'thin' beds measured for the individual drillholes was then calculated and plotted. This ratio is interpreted to provide a simple synoptic parameter summarising the usual proximality trends used by sedimentologists (e.g. Sami and Desrochers, 1992) when examining sequences with tempestite or gravity flow derived beds. Results are presented in Figure 3.5. An inspection of this diagram indicates that the thicker beds are more numerous relative to the thin beds in the north-west portion of the deposit area, suggesting a more proximal environment of deposition to the north-west.

In addition to the ratio plot, a simple plot of total thickness of the hanging wall siltstone shows a general thinning to the south-east of the deposit (Fig. 3.5B). The significance of these observations is discussed further in section 3.7.2, in the context of additional data on thickness and sedimentary facies of the mineralised sequence from section 3.4.

3.4 Mineralisation Sequence

Facies in the sequence that hosts the mineralisation are essentially the same as those in the hanging wall sequence. No major differences can be reasonably inferred for sedimentary processes responsible for the original deposition of the lithologies. The major differences lie in the 'packaging' of the various facies types into thicker shale dominant units, separated by discrete intervals of interbedded siltstone and shale facies (Fig 3.4). The development of irregular stylolitic surfaces along bedding contacts within the siltstone-rich units is diagnostic of the mineralised stratigraphy. The lithological sequence is laterally continuous across the approx 2 km width of the

deposit in the sense that the identity of the major units is maintained. However, important textural and thickness variations are present in detail.

CENTURY DEPOSIT – SEDIMENT PROXIMALITY AND THICKNESS TRENDS.

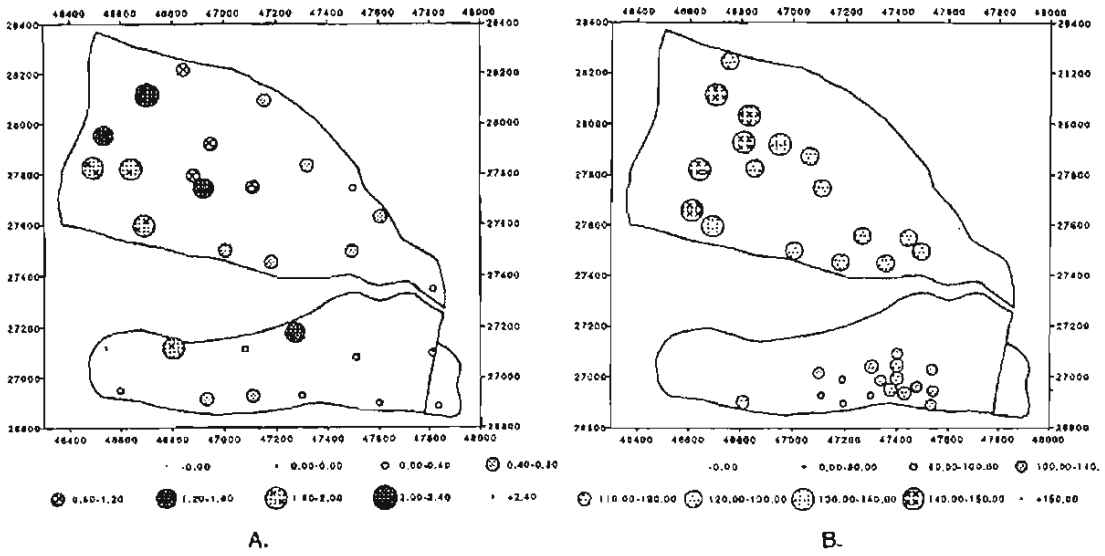

Figure 3.5 Century Deposit -A. sediment proximality trends. (ratio of aggregate thickness of >100mm siltstone beds to >50<100mm siltstone beds in hanging wall sequence). Raw data are in Appendix 8. B. Overall thickness changes of hanging wall siltstone sequence, from base of last massive sandstone interval to top of mineralisation sequence. Data are from deposit database (RTE unpublished data) and have been corrected for dip angle to give approximate thicknesses. Data in the southern block may be anomalously thin due to structural thinning. Notwithstanding this, a clear trend of decreasing thickness from west-north-west to east-south-east in the northern block is evident.

3.4.1 Stylolitic Siltstone Facies

The stylolitic siltstone facies is represented in units 1, 3.2 ("cappucino horizon") and 4.4 of the mineralised sequence (Fig. 3.4). Sedimentologically, it closely resembles the interbedded siltstone and shale facies of the hanging wall sequence. It is characterised by the extensive development of irregular stylolitic contacts along bedding surfaces and a much higher average siderite content (Plates 2D, 2E). The top of unit 1 is not strictly a stratigraphic division, but rather is a textural change defined by the occurrence of abundant stylolitic partings. The precise boundary appears to vary by several metres vertically across the deposit relative to the tuff marker beds. Massive siltstone beds up to 0.5m thick are widespread throughout the stylolitic siltstone and shale facies. These are sedimentologically similar to those in the hanging wall

sequence, except they have more pervasive siderite as well as the presence of minor disseminated sphalerite in some areas.

The stylolites appear to be surfaces of locally intense dissolution of the siltstone beds, or, in some cases, siderite-rich areas. Timing relationships of siderite to stylolites are complex; siderite spheroids are in places truncated by stylolites (Plate 8A) and in places stylolites are overgrown by siderite/sphalerite (Plate 21D). Plate 12 shows typical hand specimens of stylolitic textures; solution features are shown in thin section in Plates 8A, 13E, 21C and 21D, with varying amounts of mineralisation.

3.4.2 Thinly Bedded Siltstone Facies

Thinly bedded siltstone is present as unit 3.1 of the mineralised zone and, to some extent, in individual sub-units within the unit 1.1 facies. The facies consists of thinly bedded siliceous siltstone with only minor proportions of carbonaceous shale and lacks extensive development of stylolites. The facies comprises a minor, but important, component of the mineralisation sequence stratigraphy and is intensely mineralised in some locations, but quite low grade in many others (section 5.2). Sedimentologically, it is indistinguishable from portions of the hanging wall sequence with low shale content.

Disseminated siderite is very common in the matrix of many of the siltstone beds. Siderite aggregates are commonly stained and infilled by mobile pyrobitumen and are often overprinted by later replacive sphalerite (Plates 6-8). In thin section, the sphalerite appears to have had a preference to replace the siliceous matrix of the unit, although siderite is also replaced.

3.4.3 Laminated Shale Facies

The laminated shale facies is represented by the various '1.2' sub-units and subunits 2, 4.1, 4.3, 4.5 and 4.6 of the mineralisation sequence (Fig. 3.4; Plates 2E, 2F). These units host the majority of the base metal mineralisation and are up to 4m thick. Detailed petrography of this facies is difficult to establish because of the high content of organic matter, which renders samples practically opaque in thin section. Excluding sulphides, the ore-host shale is compositionally similar to the laminated shale facies of the hanging wall sequence, with the majority of the matrix consisting of silt to clay size clastic quartz and illite. They are, however, much thicker and more laterally continuous.

There is no evidence in the mineralised shale for the presence of any cryptocrystalline or amorphous gangue facies such as silica or barite. There is also no evidence for any substantial component of volcanic detritus as in the tuffaceous marker beds. Signs of primary or early diagenetic dolomitic carbonates are also absent, which is an important difference to the described ore host lithologies for Mt Isa, Hilton, or HYC. Organic carbon is abundant, as both fine laminae and partings of seemingly originally incorporated algal material and as lamellae of pyrobitumen which appears to, at least in part, have been introduced as a mobile phase (Plates 13A-H, 21E; Chapter 5).

3.4.4 Massive Silty Mudstone Facies

Unit 4.2 is the characteristic example of this facies in the mineralisation sequence and is the most useful stratigraphic marker horizon in the deposit. Unit 4.2 is a dark grey- to black-coloured, single, massive silty-mudstone bed. Sedimentologically, it resembles the massive siltstone facies, but has some subtle differences. It has a component of coarse silt to very fine sand and is more micaceous. Very similar facies are present in a small interval of the upper footwall sequence, about 5-10m below the mineralisation. These are grey in colour, with some specimens showing irregular fronts of black staining by mobile organic matter (Plate 6A). The matrix of unit 4.2 is stained totally black, implying that at some stage it was completely invaded by fluids

carrying mobile organic material. Disseminated siderite (predominantly as small rhombic grains in the matrix) is quite common in this facies. Unit 4.2 is almost completely barren of sulphides apart from some rare disseminated galena and sphalerite and small transgressive veinlets.

Unit 4.2 shows systematic changes in thickness across the deposit from 1-2m in the north-west to 0.5-1m in the south-east (Fig.3.6). It may represent a distal fine-grained massflow sourced from the north or west. Mineralogically, the silty mudstone facies resembles the hanging wall sandstone more than it does any of the other facies and may represent a very distal low-energy equivalent to massive sandstone beds in this sequence. More work needs to be done on the sedimentary provenance of the ore host sequence.

3.4.5 Stratigraphic Analysis of Mineralisation Sequence

The overall sedimentary package at Century has good lateral continuity. Major units and facies packages can be distinguished in every structurally undisturbed drillhole, showing only gradual lateral changes over tens to several hundreds of metres. To illustrate this, some individual beds have been correlated, to show the scale of lateral thickness changes across the deposit. Specifically, these are the tuffaceous unit immediately overlying the mineralised sequence and the internal '4.2' marker unit within the mineralised sequence (Fig 3.4).

Thicknesses of each intersection of these units made within the deposit area were compiled from the deposit drillhole database (up to drillhole LH342), in the case of unit 4.2, and from core photographs and drillcore in the case of the tuffaceous marker bands. Thicknesses of the intervening stratigraphy between these two units were also recorded, together with the total hanging wall sequence from the base of the last massive sandstone to the top of the tuffaceous marker bands. Thicknesses were then dip-corrected to true stratigraphic thicknesses using core to bedding angles from the deposit geotechnical database. A final procedure was to rotate the coordinates of the drillhole intercepts from the northern block by 15 degrees anticlockwise to effectively close the gap created by the Pandora's Fault (Fig. 3.6).

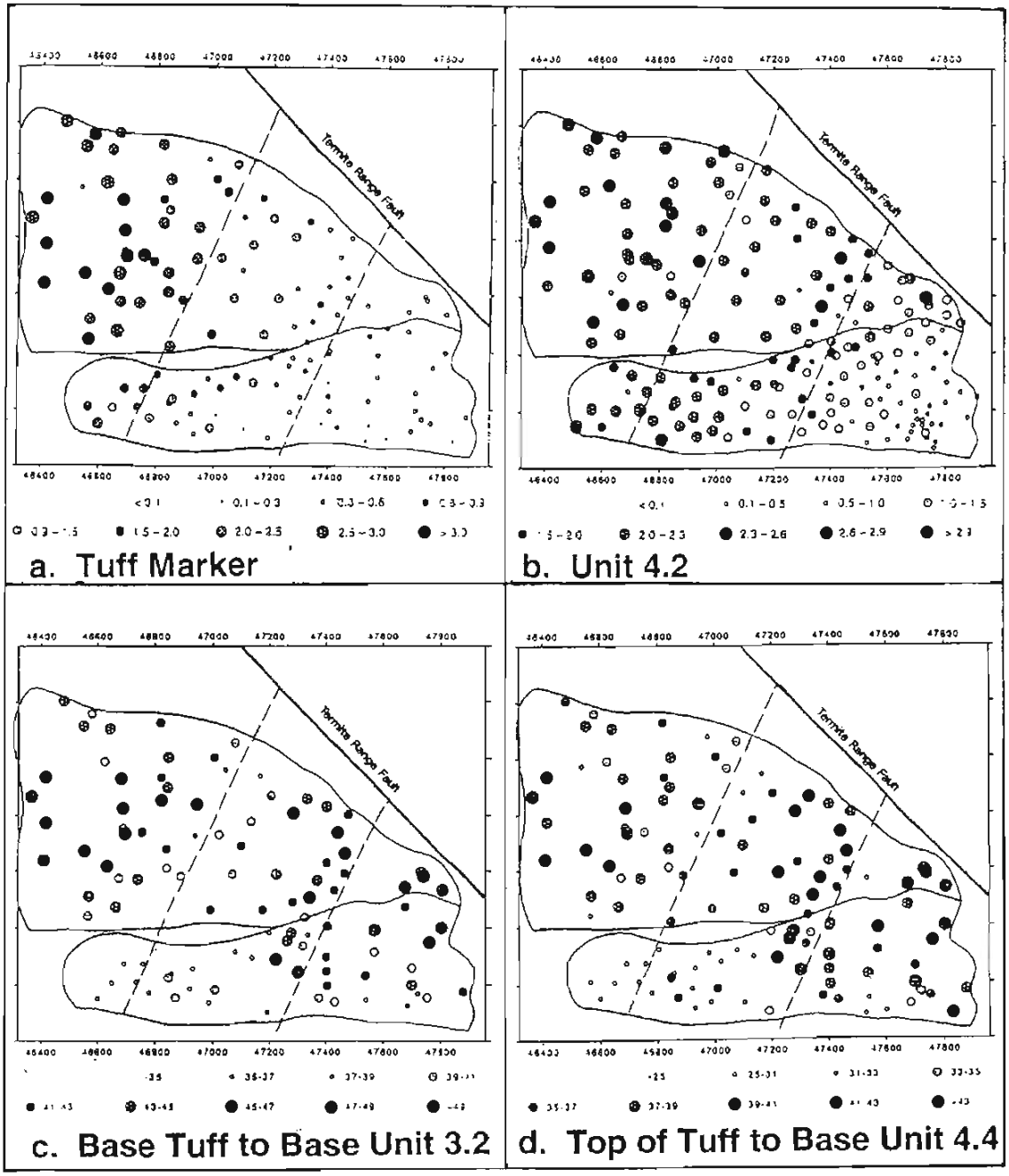

Figure 3.6 Dip corrected stratigraphic thicknesses - Century deposit. The southern block of the deposit has been rotated 15 degrees anticlockwise to close the apparent gap created by the separation on the Pandoras fault; thicknesses in metres.

Although many individual holes show anomalous departures due to later structural complications (folding, fault repetition, fault truncation), collectively, the data in Figure 3.6 show the following:

- The tuffaceous marker horizon shows a systematic decrease in thickness from west-north-west to east-south-east (Fig. 3.6). There are two linear discontinuities that strike north-north-east. These separate abrupt changes in average thickness

from greater than 1m in the north-western portion of the deposit to about 0.5m in the centre, with a further change from this 0.5m thickness to an average of 0.1m in the south-eastern third of the deposit.

- Unit 4.2 shows a sympathetic systematic change in thickness from ~1.5m in the north-west to ~0.5m in the south-east, but this is more gradual in nature, without the linear discontinuities evident in the tuffaceous marker horizon.

- The remainder of the sequence exclusive of these units show a consistent range of thickness from ~48m to ~55m. However, there are subtle north-north-east trending patterns of thickening and thinning, with the total thickness of the package varying by up to 5m across the linear changes within the tuffaceous marker bed.

In contrast to these observations in the (relatively) coarser grained facies, the laminated shale units, which are the important base-metal host rocks (Fig. 3.4), have relatively uniform thickness. This is exemplified by unit 4.3 (Fig. 3.7) which shows no systematic change in thickness across the deposit despite variation in total zinc grade from <1% to 25% (section 5.2).

The implications of these thickness variations are discussed further in section 3.7.2, after a brief description of the deposit footwall stratigraphy.

3.5 Footwall Sequence

The sedimentary beds become finer-grained progressively downwards from the base of the mineralised sequence, and the abundance and thicknesses of massive siltstone beds decreases. The basic sedimentological motif of the sequence remains similar. The amount of siderite alteration steadily decreases as massive siltstone facies become less abundant. Informally within the deposit, an upper and lower footwall sequence is defined by differing proportions of shale and siltstone and thickness variations in siltstone bands (Andrews and Stolz, 1991). Aggregate thickness of the footwall sequence is approx 180m, with the upper footwall being approx 50m of this.

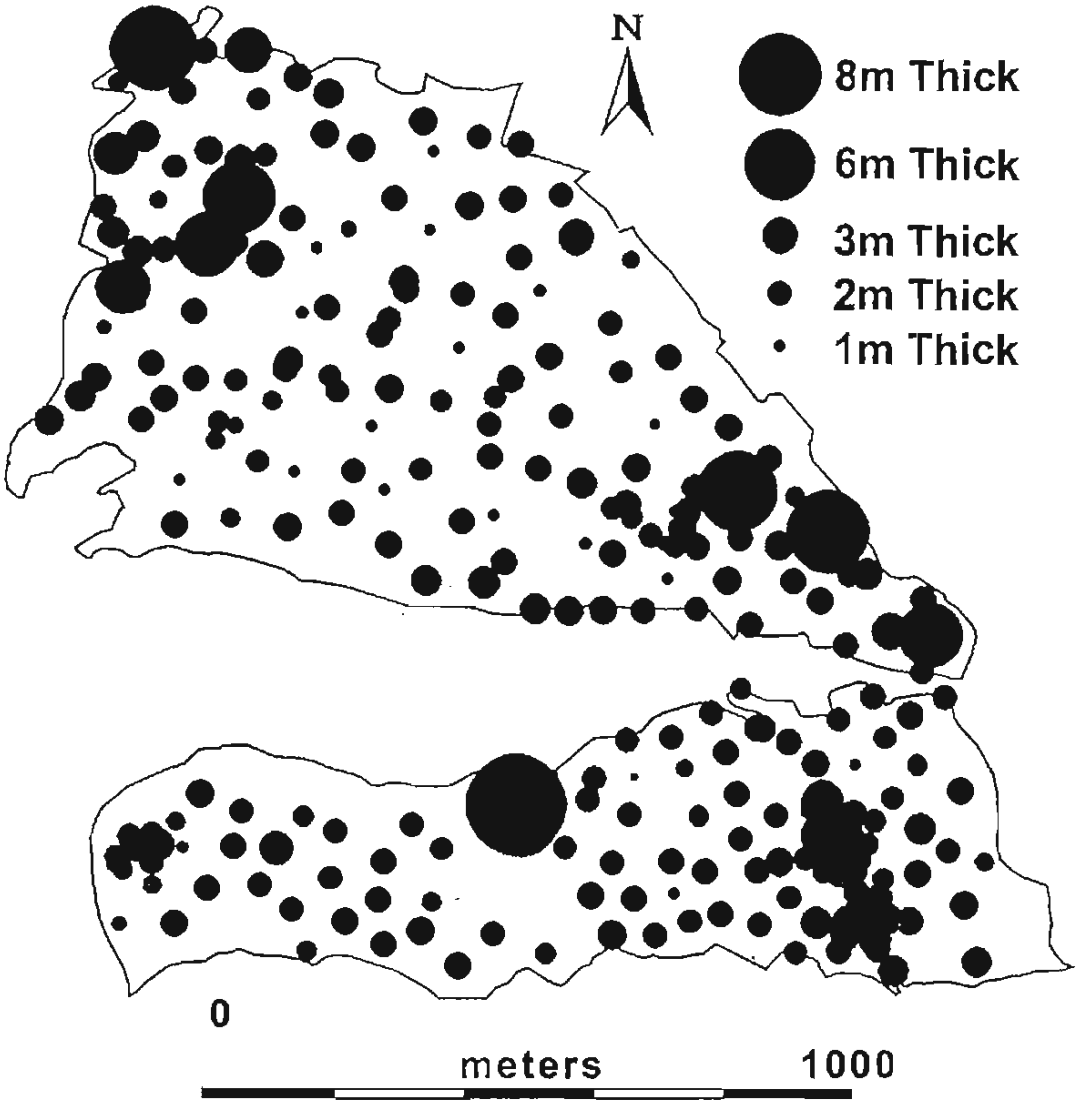

Figure 3.7 Mineralisation sequence - Unit 4.3 thickness plot. Drilled thicknesses have been corrected for dip, but otherwise represent raw data. Data show locally anomalous thicknesses created by thrust fault repetition or normal fault truncation, but overall the pattern is of a unit with uniform depositional thickness.

3.5.1 Upper Footwall Sequence

Sulphide abundance declines rather abruptly below the base of the mineralised sequence. However, depending on position within the deposit (section 5.2), traces of sphalerite, galena and pyrite occur for up to 30m below the high-grade mineralisation in some laminated shale beds. Minor amounts of pyrobitumen occur in fine lamellae and as fracture infills (Plate 6D). Stylolites abruptly disappear below the mineralised interval despite the sedimentary facies similarity.

A short stratigraphic interval with several similar beds to unit 4.2 (massive silty mudstone facies) is present immediately below the mineralised sequence in the upper footwall sequence. No detailed analysis of lateral thickness variations or correlations has been attempted, because relatively few holes fully intersect this zone, but it appears to be laterally persistent. In contrast to unit 4.2, these beds are pale grey in colour, without pervasive staining by organic material. They seem to be more abundant in the north west of the deposit, but this may only an artefact of increased drilling of the upper footwall rocks in this area. As mentioned above, in some specimens the siltstone beds show evidence for local invasion by mobile organic material (Plate 6A). In the south east of the deposit, massive siltstone beds in the upper footwall may have remained unrecognised because of pervasive staining by organic material. Below the zone with massive siltstone beds, the average thickness of siltstone interbeds progressively declines to a few centimetres. The footwall sequence becomes more thinly and regularly bedded, with increasing shale content downwards.

3.5.2 Lower Footwall Sequence

This sequence comprises finely laminated silt/mud facies, consisting of alternating grey silt and black shale beds (Plate 2G). The transition from the upper footwall sequence is gradational over several metres. Nodules filled with pyrobitumen and quartz (Plate 6C) are present below the transition zone and are viewed as diagnostic of the higher levels of the lower footwall sequence. The base of the lower footwall sequence passes relatively rapidly, but conformably, into the monotonous finely-laminated black shale of the middle and base of unit Pmh4. New whole-rock geochemical data indicate that the lower footwall sequence may have appreciable (up to 5%) authigenic dolomite cement (S. Tear, pers comm. of RTE unpublished data, 1998).

3.6 Deep Footwall Laminated Black Shale Sequence

Below the main footwall sequence, a very thick succession of monotonous finely laminated black shale occurs. These have abundant carbonaceous matter (up to 5% TOC from random analyses) and some zones are rich in pyrite. Base metal concentrations rarely exceed 100ppm, if assays from various regional drillholes that penetrate the unit are typical (RTE, unpublished data). Petrographically, the shale consists of very fine-grained clay- to silt-sized clastic silica with subordinate clays. Organic matter occurs in disseminated habit and also in compacted seams reminiscent of algal detritus (Andrews, 1998). The thicker lamellae of pyrobitumen noted in the mineralised sequence appear to be absent. The unit was probably deposited in a deeper water, more quiescent, setting to that of the overlying strata.

3.7 Discussion

The stratigraphic framework described above provides necessary boundary conditions for interpreting the Century mineralisation. Understanding the stratigraphy and geometry of the host rock package is fundamental to correctly interpreting patterns of metal distribution, geochemistry and textures of mineralisation.

Before the discovery of Century, major known zinc-lead orebodies were only known in the evaporite-rich Lower McNamara Group and its correlatives within the western Mount Isa Province and the McArthur Basin. Much attention was therefore placed on interpreting depositional environments in this context (e.g. Neudert and Russell, 1981; Muir, 1985). In some generalised ore genesis models for major deposits of the Mt Isa-McArthur province, evaporite-rich environments are regarded as fundamental to ore genesis (section 2.3). Stratigraphic observations from Century are discussed progressively in this section to show that this conclusion may not necessarily be appropriate.

There has long been a controversy between advocates of "syngenetic" versus "epigenetic" modes of origin of major "sediment hosted" ore deposits (e.g. contrast McGoldrick and Keays (1989) with Perkins (1997) interpretations of the Mt Isa

deposit). Virtually all strands of conceptual thought have the delivery of exotic metal carrying fluids to the ore deposit area as a necessary model ingredient, although interpretations of relative timing and depositional mechanisms vary greatly. It is well known in the oil industry that sediment porosity and permeability exerts a critical influence on timing and mechanisms of fluid transfer at all stages of basin evolution (e.g. Tissot and Welte, 1978). Considerable sophistication has been reached in hydrocarbon geology concerning the understanding of depositional environments and facies architecture as essential ingredients for developing conceptual fluid-transfer models (e.g. Oliver, 1986). Much remains to be learned about these issues in the field of base metal mineralisation, however. The following discussion attempts to bring together the foregoing observations in the context of both hydrocarbon geology and metal deposition processes.

3.7.1 Interpreted Depositional Environment

On the basis of the observations and discussion presented above, the following inferences can be made for the depositional environment of the Century stratigraphy:

- The thickness and lack of fine-grained facies within the Pmh5 hanging hall sandstone reflects a relatively sudden increase in sediment supply. A likely environment for the channelised turbiditic Pmh5 sands (Wright, 1992) is a progradational submarine fan, supplied by sediment from a deltaic and/or shallow marine source

- Several critical features of the hanging wall siltstone sequence are relevant to interpreting its depositional environment:

  - The abundance of the massive siltstone beds ('unifites') in the hanging wall sequence and their thickness ratio trends (Fig. 3.5).

  - The overall coarsening upward nature of the sequence.

- The locally thickened sequence and the relatively rapid thickness changes of the unifite beds within the immediate deposit area.

- These observations suggest that the hanging wall sequence originated as a lateral more-distal equivalent muddy-facies to the prograding sandy submarine-fan (Pmh5 facies). As the fan approached, the supply of coarser sediment steadily increased, giving the coarsening-upwards sequence.

- Most sedimentation occurred in a dynamic environment, below fair-weather wave base and largely below storm wave base, but possibly within the photic zone (120-200m?), as suggested by the following features:

  - The presence of deformed fragments of carbonaceous matter in the various thicker (presumably storm re-worked) silty beds ("unifites").

  - The good lateral stratigraphic continuity of the thick shale packages.

  - The lack of any facies indicating emergent conditions.

  - The possible *in situ* algal mat material in the more laminated shale facies.

- A depositional environment within a siliciclastic ramp-style depositional system (Fig. 2.6), within a middle- to outer-marine-shelf setting is indicated (e.g. studies by Myrow, 1992; Sami and Desrochers, 1992). If the organic material represents algal mats, the sedimentation may have been within the photic zone (Scheiber, 1989).

- In contrast to the siltstone beds, the uniform thickness (Fig. 3.7) and textures of the shale units indicates that they were most likely deposited in quiescent conditions, from suspension or from very low-energy density currents. Such a depositional environment may have been induced by either major transgressions in the basin, or extended periods of impoverished sediment supply.

Further work is required to constrain the lateral extent of these facies variations. The scale of major variations in ramp geometries would be of the order of tens to possibly hundreds of kilometres, with smaller local depocentres perhaps approaching the order of size of the mineralised system itself (2-10km). The possible significance of these scale variations with respect to conceptual mineralising processes is discussed in Chapter 6.

The interpreted environment of deposition contrasts markedly to that interpreted for other major base-metal deposits in the Mt Isa/ McArthur province. These have abundant carbonates, sulphates, pyrite and/or evidence of restricted near-shore evaporitic/anoxic environments (e.g. Neudert and Russell, 1981; Logan et al., 1990). Several popular genetic models for these deposits implicate these facies either as sources of sulphur, or indicative of periodic episodes of sulphide fixation in environments with restricted circulation (Williams, 1978; Neudert, 1983; Muir, 1985). It seems that these models are not really appropriate for the carbonate- and sulphate-poor, siliciclastic-rich Century host sequence. Sulphates are known in reduced deep-marine sediments (Seisser and Rogers, 1976; Corselli and Aghib, 1987) and also open-shelf marine sediments (Hashimi and Ambre, 1979). However, the resultant gypsum is texturally distinctive and unlike any of the textures in the Century ore zone. Implications for possible sulphur sources for the deposit are discussed further in Chapter 5.

3.7.2 Implications of Stratigraphic Thickness Variations

An idealised section of averaged sediment thickness perpendicular to the linear stratigraphic discontinuities (Fig. 3.1) is shown on Figure 3.8. It is postulated that the north-north-east striking changes in thickness in the mineralisation sequence itself are caused by the presence of original growth faults trending north-north-east. Alternative explanations could include the presence of intrafolial fold zones with relatively flat axial planes to create apparent local thickening trends within the mineralised sequence stratigraphy, or possibly shallow thrust repetition. Minor folds with north-east trends are indeed known in the deposit area (Chapter 4). However, structural explanations are not favoured because large-scale structural flexures or thrusts that could cause

systematic thickening over distances of 5-600m (Fig. 3.6) should be reflected by sympathetic changes in apparent thickness of both silt-rich and shale units. Deformation has indeed induced local thickness variations in shale beds (Fig. 3.7), but these are developed at much smaller scales than the overall stratigraphic variation shown in Figure 3.5. When the depositional characteristics of unifite beds (Stanley, 1981) and associated shale beds are considered, it seems more likely that the thickness variations within the siltstone units, unit 4.2 and the tuffaceous marker bed are more consistent with a small sedimentary depocentre. The growth faulting explanation is therefore more likely.

The pronounced "wedge" geometry of the hanging wall sequence deserves comment. The sequence thins from around 140m to about 80-100m from north-west to south-east (Figs 3.5B, 3.8). Stratigraphic thinning in some areas of the southern block may be tectonic, caused by bedding slippage during folding and rotation during movement on the Magazine Hill Fault. However, the trend is also present in the relatively undeformed northern block. It seems more likely that the overall change in thickness of the hanging wall sequence represents a genuine stratigraphic thinning over the width of the deposit. The nature of the reduction in thickness is interesting. From Figure 3.5A and Enclosure 1, it almost certainly relates to the larger siltstone interbeds being both fewer in number and thinner to the south-east, with the shale facies comprising relatively constant thickness "blankets". It is well known that many hydrocarbon traps occur in such "pinch-out" positions in conventional coarse-grained clastic reservoirs (e.g. Tissot and Welte, 1978), probably because the reduction in volume of more permeable facies simply acts to constrict lateral movement of fluids. Many positions of stratigraphic thinning appear to be controlled by classic growth fault-related "rollover" anticlines (e.g. Xiao and Suppe, 1992). A conceptual diagram showing lateral relationships within a fault-controlled roll-over anticlinal fold is presented as Figure 3.9. Such a geometry can only be inferred for Century, as insufficient data are available to the north-west and north-east of the deposit area. Figure 3.10 gives a reconstructed geometry of the preserved Century deposit area during upper Pmh4 sedimentation.

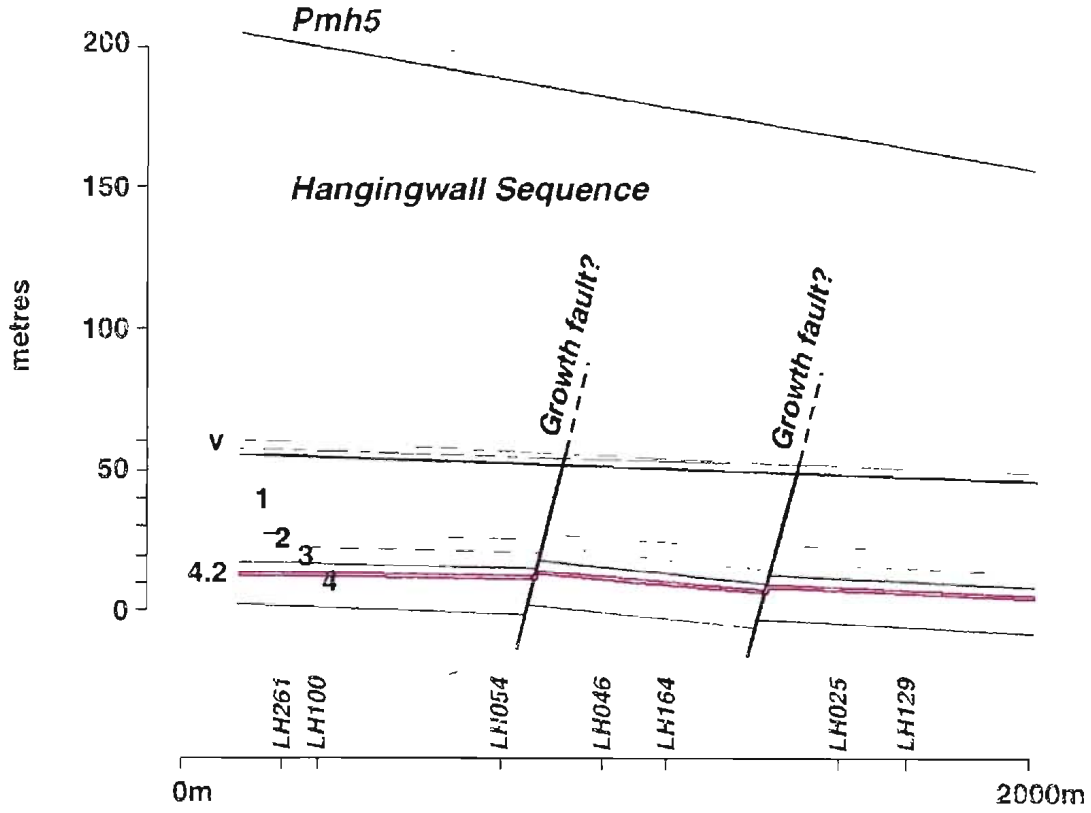

Figure 3.8 Century mineralised zone stratigraphy - generalised section of lateral thickness variations. The diagram has been constructed assuming a flat surface for the tuffaceous marker bed above the ore zone and then by taking average stratigraphic thicknesses above and below this in a west-north-west-east-south-east transect across the deposit. Local structural variations have been smoothed; approximate positions of critical drillholes (locations shown on Figure 3.1) on the transect are shown. Later faults such as the Pandora's Fault have been ignored. Probable small-scale growth fault locations are indicated.

Unfortunately, the lateral terminations of these stratigraphic patterns have all been removed in the deposit area. There is no way of re-constructing the actual dimensions of the interpreted fault controlled depocentre to take this analogy to a testable conclusion. However, it seems probable, in the context of the overall style of sedimentation, that it was not very large - perhaps only as big or slightly bigger than the area of the total ore system. Further to the south in the Lilydale area, the upper

Pmh4 maintains a constant thickness of 40-60m for distances greater than 10km, for example (Andrews, 1998).

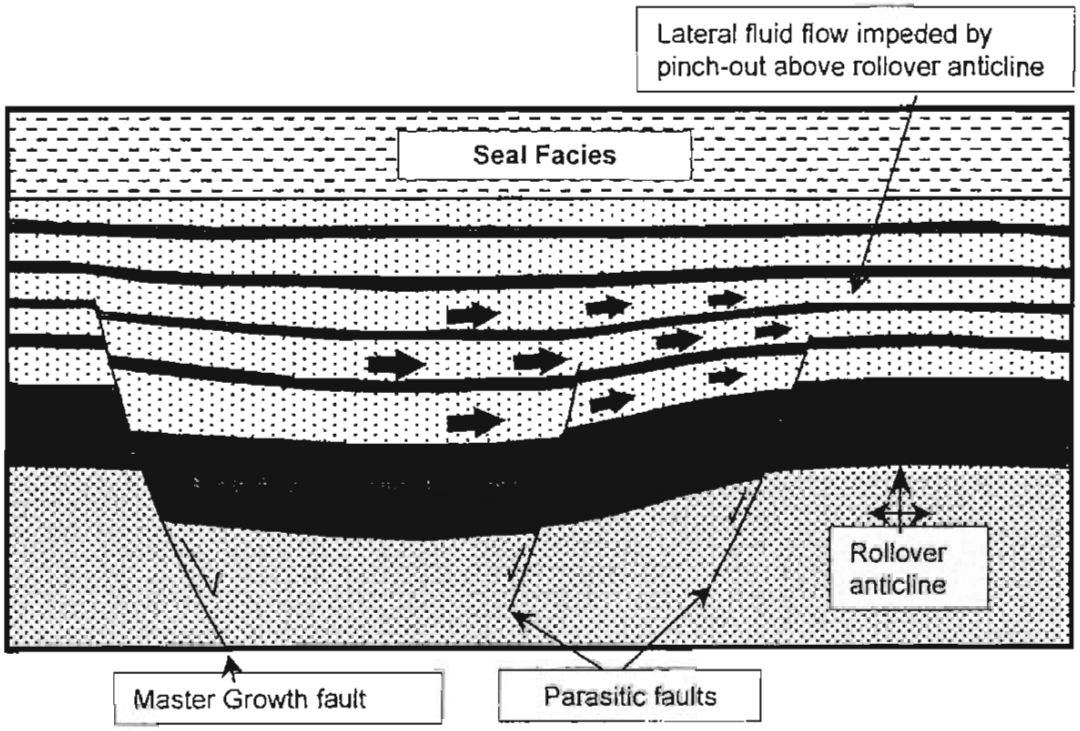

Figure 3.9 Schematic diagram of a rollover anticline with associated hanging-wall stratigraphic pinch-out. Thinned stratigraphy in the pinch-out impedes lateral fluid flow. Such a rollover structure could develop on minor growth faults parasitic to a larger displacement master growth fault (left). The deposit area is interpreted to have analogous geometry to the right hand portion of the diagram. This interpretation would require that a master growth fault would have existed to the north-west, outside the preserved deposit area. The local north-north-east growth fault trends at right angles to the Termite Range fault shown on Figure 3.10 are all that can be interpreted on available data.

It cannot be established from available data whether the Termite Range Fault was active at the time of deposition of the upper Pmh4 sediments. Unfortunately, no exposures stratigraphically above lower to middle Pmh4, well below the mineralisation sequence, are presently known east of the fault. Andrews (1998) has demonstrated that movement on the fault influenced deposition of the lower Lawn Hill and Riversleigh Formations. It seems possible that the small north-east growth faults could represent parasitic structures to minor syn-sedimentary movement on this larger structure in late Lawn Hill Formation time. However, the Termite Range Fault does not appear to have influenced deposition of the Termite Range Formation, so there must also have been periods when it was basically inactive. There are also important south to north

thickness changes in parts of the lower Lawn Hill Formation that implicate the existence of more east-west or east-north-east growth faults in the region to the north of Century, at least at that time (Andrews, 1998b). Until more data are available on detailed thickness trends within the upper Lawn Hill Formation at other localities than Century, questions of the large-scale growth fault architecture during deposition of the upper Pmh4 and Pmh5 must remain speculative.

The foregoing discussion concentrates on the important role of the coarser-grained silty facies in controlling the overall geometry of the total sediment package in the immediate orebody area. However this must not be confused with the equally important observation of lateral continuity and consistency of stratigraphic thickness of the laminated shale horizons (Fig. 3.7), which host most of the sulphide mineralisation. This is a crucial observation in the context of overall metal distribution and is discussed in detail in Chapter 5.

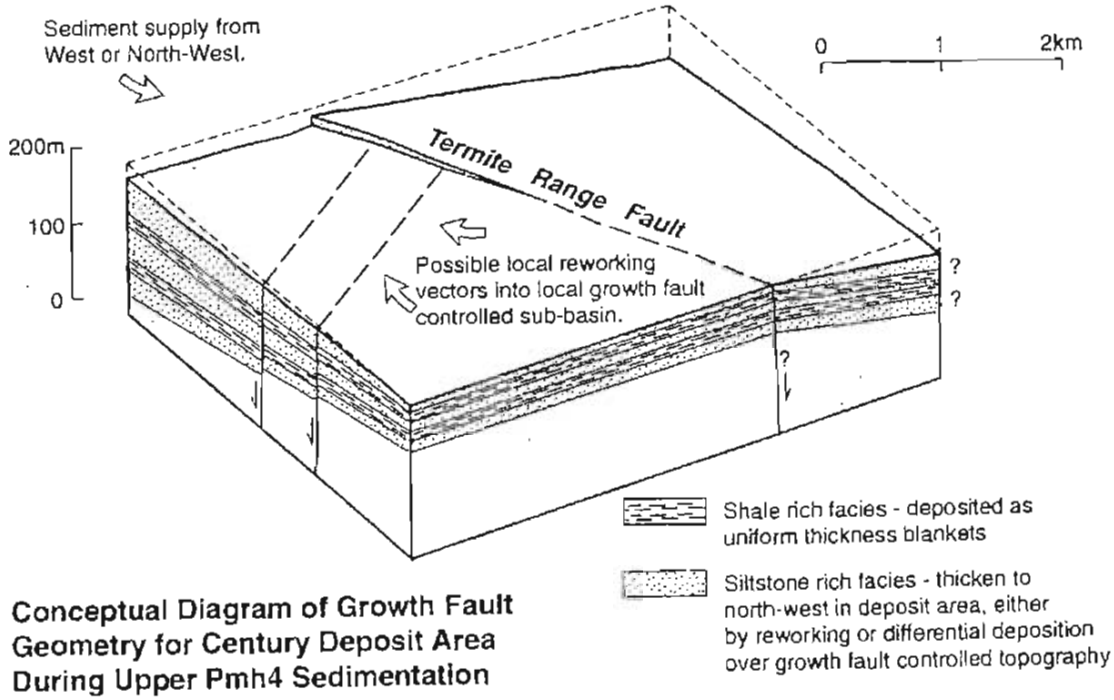

Figure 3.10 Diagrammatic representation of growth fault geometry for Century deposit area during upper Pmh4 sedimentation.

3.7.3 Stylolites and Solution Textures

Because of the intimate association of stylolites and solution features with mineralisation, a search of the literature for references to stylolite development in siliceous rocks was made. Surprisingly few references were found, with most literature concentrating on carbonate rocks (e.g. Prokopovich, 1952; Wanless, 1979, Simpson, 1985). The traditional view of stylolite development is that it is exclusively due to dissolution in response to applied compressive stresses (whether tectonic or compactional). A review of stylolite textures and their likely significance by Braithwaite (1988) concluded that, in contrast to this, some stylolites represent former open fluid-pathways developed in systems with high internal fluid pressures. Gundu Rao (1979) noted enhanced reservoir permeabilities to be associated with flasers and diagenetic compaction seams in carbonate rocks. Some workers have postulated that stylolite morphologies, traditionally interpreted as being due to pressure solution, originally developed as open fractures in internally overpressured sediments, with the irregular morphologies enhanced by collapse of sediment fabrics as pore fluid pressures declined. This idea was advanced by Prokopovich (1952) to explain vertical stylolites in fine-grained carbonates, but has been subsequently little remarked. Recent work in epithermal veins in the Drummond Basin has shown stylolitic fractures to be present in material of undoubted hydrothermal origin, without evidence of substantial later tectonic deformation (G Morrison, pers. comm., 1991).

At Century, areas of intense siderite deposition, hydrocarbon mobility and base-metal sulphide mineralisation appear to overlap the most intense development of stylolites. Stylolites rarely overprint early spheroidal siderite (Plate 8A). However, sulphide-siderite-hydrocarbon assemblages commonly overprint and infill both bedding-parallel stylolites and stylolitic fractures at high angles to bedding (Plates 7E, 7F; 12B, 12D, 13E, 13F, 13H, 19F, 21C, 21D). It may be argued that the hydrocarbon material (and, by extension, the sulphides and siderite) simply represents an insoluble residue concentrated after dissolution of silica from siltstone or shale beds. However, this does not explain clear overgrowth textures of the sulphides (Plates 13E, 21C, 21D), differential abundance of hydrocarbons and sulphides around and in stylolitic fractures (Plates 7F, 12D, 13F, 13H, 21E), or multiple overprinting relationships of sulphides

and hydrocarbons along high-angle stylolitic fractures (Plates 21E, 21G). These textures suggest that either appreciable movement of hydrothermal fluids has occurred along stylolites and high-angle stylolitic fractures during their development, or afterwards. The strong spatial coincidence of stylolite textures with mineralisation (and the apparent complete absence of stylolites in equivalent lithologies away from mineralisation), together with evidence for multiple overprinting, suggests that they may represent the remnants of formerly open fluid-filled fractures developed during main-stage mineralisation. Relationships at Century may therefore offer support for the previously cited, unconventional ideas of Prokopovich (1952) and Braithwaite (1988).

The interesting feature of the stylolitic surfaces at Century is that extensive dissolution of silica has occurred. Few detailed descriptions of the occurrence of stylolites in siliceous rocks are available, although many workers have noted diagenetic silica cements and overgrowths to be ubiquitous in clastic rocks. Increases in the intensity of diagenetic processes and the precipitation of siliceous pore cements in sandstone adjacent to shale contacts are well recognised as related to extensive silica mobility during burial diagenesis (Sullivan and McBride, 1991). Silica cements and overgrowths precede calcite and ankerite growth in the classic paper on burial diagenesis in sandstone by Boles and Franks (1979). At higher metamorphic grades, pressure solution of silica is ubiquitous during cleavage development in black carbonaceous shale (e.g. Wright and Platt, 1982). Enhanced dissolution of siliceous material in the more graphitic portions of shear zones has also been commonly recorded (e.g. Valenta, 1989a). In general, the carbonaceous material typically present in stylolites has been interpreted to be an insoluble residue, particularly at moderate to high temperatures where the stable residual phase of organic-rich material is graphite. However, at lower temperatures, reactions involving organic compounds may be profoundly important in other ways, influencing both metal and silica solubilities.

The formation of bedding-parallel stylolitic solution seams in sandstone was described by Lerbekmo and Platt (1962). They noted that solution of silica was increased in the vicinity of carbonaceous material and iron-bearing smectite phases. They suggested a mechanism involving the reduction of iron III derived from the breakdown of clay

minerals, in the presence of sulphur bearing organic phases, to produce pyrite and hydroxyl ions. The increase of alkalinity would promote the solution of silica. Fine-grained cherty or amorphous silica was noted to be more susceptible to solution than large crystalline grains.

McMahon et al. (1992) noted the problems of derivation of carbonate and pyrite cements and secondary porosity creation in sandstone at shallow burial depths. They concluded that the processes of microbial organic-acid production (by fermentation) and organic acid consumption (by sulphate or iron III reduction) were adequate to link the diagenesis of organic-rich clays to the production of 10% calcite cement, 0.1% pyrite and 1.5% porosity in sandstone. Carbonate was derived from the breakdown of organic acids, in particular acetate. Implicit in their scheme is extensive CO_2 production, which will promote weakly acid conditions by way of hydrolysis, producing carbonic acid (Fig. 3.11). Calcite dissolution or precipitation is possible depending on the bicarbonate buffering of such a system, but it is difficult to explain the dissolution of silica. Silica dissolution requires either extremely acid conditions, in which case the associated calcite pore cements would be unstable, or highly alkaline conditions, which are not compatible with CO_2 hydrolysis. Silica mobility is promoted by alkaline conditions (Dove and Rimstidt, 1994). Alkaline conditions are predicted by the reaction scheme of McMahon et al. (1992) if sulphate is available (Fig. 3.11). However, H_2S produced by sulphate reduction would react rapidly with any ferric iron derived from oxides or smectite breakdown, generating pyrite and acidity and, consequently, reducing the mobility of silica.

An integrated overview of burial diagenesis by Surdam et al. (1989) includes silica and alumina dissolution and reprecipitation related to organic acid creation and destruction as a normal burial process. They note that monofunctional and difunctional carboxylic acids have the capacity to complex aluminium directly, but do not specifically discuss mechanisms and conditions of silica mobility. Once again, implicit in their stated reactions involving sulphates and organic matter is the production of alkalinity by early reactions and the eventual production of acidity as the products of these early reactions re-equilibrate.

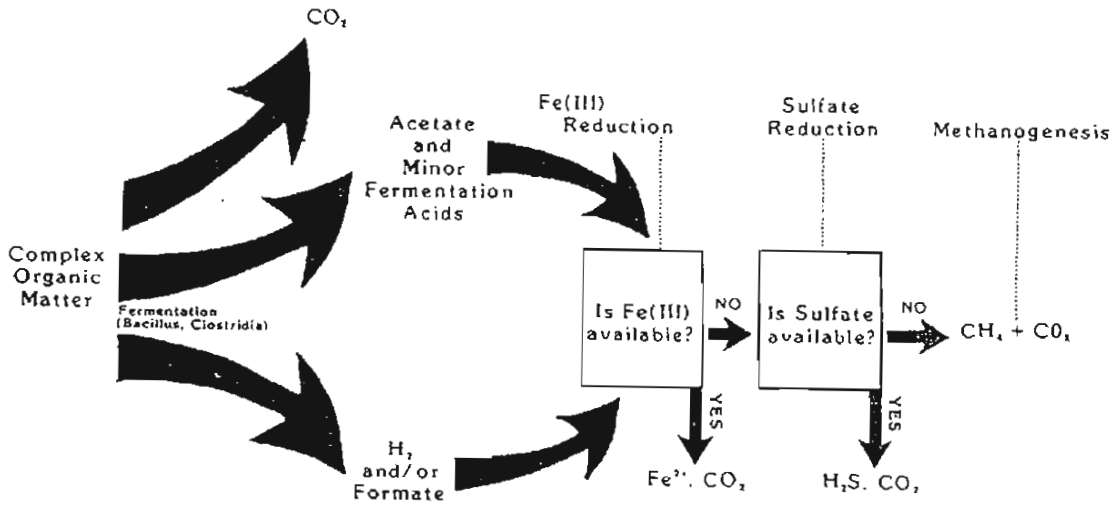

REACTIONS:

1. ACETATE FROM KEROGEN.

Thermocatalytic Cleavage of Carboxylic Acids from Kerogen

I.

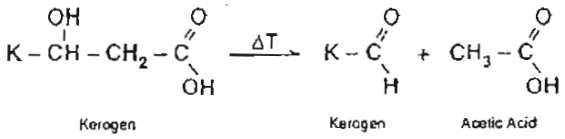

(From Surdam, 1989)

K - Indicates main kerogen molecule.

2. ACETATE DESTRUCTION.

A. Iron Reduction

$CH_3COO^- + 8Fe^{3+} + 2H_2O \Rightarrow 8Fe^{2+} + 2CO_2 + 7H^+$

B. Sulphate Reduction

$CH_3COOH + SO_4^{2-} \Rightarrow H_2S + 2HCO_3^-$

C. Thermal Decarboxylation (> 100 C)

$CH_3COOH \Rightarrow CH_4 + CO_2$

$CH_3COO^- + H_2O \Rightarrow CH_4 + HCO_3^-$

3. METHANE/SULPHATE REDUCTION.

$CH_4 + SO_4^{2-} \Rightarrow H_2S + HCO_3^- + OH^-$

Figure 3.11 Scheme for organic matter degradation and sulphur fixation in relation to carbonate generation and silica mobility (adapted from Surdam et al., 1989; McMahon et al., 1992).

Recent experimental studies have shown that carboxylic acids at modest temperatures (100°C) can cause appreciable dissolution of silica and aluminium from granitic sand in open system conditions (Reed and Hajash, 1992). It seems that, although much more work is required to define precise reactions, the involvement of organic phases can certainly be important in silica destructive and carbonate generative reactions (refer also the extensive work by Curtis, 1978; Curtis and Coleman, 1986).

The "self cancelling" nature of the reactions in relation to alkalinity and acidity generation is likely to promote the development of "feedback" style geochemical systems. Repeated local dissolution and reprecipitation of reaction products will be the most likely consequence of closed-system fluctuations in local diagenetic conditions.

At Century, this question has considerable implications for the observed extensive silica mobility, namely the early silica cements, the development of stylolites and the widespread replacement of silica by base-metal sulphides. The following reaction, although simple, does not appear to have been proposed in the literature in the context of diagenetic silica mobility, although it has been inferred to be an active process in modern marine sediments (Masuzawa et al., 1992) :

$$CH_4 + SO_4^{2-} \Rightarrow H_2S + HCO_3^- + OH^-$$

In applying this scheme to burial diagenesis, the methane could be derived either from fermentation at low temperatures (Curtis, 1978), or from the well-known inorganic processes of gas generation from organic matter or carboxylic acids at higher temperatures (Tissot and Welte, 1978). Sulphate would come from either residual pore fluids (shallow burial) or be introduced from elsewhere (deep burial). The main implications of the scheme are:

- that it can proceed without the presence of local ferric iron from either clay or haematite as an oxidant

- carbonate precipitation would be expected

- the reaction would only proceed if sulphate and methane abundances are high.

- it would create reaction products (alkalinity) which facilitate the subsequent dissolution of silica. This would be accomplished by the following reaction scheme:

$$SiO_2 + 2H_2O \Rightarrow H_4SiO_4 \quad \text{(Dove and Rimstidt, 1994)}$$

This is subject to the following dissociation reaction if the pH is sufficiently high to allow consumption of hydrogen ions:

$$H_4SiO4 \Rightarrow H_3SiO_4^- + H^+. \quad \text{(Dove and Rimstidt, 1994)}$$

In alkaline conditions, the above reactions can therefore be re-written in terms of OH^- to give a net reaction of:

$$SiO_2 + OH^- + H_2O \Rightarrow H_3SiO_4^-$$

The real life situation is one of considerable complexity. This proposal does not exclude other reactions documented in the literature, as many of them could probably be proceeding contemporaneously. However, it is worthy of consideration as a reasonably simple mechanism for explaining the development of many textural features. At shallow burial depths in sediments with low iron content, alkalinity created by reduction of pore water sulphate could catalyse extensive silica mobility because free H_2S would be lost from the system. Pore fluid alkalinity produced by breakdown of organic acids such as acetate could be a potent mechanism for catalysing silica mobility during deeper burial diagenesis.

A possible explanation for the selective confinement of stylolites to some laminated siltstone and organic-rich shale horizons within the mineralised zone at Century may therefore be that they have the following coincident factors:

- sufficient intrinsic organic material in black shale laminae to produce locally abundant organic acids and methane during burial/thermal processes.

- sedimentologically these shale bands in the favourable facies are juxtaposed directly against silica-rich material of very fine (silt to shale) grainsize, sufficiently fine grained to promote solution reactions by decay of organic acids.

Speculatively, access of a hypothetical sulphate-rich fluid phase along organic-rich horizons during deep burial could be an alternative way of developing pore fluid alkalinity, thereby promoting silica solution and stylolite development. This alternative would require a mechanism for the removal of free H_2S from the system.

3.7.4 Diagenetic Cements and Influence on Permeability

The rapid deposition of the Pmh5 sandstone as a prograding submarine-turbidite fan has significant implications for the possible development of under-compacted (and eventually overpressured?) zones in the underlying mudrocks of upper Pmh4. The emplacement of such a thick uniform sand body (Andrews, 1998) over sediments with high initial pore-water content could be expected to increase pore fluid pressure within the upper portions of the muddy sequence by simple gravitational loading. Normally, this would create accelerated de-watering of the mudrock by either vertical or lateral fluid movement (Cartwright, 1994). In areas with locally increased depositional thickness of mudrocks, such as the deposit area, there would be a correspondingly higher amount of pore fluid to be removed.

If there is appreciable vertical movement of pore fluids from the mudrock into the sandstone, compaction will initially proceed from the edges of the muddy section as fluid escapes into the more porous overlying sandstone beds. As time goes on, the reduced permeability of the de-watered boundary zone makes escape of fluid from lower down in the shale-rich stratigraphy more difficult. Additionally, there is a strong possibility that diagenetic cementation reactions will take place close to the contact

zone of the two facies (Boles and Franks, 1979). If the pore fluid from the shale is in chemical disequilibrium with the pore fluid in the sand, precipitation of new mineral phases will begin to hydrodynamically seal the two units from each other by blocking permeability in the sandstone aquifer. In the Century context, the operation of such cementation processes close to the Pmh5 sandstone contact would have the effect of progressively confining fluid within the underlying mud-rich Pmh4, thereby suppressing normal compactional-dewatering processes. In such a scenario, areas of locally thicker upper Pmh4 stratigraphy could therefore remain under-compacted relative to their thinner lateral equivalents.

The Pmh5 hanging-wall sandstone has experienced early cementation by chlorite and clays, sufficient to arrest the decay of detrital feldspars (Plates 3A, 3B). Most of this early cement appears to have been derived from the matrix of the sand itself. Cementation is pervasive and ubiquitous at regional scale (Andrews, 1998b). Early stage supply of solutes from the underlying shales could also have acted to reinforce the tendency of the Pmh5 to develop an impermeable cement matrix. It is argued that there is a good probability that the Pmh5 sandstone acted as a regional seal facies during burial diagenesis of the underlying sediments.

A direct consequence of this would be the probable development of overpressured conditions in the underlying mudrocks of the lower Lawn Hill Formation during later burial. Localised areas of overpressure could be expected to develop first in thicker (under-compacted) portions of the underlying mudrock stratigraphy and to persist in these areas for longer periods of time. The concept is shown in cartoon form in Figure 3.12.

One of the consequences of overpressure development is the local establishment of higher porosity and/or permeability conditions within overpressured compartments beneath the seal facies (Spencer, 1985; Hunt, 1990; Luo and Vasseur, 1992; Weedman et al., 1996). Movement of fluids at a regional scale beneath the overall seal could be focussed into such local environments. To the present authors' knowledge, this concept has not been advanced in the context of sediment-hosted base metal mineralisation processes.

3.7.5 Early Faults as Potential Fluid Conduits

It seems likely that north-east trending growth faulting influenced the deposition of the host sediments at Century, probably parasitic to the larger scale north-west trending Termite Range Fault. Such growth faults are often implicated as fluid conduits for "SEDEX" style genetic models (e.g. Large, 1980), and this possibility must be included among the spectrum of alternatives to be considered for the genesis of Century (Chapter 7).

However, once established, early fault trends are characteristically "recycled" during subsequent deformation and fluid transmission events (e.g. Cartwright, 1987, 1992; Sibson, 1994) and can function to deliver fluids at later times. They can therefore be equally inferred to be potentially important fluid conduits in epigenetic mineralisation models. In this context, the dominantly north-east orientation of the transgressive lodes of the Lawn Hill area (section 2.4) is particularly interesting. The lode mineralisation is interpreted by Bresser (1992) as being emplaced syn-tectonically with N-S striking folding that can be correlated with the regional D2-D3 events of the Isan Orogeny. One would expect that there would be a wider scatter of orientations of these faults if they had been initiated solely during the folding events, without being influenced by pre-existing weaknesses. It is possible that the predominant north-east orientation of the lode structures is the result of reactivation of a family of earlier, syn-depositional structures. In subsequent sections, isotope geochemistry and paragenetic relationships of the lode mineralisation in the Lawn Hill area are compared to those of Century.

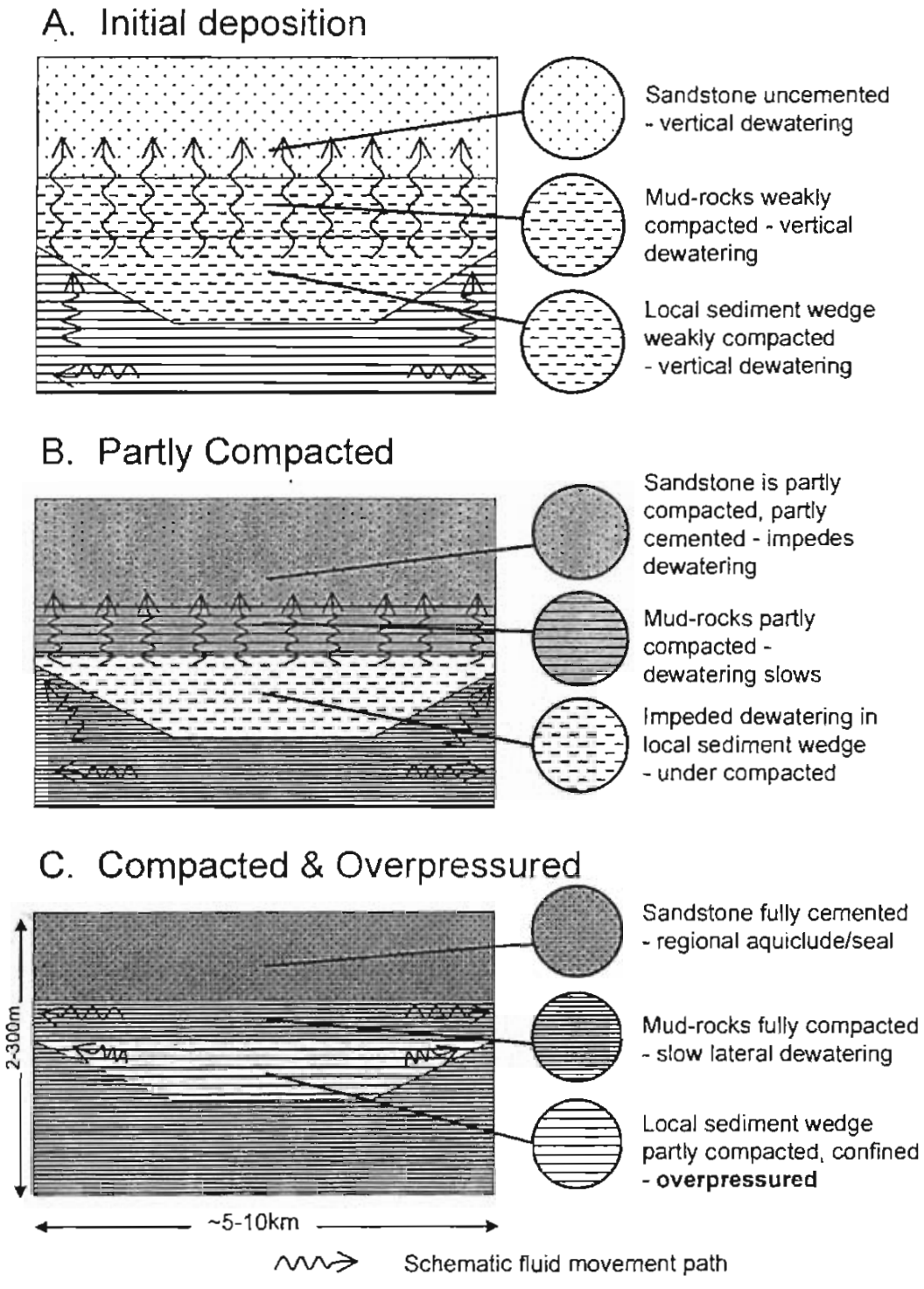

Figure 3.12 Cartoon of possible evolution of undercompacted/overpressured zones during burial evolution of a reactive sand:shale contact.

3.8 Summary

The host sequence to the Century deposit differs from the well-documented Mount Isa and HYC orebodies in that it is hosted by deeper water siliciclastic deposits rather than shallow water carbonate or evaporite-rich lithologies.

There are no barium- or silicate-rich sedimentary rocks suggestive of exhalite facies anywhere in the deposit stratigraphy, the hanging wall stratigraphy, or the footwall sequence. Any genetic model must account for this absence.

Most sedimentation occurred in a dynamic environment, below fairweather wave base and largely below storm wave base, but possibly within the photic zone (120-200m?). The coarsening upwards nature of the hanging wall sequence suggest that it originated as a lateral more-distal equivalent muddy-facies to a prograding sandy submarine-fan (Pmh5 facies). Overall sediment supply was likely to have been from the west or north-west.

The thickness changes within the deposit area suggest that Century was a possible local structurally-controlled sub-basin with active north-east trending growth faulting during the progradational event. This sedimentary depocentre was probably of comparable dimensions to the mineralisation system, and this factor must also be considered in any genetic model for the mineralisation (Chapter 6).

Rapid loading by the Pmh5 sandstone, in combination with the locally increased thickness of the underlying mud-rich sediments, could have created a discrete under-compacted compartment of sediment in the deposit area during earliest burial and compaction. Also, the Pmh5 sandstone was extensively cemented by chlorite and clays during early diagenesis. It is proposed that this caused it to become a regionally extensive seal during later burial diagenesis, giving a high probability that overpressured conditions would develop regionally in at least some of the underlying mud-dominated units of the Lawn Hill Formation during progressively deeper burial.

Distinctive solution and cementation textures indicate the early diagenetic history in the hanging wall and mineralisation sequences to be complex, but apparently controlled by the interaction of organic-rich material in the shale facies and silicates in the adjacent organic-poor siltstone facies. Organic acid breakdown during deeper diagenesis and possibly hydrothermal activity would contribute reactants that could have materially contributed to silica solution processes and both carbonate and silica cementation.

The coincidence of the dominantly north-east orientation of the transgressive lodes of the Lawn Hill area (Bresser, 1992) with the early growth faulting at Century needs to be further examined. It is inferred that reactivated early fault structures have functioned as fluid conduits for base metal mineralisation in at least the late stage history of the area. The question of whether lode mineralisation was related to the Century mineralisation is further examined in later sections.

The combination of all of these possible processes indicates an environment of considerable complexity surrounding the area of mineralisation. Interesting issues of sediment geometry and supply, structural geometry and localised anomalous sediment textures require to be integrated in any genetic model. Subsequent chapters consider detailed aspects of these issues in relation to base metal distribution and timing.

Chapter 4
Structure

4.1 Introduction

This Chapter presents structural observations of various fabrics in the Century mineralisation, made from drill core and the limited outcrops available. Broad timing of the mineralisation emplacement at Century is then established relative to the major deformational events of the Lawn Hill region. This, in turn, enables a correlation with the regional deformation history of the Upper McNamara Group (Isan Orogeny; Chapter 2).

One of the difficulties in making structural observations at Century lies in the lack of outcrop and underground exposures and the preponderance of vertical drillholes without oriented drill core. The only areas for direct observation were the weathered exposure at Discovery Hill (now substantially removed by trial mining) and limited faces created during the sinking of an exploration shaft during 1992. The shaft is now flooded and not available for further examination. Approximately 100 metres of driving was done from the shaft and obvious structural features from these exposures were recorded (Appendix 7). Oriented samples were also collected for future microstructural work (Appendix 1). Samples are stored in the James Cook University collection.

These exposures only represent a fraction of the area of the orebody and are biased insofar as they only represent the southern block of mineralisation. To gain structural data over a wider area of the orebody, the magnitude of the dip of the surrounding beds and its direction were estimated from the structural contours of the 3.2 marker horizon at various locations. Calculations of orientations of macroscopic structural features were then made from the appropriate vertical drillholes, using the assumed orientation of bedding surfaces to orient the core. The assumed dips used to control measurements have been recorded with the observations of the various structural fabrics in Appendix 7.

It is acknowledged that this approach will lead to some scatter in results. Bedding surfaces will not have uniform directions vertically throughout the drillhole, and some assumed orientations will be wrong due to unforeseen local structural complications. Structurally complex areas, such as the immediate vicinity of major faults, were therefore avoided. Although the orientations of measured features are therefore slightly imprecise, the data should be sufficiently accurate for a general interpretation to be made because of the good stratigraphic control in the mineralised sequence. Future more comprehensive structural work will be required to verify the preliminary conclusions made in this study.

4.2 Macroscopic Geometry

The overall structure and boundaries of the mineralisation are described above (Chapter 3, Figs. 3.1, 3.2, 3.3). Structural contours for the base of unit 3.2 at 10 metre intervals relative to the deposit datum are shown on Figure 4.1. The most striking feature on this diagram, apart from the separation between the northern and southern blocks induced by the Pandora's Fault, is the steep north-south striking upturn of bedding on the western side of the northern block. This upturn and the northerly striking minor anticline in the vicinity of the shaft site are parallel to the axis of the major Pages Creek syncline (Fig. 2.3).

The Pandora's and Magazine Hill faults offset and postdate the main north-south fold axes, so a structure contour map was prepared for a pre-Pandora's Fault geometry (Fig. 4.2). Some distortion of the pre-fault geometry is still evident because of the presence of numerous small displacement faults that have not been compensated for. These are visible as irregular closures and subtle discontinuities in the contours. Some rotation of the southern block relative to the northern block has probably occurred because of the differing dips and relative displacements of the Pandora's and Magazine Hill fault planes. Nonetheless, the exercise clarifies the apparent original fold geometry.

The south-plunging fold geometry noted above is present in the reconstructed data (Fig 4.2) and is consistent with the position of the deposit along strike from the Pages Creek syncline. However, an overall east-north-easterly strike and south-south-easterly dip to

the sequence is also clearly evident. This direction is similar in strike to the sedimentological and possible early growth fault or structural trends discussed in section 3.7.2 (Figs. 3.8, 3.10). It is suggested that two structural fabric orientations are present in the deposit area, with an earlier subtle north-east trending fold direction being overprinted by later more pronounced north-south folding.

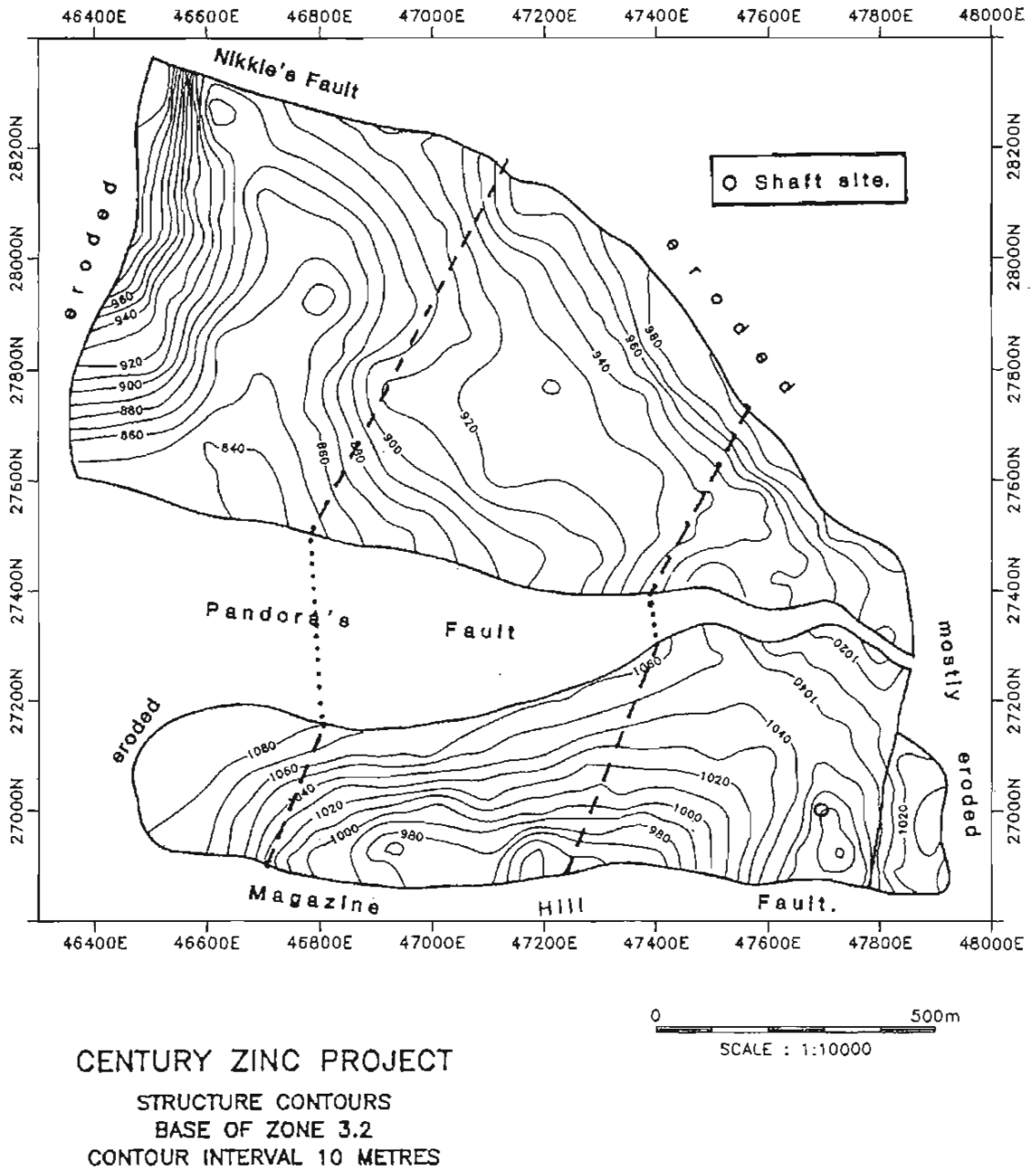

Figure 4.1 Century deposit. Structural contours of base unit 3.2; 10m intervals. (Datum is Australian Map Grid surface elevation plus 1000 metres)

In the following sections other meso- and macroscopic structural features within the deposit are examined for their consistency with this concept before the structural evolution of the deposit area is considered in section 4.7. Plates 17-21 illustrate most of the features discussed in the text.

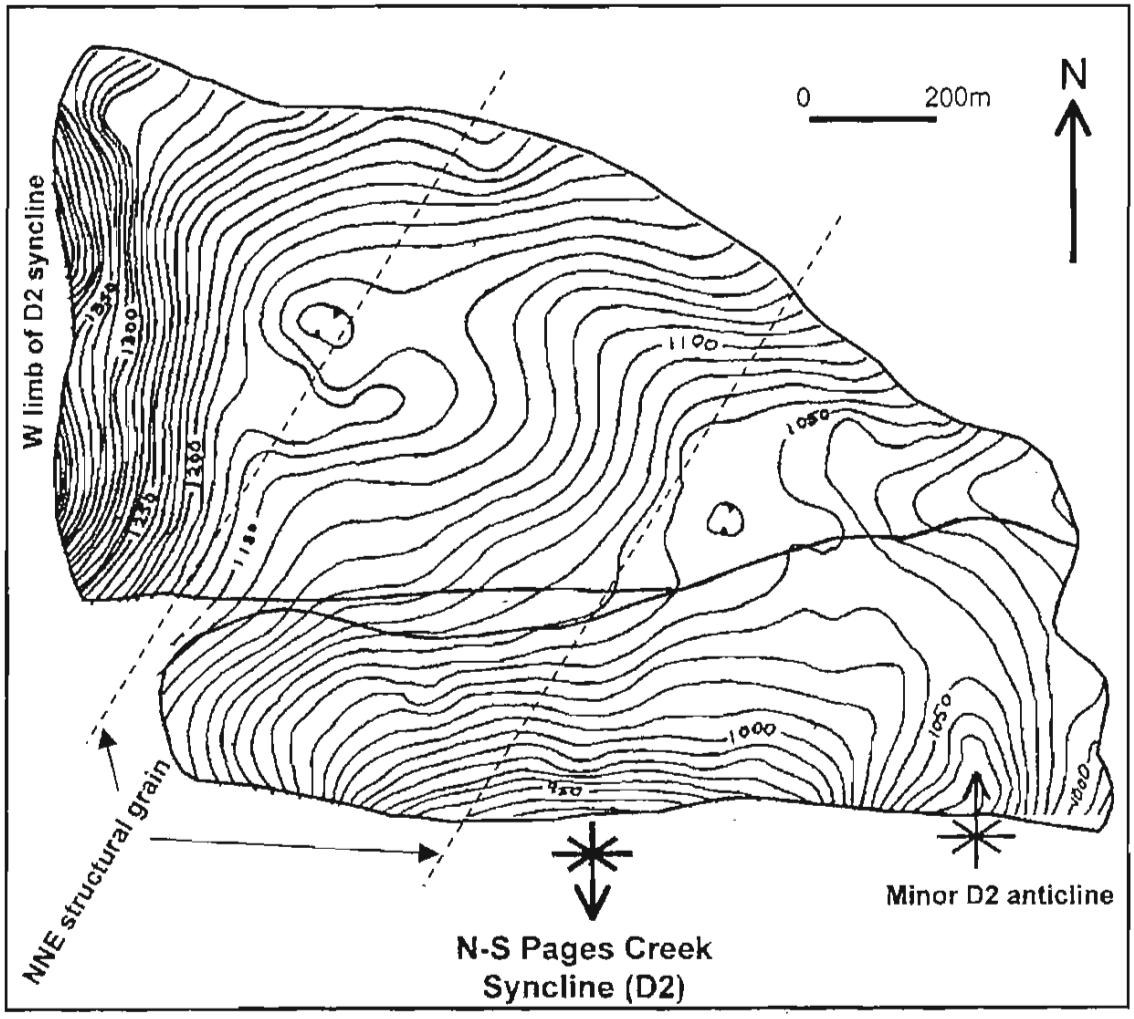

Figure 4.2 Century deposit. Structure contours of base of unit 3.2 for a pre-Pandora's Fault geometry. Rotational displacement along the Pandora's Fault was corrected for by counter-rotating the heights of the base of unit 3.2 in the northern block 15 degrees anticlockwise about a pole at right angles to the fault plane on the extreme eastern edge of the orebody. This point is where the displacement of the fault is inferred to be zero. The resultant heights were contoured at 10m intervals.

4.3 Early Deformational Fabrics

The earliest hand specimen-scale deformational features visible in the mineralisation sequence and hanging wall sequences are small intrafolial "glide" folds and poorly defined shears at low angles to bedding. These are often overprinted and truncated by later brittle fractures (Plates 18A, 18F, 18E; 17E; 11A, 11C, 11E, 11H).

Axial surfaces to many of the small folds lie at low angles to bedding. Some are overprinted by dissolution/compaction fabrics (Plate 4A). These folds are inferred to have developed during compaction and diagenesis. There is clear evidence for overprinting and replacement of the compactional fabrics by siderite and all sulphide species and generations (Plates 18E; 21A; 9F, 9H). Within a single hand specimen individual fold geometries often have opposing symmetries (Plates 11A, 11C). Piercement structures into the enclosing sediment lamellae (Plate 18A) are common, also with superimposed compactional features. Mesoscopically-similar small conjugate folds surrounding siderite nodules are relatively common (Plate 17B), but have an uncertain relationship to compaction. These are asymmetrical, because they are overprinted by later more brittle folding and shearing (Plate 17C).

Available data on the orientations of axial planes to small-scale folds are plotted stereographically on Figure 4.3A. Strike directions of the glide fold axes are plotted as a rose diagram on Figure 4.4A. The fold axes have a preferred orientation at around $N30^0E$, aligned with the trends in variations in stratigraphic thickness discussed above (Figs. 3.8C and 3.8D). This preferred axial orientation could be a product of either slumping (e.g. Miyata, 1990) or early tectonism (Elliot and Williams, 1988; Maltman, 1984, 1988).

The axial planes of the glide folds are flat lying (Fig. 4.3A), sub-parallel to the bedding and have been rotated by the later north-south folding. The low-angle compactional/solution fabrics associated with the folds have a weakly penetrative character through compacted sediment fabrics (Plates 18B; 4C, 4D, 4F). This may indicate that development of these fabrics occurred at burial depths greater than 100 metres (Elliott and Williams, 1988; also see section 5.4).

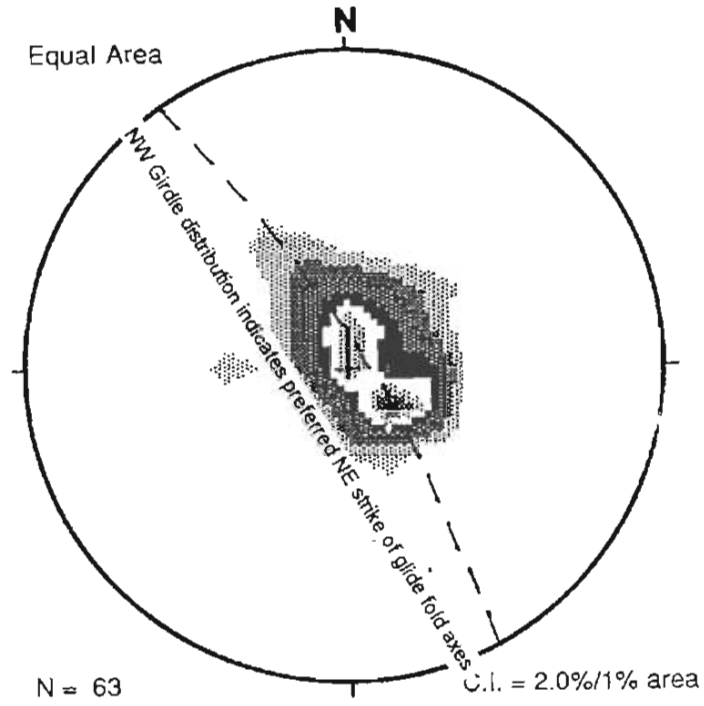

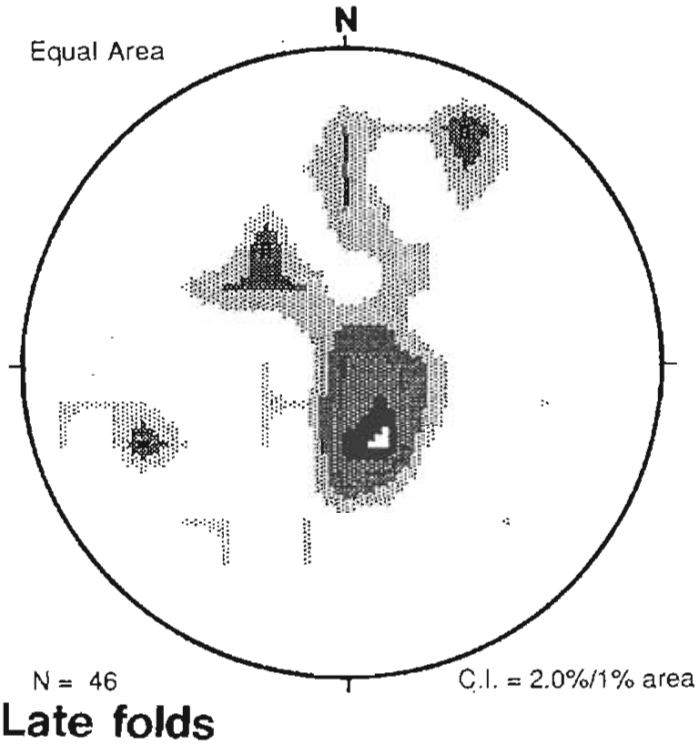

Figure 4.3 Century deposit. Stereoplots of poles to early- and late- small-scale fold axial planes.

Two interpretations of the genesis of these folds are possible;

- early tectonism or sediment gliding (possibly related to growth faulting) may have induced slump and fold structures which have then been a focus for later deformation, possibly in under-compacted/overpressured conditions.

- later tectonism in under-compacted or overpressured sediments, producing shallow-dipping fold axial planes with north-east to north-north-east trending fold axes.

These interpretations cannot be easily separated on textural grounds alone, because of the similarity of the mechanical state of the sediments in either case. The first interpretation implies that the small-scale deformation fabrics were initiated early in the sedimentation history and were then overprinted by a later south-east to north-west fold event of unknown age. The second interpretation implies that deformation occurred much later, independently of sedimentation. As a possible analogue, Roehl (1981) and Redwine (1981) document mesoscopically similar intrafolial folds with flat-lying axial planes from overpressured shale environments in the Monterey Formation.

A kinematic reconstruction of the Lawn Hill region has been made by Flottmann (1996). Based on mapped geology and overprinting fabric relationships, Flottmann (1996) argues for an initial phase of mild east-west shortening, followed by a south-east to north-west episode of folding, which is, in turn, followed by east-west shortening. Based on their strike orientation, the Century intrafolial folds could be correlated with the second deformation event in Flottmann's (1996) scheme.

The first interpretation, involving early sediment flowage followed by later reactivation, is preferred for the following reasons:

1. The deformation appears intrafolial, being confined to narrow zones within individual beds. There seem to be compensatory zones of extensional and compressional deformation along individual beds, giving rise to local thickness

variations up to 25% in individual units (e.g. Fig 3.7). Both extensional and compressional types of deformation appear to be overprinted by later compactional and solution fabrics (Plates 4A, 4B).

2. The changes in thickness of the sedimentary sequence across the north-north-east trending discontinuities (Figs. 3.8, 3.10) are more consistent with early growth faulting.

3. There should be more consistent trends in symmetries of the individual small folds if a penetrative shear event was involved in producing the thickening trends in the stratigraphy.

If Flottmann's (1996) interpretation of the structural sequence is correct, the mid-stage south-east to north-west regional shortening would logically have acted to re-activate early structures. The two phases of east-west shortening would have had the effect of causing some of the scatter in fabric orientations. Further structural work to resolve this fascinating question awaits the creation of three-dimensional exposures by mining, to better integrate the detailed textures of the small-scale folds with mesoscopic structures.

4.4 Siderite Nodules

Siderite in the mineralisation sequence commonly occurs in nodules or concretions up to 20cm across (section 5.3.2). Geometry of these bodies ranges from almost spherical to elongate shapes reminiscent of French bread sticks. Many of the elongate bodies (Plates 17B, 17D, 17F;) display compactional and rotational effects around their terminations (Plates 18C, 18D; 5C, 5E, 5G), and, in some cases, small-scale deformation structures develop in the enclosing beds (Plates 17B, 17C; 19B). These may take the form of conjugate folds (Plate 17C), or pinch and swell structures (Plates 17B; 18C, 17D). Asymmetric development of stylolitic surfaces and siderite growth in the stylolitic siltstone facies is a related phenomenon (Plate 18B).

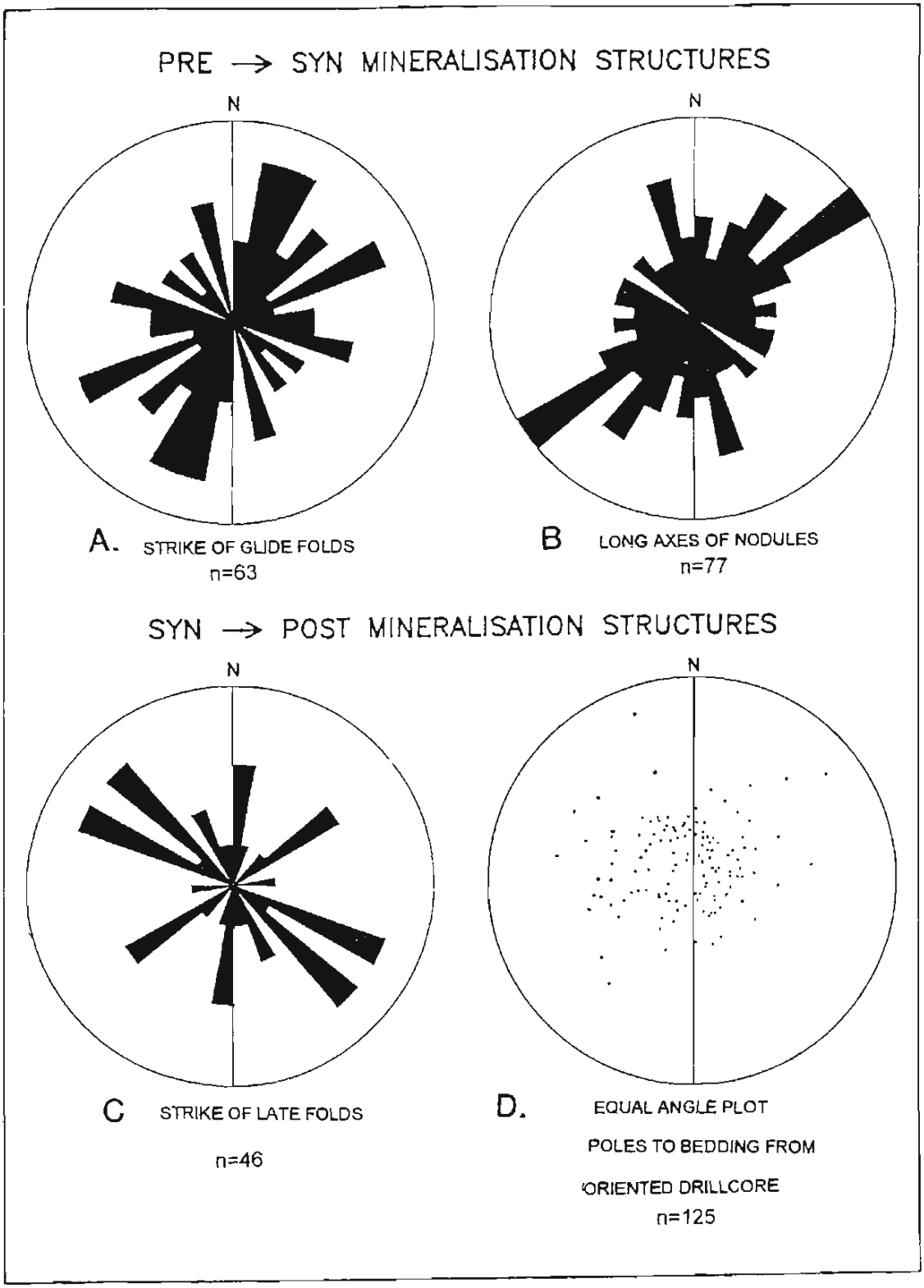

Figure 4.4 Century deposit. Rose diagrams of structural features and poles to bedding planes.

Early fold or dislocation structures and related compaction features in surrounding beds are sometimes overprinted by disseminated siderite aggregates (Plates 18A, 18G).

When the axes of elongation of the nodules are plotted on a rose diagram (Fig. 4.4B), a north-east trending preferred orientation is evident. The siderite nodules preserve less compacted sedimentary beds (Plates 18C, 18D). Whether the nodules have grown early in the compaction history or have grown in under-compacted sediment in later time is discussed in Chapter 5. Their preferred orientation may be caused either by early tectonism or sediment movement influencing growth, or growth being nucleated on primary sedimentary fabrics (Colton, 1967). Some specimens do give the impression that they preserve sediment cross-lamination (Plate 5H), but these occur too rarely to get sufficient data to establish any statistical orientation.

The preferred orientation of siderite nodules is sufficiently close to the strike of the early fold axes to suggest that they are related features. The elongate nodule geometries can be considered analogous to boudin structures. The other peaks on the rose diagram may therefore indicate fabric elongations analogous to 'chocolate tablet' terminations (Ramsay and Huber, 1987).

Siderite nodules are cut by pyrobitumen veins, and pore space in the nodules is commonly infilled by mobile pyrobitumen. Pyrobitumen is, in turn, partly replaced by sphalerite. Timing relationships of these features are more fully described in section 5.3.2 and further discussed in section 5.4.

4.5 Early Stylolitic Fractures

Early stylolitic fractures are ubiquitous throughout the mineralisation. In hand specimen, they are difficult to detect in black shale facies, but are easily visible microscopically (Plates 19B, 19C, 19D, 19F). In hand specimen, in the siltstone beds, stratabound stylolitic fractures have sinuous margins and high pyrobitumen content. These may die out at bedding plane boundaries or else refract laterally into bedding-parallel stylolites. Where observed in polished section, high-angle stylolites are characteristically filled with sphalerite, galena and pyrobitumen (Plates 19B, 19C, 19D,

19F). They display variable angles to bedding and mostly terminate against layer-parallel stylolites bounding siltstone beds, or bituminous seams in shale. The apparent lack of consistency in overprinting relationships between high-angle stylolitic fractures and layer-parallel stylolites is interpreted as evidence that they are co-genetic. Both stylolites and stylolitic fractures contain similar mineralisation infill (Plates 21C, 21D, 21E, 21F, 21G). They are commonly cut by later brittle fractures (section 4.6, Chapter 5) and overprinted by later fracture and breccia mineralisation (Plate 21H).

Early stylolitic fractures seem for the most part to post-date disseminated siderite deposition (Plate 19B). In many specimens layer-parallel sulphide and hydrocarbon mineralisation decreases in intensity away from stylolitic fractures, suggesting they may have acted as micro-scale fluid conduits during early-stage mineralisation (Plates 21E; 15B, 15E, 15F, 15G; 13F, 13H). Stylolitic fractures closely resemble some styles of hydraulic fractures documented by Kulander et al. (1990). They are considered as good evidence for the existence of overpressure within the sediments during pyrobitumen mobility and at least some sulphide mineralisation. Insufficient data exist to determine whether early high-angle stylolitic fractures have any systematic orientation relative to early versus late folds. This potentially important relationship requires further micro-structural analysis, as it could provide insights into the directions of far-field stresses during mineralisation development.

4.6 Late Shears and Fractures

Brittle fractures, with sharp contacts, are ubiquitous throughout the mineralisation ('crackle' mineralisation; Plate 20). These are partly to completely infilled with quartz, pyrobitumen, sphalerite, siderite, galena and pyrite. Petrography is described in Chapter 5 and sulphur isotopic values in section 6.4. In hand specimen and thin section (sections 5.3.8, 5.3.9), brittle fractures truncate and disrupt earlier-formed layer-parallel sulphides. There appears to be a continuous progression of geometrically similar mineralised veinlets to virtually unmineralised small-scale late shears and breccia zones.

When the orientations of these shears are plotted stereographically, a wide scatter of directions is apparent (Fig. 4.5A), with no apparent preferred orientation for either mineralised or unmineralised varieties. The plot of raw bedding data shown on Figure 4.4D shows a similarly scattered distribution. During core logging and outcrop mapping it was noticed that the late shears and 'crackles' predominantly intersect bedding at high angles. Orientations of the fractures were therefore rotated to an assumed constant bedding-plane orientation to determine whether this impression was statistically correct. Figure 4.5B shows the result for the poles to the fracture surfaces relative to an assumed constant bedding-surface dipping 30^0 to true north. A definite girdle distribution around the hypothetical bedding surface is present, indicating that many fractures indeed occur at high angles to bedding. An equal distribution of mineralised and unmineralised fractures occurs within and outside the girdle.

This can be interpreted to indicate that the brittle fractures are, for the most part, a systematic set of extension fractures developed during a major late folding event. Since from section 4.2 the major folding geometry is represented by the north-south striking Pages Creek fold structure, these systematic brittle fractures are therefore almost certainly linked to this event.

The brittle fractures truncate and overprint earlier-formed fold and concretionary structures, layer-parallel sphalerite and stylolitic fractures. The vein mineralisation within them is therefore timed quite specifically to the period between the establishment of early north-north-east trending folds and siderite nodules (hereafter called "D1") and the onset of conditions suitable for brittle fracture during the north-south fold deformation (hereafter called "D2"). Most layer-parallel mineralisation shows evidence of being overprinted by the late brittle fracturing, and can therefore be construed to have been partly folded and deformed D2 north-south folding. However,

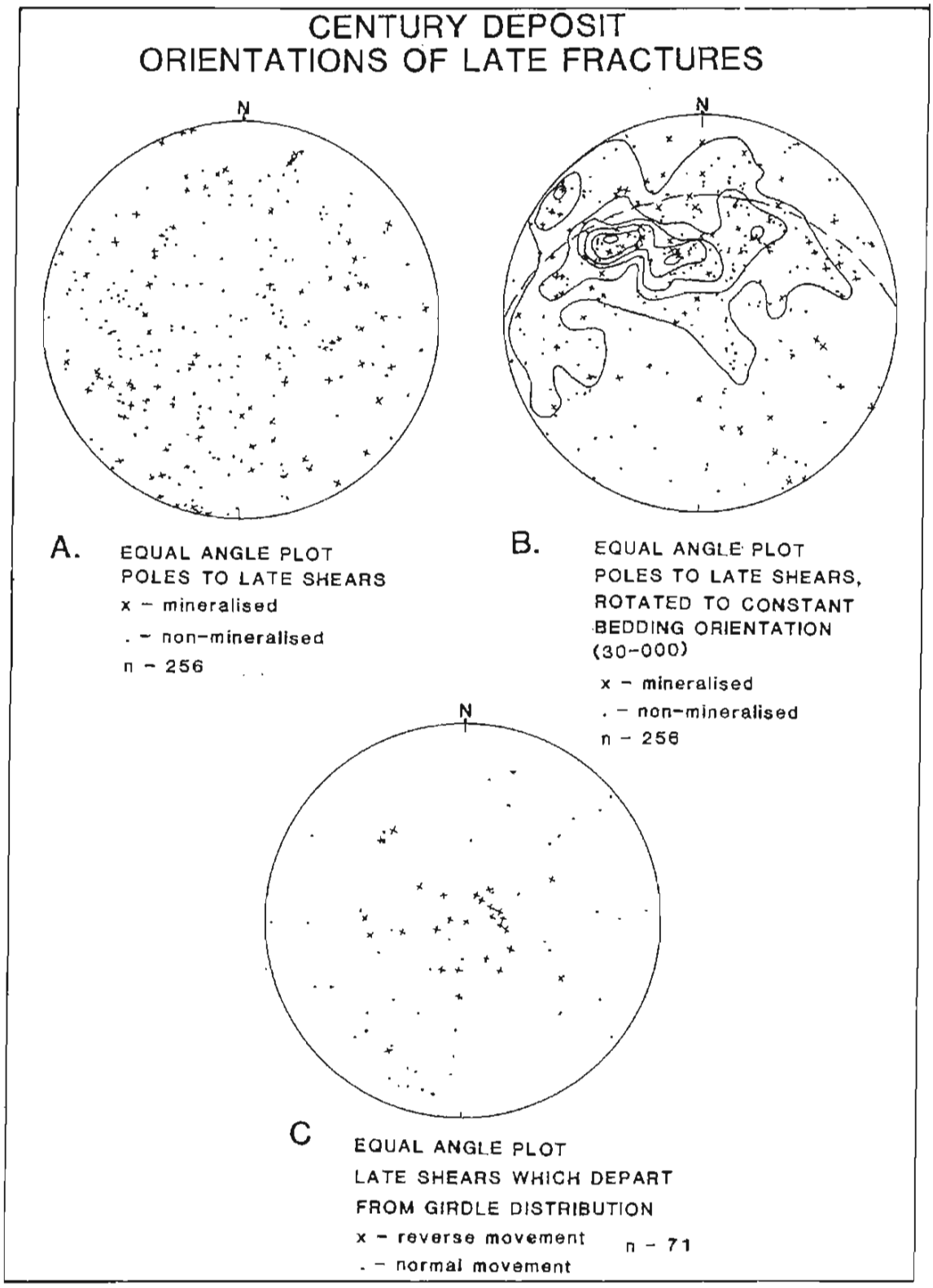

Figure 4.5 Century Deposit. Stereoplots of joint and mineralised fracture directions.

volumetrically minor fracture-filling sulphides and gangue species were emplaced synchronously with the main-stage D2 folding.

The large scale synclinal D2 fold structure is plainly cut by later faults such as the Pandoras and Magazine Hill normal faults and also by small-scale thrust faults (Plate 17G). Continued movement of these late shears is indicated by curvature and displacement of earlier-formed failure planes (Plate 17G). An attempt has been made to discriminate orientations of minor fractures related to this later faulting from the larger population of fold-related extension fractures. Data from Figure 4.5B which clearly depart from the girdle distribution were selected out and replotted in its original (i.e. unrotated) orientation. Separations on the fractures were discriminated as to whether they are normal or reverse (Fig. 4.5C).

Even though the data is sparse, a cluster of flat-dipping reverse structures is evident (Fig. 4.5C). These reverse structures are congruent with the orientations of the late thrusts recorded in underground mapping (Plate 17G). Stratigraphic repetitions are evident in many drillholes (RTE unpublished data), and are almost certainly caused by small thrusts.

Although there is a wide scatter of strike directions, fractures with normal separation plot in a field consistent with broadly east-west to north-west striking, steeply-dipping extensional structures. The orientation of these steep fractures with normal separations are congruent with the orientations of known major faults in underground exposures (Plate 17H) and the orientation of the bounding faults to the deposit.

A limited number of observations of axial planes of small late kink folds were also plotted stereographically (Fig. 4.3B). The data show a girdle distribution about a plane striking north-east and dipping north-west, which may be sympathetic to the flat-lying thrust trends. Note that the main cluster of poles occurs in a similar quadrant to the early folds, but is rotated approx 30^{O} clockwise. This is interpreted as asymmetric reactivation of the earlier-formed fold trends (Plate 17C), and indicates the late folds to

have dominantly west-dipping axial planes, consistent with incipient north-west over south-east thrusting within the ore zone.

Although these observations are somewhat fragmentary and limited in scope, they possess sufficient internal consistency for a speculative discussion of the structural evolution and timing of the mineralisation.

4.7 Discussion

Insufficient data are available to reconstruct detailed structural kinematics during formation of the north-east to north-north-east trending early folds and elongate siderite nodules associated with D1 deformation at Century. The lack of consistent asymmetry of axial planes to these structures within major fold limbs indicates that they are substantially earlier than, and unrelated to, the major north-south fold events. The consistency of orientation of the early fold axes suggests development (or enhancement of even earlier slump structures) during south-east to north-westerly directed compression, parallel to regional-scale north-east macrofolds of the D2 events recognised by Flottmann (1996). The data from within the orebody do not permit any comment as to the existence of earlier north-south D1 folds interpreted by Flottmann, as this event is very weak and only arguably deduced from map interference patterns. Some of the early folds may have nucleated east-west directed strain during the later D2 folding events and been reactivated, giving some of the scatter in orientations.

In hand specimen, individual sedimentary bands characteristically have different populations of fracture abundances (e.g. Plates 18A; 19G). In underground exposures, a hierarchy of fracture sizes is evident, but the bigger fractures tend also to be stratabound. Orientations of the early stylolitic fractures have not been established due to sparse data, but their close association with layer-parallel stylolites, early folds and pinch and swell structures suggests a genetic relationship. They may have initially propagated in under-compacted sediments or in an overpressured environment. In some instances, sediment material from adjacent beds has been physically remobilised into geometrically similar fractures (Plate 19H) within more competent adjacent lithologies.

The overall geometry of the orebody suggests that the majority of the stratabound mineralisation was folded by the north-south syncline which is the logical extension of the Pages Creek syncline. This includes rotation of small-scale north-north-east trending fold fabrics and siderite nodules. The folds and siderite nodules appear to be in part synchronous with, and in part overprinted by, assemblages related to mineralisation, in particular the early stylolitic fractures. The orientations of most of the late more-brittle fractures are interpreted to be compatible with their origin as extension joints developed during folding. The assumption is made that the geometry of the late fractures correctly records final stage relationships of the entire mineralised fracture progression. Therefore, rather than trying to artificially constrain the fractures into sets of discrete events with differing orientations and timing, it seems more logical to consider a continuum of fracture development during mineralisation. The implications of this in terms of the overall mineralisation timing are discussed more fully in section 5.4.6.

As the east-west shortening continued, north-west structures such as the Termite Range Fault assumed a pivotal role in the regional stress system. Late in the deformation, when shortening by folding had reached its peak, faults with this transpressive orientation would logically begin to accommodate part of the regional strain by commencing left-lateral wrench movement. The natural consequence of this strike-slip movement of the fault would be the creation of local environments of extension and compression, caused by irregularities in the fault plane and various intersecting structures.

Century is preserved in an extensional graben complex created by the post-folding extensional Magazine Hill, Pandoras and Nikki's normal faults. This graben formed post-folding and prior to deposition and deformation of the Cambrian limestone sequence (Figs. 3.1 and 3.2), but is otherwise temporally unconstrained. An argument is advanced below for the timing of the graben complex to be logically linked to late strike-slip movement on the Termite Range Fault, in the closing stages of the regional deformation. This is admittedly made on reductionist grounds, but seems kinematically plausible, and, in any case, the timing cannot be proved or disproved on

current data. The alternative hypothesis is that the Century graben structure formed after the Isan Orogeny during a later, cryptic, extensional event.

The geometry of the ore-bounding late normal-fault network has similarities to an extensional strike-slip duplex, or 'negative flower structure' (terminology from Dooley and McClay, 1997), parasitic to the Termite Range Fault. In model experiments, such extensional duplex or pull-apart structures form as the result of an oblique step between main strike-slip zones (Rahe et al., 1998). Such duplexes are characterised by short-strike length, curved, normal-faults with rotational displacement that sole into a basal detachment, which, in turn, terminates against a master bounding fault (Rahe et al., 1998). The ore-bounding faults have these geometric attributes.

There is a significant space problem in accommodating the approximate 500m normal displacement of the Magazine Hill and Pandoras faults. The two faults must swing to a northerly strike close to the western margin of the orebody and join together, as the Pmh2 only 500m west of the orebody is not cut by them (Fig. 2.3). Further, they most likely also connect to the south-facing Nikki's Fault, as there is likewise no south-block down east-west fault cutting Pmh2 along the projection of Nikki's Fault (Fig. 2.3). The three faults therefore must sole together at relatively shallow depth on an upward-concave, spoon-shaped, listric base surface. No vein or breccia mineralisation has been detected in drillcore intersections of the boundary faults, suggesting that they post-date regional lode mineralisation.

Such upward-concave listric geometry of the faults is consistent with kinematics related to sinistral strike-slip movement of the Termite Range Fault. A substantial stepover in the Termite Range Fault may not be required if the fault array simply represents an accommodation structure developed during sinistral strike-slip torsion on a small releasing bend in the fault. Sinistral strike-slip kinematics on north-westerly structures are a feature of the regional "D3" phase of the Isan Orogeny (section 2.2). Minor sinistral strike-slip separations are consistently portrayed on maps of the present day Termite Range fault trace (Bresser, 1992).

Within the deposit, timing of the small-scale late thrusts is uncertain. They post-date minor folding (Plate 17H), but insufficient orientation data are available to give a statistically valid picture of their orientation and timing. They may represent late-stage accommodation structures developed during final stages of the D2 folding, as some are mineralised. The steep fractures with normal separations are interpreted as parasitic small-scale structures to the bounding faults.

Figure 4.6 summarises within-deposit deformation events and correlates them to the regional structural framework discussed in Chapter 2. Figure 4.7 schematically illustrates the interpreted structural evolution of the Century deposit. Further work to clarify structural relationships relies on the creation of three dimensional exposures by mining.

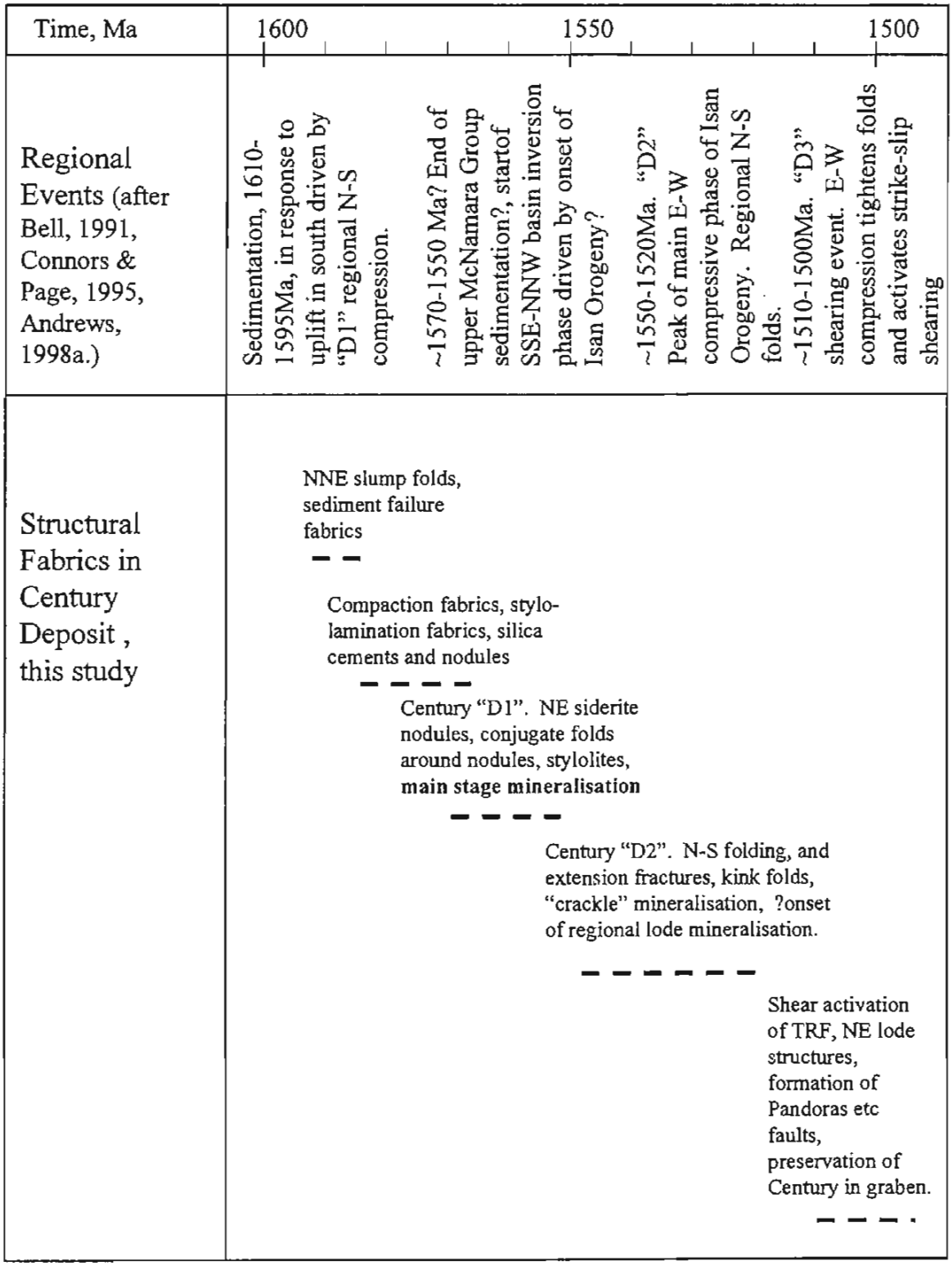

Figure 4.6 Summary diagram comparing within-deposit deformation events to the regional structural framework.

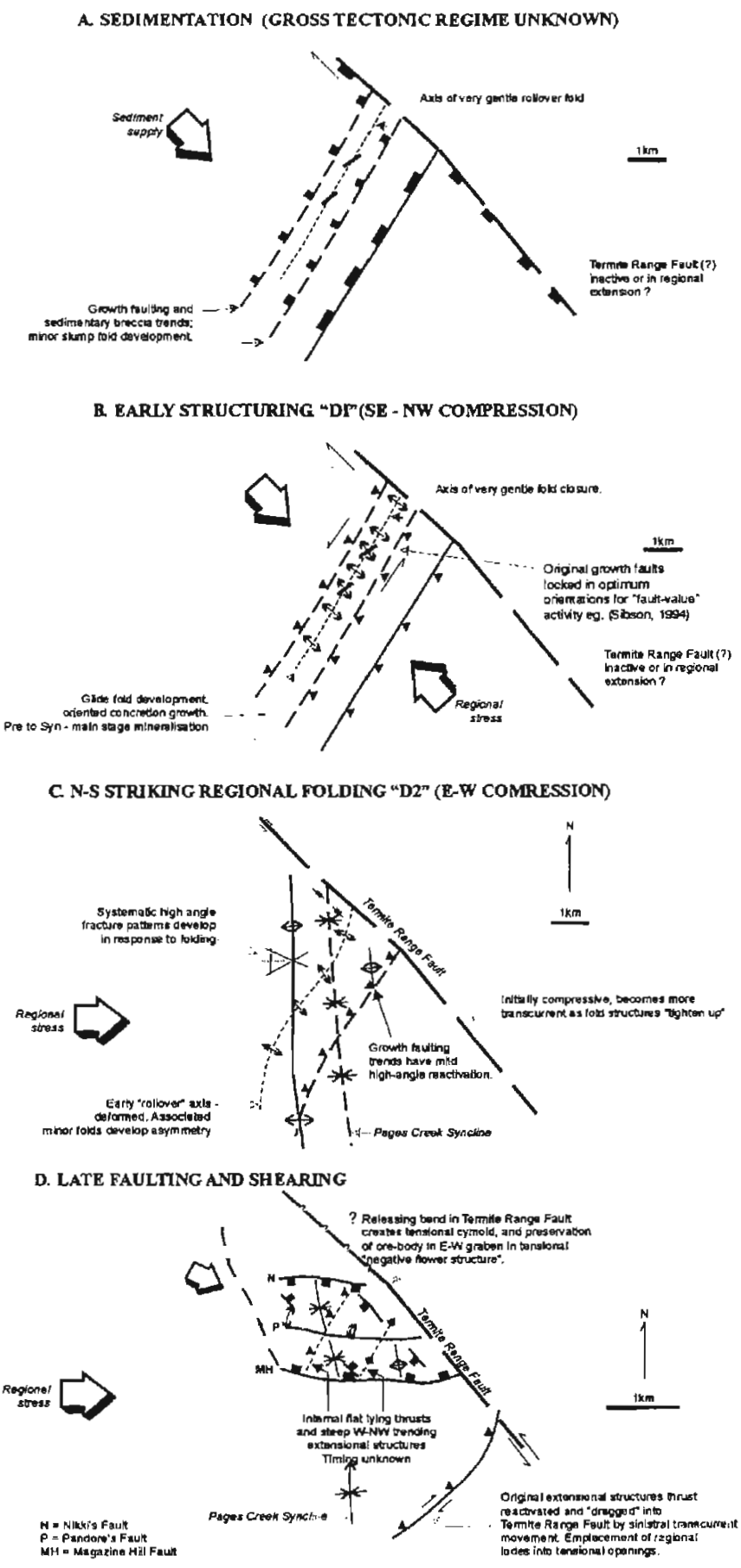

Figure 4.7 Interpreted structural evolution of the Century deposit area.

4.8 Summary

From the foregoing discussion the structural evolution of the Century deposit area can be summarised rather simply (Fig. 4.7):

1. Orientation of the earliest deformational fabrics is consistent with sedimentation trends and possible syndepositional tectonism about local north-north-east trending structures. Pre-compaction slump folding associated with growth faulting on north-east trending structures is plausible (Fig. 4.7A). No firm conclusions can be drawn about the orientation of the gross tectonic regime during this event; it could belong to the early north-south extension-compression event recognised by Comalco workers to the north (McConachie et al., 1993), making the sedimentation part of Comalco's foreland cycle (McConachie et al., 1993).
2. Some folds with soft-sediment textures are interpreted to belong to the earliest stages of later south-east to north-west directed "D1" deformation, which is also associated with growth of oriented siderite boudins and conjugate folds around siderite nodules. Irregular, mineralisation-related stylolitic fractures and bedding-parallel stylolites formed at or after this stage. In the wider Lawn Hill area, already established north-east growth faults could be expected to have either localised development of north-east folds or experienced reactivation as high-angle reverse faults, thus explaining the kinematic sequencing postulated by Flottmann (1996). Detailed petrographic relationships of mineralisation to folds and fractures are presented in Chapter 5.
3. Early fold and fracture fabrics, including the majority of main-stage Century mineralisation, were overprinted and rotated by the main stage local "D2" north-south folding event, which created the major fold geometry at Century. Crackle mineralisation, overprinting the main-stage mineralisation, progressively developed within internal extension fractures in the early stages of this event (Fig. 4.7B).
4. This north-south fold deformation in the Lawn Hill area occurred in response to the east-west directed shortening of the regional D2 phase of the Isan

Orogeny. As regional shortening continued, transpressional reactivation of the large, obliquely-oriented, north-westerly striking Termite Range Fault would have commenced, with a strong sinistral component. In this regime, steep north-east trending fault and fold corridors would logically also have been dextrally re-activated, as a natural conjugate set. The north-east faults would have been progressively rotated to more northerly trends in the proximity of the Termite Range Fault. This sense of movement is consistent with the reconstruction made for the emplacement of the Silver King and Watsons lodes by Bresser (1992).

5. In the final stages of such a transpressional shear regime, when folding had ceased, final-stage sinistral wrench movement of the Termite Range Fault could be expected to create local extensional environments at releasing bends or irregularities. The post-folding, post-mineralisation normal bounding faults to the deposit have contributed materially to the preservation of the orebody in a parasitic graben to the Termite Range Fault. They are tentatively interpreted on geometric grounds to have been initiated in response to late-stage sinistral transcurrent movement of the Termite Range Fault, although they could have been initiated in a later, as yet unconstrained, extensional event.

The low angle thrust faults and brittle kink folds within the deposit are probably small scale accommodation structures related to late phases of structural development, but insufficient data are available to constrain them further.

The variable development of sulphide and carbonate mineralisation in stratabound late brittle fractures, their similar style and the overlap in orientations with earlier fracture fabrics is of special relevance to mineralisation processes and timing. The repeated activation of fractures, overprinted textural fabrics, and the overall stratigraphic confinement of the fracture network are interpreted as evidence of the periodic development of overpressure within some strata. The fracture network (particularly the transgressive stylolites) in the Century mineralisation shows striking similarities to fracture fabrics interpreted as hydraulic or fluid expansion fractures (Kulander et al., 1990).

Fractures of all generations, in combination with selective diffusion along sedimentary layering, are speculatively interpreted as the main fluid conduits for accomplishing mass transfer within the deposit during the mineralising process. This assertion is further discussed, after consideration of detailed textures and paragenesis, in Chapter 5.

Chapter 5
Mineralisation

5.1 Introduction

This chapter commences with an overview of the distribution of the major metals within the deposit. This is followed by descriptions of common textures of gangue and base-metal sulphide minerals. Patterns of sulphide zoning relative to the deposit stratigraphy and major metal-grade trends are then established. The significance of various textural relationships is then discussed and a deposit paragenesis developed. Patterns of sulphide zoning are then linked to metal distribution and the distribution of gangue phases (especially pyrobitumens), and a preliminary scenario for processes and relationships at the time of main stage mineralisation is developed. The Chapter concludes with a discussion of possible depths of emplacement of the mineralisation, in the context of the structural history developed in Chapter 4.

5.2 Metal Distribution

The most crucial relationships to be explained at Century are the vertical and lateral metal zoning and distribution of major sulphide and gangue species. The mineralogy of the deposit is relatively simple, with only three principal sulphide species present; galena, sphalerite and pyrite. No effort has been made in this study to document the existence and distribution of other sulphide species (chalcopyrite, sulphosalts etc), or the distribution of minor elements such as arsenic, cadmium, mercury and thallium, which are present in trace amounts within the mineralisation (RTE, unpublished data). These undoubtedly are of academic and possibly metallurgical interest, but are considered subordinate in importance to the definition of patterns of distribution of the major ore and gangue phases and the explanation of relationships between them. Interestingly, the Century deposit has very low copper (the maximum in composite analyses from ore grade zones is 150 ppm) and barium (max 300ppm) (Waltho and

Andrews, 1993). Both these elements are common in trace to major amounts in other major sediment-hosted lead zinc deposits (e.g. Goodfellow et al., 1993; Large, 1980).

An idealised vertical profile of distribution of lead, zinc and silver within the mineralised stratigraphy, together with the generalised vertical distribution of the main sulphide species, is shown on Figure 5.1 (Waltho and Andrews, 1993). There is a close correspondence between base-metal sulphide abundance and the shale facies units of the stratigraphy (Fig. 5.1). Peak metal concentrations commonly approach or even exceed 30% in individual 1-1.5m. assay intervals within the shale horizons. The intervening siltstone-rich facies are also mineralised, but average zinc+lead concentrations rarely exceed a few percent. Whilst these units are considered as internal waste in the economic sense, they still provide useful paragenetic and textural information. Only moderate correlation exists between zinc and lead assays overall (Waltho and Andrews, 1993). Not unexpectedly, silver assays correlate with lead content (Fig. 5.1). Interestingly, much of the silver apparently occurs mineralogically in solid solution within sphalerite rather than galena (Minenco, 1991; Waltho and Andrews, 1993). The reasons for this are not known.

In major element terms, Century sphalerite is exceptionally pure, approaching the stoichiometric composition of ideal sphalerite (Waltho and Andrews, 1993; unpublished RTE data). There are several textural varieties of sphalerite (see following sections). However this textural variation does not appear to correlate with any major changes in sphalerite composition.

Pyrite is also preferentially localised within the shale facies beds (Fig. 5.1). However, pyrite is not particularly abundant within the higher-grade zinc mineralisation. It is developed mostly on the periphery (above and below) of the zinc and lead-rich zones, with concentrations up to 10-15 percent over individual 1m intervals, and rapidly declines in abundance vertically away from the main zone of mineralisation (Waltho and Andrews, 1993). Siderite-rich bands and nodules are relatively common in pyrite-rich shale and less so in zones with high galena or sphalerite contents. The mineralisation appears to be symmetrically zoned in a vertical sense, having a central base-metal rich core that is surrounded by an envelope of iron sulphides and siderite. In

the south-western portion of the deposit, the shale units have generally lower base-metal grades and higher pyrite and siderite content. To the north-east, these same beds have high-grade sphalerite with little pyrite. This suggests that the vertical zonation also occurs laterally (see section 5.3.12).

The consistent thickness of shale-rich units across the deposit is described above (section 3.4.3; Fig. 3.7). Average grades of the representative shale units 2 and 4.3 for both lead and zinc are shown on Figure 5.2 (see also Waltho et al., 1993, for details of other units and elements). There are some short-range (50-100m) variations caused by incomplete sampling of the units where they have been structurally disturbed. Despite this, examination of the data shows several important trends. Taking unit 4.3 first, there is:

1. A striking decline in grade from north-east to south-west away from the Termite Range Fault, with grades diminishing from >25% to 3-5% zinc.

2. A more subtle decline in grade from south-east to north-west, with grades diminishing from >20% to 10-15% zinc.

Unit 2 has quite a different pattern of zinc distribution (Fig. 5.2A). Within this unit, zinc is relatively low grade in the south-east and much higher grade in the north-west. There is still a gradual decrease in grade to the south-west, away from the Termite Range Fault. Unit 2 has higher lead content than unit 4.1 (Fig 5.2B). Both units show decreasing lead grades from south-east to north-west and also from north-east to south-west. However, the main focus of lead mineralisation shifts to the south-west and slightly to the north-west between unit 4.1 and unit 2. In unit 2 high lead content is distributed parallel to the Termite Range Fault, but is offset from it by several hundred metres. Unit 4.2 has high lead content closer to the fault. These puzzling patterns suggest that mineralisation is stratabound and may be subtly transgressive to the stratigraphy.

Representative vertical profiles of zinc grades have been drawn to further clarify the three-dimensional grade variation in zinc (Figs 5.3 and 5.4). The correlation of high

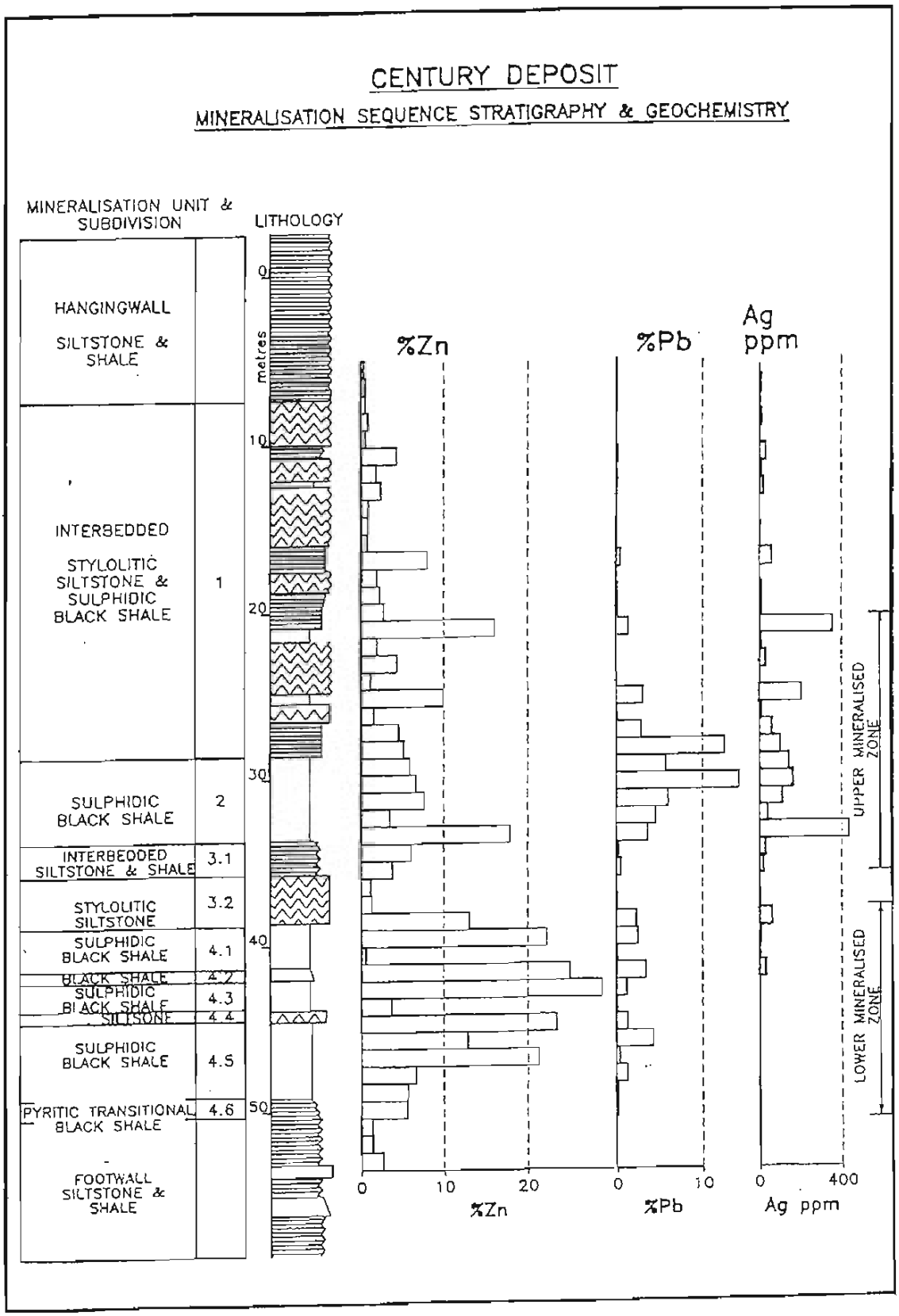

Figure 5.1 Base metal abundances relative to stratigraphy of mineralisation sequence, Century deposit (from Waltho and Andrews, 1993). Graphic symbols on lithological log: horizontal lines – interbedded siltstone & shale; wavy lines – stylolitic siltstone; white background – siltstone and shale.

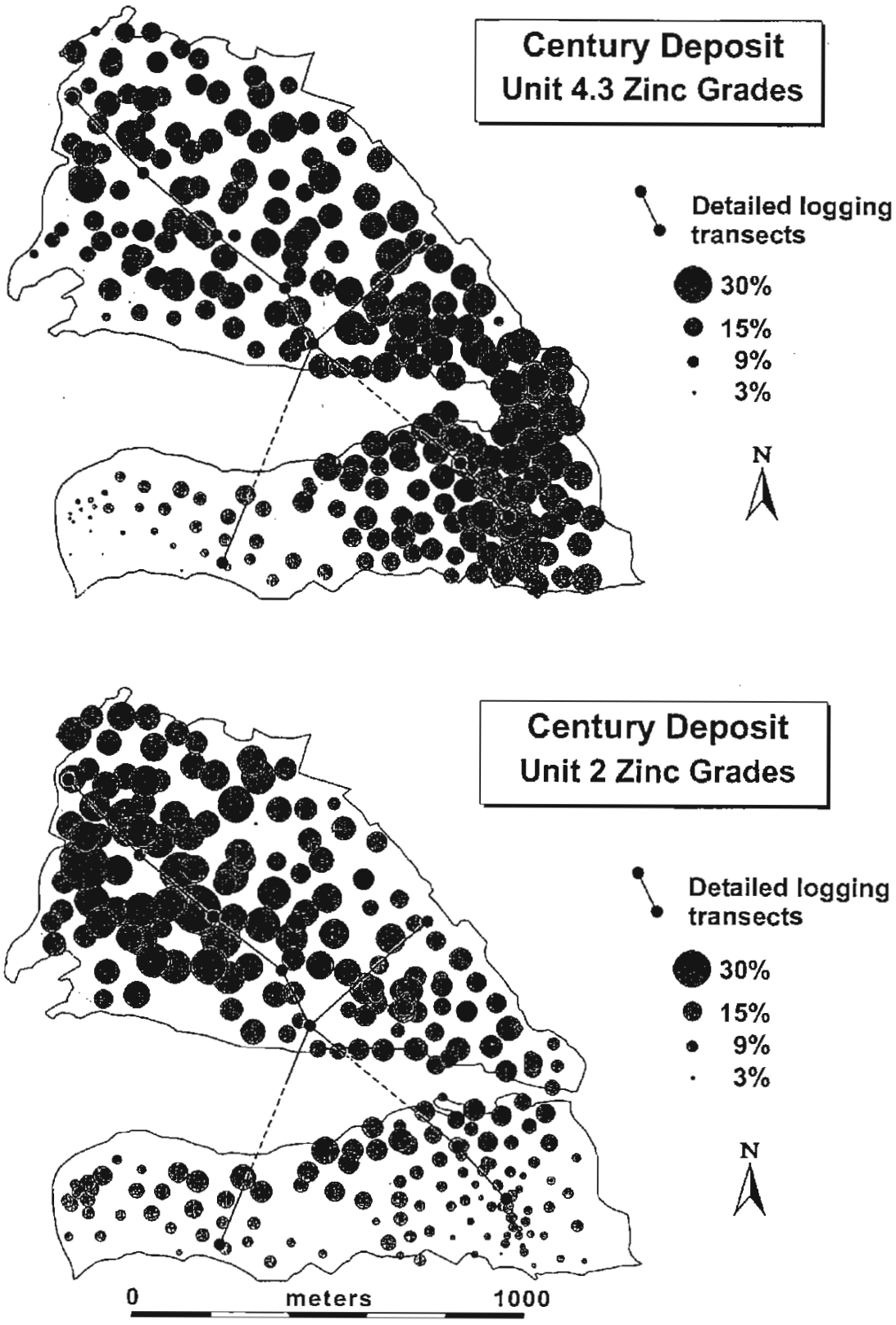

Figure 5.2A Zinc grades in units 4.3 and 2, Century deposit. Solid lines connecting boreholes indicate positions of detailed logging profiles See fig 3.1 for details of hole numbers for these traverses.

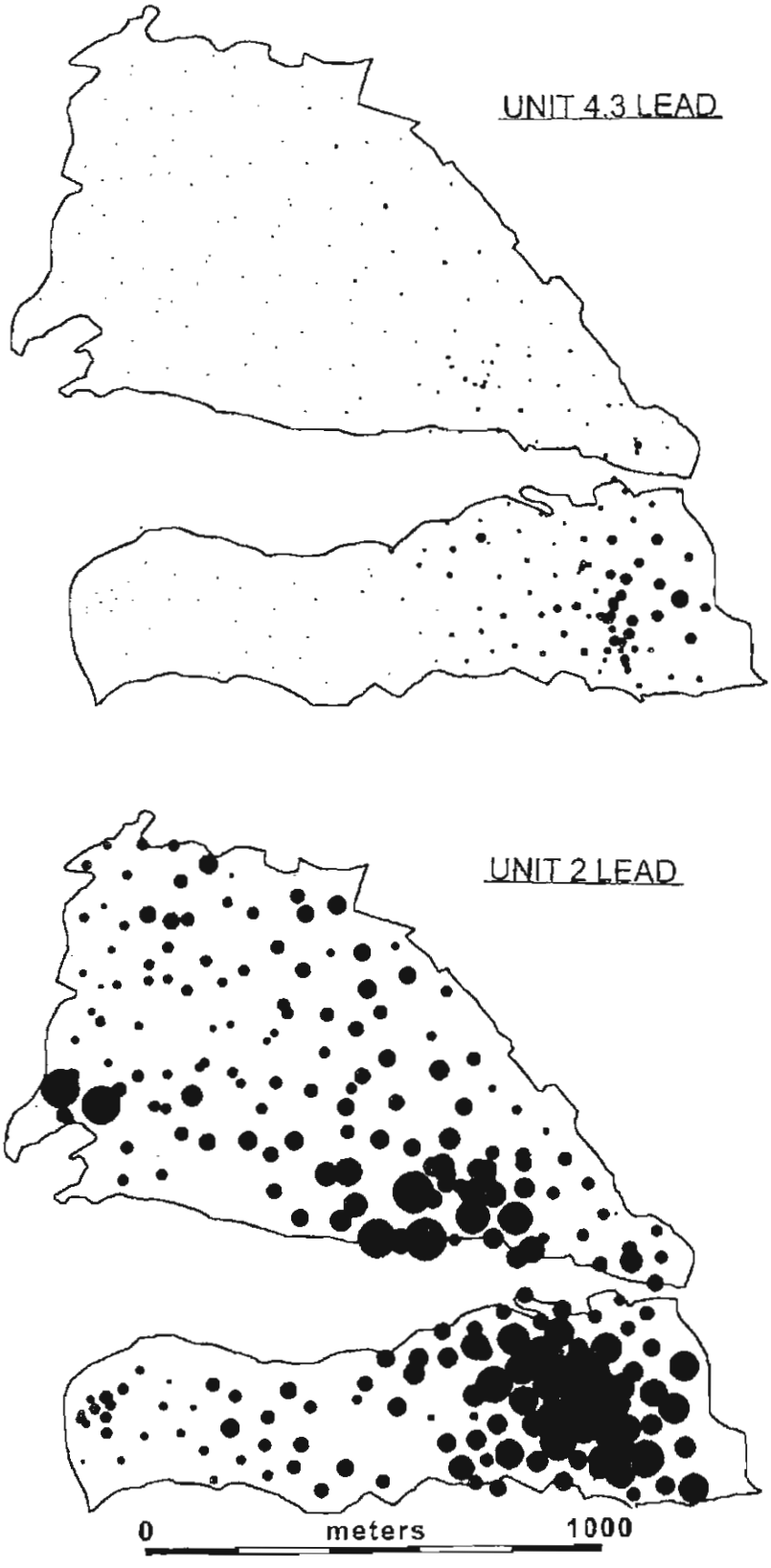

Figure 5.2B Lead grades in units 4.3 and 2, Century deposit. Graduated circles same scale as Fig 5.2A.

grades with individual shale units is clear from the individual assays. Figure 5.3 confirms the decrease in grade in all units from north-east to south-west. Figure 5.4 shows a different relationship, normal to this trend. In the south-east, the main bulk of the mineralisation is centred in unit 4. In the north-west, the centre of the main grade envelope lies in unit 2; a vertical cross-stratigraphic transgression of approximately 20 metres over approximately 1500 metres. From a genetic perspective, this cross-stratigraphic grade migration presents one of the most interesting and challenging features of the deposit. It is discussed in detail in sections 5.3.12 and 5.4.5.

Volumetrically, most of the lead and silver in the deposit occurs in units 1 and 2. The lower units of the mineralised sequence are dominated by zinc (Figs 5.1, 5.3, 5.4), with average lead values less than 1%. The deposit can be subdivided in an economic sense into an upper and a lower zone with differing metal ratios, separated by the generally poorly mineralised units 3.1/3.2 (Waltho and Andrews, 1993). However, although this division is useful in a general way for some portions of the deposit, it is artificial and breaks down when metal distribution patterns are considered in detail. In the south-eastern portion of the deposit, significant laminated and disseminated galena is present in the upper portion of unit 4 (the notional lower zone), to concentrations of several percent. Also in the south-eastern portion of the deposit significant zinc mineralisation extends into the top of the upper footwall stratigraphy, an interval that is only weakly mineralised in the remainder of the deposit. In the north western portion of the deposit, unit 2 (the core of the upper zone) has virtually no significant lead, but has abundant zinc. The lead in unit 2 extends further to the north west in unit 2 than it does in unit 4.1; this pattern is confirmed by trends in over- and underlying units (RTE, unpublished data).

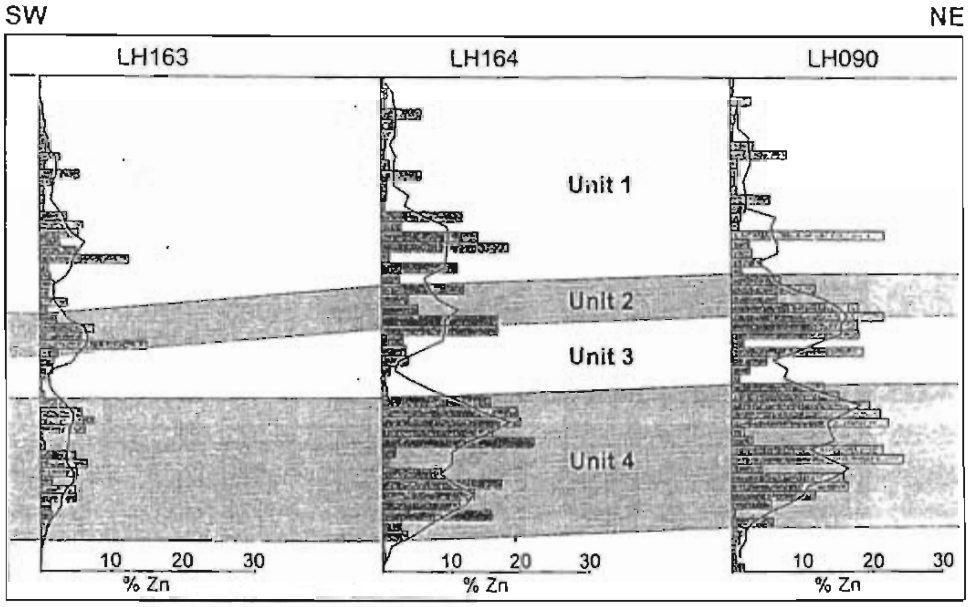

Figure 5.3. Vertical zinc grade distribution along a south-west to north-east transect. A five-point moving average has been superimposed to highlight the overall trends of zinc concentration.

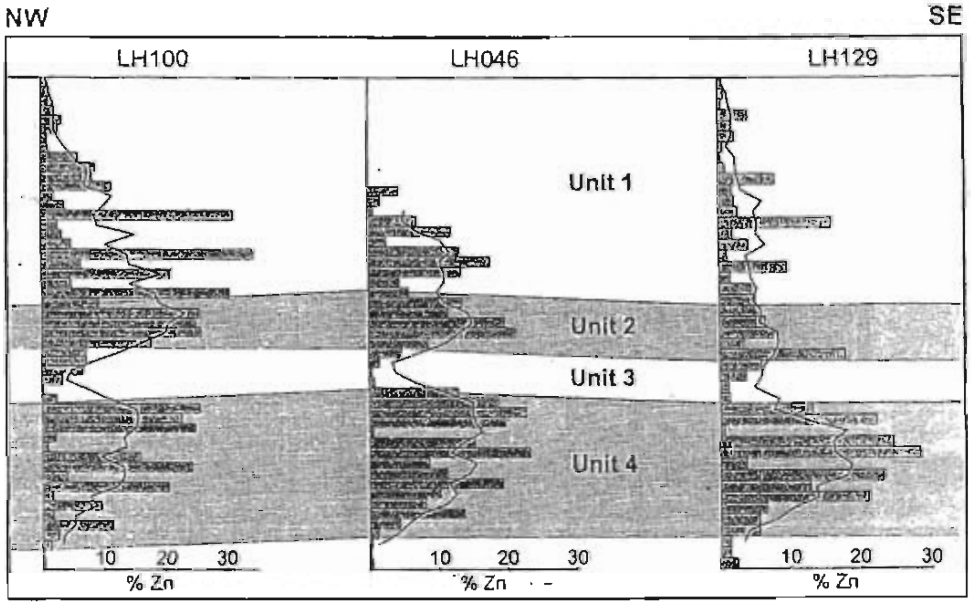

Figure 5.4. Vertical zinc grade distribution along a north-west to south-east transect. A five-point moving average has been superimposed to highlight the overall trends of zinc concentration.

In summary, the following generalisations concerning metal distribution can be made:

- Shale is preferentially mineralised and contains the bulk of economic metals, but, from a genetic viewpoint, siltstone facies also have mineralisation that requires explanation.
- Pyrite and siderite content are higher both above and below the mineralisation.
- In a vertical sense, lead and zinc are concentrated in the centre of the mineralised envelope. The ratio of lead to zinc is higher in the core of the envelope.
- The position of peak metal concentration moves systematically vertically upwards through the stratigraphy from south-east to north-west.
- In a lateral sense, zinc varies in abundance relative to lead. Lead:zinc ratios are higher in the south-eastern portion of the deposit.
- Metal grades decline systematically from north-east to south-west. In some units, pyrite and siderite appear to increase along this vector as zinc and lead grades decline (section 5.3.12).

5.3 Hand Specimen Textures and Petrography

This section describes typical textural features of the mineralisation noted from detailed logging and thin section examination. Several aspects of the mineralisation were examined in detail, including lateral and vertical changes in mineralisation assemblages as well as mineral paragenesis and textures. Over four hundred samples were collected during detailed logging of drillholes along the two deposit transects (see section 5.3.12), other representative drillholes and exposures made in the exploration shaft. The intention was to provide a comprehensive overview of mineral paragenesis and textures over the entire deposit. A list of samples and their locations is presented as Appendix 1.

Specific textures and features are presented as a series of thematic plates (4 to 21) with detailed captions describing features. The sub-sections below describe major textural features, cross-referenced to individual plates. Some low-level discussion of the

significance of various features is made where appropriate. Major inferences for timing and the deposit paragenesis are developed in section 5.4.

5.3.1 Silica Cements and Stylolites

Silica Nodules

Throughout the hanging wall sequence and in the mineralised sequence small patches and nodules of siliceous cement are present. They are most common in the massive and thinly bedded siltstone facies (Plates 4D, 4E, 4F). Individual nodular aggregates are up to 5mm across. They are one of the earliest textural changes observed, as stylolitic solution seams and bedding-parallel foliations appear to deflect around them (Plate 12C). In some specimens, nodular patches of silica cement overgrow undulose bedding fabrics marked by organic-rich laminae, but these aggregates are uncommon and are almost invariably overprinted by later-stage compactional fabrics. Maximum volume loss up to 20-30% is estimated by comparing under-compacted thicknesses in the nodules to the surrounding compacted beds (Plate 4D).

Silica Cement

The silica cement consists of very fine-grained micro-crystalline to amorphous silica, interstitial to original clastic quartz and clay grains (Plates 4D, 4E, 4F, 4G). Under cross polars in transmitted light (Plate 4E), the silica is a uniform medium grey colour, suggesting an array of randomly oriented micro-crystals. This crystallisation is interpreted to be relatively early in the compaction history, as subsequent compaction/solution features and associated siderite spheroids truncate the micro-crystalline material (Plate 4E). There is no evidence for internal stylolite development or patches of undulose extinction within bodies of silica cement. This suggests that silica crystallised quickly after precipitation and did not suffer appreciable deformation during subsequent compaction.

Stylolites

The significance and possible causative mechanisms for the stylolites are discussed above (section 3.4.1). The main significance of the patches of early silica cement and their relationship to enveloping low angle to layer-parallel compactional textures lies in their importance for timing the development of later sideritic carbonate. Siderite consistently overgrows compactional foliation fabrics (Section 5.3.2; Plates 4E, 4F, 4G, 4H; 16E), indicating that siderite commenced deposition *after* significant compaction and silica cementation had occurred.

Silica continued to be mobile after development of these earliest cementation textures. Some varieties of authigenic silica appear to reflect late diagenetic precipitation which overprints compacted fabrics in the siltstone. These are easily distinguished from the distinctive early micro-crystalline nodule fabrics, consisting of 1-10 micron quartz crystals which are not truncated by compactional fabrics (Plates 13A, 13B). They may be associated with organic carbon and sulphides (Plates 13A, 13B), and have a variable timing relationship to siderite. In some specimens, siderite spheroids have been replaced by late silica, giving distinctive pseudomorph textures (Plate 16D). Euhedral quartz crystals may overgrow, or be intergrown with, laminated sphalerite and hydrocarbons (Plates 15D, 15E, 21D). Early euhedral galena crystals are invariably corroded and overgrown by later euhedral quartz crystals (Plates 10C, 10D, 14A). These quartz crystals have euhedral terminations which point into the centres of the galena crystals, indicating nucleation on the margins of the galena grains and dissolution of galena contemporaneously with quartz precipitation.

Silica mobility has been clearly been continuous throughout the paragenesis, with evidence for repeated dissolution and precipitation processes at the microscopic scale. The resultant quartz cements and textures evolve to progressively more crystalline and crosscutting forms with time. Amorphous silica in the matrix of the sediments appears to have been a target for preferential replacement by other mineral species. The significance of these relationships are discussed further in section 5.4 and Chapter 6, after detailed consideration of the deposit paragenesis.

5.3.2 Siderite

Several textural varieties of siderite are present in and around the mineralised zone. Plate 5 illustrates an assortment of typical hand-specimen siderite textures. In siltstone, these range from preferential impregnation and replacement of siltstone bands (Plates 5A, 5B, 5D) to irregular concretionary aggregates developed in essentially compacted sediments (Plate 5F). In shale facies, siderite occurs as nodules and concretions or as planar bedding-parallel siderite-rich bands up to 5 centimetres thick (Enclosures 3 and 5). Siderite nodules and concretions are enveloped by compactional/deformational fabrics in the surrounding beds (Plates 5C, 5E, 5G), suggesting growth in un- or de-compacted sediments. Siderité in the planar bands is more replacive and immediately adjacent sedimentary layers show little evidence of deformation. Siderite in these bands is interpreted to have formed by selective replacement of beds with subtly coarser grainsize. Section 6.3 describes the composition of the siderites from electron microprobe analysis; carbon and oxygen isotope chemical data are in section 6.4.

Petrographically, five distinct forms of siderite are present:

1. euhedral rhombs which grew replacively in massive siltstone beds (Plates 7A, 7B; 16G, 16H). This variety is characteristic of siltstone in the footwall sequence. It is not known whether this variety is a direct equivalent of the clear siderite which infills the spheroidal aggregates (see below), or is a separate variety. This issue is further discussed in section 7.1.

There are possibly other complexities in the footwall carbonates. This study has selectively concentrated on samples collected in siderite-rich beds that have the characteristic brown surface-oxidation stain developed after core is exposed to the atmosphere for several months. However, some samples have appreciable ankerite content (C072, C073). In one of these samples (C072), ankerite seems to be related to late veining (Plate 16D), but it could also represent an early authigenic cement (C073), as early authigenic dolomitic carbonate may occur regionally in the lower footwall stratigraphy (S. Tear, RTE, pers. comm., 1998). This issue has not been investigated

in detail because of the necessity to concentrate on the near-mineralisation siderites. It does not materially alter facies or environment interpretation of the sediments, but it could complicate interpretation of chemical and isotopic data (sections 6.3 and 6.4) and is a topic for future research.

2. fine-grained mosaics of grains which grew replacively in the matrix of massive siltstone beds (Plate 7C, clast in 7D). These could in part have replaced original authigenic carbonate. This texture is represented in both the hanging wall and mineralisation sequences.

3. rounded, concentrically zoned, replacive grains, termed spheroids, which overgrow compacted fabrics in the hanging-wall and ore zone siltstone (Section 5.3.1; Plates 4E, 4H; 8A, 8B; 16A, 16B, 16C, 16E; 21D). The siderite nodules and concretions typical of shale lithologies are also composed of aggregates of spheroids. In thin section, individual grains are up to 0.5mm across (Plates 8A, 8B, 8C, 8G, 8H; 16A, 16B, 16C). In transmitted light, they are characteristically brownish but may be colourless, depending on their composition (section 6.3).

4. infilling rhombic grains. These typically appear as overgrowths on the spheroids, growing into pore space within siderite nodules (Plates 8D, 8E, 8F).

5. clear polycrystalline aggregates in late fractures, veins and breccias, with sphalerite, quartz and galena (Plates 7D; 8A, 8B; 13D, 13F; 16D, 16F; 20B, 20G).

Detailed logging indicates that siderite-rich bands can be correlated between drillholes, but the intensity of siderite development within them varies (Enclosures 3 and 5). The nodular aggregates with deformed margins characteristically show evidence of rotation synchronous with growth and compaction and are commonly elongated (Plates 18C, 18D; 17D, 17F; 19B). Spheroidal siderite within these nodular to concretionary masses appears to be identical in texture and composition to that which overgrows the patches of silica cement in the compacted siltstone beds (e.g. compare Plates 4H; 8A, 8B). This suggests strongly that the shale beds were under-compacted relative to the siltstone beds during growth of spheroidal siderite aggregates. The elongate, possible

boudin-like, nature of some siderite concretions is discussed above (section 4.3; Plates 17B, 17D).

Both the spheroidal and rhombic overgrowth siderite forms appear to unambiguously predate at least some, and probably most, of the mobile organic carbon phase, as residual porosity in siderite aggregates is typically infilled by invasive pyrobitumen (section 5.3.3; Plates 6F; 8C, 8D, 8E, 8F). Both the deep footwall siderites and the mineralisation sequence siderites show a similar early timing relative to hydrocarbon mobilisation. Pyrobitumen, in its turn, is clearly replaced and infilled by base metal sulphides (Sections 5.3.4-5.3.9; Plates 8B, 8F, 8G; 16A, 16B), which have associated colourless siderite and quartz. Compositional data on the various siderite varieties are presented and discussed in detail in section 6.3.

5.3.3 Pyrobitumen

Pyrobitumen with various textures is widespread, particularly in the laminated shale facies of the mineralisation sequence. Pyrobitumen occurs sporadically in every unit of the Lawn Hill Formation, but, from the limited available regional drill core, is more abundant in the stratigraphy surrounding the deposit. In hand specimen (Plate 6), a variety of impregnating, dispersed, nodular and fracture controlled modes of pyrobitumen occurrence are evident. The pyrobitumen is now amorphous carbon, which is pregraphitic in character and retains virtually no hydrogen or oxygen (section 6.2). It is interpreted to represent the degraded residue of a mobile hydrocarbon phase. As mentioned above, much of the pyrobitumen infills porosity in siderite aggregates (Plates, 6F; 7D, 7G, 7H; 8C, 8D, 8E, 8F) and therefore post-dates their development.

The transgressive fracture and nodular infills are of particular interest, as they unambiguously indicate physical mobility of the carbon phase (Plates 6B, 6C, 6D, 6F). Petrographically, the pyrobitumen in these fractures (and the stylolitic dissolution surfaces) consists of massive infilling amorphous carbon with various admixtures of colourless siderite, quartz and sulphides (Plates 7E, 7F; 8C, 8D, 8E, 8F; 13F, 13H). Some patches of pyrobitumen adjacent to infilling sulphide grains display a speckled pattern of interference under cross polars in reflected light. This suggests incipient

pre-graphitic ordering of the carbon, but no actual graphite is present (S. McKnight, pers. comm., 1992). No features suggestive of a thermal mesophase, as shown by Gize (1985), have been noted in the pyrobitumen, suggesting that degradation of the original hydrocarbon did not occur at temperatures greater than 250-300^0 C (see section 6.7.1 for further discussion).

Pyrobitumen, sulphides (Plate 15) and quartz (Plates 15D, 15F) overlap each other in the paragenesis. This indicates substantial mobility of silica concomitant with organic material and sulphide emplacement. Possibly, silica dissolution and precipitation reactions (section 3.7.3) were associated with the continuing breakdown of organic materials, including hydrocarbons, after they were generated, throughout the life of the system. Potential reactions are further discussed in Chapter 7.

5.3.4 Pyrite

A halo of pyrite-rich strata surrounds the base-metal rich zones, but the richly mineralised sphalerite zones have relatively little pyrite. Pyrite is also sporadically present in the hanging wall and footwall stratigraphy of the mineralisation sequence, but only rarely exceeds a few percent over significant thicknesses (1-2m.).

In hand specimen, pyrite in the ore zone mostly occurs concentrated in fine lamellae parallel to bedding, giving a brassy yellow sheen to the bands (Plates 9E; 11A, 11B, 11F). This variety has been named pyrite a (Figure 5.6). Concretions of massive pyrite to 3 centimetres occur rarely; surrounding beds are compactionally deformed about these bodies. A late textural variant (pyrite b; Fig. 5.6) occurs occasionally within concretionary siderite bodies as irregular replacive aggregates up to 1.5mm across (Plate 8H). Sparse pyrite rarely infills late-stage cross-cutting veinlets.

Petrographically pyrite a comprises euhedra approx 1 - 2 um in diameter dispersed along sedimentary layering (Plate 15A). Rare spherical clusters of such euhedral grains are suggestive of framboids (Plate 13G). Abundant pyrite, with some textural similarities, is present in other base metal deposits in the Mt Isa/McArthur province (Solomon, 1965; Croxford and Jephcott, 1972). Traditional interpretations of such

textures invoke synsedimentary or early diagenetic processes, with a strong inference made that biologic processes were involved in sulphide fixation (e.g Muir, 1985). However, several textural features of the Century pyrite suggest that at least some of it may have a later origin.

- Pyrite is commonly present around the edges of siderite concretions. These have substantial compactional deformation around their margins, but, in many specimens, the pyrite bands seem to overprint compacted sediment fabrics (Plates 5E, 5G). This makes at least these pyrite aggregates coeval with, or younger than, the main phase of siderite deposition. Some spheroidal siderite grains overgrow euhedral pyrite grains (Plate 7B), making relationships more complex. Possibly siderite and euhedral pyrite were co-deposited.

- Pyrite of identical 1-2 micron crystal morphology is frequently observed to occur disseminated within cross-cutting fractures which are filled with mobile pyrobitumen (Plates 13F, 13H). This is an unambiguous indicator of late deposition of fine-grained euhedral pyrite.

- Pyrite-rich zones in the hanging wall and footwall shale facies close to the mineralised sequence are texturally similar to those in the ore zone. Texturally, much of the euhedral pyrite in the hanging wall siltstone sequence appears to overgrow compactional foliation and occurs in transgressive relationships (Plates 13F, 13G, 13H).

An interesting large-scale observation concerning pyrite abundance is the symmetry of the mineralisation system zoning, from base metals in the core of the deposit outwards to pyrite- and siderite-dominant zones (Fig. 3.4; Waltho and Andrews, 1993; see detailed lateral zoning in unit 4.1 on Enclosure 5). Correlative upper Pmh4 stratigraphy at Lilydale has low bulk pyrite content, but the pyrite still occurs as fine-grained euhedra. This suggests that, at Century, much of the pyrite is an integral part of the mineralised system, but, in detail, no confident judgement can be made as to the origin of pyrite in a particular specimen because of the potential textural ambiguity.

From observation of numerous specimens, there are too many contradictory relationships between euhedral pyrite and different mineral species to interpret simple unambiguous temporal phases of pyrite a deposition. Detailed textural work using an ion microprobe for sulphur isotope compositions (e.g. Eldridge et al., 1993) could potentially establish statistical populations of various types, but this would be very expensive and subject to error anyway because of the small size of the grains. It is simpler to interpret a continuum of pyrite deposition throughout the life of the deposit, with conditions proximal to the ore system favouring the development of discrete euhedra.

Pyrite b is undoubtedly late using conventional textural criteria (Plates 8H; 14G). It overprints and pseudomorphs earlier minerals such as siderite and sphalerite. This type of pyrite, and the pyrite in transgressive veinlets, are volumetrically unimportant, but could yield some useful insights into sulphur isotopic evolution of the late stages of the system because of their larger grain size and undoubted late timing relationship (section 6.5).

5.3.5 Euhedral Galena

An estimated 10 - 20% of the galena at Century occurs as discrete grains up to 1mm across (Plates 9A, 9B), typically disseminated rather evenly through discrete bands up to 5 centimetres thick in the shale units. Unit 4.2 also has sparsely disseminated euhedral galena. Petrographically, some crystals appear to have been precipitated relatively early, as the bedding-parallel foliation wraps around some grains (Plate 10A). However, most euhedral galena grains appear to overgrow compactional/deformational fabrics (Plate 10B). Early euhedral galena crystals are almost invariably corroded and partly replaced by silica and sphalerite (Plates 10A, 10D). Delicate internal growth structures are common in these grains, as revealed by etching (Plates 10C, 10D).

Porphyroblastic galena grains up to 5 mm across occur as overgrowths on delicate fold structures, including bands of sphalerite mineralisation (Plate 9F). These porphyroblastic grains are interpreted to have developed during later phases of galena deposition (section 5.3.9). They are distinguished from the early euhedral grains by

their large grain size, association with brittle deformation features and sharp uncorroded margins.

A further 10% of the total galena is estimated to occur as fine-grained galena-rich lamellae, which show development of dynamic recrystallisation textures (Plates 10E, 10F). These lamellae may originally have been small bands rich in early euhedral galena that were weakly deformed by shear parallel to bedding planes. The deformation has been partitioned into discrete domains, which makes microstructural interpretation difficult. Insufficient detailed microstructural work has been completed on these textures to determine relationships of shear fabrics to macrofold geometry. However, the existence of a deformed phase of galena places some constraints on the timing of at least some of the mineralisation. The volumetrically more important later galena (section 5.3.9) plainly occupies transgressive fractures associated with later structural events. These overprint earlier small-scale deformation structures and rarely show evidence of deformation in etched specimens.

5.3.6 Porous Sphalerite

This textural variety of sphalerite comprises 40 - 50% of the total zinc mineralisation. The term porous sphalerite was coined by metallurgical investigators working on the project because of the very fine grainsize of the sphalerite crystals (as small as 60 Angstroms, from TEM work by S. McKnight, unpublished Minenco data, 1991) and their occurrence as porous aggregates intimately intergrown with pyrobitumen. The term has been retained despite its apparent clumsiness, for lack of a simpler, unambiguous, name.

In hand specimen, porous sphalerite consists of steel-grey coloured lamellae which mostly lie parallel to bedding planes in the host carbonaceous shale facies (Plates 9B, 9C, 9D; 5E; 19B; 11A, 11B, 11E). Some lamellae occur along low-angle bedding discontinuities (Plates 11C, 11E). The distinctive grey colour in hand specimen is due to differing proportions of finely admixed pyrobitumen and host sedimentary material, which imparts a grey colour to otherwise pure white sphalerite. Apart from this textural difference, this type of sphalerite shows no appreciable chemical or isotopic

differences to the other major variety of early sphalerite (non-porous; section5.3.7) in the deposit. It is regarded as a textural variant related to differences of host lithology, rather than comprising a specific sphalerite generation.

Petrographically, the porous sphalerite is finely disseminated in discrete pyrobitumen-rich lamellae up to 5 mm wide, forming locally massive bands up to several millimetres thick. Plate 15 illustrates the most common pyrobitumen and sulphide textures. There seems little doubt that the majority of the pyrobitumen was either a pre- or co-existing phase and that the porous sphalerite intimately occurs within microporosity developed in pyrobitumen. Confirmation of the relationship of some sphalerite and pyrobitumens is provided by the textures within siderite aggregates (Plates 8D, 8E, 8F, 8G). These clearly show that sphalerite was preferentially deposited in association with and slightly later than degraded pyrobitumen. Within the siltstone facies, blebs and irregular aggregates of pyrobitumen and sphalerite are dispersed in siliceous nodules (Plate 13A, 13B), in irregular transgressive fractures (Plate 13C, 13D), or preferentially within pyrobitumen-rich stylolite surfaces (Plate 13E; see also Plate 21E which shows the progression sphalerite – pyrobitumen away from a feeder fracture). This timing relationship with pyrobitumen is quite unambiguous. In the context of the other relationships of siderite and pyrobitumen, the timing of sphalerite is therefore constrained as being quite late in the burial history of the host sequence.

In hand specimen, the porous sphalerite/pyrobitumen lamellae apparently show good continuity along bedding. Microscopically, these apparently simple lamellae are revealed to have myriad across-layer microfractures with fronts of pyrobitumen and sulphides (e.g Plate 21E). Mobility of mineralising fluid was therefore controlled by across- and along-layer permeability, with an associated intricate stratabound mesh of microfractures. The widespread occurrence of later cross-cutting pyrobitumen- and sphalerite-filled fractures (Plate 21; section 5.3.11) shows that mobility of sphalerite and hydrocarbons proceeded for some time through the subsequent mineralisation history.

The relationship of pyrite and porous sphalerite is problematic. Pseudomorphs of sphalerite after pyrite, or inclusions of pyrite within sphalerite lamellae, should be expected to be common if pyrite was an earlier mineral species, whereas, in fact, they are very rare (as are inclusions of pyrite in massive non-porous sphalerite bands). It seems more likely that the pyrite and sphalerite were partly contemporaneously deposited but perhaps spatially separated, when their relationships within the larger mineralising system are considered.

The strong relationship of the porous sphalerite variety with pyrobitumen is perhaps understandable given the strong reducing capacity of what must have been original hydrocarbon liquids at the time of mineralisation. Ample precedent exists in the literature for processes such as thermochemical sulphate reduction to trigger sulphide precipitation in the presence of strong reducing agents (e.g. Williams, 1978; Leventhal, 1990; Anderson, 1991; Arne et al., 1991; Davidson and Dixon, 1992). This is discussed further in section 5.4 and subsequent chapters.

5.3.7 Non-porous Sphalerite

This sphalerite variety comprises the other major source of zinc in the deposit, being approximately as abundant as the porous sphalerite (Minenco, unpublished data, 1991). In hand specimen, it again delicately follows layering in the black shale units, but a wider variety of subtly transgressive relationships are evident. For the most part, non-porous sphalerite consists of almost pure sphalerite bands from 0.2 to 5mm thick (mostly around 0.5-1mm), as in Plates 9A, 9B, 9F; 11D, 11G, 11H; 19G. When in association with the porous sphalerite, it appears in the main to be slightly later (Plates 9F; 11B, 11C), although thin section relationships are often ambiguous. Thin high-grade lamellae of this sphalerite variety are the main constituents of the better mineralised portions of the siltstone facies. These lamellae occur preferentially concentrated along shale partings or stylolites (Plates 12B, 12D, 12E).

Petrographically this type consists of aggregates of very fine-grained pure sphalerite, intergrown with, and almost completely having replaced the fine siliceous matrix cement of the host shale and siltstone (Plates 14B, 14G; 21A, 21B, 21F). Non-porous

sphalerite development is remarkably selective to individual sediment lamellae. Pyrobitumen is not particularly abundant. Evenly-dispersed fine non-porous sphalerite occurs in some micro-layers, having preferentially replaced silica (Plates 14A, 14B, 14G; 21F, 21H). It seems that, if the mineralising process had continued in these diffuse bands, they would ultimately have been transformed to massive sphalerite.

Dispersed replacive sphalerite in the matrix of siltstone bands and in the siderite concretions (where pyrobitumen is not present) are also included in this variety. Where sphalerite occurs within siderite concretions, it most commonly replaces interstitial silica (Plates 8G, 16A, 21D). Direct replacement of siderite grains (Plate 8G) is relatively uncommon. Stylolitic surfaces may serve as departure points for delicate diffusionary coronas of non-porous sphalerite into surrounding siltstone beds (Plate 12D, 12E). Intraformational breccia zones (Plate 12D) and small shears (Plate 18E) contain non-porous sphalerite which clearly post-dates brecciation. Replacement fronts are clearly visible in the matrix of some black shale bands (Plate 9B); these surround early irregular fracture planes (Plate 11B). This texture appears to be gradational to coarse-grained irregular replacive masses (section 5.3.8).

The emplacement of approximately half of the sphalerite at Century as non-porous sphalerite, without obvious involvement of organic matter, needs to be reconciled with most of the remainder being present as porous sphalerite intimately associated with pyrobitumen. Zoning relationships of the two sphalerite varieties is described in section 5.3.12. A scenario for possible processes is developed in subsequentsections.

5.3.8 Transgressive Sphalerite

Numerous bedding-transgressive forms of sphalerite are present throughout the deposit. These vary from irregular fractures with corroded margins and high pyrobitumen content, which seem to be early features, to irregular replacive bodies up to several centimetres across (Plates 19A; 20F). Despite their seeming simplicity, when Century specimens are examined carefully (particularly microscopically, virtually all have an abundance of transgressive textures, at various scales. It is difficult in many instances to draw a line demarking transgressive from layer parallel

sphalerite. There are also difficulties in unambiguously separating replacive sulphide surrounding transgressive fractures and the infill sulphide of the fracture (Plates 20F, 20G; 12D, 12F, 12G, 12H).

A volumetrically minor, but texturally distinctive, pale-yellow coloured late-sphalerite variety has coarse grainsize and a sugary-textured, replacive habit (Plates 9H; 18H). This variety overprints small fractures which displace earlier non-porous sphalerite bands, but predate the ubiquitous late-stage transgressive crackles and vein/breccia infills (see 5.3.11). It therefore lies paragenetically between the mostly layer-parallel porous and non-porous varieties and the later transgressive forms emplaced in more brittle fractures. Sugary textured sphalerite appears to be limited in distribution to areas with 'swirly' textured late galena (Plate 9H) and to plastically deformed/sheared zones in shale facies within unit 2 (Plates 18H; 19E; 20C). Microscopically, it consists of euhedral single sphalerite grains apparently replacing the weakly carbonaceous shale host. Some small (1-2 micron) fluid inclusions have been observed in this phase; a single determination by J. Wilkinson of Imperial College has given a homogenisation temperature of 120^{0}C (Wilkinson, written comm., 1992). It appears to be the only sphalerite within the deposit suitable for fluid inclusion work, apart from the ubiquitous vein-infill sphalerite or possibly some of the coarser grained sphalerite which has replaced siderite concretions. Some specimens have been sampled for sulphur isotopes in this study (section 6.5).

5.3.9 Transgressive Galena

An estimated 70-80% of the galena occurs transgressively and paragenetically late. Transgressive galena is variably present as stratabound veins; irregular replacive masses up to several centimetres across at high angles to bedding; fine stringer-type fracture infills or as 'swirly' irregular lamellae stratabound within shale beds (Plate 9). From detailed core logging (section 5.3.12), the lead-poor north-western portion of the deposit mostly has disseminated euhedral galena. The lead-rich south-eastern corner is dominated by more transgressive forms (progression Plates 9B - 9H). The late timing of transgressive styles of galena is best developed in the south-east of the deposit. Sphalerite of various types is typically deformed, fractured and overprinted by

replacive/infilling galena where they occur together (Plates 9A-H;12F, 12G, 12H; 20A).

Petrographically, transgressive galena preferentially replaces fine-grained silica (Plates 15H; 13C) and truncates earlier layer-parallel mineralisation species (Plates 10F, 10G, 10H). Minor galena may fill circular cavities in degraded pyrobitumen (interpreted as gas vesicles) or occurs intimately intergrown with pyrobitumen in cavity fills within siderite aggregates (Plate 8F). This is not a volumetrically important association, but confirms the late timing relationship of sulphide emplacement as post-dating destruction of original hydrocarbon.

Within the laminated pyrobitumen-rich shale, there appears to be no galena texture strictly analogous to the porous sphalerite texture. Rather, galena appears to be preferentially associated with siliceous material where all phases are present within the same specimen (Plate 15H). In many respects the transgressive galena texturally resembles (and is closely associated with) the more transgressive varieties of non-porous sphalerite. Porphyroblastic galena infills cavities lined with crystalline sphalerite and/or quartz (Plate 10H). Transgressive fractures with galena infill commonly have corroded margins, particularly where they contain appreciable pyrobitumen (Plates 21G, 21H), giving clear evidence of at least partial creation of solution-related porosity late within the paragenesis.

5.3.10 Chlorite

Trace amounts of a transparent fine-grained mineral with high iron, magnesium, aluminium and silicon were noted in thin section and microprobe examination of specimens from the hanging wall and mineralisation sequences. A preliminary identification as chlorite has been made. Diagenetic chlorite cement appears to almost completely occlude porosity in the hanging wall sandstone (Plates 3A, 3B; section 3.2) and is developed throughout the Lawn Hill region in this formation (Andrews, 1998b). It is not known whether the hanging wall and mineralisation sequence chlorite is related to these, or is a separate hydrothermal species. Within the deposit, at least some chlorite unambiguously seems to be a hydrothermal species, as it fills gas

vesicles within pyrobitumen (Plates 8C, 8D) and infills late fractures. The relationship of the more disseminated chlorite in the hanging wall siltstone and this hydrothermal chlorite is not known. Further research into the chlorite compositions and relationships in the hanging wall of the deposit in particular would potentially be productive; this has not been attempted in this study. Available data have been included here to prompt consideration of the following additional speculative questions:

- From a limited number of microprobe analyses (Appendix 2), the chlorite is compositionally unusual, with high ratios of iron to magnesium. Chlorites with these unusual compositions are apparently common in oilfield environments (C. Cuff, pers comm., 1992).

- From the limited number of analyses to date (Appendix 2), it seems that the iron to magnesium ratio of the chlorite increases systematically towards the mineralisation. Further work should be carried out to assess the validity of this relationship because it may be useful in exploration.

No comment can be made on the potential uses of the chlorite composition as a geothermometer at this stage.

5.3.11 Vein and Breccia Mineralisation

As discussed above, transgressive fabrics with varying amounts of sulphides, quartz, siderite and pyrobitumen mineralisation are ubiquitous throughout the mineralised zone. These grade from the more replacive fabrics discussed above to simple fracture and breccia infills, which are the subject of this section. A representative range of hand specimen textures is shown in Plates 19 and 20, with the bottom of Plate 21 showing petrographic evidence of the late timing of various infilling sulphide, siderite and quartz phases relative to earlier formed sulphides. Most vein and breccia infills clearly cross-cut previously mineralised material.

The crackle veins and breccias are more abundant within, but not solely confined to, the ore zone at Century. From core logging they form a definite halo around the mineralisation, extending vertically for several tens of metres into the footwall and more particularly the hanging wall sequences. Although some preferred orientation of the larger veins is present, for the most part they appear to fill a network of fracture sets analogous to extension joints developed during folding (Chapter 4). Many of the small-scale faults which disrupt the orebody are infilled by such mineralisation.

5.3.12 Sulphide Zoning

Zoning of the various sulphide textures was examined in the context of bulk metal zoning patterns (section 5.2). A transect from north-west to south-east across the deposit was examined by detailed logging of the interval from the top of unit 2 to the base of unit 4.2 on drillholes LH261, LH100, LH54, LH46, LH164, LH25 and LH129 (Fig. 5.2; Enclosures 2 and 3). A further detailed logging transect to examine changes in units 4.1 and 4.2 was conducted from north-east to south-west across the deposit, encompassing drillholes LH90, LH60, LH164, LH177 and LH163 (Fig. 5.2; Enclosures 4 and5).

Generalised lateral changes in major sulphide and gangue assemblages are shown diagrammatically in Figure 5.5. Estimates of grainsize and scale of bedding and lamination, together with stylolite development and the abundance of siderite, are presented graphically on enclosures 3 and 5 as a master lithologic column. Visual abundances of pyrite, porous sphalerite, non-porous sphalerite and galena were estimated and their geometric distribution in the core sketched on to the graphic logging columns adjacent to the lithological log. For ease of lateral stratigraphic comparison, the individual logs were dip corrected to a common scale (1:40), as shown by the metreage indicators on the logs. Observations interpreted to be of major significance are as follows:

- in unit 4.1 from the north-west to the south-east, porous sphalerite is the dominant sulphide species. Some indications of an increasing proportion of bedding-parallel non-porous sphalerite are present in holes in the south-eastern corner of the

deposit, together with an increased proportion of finely disseminated and lamellar fine-grained galena. Pyrite content is low (<2%) and relatively uniform.

- From south-west to north-east, unit 4.1 shows some quite substantial changes. In the extreme south-west, porous sphalerite has low abundance. Zinc is mostly present as the dispersed non-porous replacive form within siderite-rich bands and as stratabound crackle veins. Siderite is noticeably more abundant than to the north east. Porous sphalerite becomes more abundant to the north-east, by the centre of the deposit (LH164) it comprises an estimated 40% by volume of the unit and then remains fairly constant. However, the location of most intense sphalerite development subtly changes from intersection to intersection. This gives a clear indication of non-stratiform, but stratabound, zinc distribution. Non-porous sphalerite content is relatively low, but shows a slight increase in abundance to the north-east. Lead content is low. The galena which is present is finely disseminated or occurs as rare fine-grained lamellae. These mineralogical changes occur without any substantial change in thickness of the host unit, apart from normal pinching and swelling due to intraformational deformation.

- On the north-west to south-east transect, unit 3.2 appears quite consistent. Sulphide content is low, where present the sulphides are disseminated replacively in massive siltstone beds or stylolaminae, or else are present in the ubiquitous crackles. The thickness of the unit does not change appreciably. Although individual beds cannot be exactly matched, packages of thinly versus thickly bedded variously stylolitised siltstone can be correlated from intersection to intersection. In equivalent stratigraphic positions, siderite content varies in intensity, generally being less abundant in the south-east. In the south east, some siltstone intervals appear to originally have been stylolitised, mineralised with siderite, and then partly replaced by later silica (Plate 16D).

- Unit 2 and the lowermost portions of unit 1 display some quite dramatic changes from north-west to south-east. In the north-west, porous sphalerite is dominant in the shale facies in unit 2; galena and pyrite contents are very low. In the north-west, the shale beds in unit 1 mostly have porous sphalerite but have an increased

proportion of layer-parallel non-porous sphalerite relative to their lateral equivalents in the south-east. Towards the south-east, unit 2 shows a steady decrease in the proportion of porous sphalerite and a concomitant increase in the proportion of layer-parallel non-porous sphalerite. This non-porous sphalerite in turn decreases in abundance, with a higher proportion of coarser grained and more transgressive sphalerite varieties in the south-eastern sector. Overall zinc content steadily decreases on average to the south-east (Enclosure 2; Figs 5.4, 5.6). It appears that, in the south-east in unit 2, the layer-parallel porous and non-porous sphalerite is confined to only a few relatively thin zones and is very much reduced in abundance relative to the north-west (Enclosure 3).

- Galena is more abundant and also more transgressive in its textures to the south-east. Pyrite is more abundant in the south-east, in a zone concentrated in units 3.1 and 2. Insufficient detailed logging has been done to determine whether this reflects a general pattern of increased pyrite peripheral to zones with lower zinc grades (as in unit 4.1 on the north-east to south-west transect), or whether it is a more local zonation.

- Siltstone-rich units (3.1 and the various 1.1s) in the north-west have appreciable quantities of non-porous replacive sphalerite in both the matrix of siltstone and disseminated in stylolaminae. The same units in the south-east have virtually no zinc apart from minor sphalerite present in transgressive crackle veinlets with galena.

- In the lower portions of unit 1, siderite is more abundant in the north-west than in equivalent beds in the south-east. In hand specimen, some intervals appear to have been originally siderite rich and then overprinted by silica. Delicate stylolamination features are perfectly preserved; the rock is harder than normal siderite rich intervals and does not develop the brownish stain on exposure to the atmosphere. Silica-replaced siderite spheroids are evident petrographically (Plate 16D). No detailed petrographic work has been done to confirm the scale of this late post-siderite silica replacement.

- These changes in sulphide mineralogy and textures occur without any substantial change in thickness of the shale and siltstone units. However, in the north-western holes, the unit 2 shale appears to be more carbonaceous and laminated. Unit 2 in the south-east is much more siliceous and more massive in nature. The increased intensity of lamination in the north-west appears to be defined by layer-parallel intrusions of pyrobitumen and sphalerite (both porous and non-porous).

- Unit 4.2 has consistently low (<2%) sulphide content, although it has appreciable siderite content. It has been stained totally black by mobile organic material, has abundant siderite and, in places, has up to 1% euhedral galena. The reasons for the lack of major sulphide mineralisation are not known, as the unit has apparently been permeated by post-depositional, hydrocarbon-rich, fluids.

The lateral variations in sulphide species and textures are generalised on Figure 5.5, for a pre-Pandoras Fault (but post folding) geometry. The zones shown should not be interpreted as indicating exclusion of other sulphide textures or species. The purpose of the diagram is to show zones where differing sulphide species and textures appear to be better and more consistently developed than elsewhere. Any or all of the other main minerals and textures may be present in varying amounts within each notional zone.

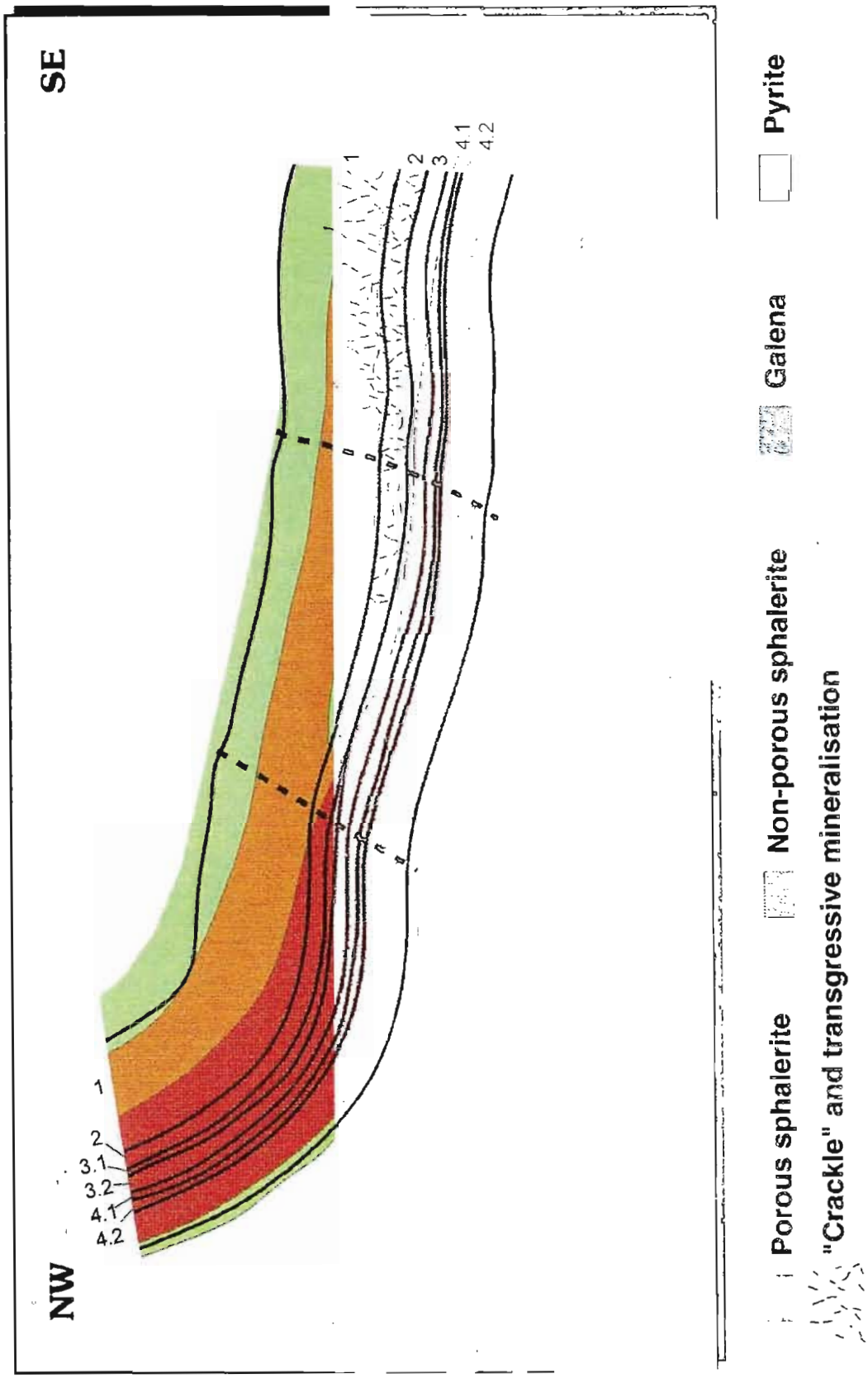

Figure 5.5 Century Deposit. Diagrammatic lateral sulphide zoning (pre faulting geometry) from north west to south east. Note specifically the stratigraphically transgressive nature of the porous/non-porous sphalerite zones and the limited distribution of the transgressive and crackle style mineralisation in the south east of the deposit.

5.4 Discussion

From the foregoing observations and discussion, a series of inferences for the development of the mineralisation are drawn.

5.4.1 Inferred Paragenetic History

A summary paragenetic diagram, synthesising the relationships of major sulphide and gangue phases to compaction and deformation events, is presented as Figure 5.6. Despite the complexity of textural relationships in individual specimens, the paragenetic progression of the main ore and gangue phases has overall consistency as shown. Siderite, hydrocarbons and main-stage sulphide mineralisation are constrained by their textural relationships to have occurred after sedimentation and early diagenesis. The following short summary of specific relationships within the paragenesis indicates emplacement of mineralisation during shallow to deep burial diagenesis and expanding in part into the early tectonic history. Discussion of more specific issues is made in subsequent sections.

Silica nodules and patches of silica cement (section 5.3.1) are the first diagenetic minerals in the paragenesis. These appear to have developed early in the burial history of the sediments, being enveloped and truncated by sediment compaction fabrics. Spheroidal siderite, the earliest hydrothermal mineral phase, systematically overgrows compactional foliations around silica nodules in siltstone facies. However, nodular and concretionary aggregates of siderite spheroids in shale units are commonly enclosed by compactional drape structures, indicating growth in under- or de-compacted sediment. This apparent paradox is discussed further in section 5.4.2.

Mobile pyrobitumen phases clearly post-date spheroidal siderite deposition, as evidenced by pyrobitumen infill of pore space in siderite nodules. Pyrobitumen is unambiguously the remains of former liquid hydrocarbon-rich phases (section 5.4.3). Most, if not all, sulphide mineralisation, including volumetrically dominant (70-80%) layer-parallel porous and non-porous sphalerite, post-dates or is partly

contemporaneous with hydrocarbon mobility. Although there is a slight tendency for non-porous sphalerite to overprint porous sphalerite, there is no convincing evidence that they represent radically different generations of sphalerite deposition. Rather, they respectively seem to be almost contemporaneously-deposited textural variants in pyrobitumen-poor and pyrobitumen-rich micro-environments. Section 5.4.5 discusses this further. Timing of some euhedral pyrite and minor euhedral galena cannot be determined exactly. Some may be earlier than hydrocarbons. The remaining (~10%) sulphides are deposited as progressively more transgressive and fracture-filling forms with associated minor quartz and siderite. Late sulphides appear to be associated with relatively lesser amounts of mobile organic material, although minor pyrobitumen is present throughout the late vein paragenesis, including the regional lode mineralisation (Bresser, 1992).

The relative timing of the lead and zinc sulphides is of interest. The ubiquitous corrosion and replacement of the volumetrically less-abundant early euhedral galena by sphalerite and quartz indicates continually changing conditions within the system, possibly related to continuous influx of hydrothermal fluid and ongoing fluid:rock interaction as main phase sphalerite was deposited. However, the main volume of the lead mineralisation post-dates the majority of the zinc, as shown by the systematic overprinting relationships of late galena to layer-parallel sphalerite textures. Further, there is little textural evidence to suggest that the lead dominated zones at Century have ever had substantial sphalerite content (section 5.3.12). This suggests either changes of metal ratios in the hydrothermal fluid with time, or that conditions governing metal precipitation within the system were locally different, and changed with time (section 5.4.4).

The textures unambiguously indicate that the layer-parallel sulphides are overprinted by more transgressive sulphide textures which are, in turn, deformed and brecciated by brittle-fracture controlled mineralisation. This is interpreted to indicate a progression of mineralisation processes within an increasingly lithified and more brittle host sequence. The orientations of many of the latest fractures are consistent with their origin as extension fractures related to major north-south fold deformation (section 4.6). Post mineralisation faulting then disrupts main stage mineralisation (section 4.7).

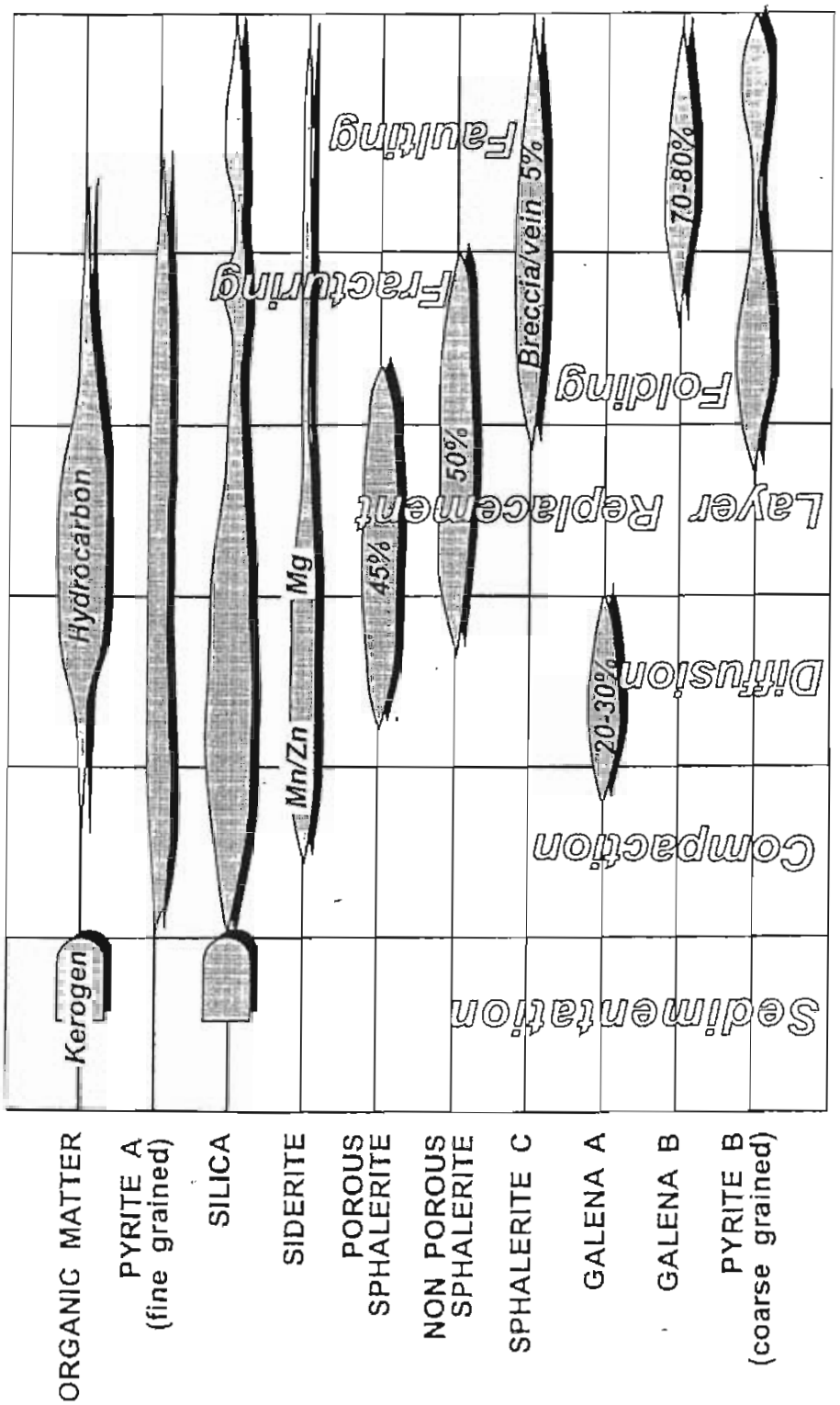

Figure 5.6 Century deposit. Summary paragenetic diagram. Percentages indicate the proportion of specific minerals represented by this stage, e.g. 50% of all sphalerite in the deposit is non-porous sphalerite and 70-80% of all galena is in late transgressive forms.

5.4.2 Siderite and Silica Relationships

Overprinting relationships of siderite to compactional foliations surrounding small folds, silica nodules and patches of silica cement are described in section 5.3.1. Development of silica nodules and cement appears to be a function of early diagenetic processes during early sediment burial. Subsequent deposition of siderite appears to be the first manifestation of the mineralising process. Stylolites are the first textural features to truncate siderite, but these are also sometimes overprinted by siderite (e.g. Plates 8A, 21D). Silica is mobile throughout the paragenesis. These observations indicate that the processes of sediment (silica) dissolution and siderite deposition were likely contemporaneous over a substantial portion of the burial and mineralisation history, with a possible common generic linkage to chemical processes outlined in section 3.7.3.

Spheroidal siderite and siderite mosaic cements in massive siltstone beds post-date early silica cementation and overlap development of stylolitic dissolution fabrics. Paradoxically, genetically-related siderite nodules and concretions have textures which suggest the siderite was deposited in poorly compacted shale beds (Plates 18C, 18D, 5G). Siltstone and shale clearly were at different states of compaction during siderite precipitation, and some explanation must be found for this. The concepts for differential compaction, seal and overpressure development that are developed in section 3.7.4 may be invoked to explain the differential behaviour of shale and silt facies. The shale facies either remained under-compacted relative to siltstone facies until accessed by mineralising fluids, or they became inflated by fluid during hydrothermal activity, effectively de-compacting them and enabling siderite concretion/boudin (section 4.5) growth.

5.4.3 Hydrocarbon Relationships

The large thicknesses of organic-rich shale in the Lawn Hill Formation would have been good source rocks for hydrocarbons. Indeed, elsewhere in the region Mid-Proterozoic sequences are still undermature (Lawn Hill Formation 50 km to north of

Century; Velkerri and Barney Creek Formations in McArthur Basin) and have been explored for hydrocarbons (Summons et al., 1988; Crick et al., 1988; Jackson and Raiswell, 1991; B. McConachie pers. comm., 1992; Comalco unpublished data). Abundant kerogens (now degraded) have long been known in the Mt Isa and HYC deposits (Saxby, 1970; Saxby and Stephens, 1973) and have been implicated as important agents for the precipitation of base metal sulphides at HYC by Williams (1978). Possible relationships of organic compounds to the production of carbonate phases in mineralisation assemblages have been infrequently considered. In normal diagenetic processes, organic matter has an important role in both organically and inorganically catalysed carbonate production (Irwin and Curtis, 1977; Curtis, 1978; Irwin, 1980; Curtis and Coleman, 1986; McMahon et al., 1992; Mozley and Wersin, 1992; Okita, 1992). This theme is discussed further in section 7.3, after consideration of chemical and isotopic data in Chapter 6.

The abundance of bedding parallel lamellae of pyrobitumen within the mineralised shale requires further discussion. It may be that these are the product of *in situ* maturation of algal mat material. This is the commonly suggested mode of origin of the carbonaceous matter at McArthur River and Mt Isa (e.g. Muir, 1985). There is no doubt that much of the organic material is intrinsic to the sedimentary beds, particularly the brownish filamental partings within the shale and the common diffuse brownish staining of siliceous siltstone lithologies adjacent to shale bands (Plates 7E; 13A, 13B; 4A, 4B, 4C). However, several factors suggest that a substantial component of the pyrobitumen may have either migrated within, or been introduced into, the mineralisation sequence. These include:

- total organic carbon contents (TOC) up to 10% in some samples have been reported by Minenco (1991). Systematic TOC analyses still require to be done. However, preliminary data (uncorrected for siderite) collected in this study indicate total carbon content of low-siderite shale intervals in the ore sequence shale beds to range from 1.1% to 7.8% (Appendix 4). Over 1 to 1.5m widths, total carbon values for unit 2 range from 1.1 to 5.5% and for unit 4.1 from 4.4% to 7.8%. Even allowing for some contamination by siderite (less than 1% in most samples analysed; compare intervals in Appendix 4 with detailed logs on

Enclosures 3 and 5), these values are comparable to normal TOC ranges for organic-rich shale reported by Huyck (1991). However, the apparently large variation of carbon content in individual units across the deposit is at odds with simple *in situ* maturation of organic matter.

- the widespread fracture filling pyrobitumen is undoubtedly exotic (albeit of possibly only minor travel distance) with respect to its present position (Plates 7F; 13F). Fronts of mobile carbon commonly impregnate otherwise non-carbonaceous lithologies asymmetrically away from stratabound fractures (Plates 6A, 6B; 7F, 7G, 7H). In thin section these fractures are ubiquitous within the shale; asymmetric distribution of pyrobitumen lamellae away from pyrobitumen filled microfractures is common (Plates 21E; 15F).

- the stylolitic dissolution surfaces are commonly filled with pyrobitumen which is not uniformly distributed. Conventionally, the carbonaceous material in stylolites would be interpreted to exclusively represent an insoluble residue from solution processes. However, the presence of apparently fluid pyrobitumen infill in many stylolites demonstrates widespread physical mobility of hydrocarbons. Along-layer mobility of hydrocarbons within the shale facies is interpreted to be a related effect (Plates 6A, 6B; 7F, 7G, 7H). Shale and siltstone facies clearly behaved mechanically differently during hydrocarbon mobilisation. Overall relationships constrain hydrocarbon mobility to at least be synchronous with stylolite development and to mostly post-date siderite precipitation.

These inferences, together with the widespread pore-filling nature of the pyrobitumen, raise the possibility that the mineralisation sequence at Century once hosted an accumulation of liquid hydrocarbons analogous to a petroleum reservoir. The host sequence of the deposit in no way resembles a conventional coarse-grained clastic reservoir lithology. However, a class of fracture associated reservoirs within mudrocks have been described in the petroleum literature, where the hydrocarbon source rock stratigraphy encloses or becomes the reservoir rock for the hydrocarbons (London, 1972; Greer and Ellis, 1991; Redwine, 1981; Roehl, 1981). These *source-reservoir* traps are characterised by the occurrence of hydrocarbons in pervasive porosity created

by intense microfracturing. The fractures occur as discrete stratabound networks within otherwise low permeability silt- or carbonate-rich shaly lithologies. Reservoir units are either organic-rich, or enclosed within organic rich shale, the organic content of which is thought to constitute the source of the hydrocarbons. The sealing lithofacies for the reservoirs are the enclosing sedimentary beds (usually clastic mudrocks). Occlusion of porosity and permeability by carbonate cements commonly provides the up-structure seal to the reservoir. Biogenic or thermal degradation of hydrocarbons, organic acids and early formed organic maturation products are possible source agencies for these carbonates (Irwin and Curtis, 1978; Curtis and Coleman, 1986; Hunt, 1990; Jensenius and Burrus, 1990). Typical vertical thicknesses of the reservoir facies are around 10-50 metres.

An example of such a reservoir (West Puerto Chiquito Field) has been described by Greer and Ellis (1991) and London (1972) and there is an extensive literature on the Monterey Shale of California (e.g. Redwine, 1981; Roehl, 1981), which hosts many fracture-controlled hydrocarbon reservoirs. Also, in the Monterey reservoirs, an intricate network of microfractures, texturally very similar to the late Century sulphide veins, hosts dolomite and hydrocarbons (see Redwine, 1981). It is possible that the process of generation of the hydrocarbons generates sufficient internal overpressure to actually initiate the network of fracturing which constitutes the reservoir (Palciauskas and Domenico, 1980; Spencer, 1987; Buhrig, 1988; Barker, 1990; Hunt, 1990).

An interesting feature of modern reservoirs of this type is that they occur at depths between about 1000-3000m (at the onset of the oil window in normal thermal conditions) and that the source-reservoir facies downdip of the reservoir are still probably actively-generating hydrocarbons. In other respects, the normal zoning of a conventional oil reservoir is present; a gas-rich cap is common, together with a lower oil-water contact (e.g. Greer and Ellis, 1991). Carbonate accumulations are a feature of fossil oil/water contacts (Burley and McQuaker, 1992).

Hydrocarbon migration occurs primarily along the source reservoir strata into more fractured areas (in particular gentle monoclinal flexures or fold warps) to produce accumulations of economic interest. Lorenz et al. (1991) give interesting data on the

orientation of these microfractures relative to regional stress fields. It seems that, in an overpressured sequence, regional stresses (far-field stresses) which would normally be insignificant with respect to the strength of the host lithologies become sufficient to induce localised failure of the overpressured horizon. A dimensional or preferred orientation could thereby be imparted to the fracture pattern of the reservoir sequence.

The pyrobitumens at Century have many features that are compatible with a source-reservoir trap model. The textures of the mineralised microfractures presented in Chapter 4 are congruent with mineralisation being formed in an overpressured environment such as a source-reservoir trap. In this context, further work on the orientations of the early mineralised stylolitic fractures could therefore be done to infer regional stress fields close to the time of hydrocarbon generation, reservoir development and, therefore, main stage mineralisation. The orientations of the paragenetically late, more brittle, mineralised fractures are interpreted to indicate their development as internal extension fractures related to the D2 north-south folding (section 4.7).

In conclusion, a source-reservoir hydrocarbon model is the preferred interpretation for the features of the pyrobitumens at Century. Zoning of different sulphide species relative to an interpreted paleo-hydrocarbon reservoir geometry is discussed in section 5.4.5.

5.4.4 Sulphide Timing Relationships

At Century, the corrosion and replacement of the early growth-zoned galena by sphalerite and quartz and the subsequent deposition of layer-parallel sphalerite require brief discussion in the context of some commonly held models for ore fluid evolution and mineral precipitation. The late timing of the majority of the lead mineralisation and the progression to more transgressive mineralisation with time are also relevant in this context.

Increases in lead/zinc ratios for many base metal deposits with proximity to feeder structures are often mentioned in the literature (e.g. Davidson and Dixon, 1992;

Waltho et al., 1993). It has been reasonably well established by numerous thermodynamic studies (Etminan et al., 1984; Sverjensky, 1984; Jaireth, 1991) that in brines thought to be typical of base-metal mineralising systems, zinc becomes relatively more soluble with respect to lead with decreasing temperature. From this solubility relationship, one would expect the deposition of lead to be more proximal to higher-temperature fluid feeder-conduits.

The lead-rich south-eastern portion of the deposit, adjacent to the Termite Range Fault, would appear on this reasoning to be the most logical point of ingress of metal-bearing hydrothermal fluid. A similar conclusion was reached by Waltho et al. (1993), who proposed an early diagenetic timing for the mineralisation. They interpreted lateral changes in lead grades and lead:zinc ratios as evidence for fluid sourcing in the south-east of the deposit.

Despite the difference in timing indicated by this study and that postulated by Waltho et al. (1993), the interpretation of metal supply to the south-east of the deposit seems reasonable. The proximal areas of the fluid delivery system may have been too hot for the deposition of large quantities of sphalerite. As mentioned above, there is no evidence that the paragenetically-late lead-rich south-eastern part of the Century deposit ever had significant bulk sphalerite content. This could imply that the transgressive galena is laterally equivalent to more distal sphalerite mineralisation. In a prograding sub-surface hydrothermal system there would be a logical expectation of considerable replacement of early layer-parallel sphalerite by galena as the system expanded. Although at Century this could be considered to be generally correct, because the majority of galena does indeed overprint sphalerite, in the early parts of the paragenesis the reverse is true. The textures indicate that the Century system was probably more complex than permitted by a simple steady-state model of fluid supply. Fluctuating temperature conditions within the system possibly explain the observed replacement relationships and are still consistent with major fluid ingress in the south-eastern portion of the deposit. This could imply major tectonically-driven pulses of hydrothermal fluids through the life of the system. Alternatively, if a paleo-hydrocarbon reservoir system was present (section 5.4.3), fluid ingress may have been episodically impeded to various portions of the deposit due to fluctuating development

of gas phases. Some high-level stratigraphic units could have been episodically starved of fluid because of their position in portions of the reservoir that were repeatedly subjected to higher fluid pressures.

A possible alternative scenario for the relative dominance and restricted distribution of late galena at Century is that much of it may have been deposited during the overall decline of the hydrothermal system. Thermodynamically based arguments, using relative solubility and stability data, have been used to postulate that the character of mineralising brines should evolve with time to lead-rich compositions because of reactions with wall-rocks in fluid conduits (Sverjensky, 1984).

Full resolution of these very interesting questions is considered to be outside the scope of this thesis, although further arguments are developed in subsequent sections and chapters to develop a preferred hypothesis. They constitute worthy topics for further research and thermodynamic modelling.

The above ideas should be briefly considered in the context of another interpretational debate concerning the significance of transgressive mineralisation in sediment-hosted orebodies. Traditional SEDEX models explain stratabound transgressive ore textures as the product of closed system remobilisation of pre-existing sulphide. Epigenetic replacement models usually interpret mineralised fractures as being feeders for mineralisation. Both of these alternatives have the logical corollary that mineralisation of varying textural characteristics and timing would be expected to have rather similar isotopic systematics.

It could be argued at Century that the textures of the transgressive sulphides are the result of remobilisation. However, consideration of the relationships of the volumetrically more-important late galena prompts some substantial objections to this. First, the early euhedral galena, which would be the logical source for any remobilised material, is associated with zones of relatively-low bulk-lead content throughout the deposit. There is no evidence for the existence of any relict textures in the lead-rich south-eastern portion of the deposit to indicate that early phase euhedral galena was more abundant in this area of the deposit (section 5.3.12), so sourcing the required

amount of lead is problematic. The feeder role of late transgressive mineralisation textures is problematic in other ways because of the consistency of overprinting relationships to earlier layer-parallel mineralisation and the large scale over which this occurs. There is, however, some textural support for early generation stylolitic fractures (section 5.3.1) to have functioned as conduits during emplacement of layer-parallel sulphides.

At Century, the transition to more transgressive sulphide textures with time suggests ongoing mineralisation in an increasingly lithified and more brittle host sediment, with an attendant decline in fluid:rock ratio at the micro-scale. In Chapter 6, paragenetically-constrained isotopic data is used to further interpret the possible genetic significance of this textural progression.

5.4.5 Sulphide Deposition in a Paleo-hydrocarbon Reservoir

This section further builds on the discussion in sections 5.4.3 and 5.4.4 by considering the patterns of metal grade distribution in the context of textural and spatial changes in sulphide and gangue species. It is already established that lateral variations in zinc grade demonstrate systematic changes from as much as 40 volume % sphalerite to about 5 volume % sphalerite without any corresponding changes in stratigraphic thickness or addition of compensating gangue phases (Figs 5.2; 3.7). This is considered *prima facie* evidence for the mineralisation to be of replacement origin.

Figure 5.7A shows the relative abundance of porous and non-porous sphalerite types in unit 2 from the north-west to south-east logging transect. Figure 5.7B simply relates this to an idealised cartoon of a speculative hydrocarbon reservoir geometry. This conceptual model should be considered in the context of the cross-stratigraphic metal migration described in section 5.2 (Fig. 5.4) and the sulphide zoning described in section 5.3.12 (Fig. 5.5). The relative abundance and distribution of the porous and non-porous sphalerite types can be related in geometric and process terms to the existence of a possible hydrocarbon reservoir prior to, or synchronous with, mineralisation. The predominance of hydrocarbon-rich porous sphalerite in the lower portions of the system is explained by postulating that this zone was oil-dominated.

The relative paucity of pyrobitumen in the zone rich in non-porous sphalerite is related to emplacement in a more gas-rich cap.

This is admittedly a radical model for a shale-hosted base-metal deposit, but Century appears relatively unique amongst major shale-hosted base-metal deposits in terms of the clear relationships indicating mobility of organic material and its intimate relationship with sulphides. Interactions between hydrocarbons, diagenetic sulphates and metal-rich fluids in paleo-hydrocarbon reservoir systems have been postulated many times for MVT-style base metal systems (e.g. Cadjebut deposit, W.A.; Tompkins et al., 1994; Admiral Bay deposit, W. A.; McCracken, 1997).

Figure 5.8 presents a schematic reconstruction of the reservoir configuration relative to the internal deposit stratigraphy. Initial top seal to the reservoir environment could have been provided by the early diagenetic cementation of the hanging-wall sandstone (section 3.7.4), augmented by siderite cementation of the hanging wall siltstone (section 5.3.2). Closure of the reservoir could have been assisted by the stratigraphic pinch-out from north-west to south-east (section 3.3.6).

Previous workers have attempted to explain aspects of the metal zoning and relate them to location of possible fluid conduits. Wright (1992) noted the congruence of the north-east to south-west decline in grade with the regional strike of the Termite Range Fault. He implicated the fault to have been a major fluid source, into a speculative hydrocarbon "kitchen", but did not establish timing, reservoir geometry or seal mechanisms. Waltho and Andrews (1993) attempted to link changes in zinc/lead ratios with subjectively assessed changes in silt content of the sequence from west to east. They speculated that the sedimentological change may have in some way caused altered internal chemical conditions in some units to give different sulphide abundances and postulated the conjunction of the Termite Range Fault and the

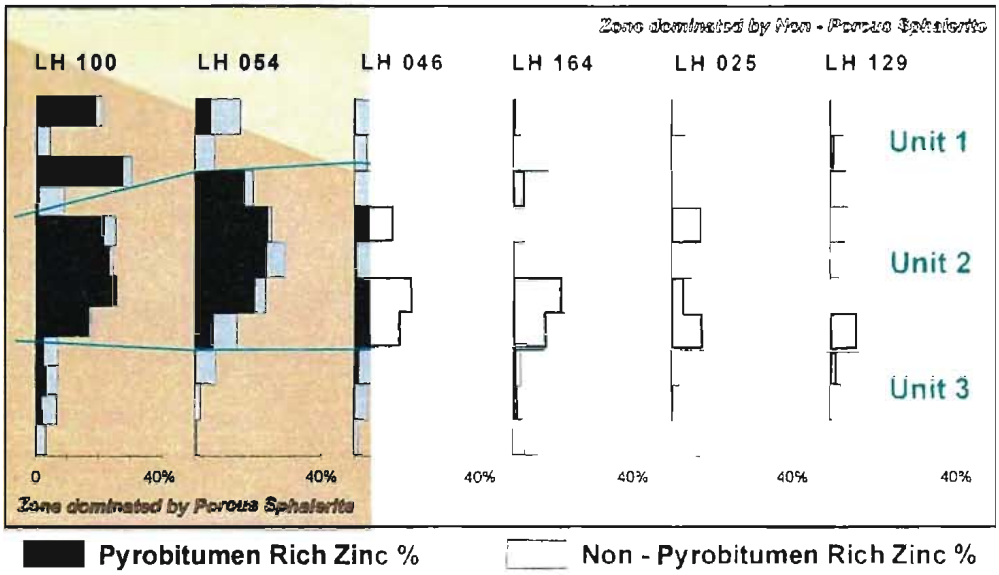

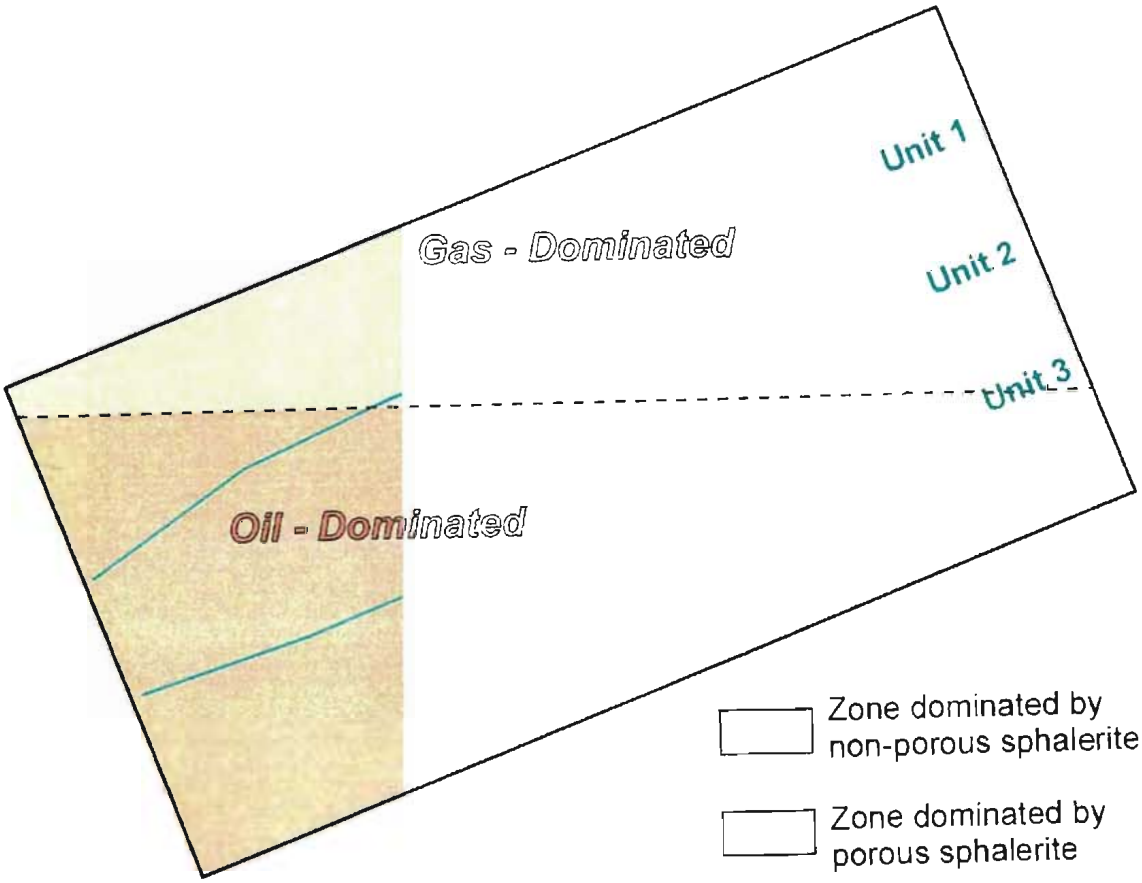

Figure 5.7 A: Relative proportions of major sphalerite types along a north-west to south-east transect, conceptually related to overall zoning of sphalerite types (Fig. 5.5). B: Schematic reconstruction illustrating pattern of cross-stratigraphic sphalerite zoning in relation to a conceptual oil:gas contact.

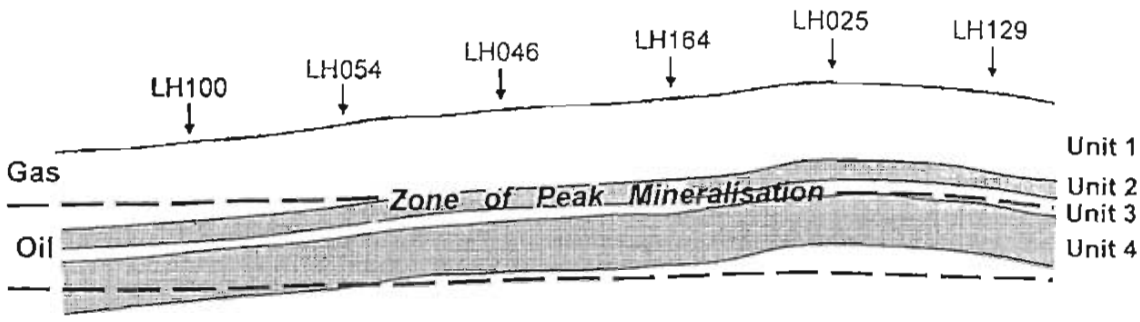

Figure 5.8 Schematic reconstruction of paleo-hydrocarbon reservoir configuration at Century. Drill holes are those shown on Figure 5.7. The zone of most intense mineralisation (i.e. highest zinc grades) is interpreted to have been concentrated along a paleo gas:oil interface. Non-porous sphalerite is more common above the interface, porous sphalerite below it (refer Figure 5.5). Sections 6.7.4 and 7.6 discusse possible chemistry of mineralising processes.

Magazine Hill Fault as a possible entry point for metal bearing fluids to an early diagenetic system.

The Century paleo-hydrocarbon reservoir scenario combines and expands some aspects of both of the above interpretations whilst rejecting others. Fluids important for the deposition of metals were most likely introduced to the deposit area along a predominantly north west striking feeder conduit (as evidenced by the north-east to south-west decline in total metal content). The north-east striking structural discontinuities discussed in sections 3.7 and 4.7 could plausibly have localised fluid flow along the plane of the Termite Range Fault, enabling focussed entry of fluid to the orebody area. Interestingly, the along-strike continuation of the north-east striking Silver King line of lode projects into the zone of peak lead grades in the deposit (Fig. 2.7). Within the mineralised sequence, fluid movement would have undoubtedly been strongly influenced by the differential porosity and permeability of the massive siltstone units, with a possible tendency for the thicker units in the north-west of the deposit to act as aquifer facies. The siltstone facies could therefore have acted to drain spent fluid away from the site of mineralisation, or they could have introduced other necessary reactive components of the mineralised system from elsewhere.

5.4.6 Depth of Mineralisation Emplacement

In a review of structural features diagnostic of non-tectonic deformation (ie slump folds and the like), Elliot and Williams (1988) suggest that axial foliations and low angle systematic foliations around slump folds are only developed by compaction after a minimum depth of burial of 100 metres. If this is correct, a minimum depth of burial of 100 metres may be assumed for the onset of siderite (and therefore hydrocarbon and sulphide) deposition. In any case, siderite alteration extends for at least 80 metres into the hanging wall, giving a minimum depth of burial of 80-100 metres. There are grounds for suspecting that the deposition of siderite commenced during deeper burial than this.

Weak siderite development and hydrocarbon staining in the ~550 metre thick Pmh5 hanging-wall sandstone sequence overprints authigenic clay and chlorite cements (section 3.2; Andrews, 1998b). If these are related to the same processes which generated the siderite and hydrocarbons in the hanging-wall and mineralisation sequences, then sulphide emplacement must post-date deposition and cementation of the hanging wall sandstone. This implies a burial depth of at least 6-700 metres and probably more.

The stylolitic bedding surfaces and high-angle stylolitic fractures (Plate 12, esp. 12C), offer additional constraints on the depth of siderite formation, hydrocarbon mobilisation and sulphide deposition. In most examples in the literature (e. g. Braithwaite, 1989), stylolites are generally interpreted as indicating even deeper burial - perhaps several hundred to several thousand metres, depending on the extent of overpressuring effects within the sequence. The mutual relationships of siderite, stylolites, hydrocarbons and sulphides (section 5.4.2) offer a further line of evidence that mineralisation commenced development at an appreciable depth of burial, in excess of several hundred metres.

Although the majority of the stylolites are sub-parallel to bedding the ubiquitous development of cross-cutting stylolitic fractures justifies the inference that the

mineralising system was probably overpressured during their development (section 4.8). Development of overpressure is widely documented in the petroleum literature in many, if not most, sedimentary basins at an average depth of around 3000 metres (Hunt, 1990). The processes involved in overpressure development in such basins are intimately related to processes of organic acid destruction and incipient hydrocarbon generation (Hunt, 1990). The juxtaposition of textural evidence for overpressure accompanying hydrocarbon mobility and mineralisation at Century is interpreted to be more than coincidental.

Overpressure development is essentially a physical phenomenon where fluid pressures locally exceed the normal lithostatic loading beneath a seal and, as such, cannot be assigned an exact depth. However, at Century, there is an interesting correspondence between the textures and mineral assemblages present and the textures and mineral assemblages expected from a normal sedimentary basin environment that experienced overpressured conditions during normal burial processes. It is well known that one of the vital factors influencing the diagenetic reactions that are linked to hydrocarbon-induced overpressure is temperature (Hunt, 1990).

At Century, a general state of advanced compaction and silica dissolution in siltstone facies precedes the earliest stages of siderite deposition. The critical temperature range for carboxylic acid generation and destruction ranges from 80 to 120^{0}C, just before the onset of oil generation (the zone of peak diagenesis as defined by Surdam et al., 1989). Textures at Century then appear to indicate the onset of overpressured conditions, including hydrocarbon mobility, during main stage mineralisation. Pre-existing under-compacted organic-rich shale units would be especially prone to localised overpressure. It seems plausible that the localised invasion of a hot fluid associated with mineralisation would accelerate the progression of normal diagenetic processes, possibly up to, and including, overpressure development and hydrocarbon generation. This hypothesis could imply initiation of the mineralising system at a depth possibly as great as 3000 metres.

5.5 Summary

The bulk of mineralisation at Century, in terms of both grades and volume of metal, is preferentially hosted by shale facies. Shale units have excellent lateral continuity and consistent thickness, but varying metal grades, in the mineralised sequence. The point of maximum development of base metal sulphides within the deposit stratigraphy is not fixed and moves progressively up through the stratigraphy from south east to north-west. The mineralisation is therefore stratabound rather than stratiform, despite individual sulphide (and pyrobitumen-rich) lamellae appearing to be bedding-parallel at hand specimen scale and, in underground openings, up to several metres across. Taking into account the lack of any apparent exhalite facies, this cross-stratigraphic metal distribution is difficult to reconcile with any model of exhalative origin for the sulphides. Post-sedimentary emplacement of mineralisation is clearly indicated, the major questions are when and at what depth this occurred.

The earliest textural change in the host sediments is the precipitation of early silica nodules and cement. Dissolution of the silica-rich matrix of the sediments occurs adjacent to organic-rich laminae, giving rise to bedding-parallel compactional foliation. Stylolitic dissolution surfaces are a diagnostic textural change within the host sedimentary beds with proximity to mineralisation. They are interpreted to be the result of chemically similar, but considerably more intense and prolonged, organic-silicate reactions. The increase in intensity was likely promoted by a substantial hydrothermal fluid component.

The sediments may have had a minor component of early authigenic carbonate cement, although derivation of siderite appears to be linked to hydrothermal processes. Siderite is widespread throughout the hanging-wall and mineralisation sequence and increases in abundance with proximity to the mineralised zone. Spheroidal siderite clearly replacively overprints compactional foliations and silica cement nodules, constraining its timing as being later in the burial history.

Textures of the siderite indicate it to have a complex history, with evidence of changing compositions and morphologies with time, from discrete spheroids and

matrix cement to later overgrowing rhombic forms in pore space. Siderite in the deep footwall sequence has slightly different morphology but similarly replaces compacted sediment fabrics. Early siderite assemblages were then subsequently invaded by mobile hydrocarbons, corroded and partly replaced by base metal sulphides. Minor siderite was deposited contemporaneously with later base metal sulphides in vein and fracture infill. It is inferred that the above-mentioned chemical and textural complexity of hydrothermal siderite could reflect progressive interaction of hydrothermal fluids with originally partly lithified or de-compacted sediments.

Organic material within the sequence occurs either as a finely dispersed phase probably deposited as algal detritus with the clastic material, or as mobilised invasive pyrobitumen. The pyrobitumen almost certainly represents the degraded residue of original liquid hydrocarbons. This mobile hydrocarbon phase postdates much of the siderite, with evidence of repeated hydrocarbon mobility during subsequent fracturing and mineralisation processes. Textures of the Century mineralisation are very similar to descriptions of source-reservoir type hydrocarbon accumulations (London, 1972; Greer and Ellis, 1991; Redwine, 1981; Roehl, 1981). It is suggested that such a hydrocarbon reservoir may have existed at Century, contemporaneous with or pre-dating sulphide mineralisation.

Sulphides were deposited in the order euhedral galena, to porous and non-porous sphalerite, to transgressive/replacive galena and sphalerite, to vein and breccia sulphides. Fine-grained pyrite on the periphery of the base metal mineralisation has complex unresolved timing relationships with other mineral species.

Porous sphalerite mineralisation, which comprises around 40-45% of the total zinc in the deposit, is intimately intergrown with pyrobitumen, thereby constraining its timing as relatively late. Non-porous sphalerite, which comprises the other main textural variety of sphalerite, is also clearly replacive and deposited almost contemporaneously with porous sphalerite. It has a more cryptic relationship with organic matter.

Zoning of the two sphalerite types is consistent with their deposition in a paleo-hydrocarbon reservoir, with a low angle of closure towards the south-east of the

deposit. The point of peak metal enrichment in the system is tentatively proposed as the gas:oil contact in the paleo-reservoir.

Early stylolitic fracture textures appear to show a progression into late, more brittle, fabrics, perhaps indicating more of a continuum of process than a series of discrete overprinting events. Microfracture conduits were prime agencies for the transmission of mineralising fluids and reaction products within the mineralised zone, in combination with layer-parallel diffusive migration of materials in the early stages of the system. From Chapter 4, the geometry of the late vein and breccia phases is consistent with their development as stratabound extension fractures during N-S striking folding; relationships of earlier fractures and siderite nodules are inferred to relate to earlier south-east to north-west shortening. Depth of emplacement of the Century mineralising system is uncertain. It most likely exceeded 700 metres, but could have been as great as 3000 metres.

Chapter 6

Geochemistry

6.1 Introduction

This chapter documents geochemical and isotopic data from paragenetically constrained samples of Century mineralisation. High temperature pyrolysis and organic reflectance techniques were used to investigate the compositional and thermal maturity of organic material, to give insights into the peak thermal regime experienced by the mineralisation. Because of their close spatial and probable genetic relationship to mineralisation, siderite compositions were investigated by electron microprobe analysis. Chemical data are then linked to changes in carbon and oxygen isotopic composition of siderite. Preliminary sulphur isotope data have been obtained from the major sulphide varieties within the deposit. The sulphur isotope data are presented in context with data obtained from the regional lodes by Bresser (1992). Lead isotope data from the Century deposit are then compared to available data from the regional lodes and to data from other major deposits of the Mt Isa-McArthur province.

Subsequent discussion focusses on the implications of these data to the temporal evolution of the mineralisation and the scale of the regional fluid system, to help establish constraints for a wider-ranging discussion of processes in Chapter 7.

Major and trace element abundances for the mineralisation and enclosing sedimentary sequence have not been examined. Full documentation and interpretation of geochemical data is beyond the scope of this investigation and is a clear priority for future workers. Waltho et al. (1993) briefly examined multi-element correlations for analyses of ore composite samples. They noted that the only elements apart from lead and zinc to show significant variation with intensity of mineralisation were iron, manganese, thallium, mercury and arsenic. Not unexpectedly, total iron and manganese appear to correlate with siderite abundance. Thallium, mercury and arsenic appear to be higher in the south east of the deposit area. The reasons for this are not known; Waltho et al. (1993) postulated that this area of the deposit was a principal feeder zone for metal-bearing fluids. Copper and barium contents of the mineralisation

are extremely low. The significance of the low abundance of these latter two elements is discussed further in Chapter 7.

6.2 Organic Material

A single sample, C201, of pyrobitumen from a siderite nodule within organic-rich shale from the mineralisation sequence was analysed to determine whether any residual complex hydrocarbons remained in the pyrobitumen phases. This was prompted in part by preliminary metallurgical work (Minenco, unpublished data, 1992), which indicated that trace amounts of complex immature organic phases were present in zinc concentrates. The analysis was conducted by AES consultants of Melbourne, using high temperature pyrolysis followed by gas chromatography - mass spectrometry (Leeder, 1992). A sample of organic-rich shale, C294, from the Lilydale stratigraphic drillhole (DD91LH265; Fig. 2.7), was also analysed, to provide a reference analysis from unmineralised stratigraphy.

Results from the pyrolysis (Leeder, 1992) indicate that no residual volatile hydrocarbons are present in the pyrobitumen-rich organic material from the mineralisation. The original Minenco results were probably due to contamination by flotation reagents. The reference sample from the Lilydale locality also had no extractable complex hydrocarbons. No clues can therefore be obtained to the original nature of the pyrobitumen – it now appears to be inert elemental carbon.

Organic matter reflectance measurements were determined for three samples (C215, C203, C214) from the mineralised zone, to obtain data on possible peak thermal conditions experienced by the mineralisation. This work was done commercially by M. Glikson of Queensland University (Appendix 4).

Reflectance values ranging from 2.1 to 2.7% were measured from both alginite and pyrobitumen phases. Data indicate likely maximum paleotemperatures between about 180°C and 200°C (M. Glikson, written comm., 1992). In one sample, mobile pyrobitumen intergrown with main stage sphalerite at Century shows slightly higher rank than alginites (R_0 of 2.7 versus R_0 of 2.2). True reflectance values (and therefore

T_{max}) may be higher than those measured, due to partial optical anisotropy created by incipient ordering of amorphous carbon phases (meso-impsonites) in the pyrobitumen (S. McKnight, pers comm., 1992). However, features suggestive of a thermal mesophase (Gize, 1985) have not been observed in the pyrobitumen, suggesting that degradation of the original hydrocarbon did not occur at high temperatures (250-300^{0}C). Additional data that may be relevant to estimates of paleo-temperature include a single fluid inclusion from late stage Century sphalerite, which gave a homogenisation temperature of 120°C (J. Wilkinson, pers comm., 1992). Bresser (1992) reported homogenisation temperatures between 110°C to 140°C from the regional lode mineralisation. Oil generation generally commences around 120°C (Tissot and Welte, 1978), which places a minimum temperature constraint on the mineralisation. These are discussed in the context of the organic maturity data in section 6.7.1.

6.3 Carbonate Compositions

The pivotal relationships of siderite within the deposit paragenesis are established in Chapter 5. Electron microprobe analyses were made of a representative collection of siderite samples from the hanging wall, mineralisation and footwall sequences, to characterise changes in elemental composition of different siderite species. Siderite-rich intervals were selectively sampled during detailed inspection of drill core. The hand specimen criterion used was the intensity of exterior red-brown staining on core samples (section 5.3.2). Three hundred and eighty three electron-microprobe analyses were performed by electron dispersive methods (EDS) on thirty samples using the JOEL JXA-840A at JCU. Spectra were collected and recorded on to floppy disc and then run through TRACOR Northern quantitation software. Particular problems were encountered with deconvoluting the iron and manganese values due to their adjacent atomic number and a difficulty in obtaining a sufficiently pure iron siderite to be used as a primary standard. Eventually, JCU silicate standards (calibration No 401; see Appendix 3) were used to obtain the quantitation corrections.

It is acknowledged that the use of a silicate standard will lead to some loss of absolute accuracy due to different matrix effects. As a check, spectra from available calcium- and magnesium-rich carbonates of known composition were calculated by the silicate standard and showed discrepancies of less than a few percent. This level of accuracy is considered acceptable given the relatively large variations in composition that were observed and in any case the internal relativities of the dataset will not be affected. Data are best treated as semi-quantitative. Data have been normalised to ideal stoichiometric proportions of cations to carbonate from the raw elemental percentages, to compensate for differences in sample surface, carbon coating integrity and grounding conditions within the SEM. Data are provided in Appendix 3 as normalised values, calculated to atomic percentages and summarised in Table 1.

Ore-zone and hanging-wall carbonates represent impure siderites, containing around 65-70 atomic percent iron and 0.4-3.7% zinc, 16-20% manganese, 2-3% calcium and 6.9-10.5% magnesium (Table 1). The late vein carbonates appear to be more enriched in magnesium relative to manganese, indicating a progressive change in siderite compositions with time during the life of the mineralising system. Plate 16 shows SEM backscatter images illustrating typical compositional and textural variations in various specimens.

As a subjective criterion for hand specimen logging, higher manganese content appears to correlate with the intensity of typical dark reddish-brown staining that develops on siderite-rich alteration after exposure to the atmosphere (refer section 5.3.2).

The data show very interesting trends in gross chemistry of siderite phases with proximity to mineralisation. Average siderite composition for entire samples are presented graphically on to a north-west to south-east cross-section of the orebody in Enclosure 2, to give an impression of the lateral and vertical changes in chemistry. Examination of the enclosure shows that four principal compositional groupings are present. These are summarised in Table 1 as averaged determinations (normalised atomic %) from various samples, grouped by their level in the stratigraphy.

TABLE 1: SUMMARY OF CARBONATE COMPOSITIONS

	Fe%	Ca%	Mn%	Mg%	Zn%	n =
Hangingwall - grain centres	67.1	2.8	19.5	6.9	3.7	26
Hangingwall - grain edges	69.8	2.6	16.5	10.5	0.4	12
Ore zone - grain centres	69.6	2.6	20.0	2.8	4.9	62
Ore zone - grain edges	68.9	1.8	19.0	8.0	2.4	94
Veins - early infill	77.5	0.6	16.7	5.3	0.0	14
Veins - late infill	70.6	0.6	15.2	13.3	0.3	21
Veins - Watson's Lode	73.1	1.0	8.0	17.6	0.3	5
Upper Footwall - all samples*	71.8	2.2	7.1	18.8	0.1	28
Lower Footwall - all samples	66.4	1.6	1.8	30.3	0.0	52

* Excludes the very high calcium analyses in sample C073, for details of these see Appendix 3.

Lower footwall sequence samples mainly comprise magnesian siderites, with low levels of calcium, manganese and zinc. Petrographically, these siderites characteristically consist of discrete rhombic crystals that selectively grew within more silt rich bands (section 5.3.2).

A single carbonate sample, C073, from the footwall sequence contains much higher levels of calcium and magnesium (Appendix 3). The (ankeritic) carbonate in this sample is a matrix cement similar in texture to the mosaic-textured siderite variety (section 5.3.2). This raises the possibility that some sedimentary facies in the stratigraphy have appreciable authigenic ankerite cement. Recent work by RTE in the region around Century has indicated the existence of ankerite-cemented facies in parts of the footwall stratigraphy (section 5.3.2; S. Tear, pers comm., 1998) and this sample may represent such material. However, a nearby sample, C072, has ankerite-rich veins which cross-cut siderite alteration (Plate 16F). The disseminated matrix carbonate in sample C073 may be related to this later vein mineralisation. Given this potential doubt, and that this study is only a preliminary investigation, sample C073 has been excluded from further consideration. However, more detailed work on the composition and textures of carbonates of the footwall sequence, in particular, is required.

A progressive change in siderite chemistry occurs with increasing proximity to the mineralised zone (Table 1). Manganese becomes progressively more abundant at the expense of magnesium. Zinc remains low until the base of the mineralised zone is reached, where it rather quickly rises to an average level of nearly four percent in spheroidal-type siderite. Manganese levels also rise rather abruptly from seven percent to around twenty percent. Magnesium declines from around twenty percent to five percent, with the iron content staying relatively constant. Hanging wall sequence siderites have a similar character to the ore sequence, but zinc and manganese are more variable.

Compositional variations within the hanging-wall and mineralisation zone siderites can be related to the morphological differences discussed in section 5.3.2. Brownish spheroidal siderite is enriched in zinc and manganese relative to magnesium. The later colourless rhombic varieties, together with the colourless phases within spheroids (Plates 8A, 8B, 8C) contain less manganese and very little zinc. A comparison of measurements on grain centres versus measurements on grain edges shows clear differences of composition, which can be related to paragenetically early versus late siderite phases (Table 1; Fig. 6.1A). Late siderite (grain edges) has lower zinc and higher magnesium content relative to early siderite (grain centres). Three samples in the late population more closely resemble the early pattern in Figure 6.1A. These samples exhibit more uniform composition, with a lesser proportion of overgrowing colourless siderite, so this is not unexpected. Figure 6.1B shows averaged bulk compositions for the same dataset in graphical form.

Elemental analysis of some siderite grains is also complicated by the presence of oscillatory zinc-rich and zinc-poor growth zoning (Plate 16B). Some rhombic siderite grains lining pyrobitumen-filled vughs are enriched in zinc. This may indicate that some early zinc-rich siderite grew into open space and was then isolated from further contact with carbonate-depositing solutions by bitumen infill.

Late vein- and breccia-infilling carbonate shows different compositions to the disseminated and spheroidal forms. Zinc is virtually absent and manganese is reduced from average contents of 16.5% in early infill to 15.2% in late infill. Magnesium

increases sharply from 5-6% in early infill to 13 % in late infill. Iron abundance decreases in abundance in sympathy (Table 1). Late infill compositions appear to be

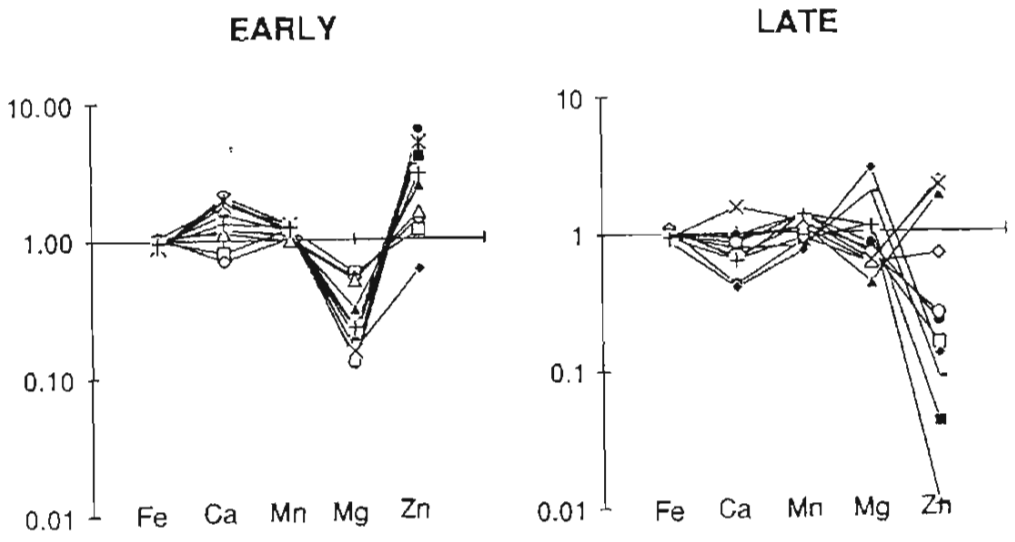

Figure 6.1A. Century deposit - Spider diagrams of early phase versus late phase compositions of siderites from nodule samples within the deposit.(samples C185; C201; C203; C205; C206; C212;C213; C214; C215; C293C). The average composition of the full EDS dataset (Appendix 3) has been used to normalise data for plotting purposes, to best illuminate trends in compositions.

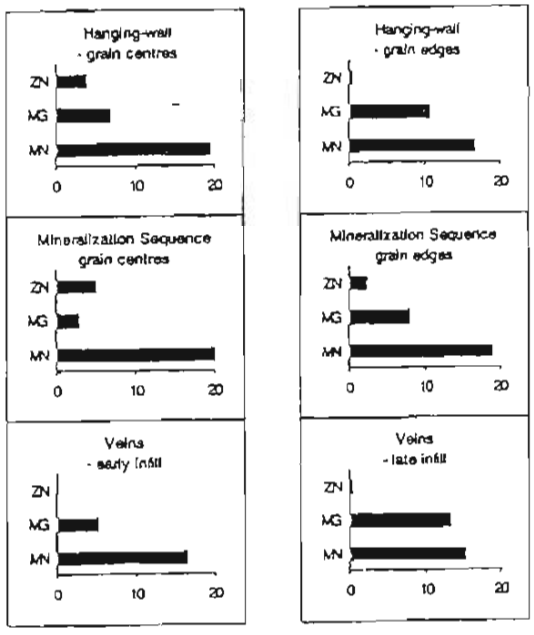

Figure 6.1B Comparison of averaged early and late siderite compositions for hanging wall sequence, mineralisation sequence and veins/polycrystalline aggregates for Zn, Mg and Mn. Data from Table 1, values in atomic %.

much more similar to that of the lodes of the Lawn Hill Mineral field, if the limited number of determinations from Watson's Lode are any guide (Table 1).

In summary, the electron microprobe data indicate two main compositional trends of siderite:

1. Footwall siderite is compositionally different from the ore zone and hanging wall siderite, with higher magnesium and lower manganese and zinc.
2. Mineralisation sequence and hanging-wall siderites change in chemistry with time, towards higher magnesium and lower manganese and zinc content. The bulk magnesium content of siderite is the most convenient parameter for comparing these trends with other data.

6.4 Carbon and Oxygen Isotopes

A selection of samples of siderite- and organic carbon-rich material were submitted for carbon and oxygen isotopic analysis, to yield insights into potential processes of carbonate generation. After hand specimen and petrographic observation, siderite-rich areas of selected specimens were drilled. The resultant sample powders were analysed commercially by the isotope facility at CSIRO Division of Exploration Geoscience, North Ryde, Sydney. Sample results and methodology are given in Appendix 5, together with average microprobe analyses for the samples (where determined; for raw data refer to Appendix 3).

It must be kept in mind that the samples consist of a mixture of different siderites in many of the samples, because of the impossibility of separating them. The trends in the data therefore partly reflect variations in the proportions of the siderite phases, and end member compositions can only be inferred.

Results for the samples are summarised on Figure 6.2, as scatter plots of carbon versus oxygen isotopic values and carbon isotope values versus magnesium content of the siderite. Magnesium was chosen as a plot parameter to assess the amount of isotopic

variation relative to the paragenetically constrained changes in siderite composition described in section 6.3. Figure 6.3 shows carbon and oxygen isotopic values and magnesium contents of siderites relative to their vertical stratigraphic level.

Data have a range of carbon isotope values from -8.3 to 3.1 ‰PDB. The majority of the hanging wall, ore zone and deep footwall disseminated siderites fall in a narrower range from -2.6 to 3.1‰PDB. The depth plot (Fig. 6.3) shows the deep footwall magnesian siderites to range from 0 to 3.1‰PDB, before a striking shift to negative values around 100m below the mineralisation.

The high magnesium siderites of the footwall sequence exhibit a strikingly narrow range in oxygen isotope values from 13 to 17 ‰SMOW until about 50 metres below the mineralisation (Fig. 6.3). The mineralisation sequence is complex and encompasses a rapid change to heavy oxygen isotope values from 20 to 25 ‰SMOW typical of the hanging wall sequence.

Carbon isotope values within the mineralisation are widely scattered. Most cluster from +2 to -2 ‰PDB, with some lighter values to –8 ‰PDB. Oxygen isotope values similarly range from 16 ‰SMOW to +25 ‰SMOW. The best constrained samples, siderite nodules from within the mineralisation, show a trend to light carbon and oxygen isotope values with increasing magnesium content. This could be interpreted as a mixing trend, with a high ^{18}O, low magnesium end member and a lower ^{18}O, high magnesium end-member. From the paragenetic relationships established in section 6.3 and 5.3.2, the lower ^{18}O, high magnesium, end-member is younger than the high ^{18}O, low magnesium, high-manganese and high-zinc end-member. The early manganese- and zinc-rich end-member composition is inferred to have slightly positive carbon isotope values (0-3 ‰PDB) and heavy oxygen isotope values (around +25 ‰SMOW). Composition of the late end-member is more difficult to judge, but could be around –2 to –4 ‰PDB for carbon and 12 to 14 ‰SMOW for oxygen.

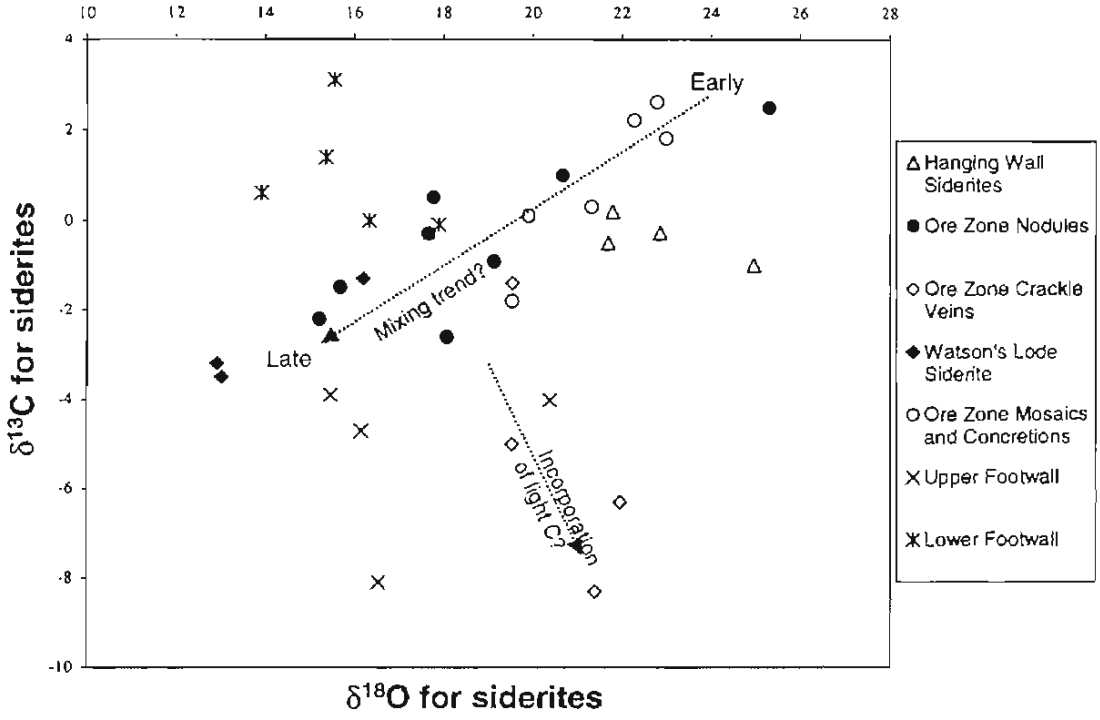

Figure 6.2A Scatter plot of carbon against oxygen isotope values of Century siderites. Inferred trends are discussed in section 6.7.3.

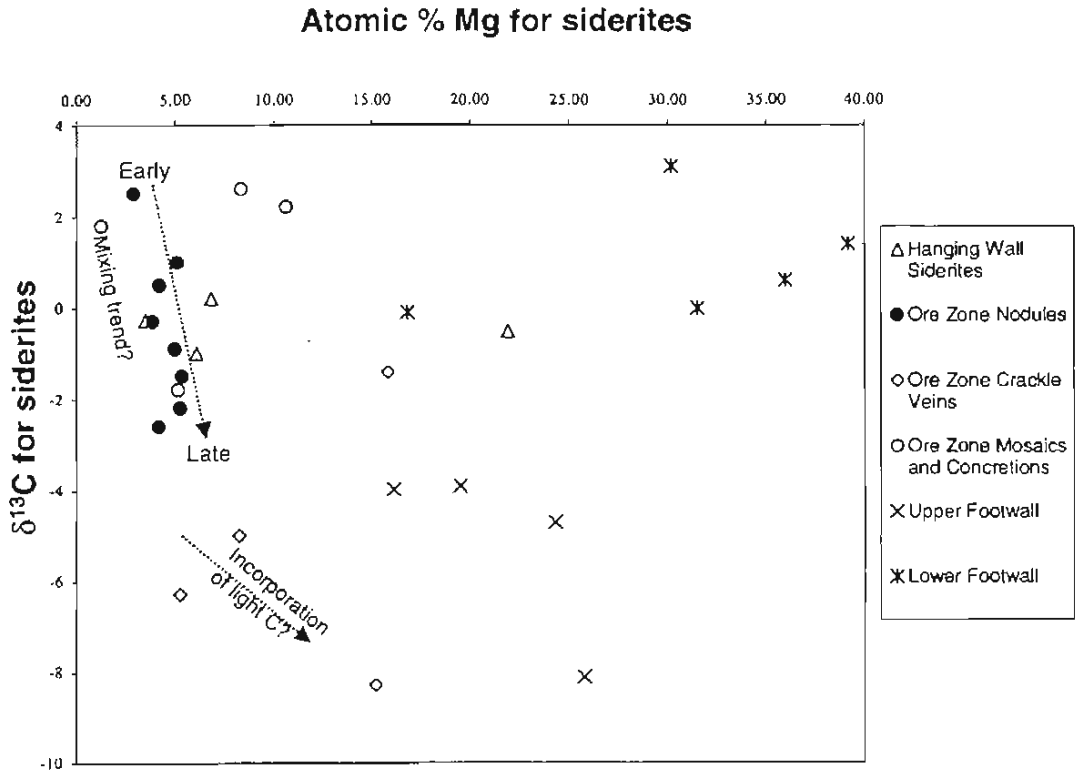

Figure 6.2B Scatter plot of carbon isotope values against magnesium content, Century siderites. Inferred trends are discussed in section 6.7.3.

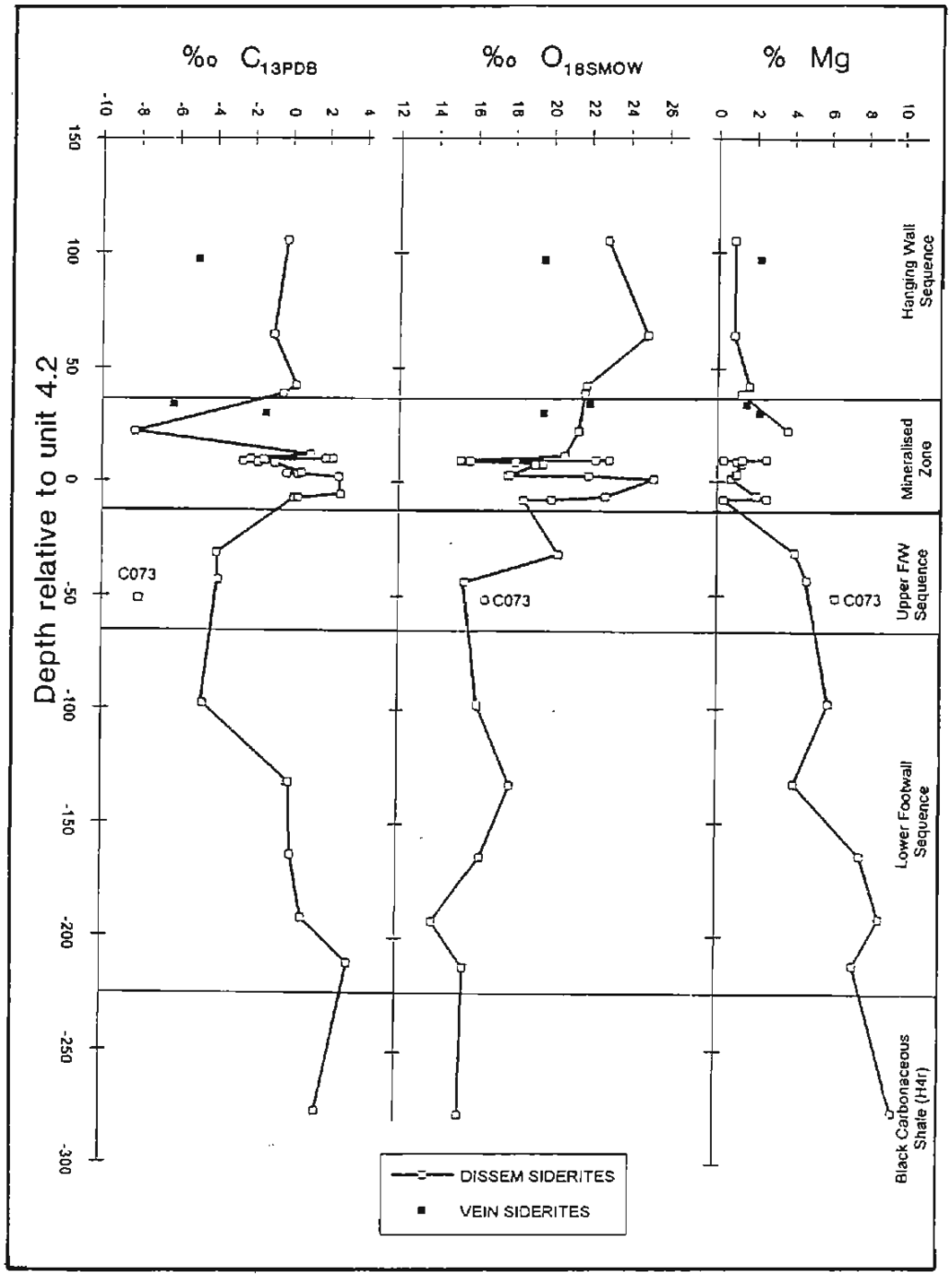

Figure 6.3 Century Deposit- Summary of carbon and oxygen isotope data shown relative to vertical stratigraphic position. Total magnesium content of samples also shown. High-Mg footwall siderites have relatively low δO_{18} content compared to low Mg hanging-wall siderites, ore zone material appears quite mixed. Significance of these observations is discussed further in section 6.7.3.

Late crackle vein-filling siderites from the mineralisation zone and immediate hanging-wall sequences have a wider scatter to light carbon (-2 to -8 ‰PDB) and lighter oxygen isotope values (20 to 22 ‰SMOW) than the disseminated early siderites. Isotopically light carbon, possibly derived from organic matter, may have been incorporated into these late siderites (Fig. 6.2, section 6.7.3). Organic $\delta^{13}C$ values in the dataset consistently lie in a narrow range from -30 to -33 ‰ PDB (Appendix 5b).

The lighter oxygen is interesting in the context of the low oxygen isotope values obtained from lode siderites. The Watson's Lode siderites give low oxygen isotope values, from 11.5 to 14.9 ‰SMOW. These have similarities to some footwall siderites at Century (the chemical similarities are noted in section 6.3), but appear to lie on the trend of mineralisation siderites (Fig. 6.2B). Local mixing of fluids could account for the intermediate values of the late vein siderites and the confused trends in the mineralised zone at Century, but more ingenuity is required to explain a continuance of the trend at Watson's lode. A speculative interpreted mixing trend for the mineralisation siderites is shown on Figure 6.2. Whether this represents a genuine mixing trend between different hanging wall and footwall fluid regimes or an evolutionary trend is discussed in section 6.7.3.

6.5 Sulphur Isotopes

Samples of sphalerite, galena and pyrite from paragenetically constrained specimens were submitted for sulphur isotopic analysis, to gain insights into the relationships between the various sulphide species and their textural variants. Some comparisons are also possible with data from other mineralisation. In particular, data from Century have been integrated with Bresser's (1992) data from the regional lode mineralisation.

After hand specimen and petrographic observation, sulphide-rich separates were prepared by drilling from hand samples. The resultant powder samples were analysed commercially by the isotope facility at CSIRO Division of Exploration Geoscience, North Ryde, Sydney. Raw data and methodology are reported in Appendix 6, with an accompanying list of descriptive textural features. Because of the very fine grainsize

of most sulphide species at Century, many of the samples have contamination from fine-grained included, or coexisting, sulphide mineral species. Therefore, estimates of amounts of contaminant phases determined by microscopic examination of the areas sampled are also given in the sample description list in Appendix 6. Samples with contamination levels less than 10-15% are judged as adequate for giving useful information for the broad scale trends judged here to be significant, whereas samples with higher contamination levels are excluded from the interpretation. Because of its relevance to wider-scale issues at Century, data from Bresser (1992) are reproduced in Appendix 6.

No attempt has been made to make sophisticated interpretations of fractionation trends to obtain temperature estimates, because the mineral phases are too fine grained for complete separation and textural relations are too complex to interpret which phases were co-precipitating (e.g. Plates 14B; 14F).

Results are presented for sulphide species in the mineralised zone in Figure 6.4, discriminated by the interpreted position of individual sub-samples in the deposit paragenesis (section 5.4.6; Fig. 28). Values from the samples from the transgressive lodes sampled by Bresser (1992) are also plotted on this figure for comparative purposes. Some interesting observations can be made from the data:

- isotopic composition of the sulphur in porous and non-porous sphalerite is virtually identical, ranging from +6 to +13 ‰CDT and averaging around +10 ‰CDT. This adds support to the deduction from the petrographic observations that the two types are co-genetic textural variants.

- pyrite from the mineralised zone has isotopically similar sulphur to the sphalerite (average $\delta^{34}S$ +9.3 ‰CDT). This is taken as evidence that much of the pyrite in the mineralised zone may be cogenetic with base metals.

- pyrite from both the hanging wall and footwall sequences (Appendix 6) has a wider and partly overlapping range (from +11.3 to +29.5 ‰CDT), but on average has heavier sulphur than the base metals (+17 ‰CDT). There is insufficient data to

assess whether if there are any systematic vertical changes stratigraphically upwards or downwards from the mineralised zone. Limited data (4 samples) from Pmh4 in the Lilydale drillhole (DD91LH265; Fig. 2.7), remote from mineralisation, show a range from +9.8‰CDT to 28.7 ‰CDT.

- the late-transgressive and coarse-grained replacive sphalerite (including crackle vein and breccia sphalerite) shows a definite progression in sulphur isotopic values to heavier sulphur. A wider range of values is present, with $\delta^{34}S$ from +9 to +18 ‰CDT, with an average of around +13 ‰CDT.

- although only a few samples were analysed, galena samples confirm the trends in the sphalerites, with $\delta^{34}S$ ranging from +5 to +14 ‰CDT in discrete early euhedral forms and from +10 to +26 ‰CDT in the late transgressive aggregates.

- data from the regional transgressive lodes, which are later in the history of the region, are heavier still, with $\delta^{34}S$ ranging from +20 to +30 ‰CDT. Lode mineralisation shows a progression towards heavier $\delta^{34}S$ values with progressively younger paragenetic stages (Bresser, 1992). A good correlation of sulphur isotope values between individual correlatable paragenetic stages in the two lodes (Watson's and Silver King) studied by Bresser (1992) is evident. This occurs despite significant differences in lead isotope values between the two lodes (section 6.6).

The significance of these observations is discussed in section 6.7.4.

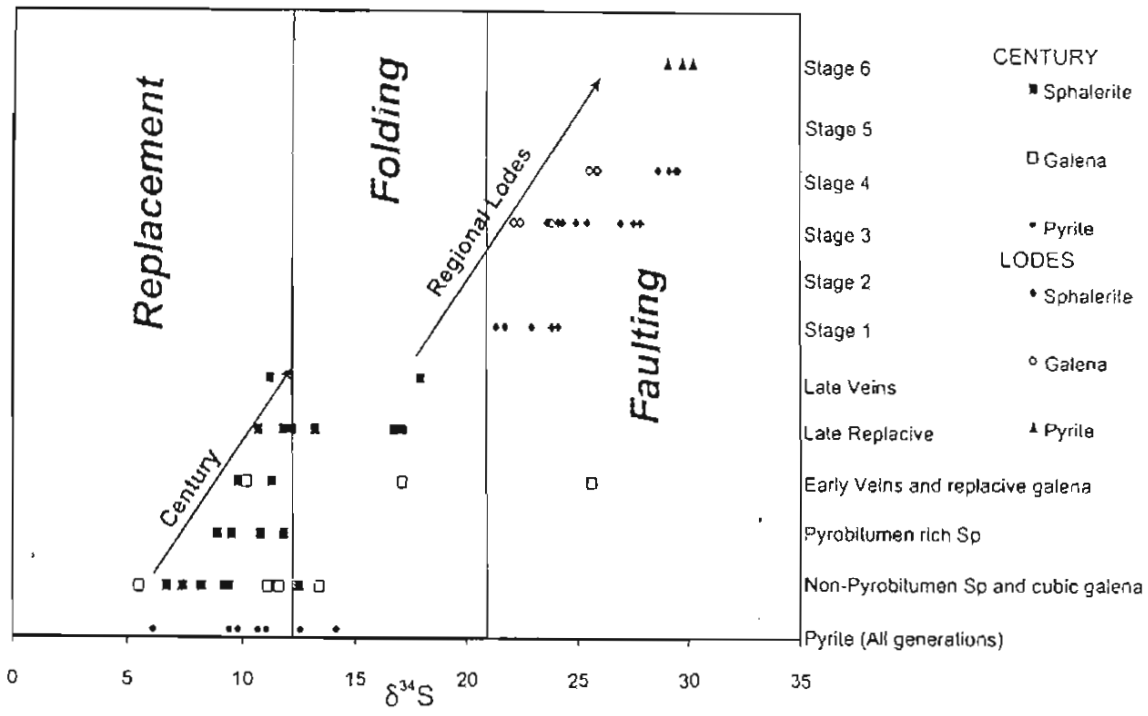

Figure 6.4 Sulphur isotope data for the Century deposit mineralised zone and regional lodes. Data for regional lodes are from Bresser (1992).

6.6 Lead Isotopes

Galena separates with various early- to late-stage textures were submitted to the CSIRO Division of Exploration Geoscience at North Ryde, Sydney, for lead isotope analysis. The objectives were threefold:

- to gain some insight into the absolute age of the mineralisation.

- to determine whether common lead from various stages of the paragenesis shows the expected internal consistency characteristic of other major stratabound lead-zinc deposits in the Proterozoic of northern Australia. (see review by Gulson, 1985).

- to investigate the relationship of the lead isotope values from the shale hosted mineralisation to the available published data on the transgressive lodes of the Lawn Hill mineral field. Samples from Watson's Lode collected by H. Bresser were also analysed, as material from this vein system had not previously been analysed by Richards (1975).

In all, seventeen samples were submitted, broken down as follows;

- 2 replacive galena in Cambrian limestone sequence (C127 and C128)*
- 2 euhedral disseminated galena (C046and C110)
- 1 replacive galena in carbonate spheroid band (C208)
- 2 replacive galena in stylolite fabrics (C043 and C113)
- 3 late stringer and replacive galena in unit 1.2 and unit 2 (C197-C199)
- 2 late galena in breccia veins (C034 and C216)
- 1 galena clast in carbonate breccia intrusive within ore zone (C132)
- 4 Watson's Lode vein hosted galena (supplied by H. Bresser, Nos 025, 103, 111A, 111B)

*These were analysed in duplicate

Full analytical results and details of sample preparation are given in Appendix 6. An initial overview of the data is made using standard graphical plots of 206Pb/204Pb versus. 207Pb/204Pb and 208Pb/204Pb (Figure 6.5).

The samples from the Cambrian limestone show widely disparate signatures (Fig. 6.5). One sample, C128, is very similar to the signature from Century and may reflect local remobilisation of lead from the weathered equivalents of the Century mineralisation. The other sample, C127, is much more radiogenic. Lead mineralisation within the Cambrian succession is a complex topic and insufficient data are present for any meaningful conclusions on Cambrian lead derivation. Experience by CSIRO on material from these lithologies regionally suggests that they are extremely variable, possibly reflecting derivation of lead from a multitude of local sources (G. Carr, pers comm., 1992).

When the limestone samples are excluded and the plot scale enlarged (Fig. 6.6), some interesting features are apparent. Most data from the Century deposit are tightly

clustered into a single population, but a smaller, slightly more radiogenic, cluster is also evident (Fig. 6.6). The linear trend of the samples from the main-stage Century population relates to slight instrumental fractionation of the different isotopes during analysis and does not have any geological significance (Carr, written comm., 1992). The main Century cluster is identical, within experimental error, to values obtained by Richards (1975) on paragenetically unconstrained samples from the Silver King and Axis lodes. The smaller, more radiogenic, population from Century is associated with samples that do not have typical textures. Some are very fine-grained replacive galena aggregates, some are vein fill, and others are clasts in later carbonate breccias. Microscopic examination of fine-grained replacive galena aggregates often shows other intergrown sulphides to be present (e.g. Plates 10F; 10H). It is possible that sufficient radiogenic lead from the inclusion of other sulphides was present to influence the results for some samples. The differences between the two Century populations are not considered substantial enough to require separate genetic consideration at this stage.

A major feature of interest in the dataset is the apparent difference of samples from Watson's Lode and Lilydale to those from Century, Silver King, and Axis. The separation of the Lilydale and Watson's lode samples may indicate that they were derived from a slightly different, more radiogenic, source region to the Century group of samples. A substantial difference in age of lode mineralisation between Silver King and the Watson's area seems extremely unlikely, given their close similarities in paragenetic stages, sulphur isotope distribution and structural regimes during emplacement (Bresser, 1992).

Published lead isotope data for the other major lead-zinc deposits in the Mt Isa province from Gulson (1985) have been plotted on Figure 6.7. The plot clearly shows that the major deposits have homogeneous signatures for the ore leads. Lady Loretta has a very complex signature, interpreted to be the result of dual sourcing of lead (Carr and Smith, 1992). Temporal relationships and implications of these regional scale observations to metal sourcing are discussed in section 6.7.5.

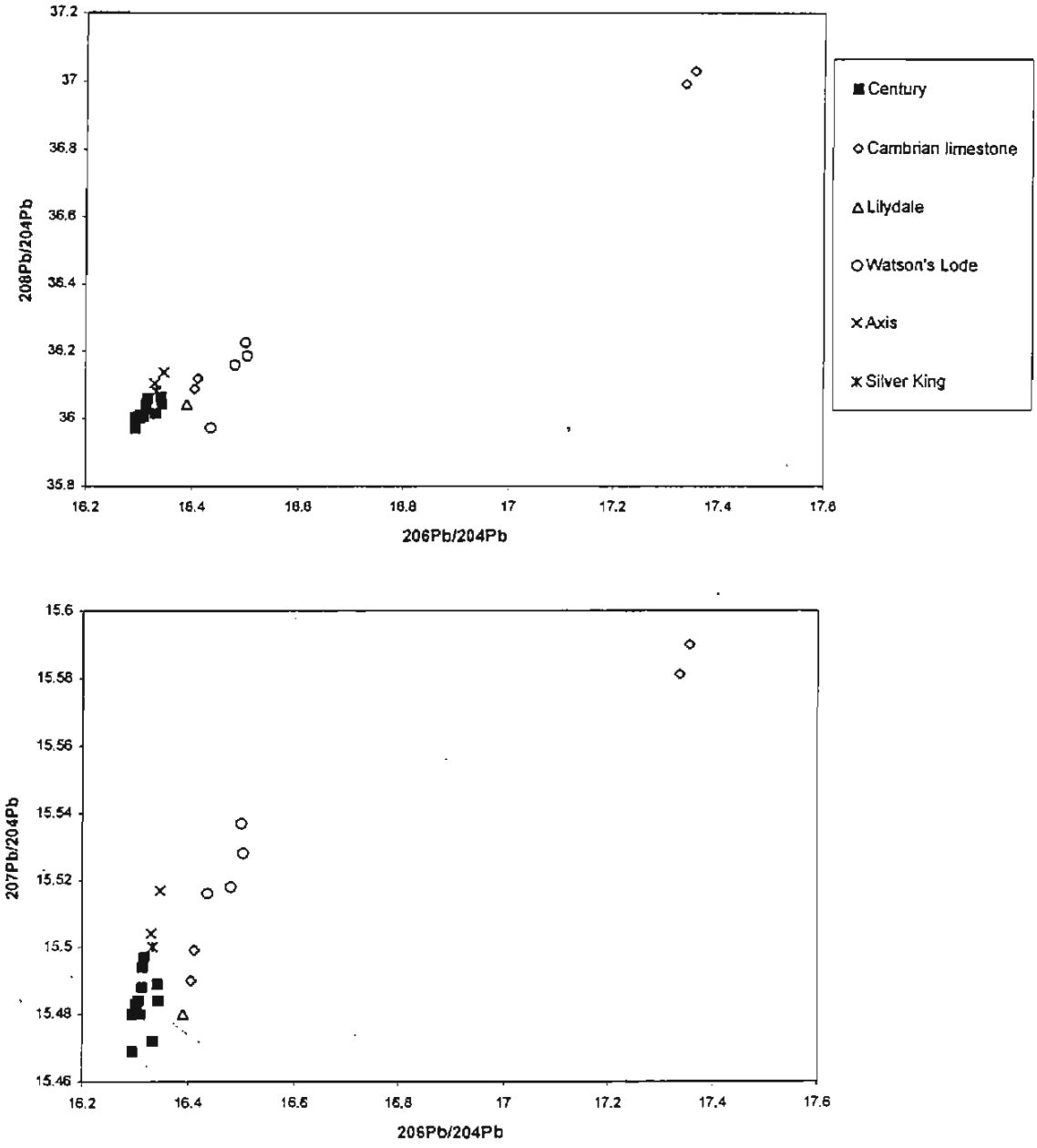

Figure 6.5 207Pb/204Pb and 208Pb/204Pb versus. 206Pb/204Pb plots for lead isotope samples from the Century dataset (Appendix 6B). Axis/Silver King and Lilydale data are from Richards (1975).

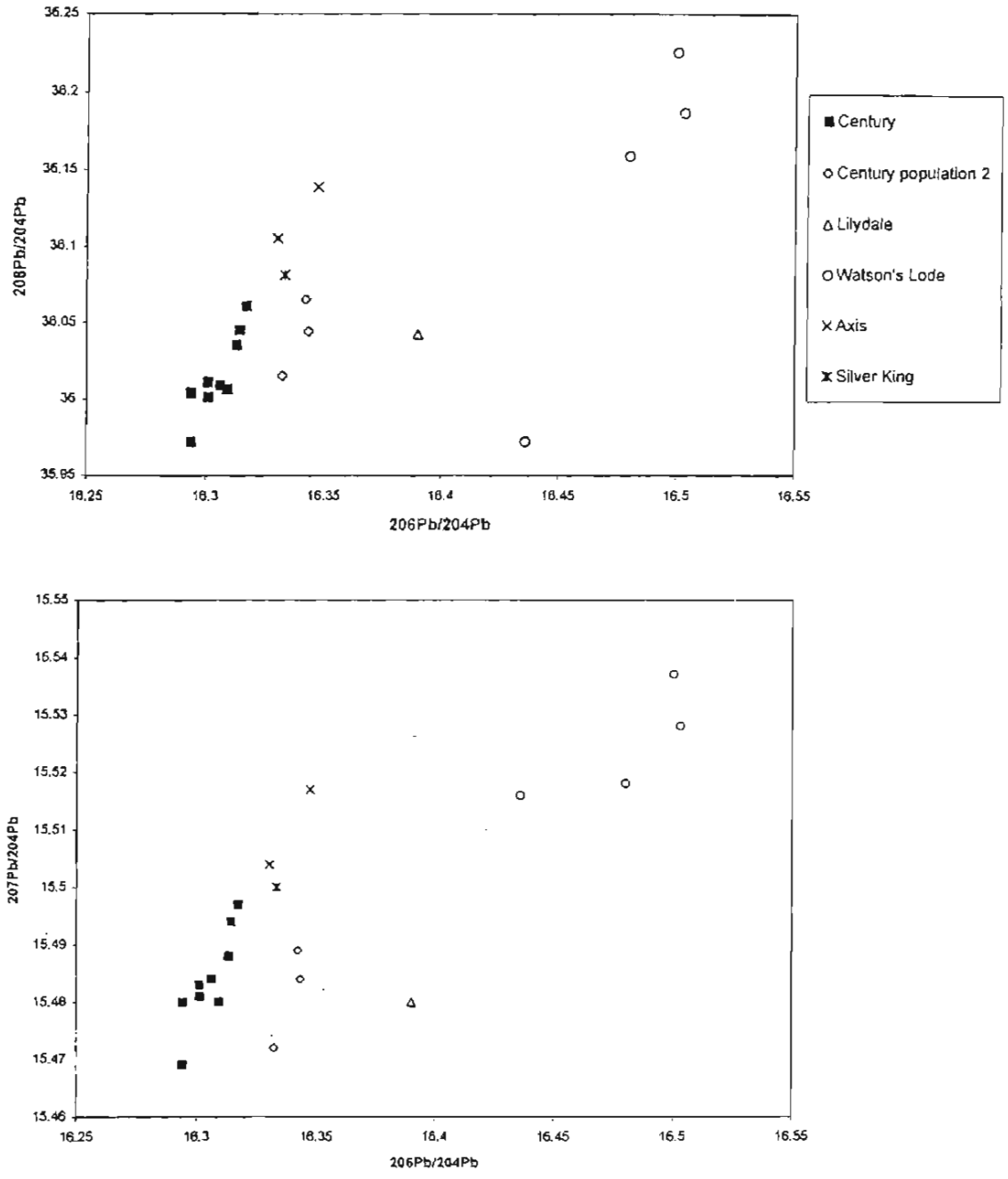

Figure 6.6 Expanded 207Pb/204Pb and 208Pb/204Pb versus 206Pb/204Pb plots for lead isotope samples from the Century deposit and transgressive lodes only, showing the difference between the tight cluster of values at Century-Silver King- Axis and the Lilydale - Watson's Lode trend. Axis/Silver King and Lilydale data are from Richards (1975).

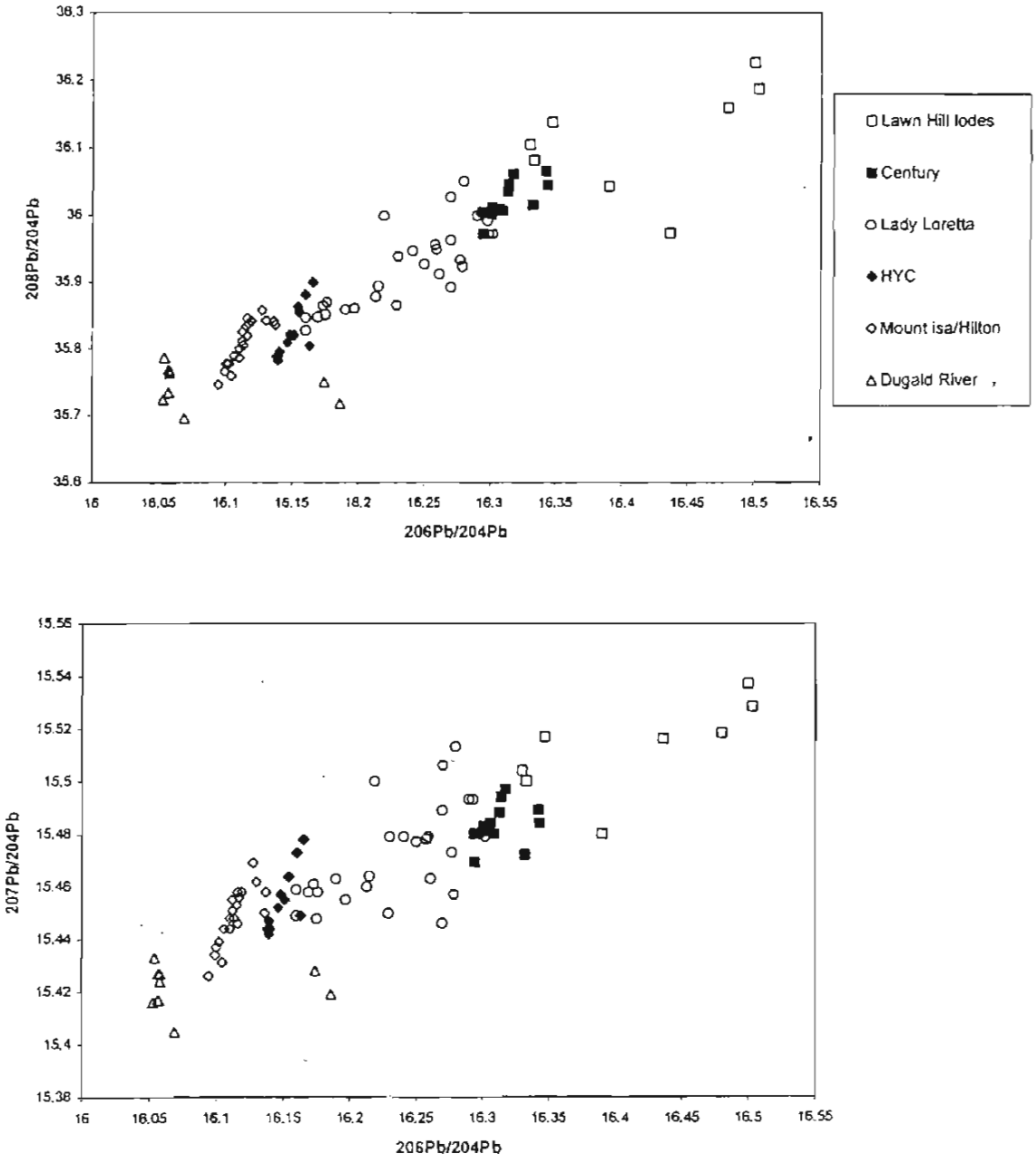

Figure 6.7. 207Pb/204Pb and 208Pb/204Pb versus 206Pb/204Pb plots of lead isotope data from the other major deposits of the Mt Isa-Macarthur province compared to Century. Data for regional deposits are taken from Gulson (1985).

6.7 Discussion

This discussion attempts to distill the most likely mechanisms responsible for the trends in the various datasets presented in the first half of this chapter. Constraints on temperature of the mineralising fluids are provided by the organic phases. These are placed into regional context prior to the more complete discussion of likely fluid-source areas and mechanisms made in Chapter 7. Chemical and isotopic evolution of siderite illuminates several key processes that are also relevant. The indicated evolutionary trend in sulphur isotopes from the Century deposit to the regional lode mineralisation does not seem to have precedent in the literature on major base-metal deposits. A conceptual model of the evolution of the regional sulphur system is therefore developed before an attempt is made to integrate it with other aspects of metal sourcing and transport in Chapter 7. Finally, some inferences concerning the possible scale and sourcing of various components of the regional fluid system responsible for Century are drawn from the lead isotope data.

6.7.1 Organic Maturity - Constraints on Thermal Regime

From the organic maturity data in Section 6.1, the most probable estimate for peak temperatures experienced by the ore environment lies in the range 180-200^{0}C, with an absolute maximum of 250^{0}C. When the likely presence of liquid hydrocarbons and the very limited fluid inclusion data are considered, it could be argued that the actual temperature during mineralisation was relatively low, perhaps as low as 120^0-140^{0}C. The maximum thermal signature of the organic material could have been imposed during subsequent deeper burial and low grade metamorphism (assuming normal geothermal gradients).

Further organic matter reflectance data from stratigraphically-equivalent barren sedimentary sequences to Century are needed to determine whether the orebody has a detectable paleo-thermal anomaly. However, at Lilydale, the compositional maturity of the organic matter from unmineralised Pmh4 is similar to that at Century, indicating that similar peak paleotemperatures were obtained. At face value, this would support

the proposition that substantial post-depositional burial is responsible for peak paleotemperatures experienced by the organic material, the question is when this loading could have occurred. Plausible alternatives for deposition of thick overlying sedimentary sequences include the unknown thickness of post-Pmh5 sequences of the Upper McNamara Group (now erosionally removed), or the younger Constance Range Group, which unconformably truncates the D2-D3 deformation of the upper McNamara Group (Hutton and Sweet, 1982).

McConachie et al. (1993) indicate the peak thickness of preserved upper McNamara Group sedimentary sequences overlying Pmh5 in the Elizabeth Creek area, approximately 80 kilometres to the north of Century, to be no more than 2500m. It is unlikely that substantially greater thicknesses than this were ever deposited, as the upper portion of the sedimentary pile is under-mature for oil (McConachie et al., 1993). Further, because of this under-maturity, later burial by Constance Range Group sedimentary rocks has also not exceeded 2500m. These burial constraints could be extrapolated to the Century area. However, because of the ~80 kilometres distance between the two areas, it could be argued that post-Lawn Hill Formation depositional histories may not be the same, and that the Century area had a substantially greater thickness of sediment, either during upper McNamara Group time, or during Constance Range Group time. The latter alternative seems unlikely because the stratigraphy of the Constance Range Group has uniform thickness between Elizabeth Creek and Century (Hutton and Sweet, 1982), so that discussion of this issue can be focussed on the upper McNamara Group.

The fluid inclusion data of Bresser (1992) from the Lawn Hill Formation lodes indicate ore-fluid homogenisation temperatures to range between 110 and 130^{0}C. Bresser (1992) made a reasonable assumption of a depth of emplacement of 2000m (53MPa) for the lodes to calculate lithostatic pressure corrections and gave an estimate of formation from 150-180^{0}C. Given that the lodes have pyrobitumen throughout the paragenesis (Bresser, 1992), the temperature range for these post-Century mineralising fluids is unlikely to have ever exceeded 250^{0}C. This upper temperature limit places a peak constraint of 125MPa for a possible pressure correction (Potter, 1977), translating to a maximum permissible depth of emplacement of approximately 4.5 kilometres.

If this argument constraining the maximum depth of burial is accepted, the data from the pyrolysis and reflectance studies indicates considerable regional thermal over-maturity of the organics relative to their maximum depth of paleo-burial. Regional geothermal gradients between 20 and 30^{0}C per kilometre appear possible in basins where cool, thermally insulating sediments overlie high heat-producing basement granites (e.g. Solomon and Heinrich, 1991). Such circumstances could be invoked for the Century area, with the Yeldham Granite 25 kilometres to the east known to comprise basement (Sweet and Hutton, 1982). However, paleotemperatures of 180-200^{0}C at a maximum burial depth of 4.5-5 kilometres require a geothermal gradient of around 40^{0}C per kilometre. A geothermal gradient of this magnitude seems unreasonable given that sections of deep-level Lower McNamara Group sedimentary rocks immediately south of Century are not significantly metamorphosed (Hutton and Sweet, 1982; Andrews, 1998b).

Abnormally high levels of organic maturity at shallow depths are probably better explained by physical transport of hot fluids from deeper levels of the basin. Regionally, Glikson et al. (1998) show pronounced elevation of organic maturity values from background levels in several levels of the upper McNamara Group, which they relate to the passage of hot basinal fluids at a regional scale. The work of Andrews (1998b) similarly indicates substantial post-depositional regional-scale hydrothermal-fluid activity in the Lawn Hill area. Finally, mobile pyrobitumens intergrown with main stage sphalerite at Century show slightly higher rank than alginites (section 6.1), strongly suggesting peak thermal maturity was achieved by interaction of hydrocarbons with hydrothermal fluids during mineralisation.

The likely time period for passage of such hot fluids most likely pre-dates deposition of the Constance Range Group because these rocks do not demonstrably affect organic maturity (Glikson et al., 1998) and unconformably truncate regional folds related to lode structures (Chapter 4). Given the timing arguments developed in Chapter 4, it seems reasonable that mineralisation in the Lawn Hill region could be related to the same pulse of regional fluid activity. The apparent thermal over-maturity of the organics at Lilydale must also indicate exposure to hot basinal fluids, but, for some

reason, substantial mineralisation was not developed at Lilydale. Speculatively, this could be because the fluids were spent of reactive constituents (i.e. equilibrated) by the time they passed through stratigraphy a long distance from fluid conduits, or that local conditions at Lilydale were simply not conducive to high intensity deposition of sulphide species.

In summary, at Century, the main-stage sulphide mineralisation demonstrably post-dates, or is synchronous with, chemical or thermal degradation of mobile hydrocarbon phases (Chapter 5). Given the intimate petrographic relationships of a substantial proportion of the sphalerite to degraded hydrocarbons, it is likely that this degradation has been caused by reaction of hydrocarbon with hydrothermal fluids. The reflectance data therefore serve to establish an absolute upper limit on the temperature regime of the Century ore fluids of 250^0C, with a likely range from 150 to 200^0C, similar in essence to the values interpreted by Bresser (1992) for the regional lode mineralisation. It is possible that the fluid system responsible for the mineralisation was linked to the regional-scale fluid activity responsible for the anomalous patterns of organic maturity documented by Glikson et al. (1998).

Unfortunately, because of the high thermal and compositional maturity of preserved organic material, no evidence is available from the pyrolysis data to either support or refute a case for introduction of exotic hydrocarbons to the deposit area. However, in the deposit context, the hydrocarbons do not need to be exotic, as hydrothermally-accelerated thermal maturation from organic-rich shale facies in the immediate vicinity of the ore environment could easily have produced sufficient hydrocarbons to develop a *source-reservoir* hydrocarbon trap (Chapter 5). This explanation of relatively local derivation of hydrocarbons by simple hydrothermally-accelerated maturation of organic-rich sediments is preferred on the grounds of simplicity. It is argued that invoking a source of exotic hydrocarbon-rich fluids simply adds to the complexity of any genetic model, for no good reason.

6.7.2 Chemical Evolution of Siderite

The evolutionary trends in siderite composition presented in section 6.3 are interpreted as giving important indications of changing chemical conditions within the deposit during the mineralisation process.

Detailed studies of the evolution of carbonate compositions within sediment-hosted base-metal systems are not common in the literature. Manganese, commonly in the carbonate form, is a common constituent of many sediment-hosted ore deposits (e.g., Meggen; Gwosdz et al., 1976), showing lateral haloes for kilometres away from mineralisation. Changes in manganese content of synsedimentary or early diagenetic carbonates are generally interpreted to give indications of changing sea-floor redox conditions (e.g. Okita and Shanks, 1992). However, whilst these concepts may be of great value in interpreting environments of interpreted syn-diagenetic mineralisation (e.g. Large et al., 1998), they may not be relevant to Century.

The petrographic relationships of the Century siderites to silica cements and stylolites (Chapter 5) are not consistent with a syn-diagenetic interpretation. Siderite was a stable species developed during burial, directly associated with the mineralisation process (section 5.4.1).

The high zinc content of the earliest siderites is best explained by postulating that the mineralising fluid had a high zinc content. This implies that it had a low reduced sulphur content, otherwise zinc would have been deposited as sphalerite. The later rhombic overgrowths and vein and crackle filling siderites were co-deposited with sphalerite. Their low zinc content suggests that zinc in the mineralising fluid has preferentially partitioned into the sulphide phase during sulphide mineralisation. Magnesium, which must have been present in some abundance in the mineralising fluid, substituted for zinc in the siderite because of the reduced zinc activity caused by sphalerite deposition. The existence of low-iron, high-purity, sphalerite such as that obtained at Century (section 5.2) indicates relatively-high reduced sulphur activity during precipitation (Scott and Kissin, 1973). The rapid change in siderite compositions associated with the onset of sulphide and pyrobitumen deposition

suggests a rapid increase in availability of reduced sulphur by some mechanism linked with hydrocarbon mobilisation.

Variations in availability of reduced sulphur and corresponding changes in partitioning of metals internally within the system are shown by the oscillatory zoned grains. Localised changes in fluid chemistry caused by non-equilibrium precipitation reactions could easily have lead to rapid and dynamic changes in fluid chemistry in very localised areas within the deposit.

At Century, early siderites, regardless of composition, texture and stratigraphic position, appear to be developed with similar timing relationships to compactional features and to predate pyrobitumen. However, the lower footwall siderites have low zinc, manganese and high magnesium compared to the mineralisation siderites. This difference may possibly indicate either different redox conditions, timing, temperature, or local fluid:rock interaction. Given that the similarities in overall composition and facies between the various sedimentary units are much stronger than their differences (Chapter 3), it seems unlikely that there were major differences in redox conditions between the footwall stratigraphy and the ore zone. It is therefore difficult to invoke differences in redox conditions to explain the differences in manganese and zinc contents of paragenetically early siderites with proximity to the mineralised zone.

The footwall siderites may simply be diagenetic carbonates unrelated to mineralisation. Mozley and Carothers (1992) noted compositional trends of non-hydrothermal diagenetic siderites to higher magnesium content with increasing depth of burial (i.e. higher temperature). The high magnesium content of the footwall siderites may reflect their formation by normal diagenetic processes during initial burial. More detailed compositional data are required on the carbonates occurring in the transitional stratigraphy between the mineralisation and footwall zones. Section 7.1 further discusses possible genetic mechanisms for siderite deposition, after consideration of other data.

It seems most likely on current data that chemical conditions during early burial were broadly similar throughout the hanging wall and footwall sequences, and that the ore

zone and the hanging wall stratigraphy were invaded by an exotic fluid high in zinc and manganese. This hypothesis is examined further in the context of carbon and oxygen isotope data in section 6.7.3.

6.7.3 Isotopic Evolution of Siderite

A general discussion of factors influencing isotope systematics of diagenetic carbonates is warranted before attempting to interpret the trends at Century. Temperatures of carbonate formation can be estimated from the isotopic composition of mineral species where the compositions of pore fluids are known. Constants used in the calculations vary depending on mineral species, ion substitution and temperature, and must be determined by experimental data. Experimental data are not available for siderites with compositions equivalent to those at Century (Mozley and Carothers, 1992), so this has not been attempted in this study.

6.7.3.1 Background Discussion – C Isotopes

In present day marine sediments, carbon in organic matter is isotopically light (-25 ‰PDB) relative to marine reservoir bicarbonate (0 ‰PDB). Organic carbon from the Proterozoic appears to have been enriched in ^{12}C relative to modern sediments (Faure, 1986). Organic $\delta^{13}C$ compositions from the Century area are consistently around -30 to -33 ‰PDB (section 6.4). Fluids sourced from seawater or a marine carbonate fluid reservoir should deposit carbonates with $\delta^{13}C$ close to zero (Irwin and Curtis, 1977).

Isotopic compositions of diagenetic carbonates developed with increasing depths of burial should reflect the existence of four zones of carbonate production (Irwin and Curtis, 1977; Fig. 6.8). Diagenetic carbonate precipitated at shallow depths (<1m) should be characterised by isotopically light carbon, because most of it is derived by direct bacterial oxidation of either organic material or methane which has been transported upwards by diffusion from the underlying methanogenic zone (zone I). Underlying this zone of direct bacterial oxidation is the zone of sulphate reduction (zone II). This likewise produces isotopically light carbon from the direct consumption

of organic matter (zone 2; approx 10m thick). A rapid change to C^{13}-enriched carbonates occurs in the zone of bacterial fermentation (zone III; ~10-1000m), because of the bacterially induced fractionation of C^{12} into methane and a corresponding enrichment of C^{13} into the CO_2 phase by the anoxic fermentation processes which dominate this interval. Carbonate is preferentially deposited from bicarbonate produced by solution of the carbon dioxide. Methane tends to be lost by diffusion.

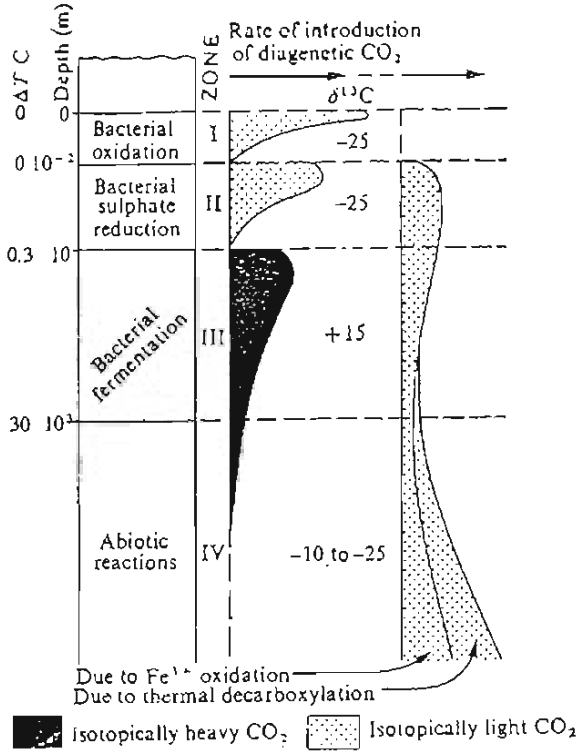

Figure 6.8 Summary diagram of isotopic compositions of carbonate within different diagenetic zones (from Irwin and Curtis, 1977).

With increasing depth of burial (i.e. increasing temperature), microbial fermentation processes decline in importance (zone IV). Thermal decarboxylation, hydrolysis, or Fe^{3+}-catalysed reactions of organic acids become important sources of carbonate (Irwin and Curtis, 1977; Surdam et al., 1989). These apparently do not impose significant isotopic fractionation between the various carbon rich products (CO_2 and CH_4). Therefore a gradual return to isotopically light values of carbon in the derived carbonates occurs with increasing depth of burial, because of increased sourcing from organic carbon. However, the compositions of the resultant carbonates rarely approach the extreme values of very early carbonates, because of the flux of existing heavy carbonate in solution and the continual dissolution and re-precipitation of existing

carbonate species. Thermal fractionation of carbon values to light values also occurs (Faure, 1986), but this appears quantitatively much less important than the changes induced by exchange between pore fluids and changes in mineral species and organic materials (Irwin and Curtis, 1977).

6.7.3.2 Background Discussion – O Isotopes

Oxygen isotope interpretation is even more complicated than that for carbon isotopes. Significant fractionation of the light (^{16}O) versus heavy (^{18}O) isotopes is both temperature (depth) and mineral species dependant (Faure, 1986). Silicates and carbonates both have appreciable exchange capacity, leading to fluctuating equilibrium relationships as fluid:rock interaction proceeds and temperature regimes shift. In general terms, ^{18}O is incorporated selectively into mineral species by both exchange reactions and precipitation of new mineral species in relatively shallow burial and diagenetic regimes (Irwin and Curtis, 1977; Gautier, 1982; Curtis et al., 1986; Mozley and Carothers, 1992; Mozley and Wersin, 1992). This leads to progressive enrichment of the light ^{16}O isotope in pore fluids with increasing depth of burial by Rayleigh fractionation (Irwin and Curtis, 1977). Therefore, there should be a progressive decrease in oxygen isotope values of new diagenetic mineral species deposited with increasing depth of burial, because they should be in equilibrium with more evolved pore fluids. This pattern has been recorded in recent marine sediments to depths up to 400 metres (see review by Longstaffe, 1989) and inferred to be feasible up to depths of several thousand metres by several studies (Irwin and Curtis, 1977; Primmer and Shaw, 1991; Mozely and Carothers, 1992).

With increasing depth, an inversion to pore fluids with higher $\delta^{18}O$ occurs, by mechanisms that are poorly understood (Longstaffe, 1989). Explanations include release of stored heavy oxygen by higher temperature substitution of light oxygen during mineral exchange reactions, or liberation of heavy oxygen by dissolution of previously formed diagenetic minerals (Longstaffe, 1989). Other things being equal, fluids sourced from deep basinal fluid reservoirs should in general have higher $\delta^{18}O$ relative to those from lithologically equivalent shallow reservoirs. If such a hypothetical fluid reservoir was dominated by marine carbonates, $\delta^{13}C$ in the fluids

should be close to zero. The carbon isotope signature from deep clastic reservoirs will understandably be more varied because of uncertainties in the relative proportions and fractionation histories of organic versus inorganic carbon, but will tend to be light rather than heavy (Fig. 6.8).

In summary, radical excursions in $\delta^{18}O$ in diagenetic carbonates formed at any given burial depth can be reasonably interpreted to indicate ingress of different fluids from quite different temperature and chemical regimes. Subsequent trends within the system are likely to reflect the attempt of mineral species to re-equilibrate to the changed fluid regime, by precipitation, thermal equilibration or isotopic exchange caused by fluid:rock interaction.

6.7.3.3 O and C Isotope Trends in Century Siderites.

With the foregoing discussion to provide a context for carbonate emplacement at shallow to medium burial depths (as indicated by the petrographic observations), trends in isotopic values from the Century siderites can be interpreted. In section 6.4, a possible mixing trend between higher $\delta^{13}C$ values in early zinc-rich siderites and lower $\delta^{13}C$ values in later, magnesium-rich, siderites is postulated. The much lower $\delta^{13}C$ values in the vein siderites from the ore zone (and arguably the more modest –3 to –4‰PDB values for Watson's Lode, Figure 6.2B) support this trend. Thermal fractionation to light values with time does not seem to be a feasible alternative because of the likely narrow range of temperature between the Century mineralisation and fluids responsible for regional lode mineralisation (section 6.7.1). Rather, the trend to light carbon isotope values with time at Century appears to be evidence of progressive incorporation of light carbon from the destruction of organic matter. The relative contribution of possible genetic processes that could be responsible for incorporation of organic carbon into pore fluids, such as decarboxylation of acetate (Irwin and Curtis, 1977; Surdam et al., 1989) and thermochemical sulphate reduction (Machel et al., 1995) are discussed in Chapter 7.

The most striking feature of the Century data are the highly positive oxygen isotope values in the hanging-wall sequence. There is a possible mixing zone coincident with

the base of the mineralisation (Fig. 6.3). Higher $\delta^{18}O$ values of oxygen in the hanging wall siderites could be attributed to simple inheritance: i.e. that they originated as shallow diagenetic siderites. However, this is considered unlikely for two reasons. First, this interpretation is inconsistent with the textural observations (section 5.3.2) and secondly, the carbon isotope data do not show the very low $\delta^{13}C$ values that would be expected (e.g. data of Irwin and Curtis, 1977; Mozley and Carothers, 1992). The $\delta^{13}C$ range of hanging-wall and early end-member mineralisation siderites (0-2‰PDB) is similar in some respects to the deep footwall siderites (Fig. 6.3). It could be possible to develop the 20 to 22 ‰SMOW values of the late mineralisation vein-fill siderites by mixing 20 to 25 ‰SMOW values of the hanging-wall siderites and the 14 to 18 ‰SMOW values of the footwall siderites. The timing relationships of both the early hanging wall siderites and the deep footwall siderites appear to be broadly similar with respect to compactional fabrics and invasion by later hydrocarbons. Isotopic exchange between locally derived pore fluids and an exotic fluid related to mineralisation is therefore permissible to explain the isotopic complexity within the ore zone.

When the petrographic and chemical evidence from previous sections is considered it therefore seems probable that the early ore zone and hanging wall siderites were deposited contemporaneously with, or heavily exchanged by, a post-depositional ^{18}O-enriched fluid which travelled laterally through the ore zone and hanging wall sequence. The lower footwall siderites may have been deposited by local pore fluid interactions (see section 7.1) and are therefore unrelated to mineralisation.

The trend to lower oxygen and carbon isotope values in the Watson's Lode siderites is interpreted to reflect progressive equilibration of the exotic fluid with sediment-derived pore fluids. Thermal equilibration trends are unlikely given the thermal constraints (section 6.7.1) that indicate a relatively narrow range of temperature variation with time.

A pronounced peak in negative carbon isotope values at the top of the footwall zone deserves some comment (Figure 6.3). It is partly defined by sample C073 (-8 ‰PDB), which has an anomalous chemical composition (section 6.3), but three other samples down to 100m below the orebody also have relatively low $\delta^{13}C$ values of around –4

‰PDB. C073 has an oxygen isotope value that conforms to the trend of underlying footwall samples. It could be argued that this sample has acquired its isotopically light carbon from the overlying ore zone, but it is difficult to see how this could occur without affecting the oxygen isotope value. In any case, this does not explain the light carbon isotope values in the other samples, which show inconsistent relationships. Stratigraphically higher samples have oxygen isotope values consistent with the mineralised zone and lower samples are more consistent with the footwall zone (Fig. 6.3). The end-member introduced fluid responsible for the hanging-wall siderite presumably had $\delta^{13}C$ of around 0 ‰PDB, providing a further disincentive to any simple mixing hypothesis.

A possible explanation is that the heat from the overlying mineralising zone has been sufficient to enhance thermal maturation of organic phases in the underlying sediments. It is difficult to see how this could have happened without any physical introduction of fluid from the mineralised zone, however. More sampling and petrographic work is required to resolve this question. It is concluded that there are insufficient data to reach any conclusions on questions of the amount and nature of possible fluid mixing until the carbonate cements from the footwall sedimentary sequences are examined in much greater detail than has been possible in this study.

Notwithstanding these cautionary observations, it seems probable that the mineralisation siderites were deposited as the result of ingress of a post-depositional ^{18}O-rich fluid, with relatively neutral (0 ‰PDB) carbon, to the ore zone and hanging wall sequence. The most likely source of such a fluid is from deep in the basin, with a strong possibility of an original marine carbonate source. The most likely reservoir of marine-carbonate buffered, deep basinal-fluid is the Lady Loretta Formation and underlying evaporative carbonate sequences (Fig. 2). Subsequent discussion in sections 6.7.4 and Chapter 7 elaborates further supporting data for this hypothesis.

6.7.4 Sulphur Isotope Evolution

A general overview of factors that may influence sulphur isotope systematics of both diagenetic and mineralisation-related sulphides is made before attempting to interpret the trends at Century.

Diagenetic sulphides that form as a consequence of open system biogenic reduction of marine sulphate have relatively low sulphur isotope compositions ($\delta^{34}S$ values may be as much as 40 to 50 ‰ lower than contemporaneous seawater). This occurs because of the pronounced fractionation imparted by bacteria and the effectively infinite nature of the marine sulphate reservoir (Ohmoto et al., 1990). During shallow burial diagenesis, downward diffusion of marine or evaporitic pore waters contributes isotopically heavy marine sulphate, which is reduced by either biogenic methane or bacteria. In some models, pore water sulphate is depleted in the light isotope by near-surface biogenic activity. Because the supply of sulphate is limited to the amount of pore fluid that can diffuse downwards, complete reduction of available sulphate occurs and isotopically heavy sulphides are produced, often as overgrowths. The maximum extent of downward sulphate diffusion in modern reduced sediments is no more than several tens of metres, because of complete reduction to sulphides by early diagenetic reactions involving either iron or organic materials (Baskin and Peters, 1972; Ohmoto et al., 1990; Zaback and Pratt, 1992).

Anoxia and high H_2S content of bottom waters may develop in sedimentary environments with restricted seawater circulation, slow sedimentation rates and abundant organic matter for metabolism by sulphate-reducing bacteria. Because of progressive removal of ^{32}S as the closed system conditions develop, sulphate in the water column incorporates $\delta^{34}S$ with time, leading to higher $\delta^{34}S$ values in younger sulphides. If a metalliferous fluid encounters such a fractionated sulphur reservoir, the resultant sulphides (and possibly barite) will likely have high $\delta^{34}S$. Episodes of global ocean anoxia have been linked to highly productive periods of base-metal mineralisation in the Paleozoic Selwyn Basin (Shanks et al., 1987).

There is an alternative, non-biologically mediated, process for the derivation of sulphide from sulphate that also has evidence for substantial fractionation. A review of sulphide depositional mechanisms by Ohmoto et al. (1990) concludes that H_2S produced by non-bacterial reaction of organic matter and sulphate (thermochemical sulphate reduction:TSR) has $\delta^{34}S$ values up to 10‰ lower than the parent sulphate, indicating a fractionation process to be operative. Machel et al. (1995) concluded that TSR had a probable $\delta^{34}S$ fractionation of 10-15‰ to light values, depending on the temperature at which reduction took place. Tompkins et al. (1994) recorded evidence for $\delta^{34}S$ fractionation of 0.5 to 4.5‰ by TSR at the Cadjebut deposit. The subject is controversial and awaits definitive work on reaction kinetics, but there seems to be adequate evidence for the process of fractionation of $\delta^{34}S$ during TSR.

With this simple background, the Century and regional lode data can be interpreted.

In section 6.5 it is established that paragenetically early sulphides have $\delta^{34}S$ between 5 and 10‰CDT, while later fracture filling and replacement styles have values up to 20‰CDT. The progression to heavier sulphur isotope values later in the deposit paragenesis occurs in sympathy with textural changes to coarser-grained, more transgressive sulphide species.

Whilst it is acknowledged that there are too few analyses from this preliminary dataset for statistical rigour, to the authors knowledge such an evolutionary progression in sulphur isotopes with time has not previously been documented in a major sediment-hosted zinc-lead deposit. The progression is at odds with classic SEDEX interpretations, which explain late coarse-grained sulphide textures as the product of closed-system remobilisation. In such a closed system, remobilised sulphides should have the same signature as their precursors. Indeed, many studies rely on the closed-system behaviour of isotopes during deformation to be able to make inferences concerning sulphur sources of highly deformed orebodies (e.g. Davidson and Dixon, 1992).

The trend to heavier $\delta^{34}S$ values appears to follow through into the syndeformational regional lodes (Fig. 6.4). In the regional lodes, early sphalerite has $\delta^{34}S$ values from 20 to 25 ‰CDT while later sphalerite generations have progressively higher values, reaching a maximum of 25 to 30 ‰CDT in the final stages of vein mineralisation (Bresser, 1992). The correlated paragenesis and $\delta^{34}S$ evolution between Silver King and Watson's Lodes establish a likely common genetic relationship for all the regional lodes in a 100 to 200 square kilometre area surrounding the deposit (Bresser, 1992; Bresser and Myers, 1993).

Although the data are preliminary and more sampling is required to confirm such trends, this apparently continuous progression in sulphur isotope values suggests that Century and the regional lodes were geochemically and genetically linked. Despite their apparent geometric and timing differences, they may well have been sourced by a common regional-scale fluid system. Lead isotope data (sections 6.6; 6.7.5) offer some support for this contention.

The structural arguments developed in Chapter 4 constrain the lodes to most likely post-date main stage mineralisation at Century, so they cannot be interpreted as direct feeders for Century-style mineralisation. The apparently systematic changes to higher $\delta^{34}S$ values with time in the lodes themselves makes a simple interpretation that they are bleeders from the Century fluid system difficult to rationalise. Rather, the progression indicates that the total mineralising fluid system over the life of both Century and the regional lodes is best modelled as accessing a large sulphur reservoir that evolved to closed-system behaviour with time. The following discussion expands a speculative model proposed by Bresser and Myers (1993) to explain progressive enrichment in heavy sulphur in the lode mineralisation.

The probable depth of burial of Century, high temperatures and undoubted late syn-deformational timing of the lode mineralisation make any kind of biological fractionation process unlikely. The same factors make sulphur supply from connate water or downward convecting seawater extremely unlikely. Given the absolute maximum temperature of about 250°C and the probable relatively small variation in fluid temperature with time (section 6.7.1), shifts of the magnitude (20‰CDT) shown

by the data over the total life of the system from thermal fractionation effects are improbable.

Sulphate in evaporites of the McArthur Basin has $\delta^{34}S$ from +15 to +20 ‰ CDT (Muir et al., 1985) and is considered representative of average Proterozoic marine sulphate in the Mesoproterozoic. In the absence of any alternative explanation, it is postulated that the Century sulphur was introduced as sulphate and the reduced sulphur for sulphide mineralisation was forming by thermochemical sulphate reduction. Sulphate reduction from an ore fluid with initial $\delta^{34}S$ of 10 to 20 ‰CDT is consistent with the initial $\delta^{34}S$ values from 5 to 10 ‰CDT in the Century paragenesis. In conditions of almost complete sulphate reduction and high CO_2 solubility, such as in limestone host rocks, very low $\delta^{13}C$ in late-stage hydrothermal carbonates will result from high rates of organic carbon assimilation (e.g. Ghazban et. al., 1990, report a range of $\delta^{13}C$ from +6 to -12 ‰PDB). In conditions where fluids have high concentrations of inorganic carbon and CO_2 assimilation is inhibited, a lesser range of $\delta^{13}C$ will result. The modest range of $\delta^{13}C$ from +2.6 to -8.3 ‰PDB at Century could be consistent with such conditions. Buffering by the silicate-rich host rocks could perhaps have contributed by inhibiting CO_2 solubility.

Direct transport of a sulphate-rich fluid to the orebody environment, by major conduits such as the Termite Range Fault, is envisaged as the sulphur source for mineralisation. Evaporite-bearing carbonates of the Lower McNamara Group (Fig. 2) provide a plausible deep sulphate reservoir.

The consistent 5 to 10 ‰CDT values of $\delta^{34}S$ early in the Century paragenesis are representative of the volumetric majority of the total sulphide in the total system. This implies relatively high throughput of fluid with $\delta^{34}S$ similar in composition to Mesoproterozoic marine sulphate. The trend to higher $\delta^{34}S$ later in the deposit paragenesis and into the regional lode mineralisation, may partly reflect a gradual decline in fluid volumes and therefore more complete reduction of available sulphate in progressively smaller, fracture controlled, fluid conduits. However, even given complete reduction, the extreme values from 25 to 30 ‰CDT of the final stage

regional lode mineralisation cannot be explained easily. They must represent products of reduction of a fluid that was enriched in ^{34}S well beyond the accepted composition of normal Mesoproterozoic marine sulphate. This implies progressive removal of ^{32}S (by pyrite cementation or H_2S loss) from the deep sulphate reservoir to fractionate residual pore water sulphate to higher $\delta^{34}S$, particularly as fluid supply declined in the later stages of the mineralising system. Because the regional lodes and Century mineralisation have no barite, the deep fluid reservoir presumably remained buffered to oxidising conditions and the volume of sulphate removed from the reservoir must not have been large. Again in the absence of any alternative explanation, incremental thermochemical sulphate reduction within the deep sulphate reservoir itself must have occurred, to differentially mobilise ^{32}S and enrich residual sulphate in ^{34}S. The model concept is illustrated diagrammatically in Figure 6.9.

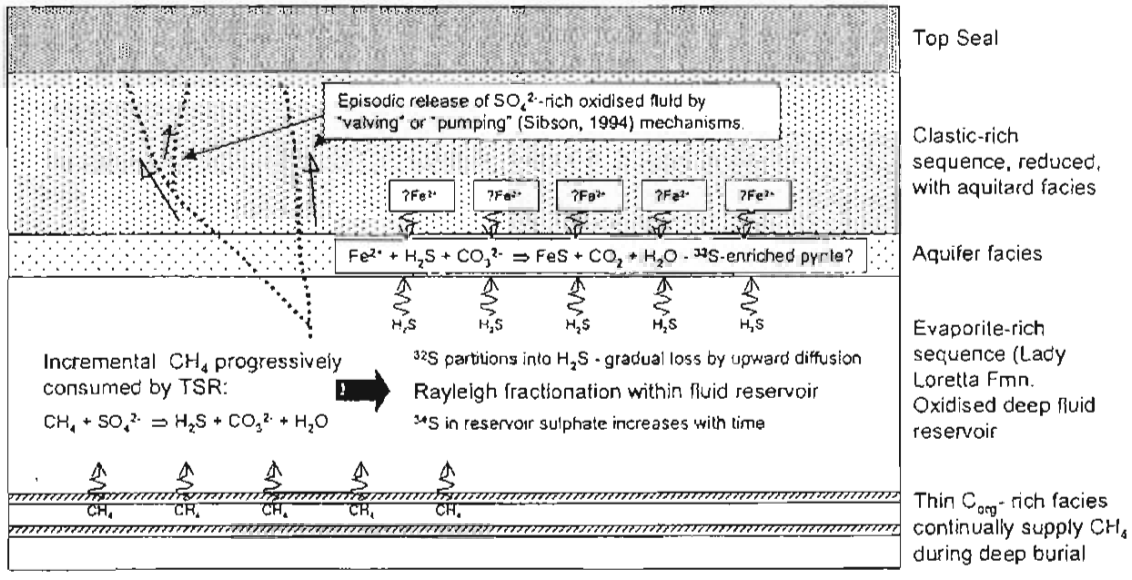

Figure 6.9 Schematic diagram for closed-system evolution of sulphur isotopes in a deep fluid reservoir.

The hypothetical closure of the sulphur system must admittedly have occurred at a very large scale, to accomodate mass balance considerations. The scale of development of the regional lode system indicates a probable fluid cell with dimensions of at least 200 square kilometres. Further discussion concerning feasible sources of sulphate versus reduced sulphur in ore fluids, timing and mechanisms of brine transport and likely

chemical reaction paths within the Century main stage mineralisation is made in Chapter 7.

6.7.5 Lead Isotopes - the Scale of the Century Fluid System

As discussed by Sun et al. (1996), lead isotope data from individual deposits show an interesting correlation with interpreted ages of the host sequences of mineralisation for Dugald River (?1700 Ma); Mt Isa (1650 Ma) and HYC (1640 Ma). Lady Loretta shows a very wide scatter, possibly reflecting dual lead sources within the deposit (Carr and Smith, 1992); its position along the growth curve suggests a younger age than Mt Isa. The Century cluster is even further along the growth curve, correlating with the younger 1595 Ma date of the host sequence (Chapter 2). Sun et al. (1996) calculate a model age of ~1575Ma for Century, 20 million years younger than the age of the host stratigraphy. This is interesting in light of the evidence developed so far in this thesis for post-depositional emplacement of the mineralisation.

However, given the controversy concerning genesis of many of the major deposits (section 2.3), local sourcing of the lead for the deposits from within their respective host sedimentary sequences could be invoked as an alternative hypothesis for explaining variations between deposits.

As a possible example, a study of regional lead isotope variations in the Irish base-metal province by LeHuray et al. (1987) shows a similar scale pattern of isotopic variation between individual deposits and ore districts. The Irish deposits were likely emplaced over a relatively short period (of geological time) and the isotopic differences therefore cannot be related to a simple temporal progression. In the Irish province, the patterns of isotopic variation appear to correlate with variations in basement lithologies (LeHuray et al., 1987). This suggests local sourcing of metals for the deposits, either directly from underlying basement, or from basin fill clastic rocks with local basement provenance.

The relationships of the clusters of vein mineralisation in the Lawn Hill area and Century itself can be interpreted as supportive of some local derivation of lead. Data

from Axis and Silver King are statistically identical to Century, indicating that the lead in both of these lode deposits and Century has probably come from the same source region. However, the more radiogenic signatures at Lilydale and Watson's Lode are different (section 6.6). These differences require reconciliation with the findings by Bresser (1992) that the correlated paragenesis, sulphur isotopes and fluid inclusions from Silver King and Watson's Lode clearly indicate the lodes to have a common genetic history.

The Watson's Lode and Lilydale systems are relatively small and a considerable distance from major fluid conduits such as the Termite Range Fault. It could be argued that their higher component of radiogenic lead simply reflects dilution/distal decay of a major regional fluid system responsible for deposits such as Century. Local leaching of radiogenic lead from wallrocks could have contributed sufficient lead to account for the shift in compositions. This scenario is testable insofar as it predicts gradual changes in lead isotopes to more radiogenic character with increasing distance from major fluid conduits.

A condition of this model would be that fluids from the master hydrothermal system would have to be in reasonable thermal equilibrium with the enclosing rocks. Otherwise, there would be systematic differences in fluid inclusion temperatures, maturity of organic matter etc as fluids cooled and moved laterally away from conduits or were diluted. No such differences are evident from work to date (Bresser, 1992). This implies fluid mobilisation at fairly substantial depths of burial.

An alternative model is that sulphur-bearing fluids and metal-bearing fluids could be sourced by different processes and therefore different source regions for individual fluid cells could exist. If a sulphate-bearing fluid from a deep reservoir commenced migrating through the entire basin sequence, and mixed with metal-bearing fluids from smaller fluid reservoirs in separate overlying basin compartments as it went, fluid cells with distinctive metal motifs but a rather more uniform temperature and sulphur signature could evolve more or less independently. This model predicts the occurrence of rather more discrete areas with different lead isotope signatures, similar to the findings from the Irish province (LeHuray et al., op cit).

Century Silver King/Axis and Watson's Lode/Lilydale have a geographic separation of some 16 kilometres in total (refer Fig. 2.3). The differences in lead isotope signatures are interpreted as providing important clues for the likely dimensions of source areas or fluid systems for the metals in the Century deposit, although ambiguity of explanations for causative mechanisms clearly exists.

Given the above uncertainties, no firm conclusions concerning the absolute age of the Century mineralising system can be made from lead model ages at present. The relatively young (1575Ma; 20m.y. after sediment deposition) model age calculated by Sun et al. (1996) is congruent with textural interpretations made in this thesis but more work may be required on this problem. Further sampling of lodes in the Lawn Hill region is required to clarify the pattern of lead isotope distribution. Some further speculations concerning metal sourcing mechanisms are made in section 7.5.

6.8 Summary

Peak thermal rank of organic matter in the deposit ranges from R_o of 2.1 to 2.7 ‰. Mobile pyrobitumens intergrown with porous sphalerite have slightly higher rank, strongly suggesting peak thermal maturity was achieved by interaction of hydrocarbons with hydrothermal fluids during mineralisation. Data suggest an absolute maximum paleotemperature of the host rock of 250^{0}C, with a likely range for mineralising fluids between 150^0 C to 200^{0}C. This estimate is compatible with the fluid inclusion data for the regional lodes obtained by Bresser (1992), and indicates a relatively narrow range in temperature of hydrothermal fluids through time. Compositional maturity of organic phases appears too high to be explained by simple burial and thermal metamorphism by now-removed sediments of either the upper McNamara Group or the South Nicholson Group. Rather, it is probable that the fluid system responsible for the mineralisation was linked to the regional-scale fluid activity responsible for the anomalous patterns of organic maturity documented by Glikson et al. (1998). This regional-scale fluid activity most likely occurred prior to the deposition of the South Nicholson Group, before or synchronous with folding linked to the Isan Orogeny. Issues of timing and source regions for mineralising fluids are further discussed in Chapter 7.

No evidence is present from the pyrolysis data to either support or refute a case for introduction of exotic hydrocarbons. The simplest mechanism for sourcing of hydrocarbons is hydrothermally-accelerated thermal maturation from organic-rich shale facies to develop a *source-reservoir* hydrocarbon trap (Chapter 5), so this is the model that is adopted here.

Petrographic relationships of the Century siderites to silica cements and stylolites indicate siderite precipitation during relatively deep burial (Chapter 5). It seems most likely on current data that chemical conditions during early burial were broadly similar throughout the hanging wall and footwall sequences. The ore zone and the hanging wall stratigraphy were invaded by an exotic fluid high in iron, zinc and manganese. Precipitation of high zinc- and manganese-siderite commenced within the mineralisation and hanging wall sequences. Overgrowths of low zinc-, manganese-

and high magnesium-siderite on this early siderite were associated with introduction of mobile pyrobitumen to the system and the onset of major sulphide deposition. This suggests a change in redox conditions over the time span of siderite deposition, from early relatively oxidized conditions to later more reduced conditions with higher fS_2, thereby favouring sphalerite precipitation. This change in system chemistry was associated with the production, or introduction, of hydrocarbon phases.

Carbon and oxygen isotope data for the siderites indicate systematic trends to lower oxygen and carbon isotope values with time. These changes occur in sympathy with the above-mentioned changes in carbonate composition. The trend to lighter oxygen is interpreted to be best explained by mixing or exchange between ^{18}O-enriched hydrothermal fluids and sediment pore fluids with lower ^{18}O and slightly heavy to neutral (0-2‰PDB) carbon. The trend to lighter carbon isotope values is interpreted to reflect progressive incorporation of ^{12}C from either hydrocarbons or the host shales.

It seems probable that the early ore zone and hanging wall siderites were deposited from, or heavily exchanged with, an ^{18}O-enriched fluid with neutral carbon isotope values, which travelled laterally through the ore zone and the hanging wall sequence. The most likely source of such a fluid is from deep in the basin, with a strong possibility of a deep marine carbonate influence. The marine carbonates of the Lady Loretta Formation and underlying evaporative carbonate sequences are a plausible source.

Sulphur isotope data from the mineralisation show changes to heavier values later in the deposit paragenesis, in sympathy with textural changes to coarser-grained, more transgressive sulphide species. Paragenetically early sulphides have $\delta^{34}S$ between 5 and 10 ‰CDT, while later fracture filling and replacement styles have values up to 20 ‰CDT. To the authors knowledge this phenomenon has not previously been documented in a major sediment-hosted zinc-lead deposit. Such an evolutionary pattern may be at odds with classic SEDEX arguments, in which late coarse-grained sulphide textures are usually explained as the product of closed-system remobilisation. In such a closed system, remobilised sulphides should have the same signature as their precursors. Derivation of reduced sulphur by subsurface thermochemical reduction of

a sulphate-bearing ore fluid, with declining fluid:rock ratios or increasing $\delta^{34}S$ of the mineralising fluid in the later stages of the system, appears the best explanation for these trends.

The trend to increased ^{34}S appears to follow through into the late syndeformational regional lodes in the 100 to 200 square kilometre area surrounding the deposit. This progression is interpreted to mean that Century and the regional lodes are geochemically and genetically linked. In the regional lodes, early sphalerite has $\delta^{34}S$ values from 20 to 25 ‰CDT while later sphalerite generations have progressively higher values, reaching a maximum of 25 to 30 ‰CDT in the final stages of mineralisation. The extreme values in the paragenetically very-late lode sulphides are incompatible with derivation from a simple fluid with $\delta^{34}S$ compatible with known Mesoproterozoic marine sulphate. It is proposed that the total mineralising fluid system was a large closed-system sub-surface reservoir that experienced progressive enrichment in heavy sulphur in the later stages of the deformation and mineralisation events. In the absence of any alternative explanation, incremental thermochemical sulphate reduction within a deep, subsurface, oxidised fluid reservoir is proposed as a process to explain the fractionation with time.

From the limited lead isotope data collected from the Lawn Hill region to date, Century has a similar lead isotope signature to the Silver King and Axis lodes, suggesting that they have similar source regions for metals. Watson's Lode and Lilydale have different lead isotopes despite Watson's Lode and Silver King having similar sulphur isotope and fluid inclusion signatures. These differences in lead isotope signatures are interpreted as having the potential to provide important clues for the likely dimensions of source areas or fluid systems for the metals in the Century deposit. It is possible that mineralising system may have accessed sulphur from a common source and lead from multiple sources. Ramifications of this possible decoupling of metal and sulphur sourcing are discussed further in Chapter 7.

Chapter 7

Mineralisation Processes

7.1 Introduction

Previous discussion of sediment textures, structural evolution, mineralisation textures, timing and geochemistry has highlighted the complexity and probable longevity of the Century mineralisation system. A series of intricate textural and chemical relationships have been demonstrated at various scales.

Specific aspects of Century which require integration into any genetic model are:

- the derivation of the siderite in the mineralisation and hanging wall sequences. Identification of potential contributions of diagenetic versus hydrothermal iron mobilisation and fixation are required.

- possible sources and migration paths of sulphur.

- the source of the base metals.

- mechanisms for precipitation of sulphides and ways of explaining the lateral sulphide zoning.

- features of hydrocarbon generation, particularly overpressuring and its likely influence on fluid movement.

- the likely late diagenetic to syn-tectonic timing of the mineralising system with respect to larger scale basin development, basin inversion and fluid processes.

This chapter commences with a discussion of diagenetic source and transport mechanisms for iron and then relates these processes to the nature of early siderite in the footwall and mineralisation sequences. This is done to establish likely burial and sediment pore fluid conditions at the initiation of hydrothermal fluid activity. Possible sourcing and transport mechanisms for carbon (both as carbonate and hydrocarbon), sulphur and ore metals are then examined, with the dual objectives of producing an integrated model for depositional processes within the ore system and establishing constraints for the district-scale fluid system which fed it. The chapter concludes by integrating this discussion into a model for large-scale fluid migration for the Lawn Hill district.

7.2 Iron Mobility - Origin of Footwall Zone Siderite Phases

As well as the obvious zinc and lead, Century represents a sizeable accumulation of iron and manganese. Many other sediment-hosted base-metal deposits have substantial iron and manganese (Lambert and Scott, 1973; Gwosdz and Krebs, 1976; Williams, 1978; Large, 1980; Forrestal, 1990). In most deposits, iron is present as pyrite, pyrrhotite, or ferroan carbonates, commonly forming aureoles around the base-metal mineralisation (Large, 1980). Manganese is typically substituted into carbonate phases. The source of the iron (and manganese) is usually attributed to high concentrations in base-metal-bearing hydrothermal fluids (Large, 1980).

Century is an unusually low pyrite system, having a rather greater proportion of iron as siderite relative to other deposits. At Century, there is textural evidence for post-burial emplacement of siderite phases (section 5.4.1). The hydrothermal fluid responsible for deposition of siderite in the hanging-wall and mineralisation zone stratigraphy was most likely high in Fe, Zn and Mn (section 6.7.2). Possible source regions for such a fluid are discussed further in section 7.5.

However, in Chapter 6 the possibility is raised that the low-manganese deep footwall siderites at Century were derived by local pore fluid reactions and are therefore unrelated to mineralisation (section 6.7.3). Chemical conditions during early burial were probably broadly similar throughout the hanging wall and footwall sequences

before the entry of hydrothermal fluid. Some discussion of mechanisms of diagenetic carbonate precipitation during burial diagenesis is therefore warranted, to give insights into the possible pore fluid chemistry of the host sedimentary rocks as mineralising fluids entered the system.

Figure 7.1 shows a typical scheme for the diagenetic precipitation of various mineral phases during deeper burial processes (modified from Boles and Franks, 1979). It resembles, in general terms, the early Century paragenesis as summarised in section 5.5, with the exception that, in their study, ankerite, rather than siderite, was the dominant carbonate species. The study by Boles and Franks (1979) is useful insofar as it illustrates general principles of diagenetic carbonate derivation and relationships to clay diagenesis (smectite to illite transformations) during deep burial. Smectite to illite clay mineral transformations at temperatures >~80^{0}C produce soluble Fe^{2+} and Mg^{2+} (Bischoff et al., 1981; Imam and Shaw, 1987; Eslinger et al., 1979; Burley and McQuaker, 1992). Such transformation reactions are also a likely source of silica for early cements (Boles and Franks, 1979). If the sediment sequence is also organic-rich, thermocatalytic cleavage of kerogen may simultaneously produce large quantities of monofunctional carboxylic acids, principally acetate, in the temperature range from 80 to 100^{0}C (Surdam et al., 1989; this thesis, section 3.7.3, Fig. 3.11, reaction 1). [For simplicity of presentation, the remainder of this discussion is phrased as if acetate was the sole carboxylic species. This is defensible in terms of the predominance of acetate in natural environments and the similar chemical properties of other carboxylic acid species (Surdam et al., 1989)]

The mechanism for iron liberation to solution may be more complex than simple liberation of relatively soluble Fe^{2+}. If iron is liberated as Fe^{3+} by the destruction of the original carrier mineral, it must be reduced to Fe^{2+} by an organic intermediary such as acetate (section 3.7.3; Fig. 3.11, reaction 2A; Fig. 7.1). If pore fluids are too oxidised, Fe^{3+} may be reincorporated into new mineral species such as diagenetic hematite.

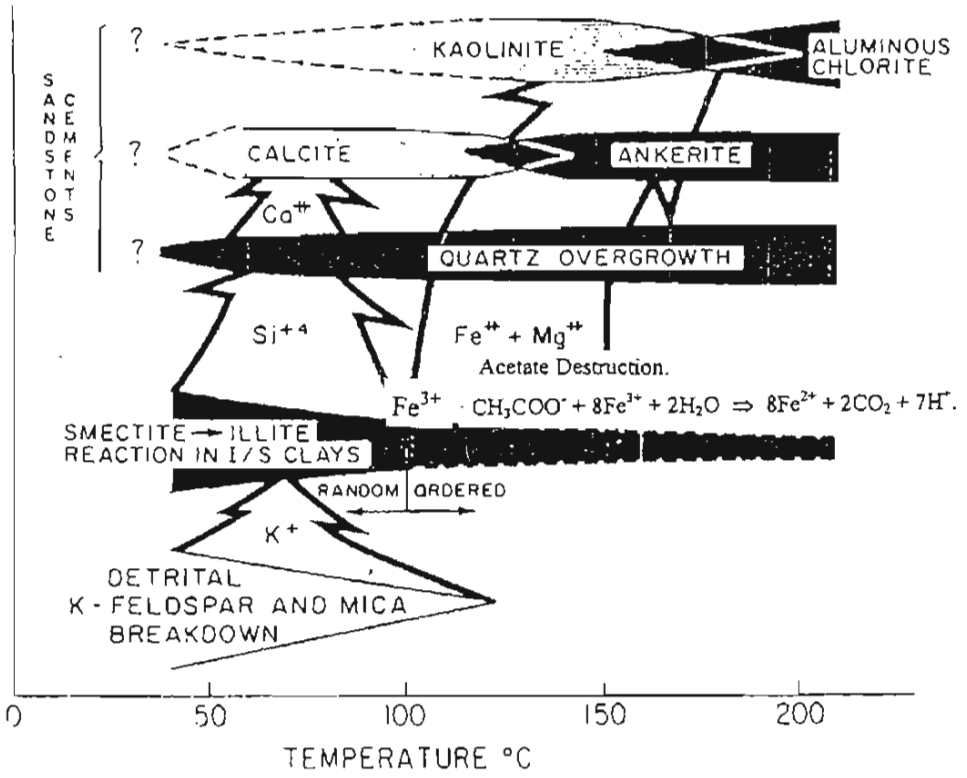

Figure 7-1 Typical diagenetic progression with burial in a mixed sandstone-shale sequence (after Boles and Franks, 1979).

The deposition of early siderite in the organic-rich deep footwall sediments at Century is postulated to have been initiated by the diagenetic liberation of iron and magnesium from disordered clay phases in the sediments. If this was ferric iron it could have reacted with acetate simultaneously being produced by the thermocatalytical cleavage of adjacent kerogens to produce carbon dioxide. High CO_2 flux in pore fluids would ultimately lead to precipitation of siderite (Fig. 7.1). Destabilisation of acetate by ferric iron also promotes acidic conditions (Fig. 3.11; reaction 2A), which would logically buffer carbonate deposition to siderite rather than ankerite. If the liberated iron was ferrous, slightly higher temperature would have been required to promote thermal decarboxylation of siderite and increased abundance of pore fluid bicarbonate (Fig 3.11; reactions 2C). The modest 0-2‰ $\delta^{13}C$ range of carbon isotope data and the relatively low oxygen isotope values ($\delta^{18}O$ 14-16 ‰) of the deep footwall siderites (section 6.4) correspond best to the lower zone III to upper zone IV of Irwin and Curtis (1977) (section 6.7.3.1; Fig 6.8).

Textures, composition and isotopic data of the deep footwall siderite at Century are therefore consistent with its derivation as a normal diagenetic species during relatively deep burial (>1000m). Reaction of organic materials with diagenetically-derived iron is a possible mechanism for the derivation of some varieties of early rhombic replacive siderite (section 5.3.2) in organic-rich units throughout the Lawn Hill Formation. However, the work of Andrews (1998b) implicates involvement of hydrothermal fluids in the regional scale deposition of siderite and ankerite cements in many units of the Lawn Hill Formation, so petrographic and compositional constraints must be established for carbonates at any given locality.

7.3 Hydrothermal Siderites - Sources of Carbon

From the discussion in the previous section, it seems logical that burial diagenesis of organic matter and acetate generation was also likely to have been well advanced in the hanging-wall and mineralisation sequences when hydrothermal fluids were introduced.

At Century, large-scale precipitation of zinc-rich siderite in the hanging-wall sequence is the most obvious early effect of the incoming hydrothermal fluid. Rapidly increasing the temperature of a system already critically poised for oil generation may partially account for this dumping of siderite, by promoting thermal decomposition of acetate-rich pore fluids. Even if thermal decarboxylation of acetate had not commenced, the additional heat from the hydrothermal fluid could have been sufficient to trigger it, thereby causing carbonate saturation of the resultant mixed fluid. If sufficient iron (and manganese, zinc, etc) was present, precipitation of siderite would have been greatly enhanced. In a hydrothermally-augmented thermally-prograding diagenetic system, intensive carbonate saturation from decarboxylation reactions is likely to have only occurred over a relatively short period of time, because of the narrow 80 to 100^{0}C thermal regime of acetate stability (Surdam et al., 1989). Soluble carbonate then reduced dramatically as acetate abundance declined and hydrocarbon maturation commenced.

The range of $\delta^{18}O$ from ~ +25‰ to ~ +14‰ of the earliest, zinc-rich, hydrothermal siderite nodules indicates substantial involvement of hydrothermal fluid (section 6.7.3). The $\delta^{13}C$ ~ 2‰ values of the earliest hydrothermal siderites are close to the (pore fluid-derived) deep footwall siderites and then shift to ~ -3‰ $\delta^{13}C$ (section 6.4). Thermal fractionation is not a plausible mechanism to explain the shift in carbon and oxygen isotope values because of the relatively small increase of temperature where acetate abruptly declined and hydrocarbon production commenced. The mixing trend line from (Fig. 6.2B) of the spheroidal siderites is therefore interpreted to reflect massive equilibration of pore fluids and hydrothermal fluids, causing dumping of carbonate. Hydrothermal fluids with $\delta^{18}O$ from ~+20 to 25‰ and $\delta^{13}C$ from 0 to -3‰ destabilised acetate-rich pore fluids with initial $\delta^{18}O$ of ~+14‰ and $\delta^{13}C$ of ~2‰. Given the inferred hydrothermal fluid isotopic composition, deep marine carbonate-derived fluids may represent an appropriate source (section 6.7.3). Part of the trend to lower $\delta^{13}C$ values with time could be the consequence of incorporation of ^{12}C from rapid destruction of organically sourced acetate.

The much lower carbon isotope values ($\delta^{13}C$ from –6 to -8‰) in the late-stage ore-zone crackle veins and lode siderites (section 6.4; Fig. 6.2A) are explained in section 6.7.3 as the result of incorporation of carbon from organic matter into hydrothermal fluids. High oxygen isotope values ($\delta^{18}O$ from +20 to +22‰) in these siderites signify continued involvement of hydrothermal fluids from the deep fluid reservoir. In process terms, if the system progressed to hydrocarbon generation and destruction in a *source-reservoir* trap (as discussed in section 5.4.2), destruction of hydrocarbon species is the most likely mechanism to have supplied the isotopically light carbon in the crackle veins. Possible chemical reactions responsible for this incorporation are discussed in the next section.

Precipitation of substantial hydrothermal siderite would also have had the effect of substantially reducing sediment porosity. The possible contribution of this cementation to progressive confinement of the hydrothermal system and overpressure development is discussed further in section 7.7.

7.4 Source and Transport of Sulphur

In this section, the merits of the preliminary hypothesis developed in section 6.7.4, for co-transport of metals and sulphur in an oxidised sulphate-rich fluid, are discussed in the context of possible alternative concepts for sulphur sourcing and transport. In addition to the established working hypothesis, co-transport of reduced metals and reduced sulphur and transport of reduced sulphur with exotic sulphurous hydrocarbons is considered.

7.4.1 Sulphate and Metals

Given the constraints on timing and access of hydrothermal fluids established in previous sections, thermochemical sulphate reduction is postulated as a key process for derivation of reduced sulphur within the Century mineralising system (section 6.7.4). The narrow range of $\delta^{34}S$ values in main stage Century sulphides is taken as evidence for the possible existence of TSR of a fluid with $\delta^{34}S$ close to that of Proterozoic marine seawater. It is further proposed that the sulphate reservoir became closed with time, from the evidence for progressive enrichment in isotopically heavy sulphur in the final stages of the deformation and mineralisation event. In the absence of any feasible alternative explanation, incremental thermochemical sulphate reduction within a deep subsurface oxidised fluid reservoir is proposed (section 6.7.4). This working hypothesis implies that sulphur was transported as sulphate in an oxidised hydrothermal fluid. Such a fluid can be calculated to have high metal carrying capacity (Large et al., 1998).

7.4.2 Reduced Sulphur and Metals

Many models for sediment-hosted base-metal deposits advocate co-transport of reduced sulphur and metals in hydrothermal fluids (e.g. Lydon, 1986; Ohmoto et al., 1991). Although solubilities are low relative to more oxidised fluids, requiring ten-fold larger volumes of fluid (Large et al., 1998), the process is probably realistic for many deposits. Ohmoto et al. (1990) point out that in many deposits with equilibrium

sulphide assemblages, excess H_2S must be present in the environment of sulphide deposition to explain patterns of sulphur isotope fractionation between different sulphur species. They argue that continuous sulphate reduction would add H_2S progressively to the ore deposit environment, stripping metals from the ore fluid in their order of sulphide solubility and making equilibrium conditions impossible to attain. They therefore postulate that, while thermochemical sulphate reduction is a valid process, it is more likely that the reduced sulphur is produced from deeper within the basin from evaporite sequences, then transported as H_2S or HS^- to the site of ore deposition with the metals in one fluid.

To some extent these points are valid, but they are based on assumptions of open-system equilibrium depositional conditions and a single ore-fluid model, which are probably not realistic for Century.

Several other factors make co-transport of reduced sulphur and metals unconvincing at Century:

1. The very low barium content of the Century and regional lode mineralisation (Waltho and Andrews, 1993; RTE unpublished data). Barium has relatively low solubility in low to moderate temperature (<250^{0}C) oxidised sulphate-rich fluids, but is soluble in more reduced, H_2S-bearing fluids (Lydon, 1986). The low barium at Century provides a strong argument that metal-bearing fluids were relatively oxidised and carried sulphur as SO_4^{2-} rather than H_2S.
2. High metal carrying capacity of reduced brines requires low pH (Large et al., 1998). Calcite or dolomite-rich rocks are required to neutralise further acidity created by metal-fixing reactions so that sulphides will continue to precipitate. Ore-host shale at Century has very low carbonate.
3. The changes in siderite composition with time. Zinc-rich siderite would not expected to be the stable zinc-bearing phase early in the paragenesis if reduced sulphur was always available for sulphide precipitation. If it was stable, then later siderite in the paragenesis should have remained zinc-rich.
4. Incorporation of isotopically light organic carbon into siderite is problematic if fluid conditions were always reduced. Hydrocarbons should further reduce the

fluid, encouraging metals to stay in solution, and discouraging oxidation of organic material.

7.4.3 Sulphurous Hydrocarbons

It could be argued that hydrocarbon phases carried the sulphur for metal precipitation, with metals supplied by a relatively sulphur-deficient oxidised hydrothermal fluid. In this scenario, sulphide precipitation would occur by simple reaction of reduced phases such as H_2S (sour gas) liberated from hydrocarbons with soluble metals.

Hydrocarbons with high sulphur content are known in many basinal environments (Baskin and Peters, 1992; Orr, 1974). In euxinic sediments with low total iron, reduced sulphur can be fixed directly on to kerogen in environments by early diagenetic processes. Kerogens with high sulphur content (up to 13 wt %) exist and are implicated in the evolution of many high sulphur oil and sour gas accumulations (Baskin and Peters, 1992). Sulphur is chemically bound to, and migrates with, the hydrocarbons after generation. Subsequent thermal and degradation effects eventually lead to the production of H_2S and elemental sulphur (Orr, 1974).

The compositional maturity of the organic phases at Century (section 6.2) makes direct refutation of the original existence of a sulphur-rich hydrocarbon accumulation impossible. However, several lines of evidence make it improbable.

1. Despite intensive reconnaissance work, no evidence exists in the immature portions of the Lawn Hill or correlative McArthur Basin sequences (Nathan Group?) for sulphur-rich kerogens or more evolved organic phases (Summons et al., 1988; McConachie, pers comm., 1992). These would be expected on a regional scale if present concepts for incorporation of sulphur in kerogen during diagenesis (Baskin and Peters, 1992) are correct.

2. The hydrocarbon accumulation at Century appears to be of the source-reservoir type (section 5.4.1), with probable relatively proximal, or internal, sourcing of

hydrocarbons. It is rather unrealistic to expect that unstable sulphur-rich kerogen would not have been abundant throughout the entire section to a greater or lesser degree and therefore led to regionally extensive iron sulphide, rather than siderite, precipitation as iron was liberated during burial diagenesis.

3. In modern environments, high-sulphur kerogens incorporate sulphur with isotopic values equivalent to, or higher than, coeval seawater (Baskin and Peters, 1992). Resultant high-sulphur hydrocarbons inherit this diagenetic signature with almost no fractionation (Baskin and Peters, 1992). During thermal degradation of high sulphur hydrocarbons, there is only a $\delta^{34}S$ fractionation of 1 or 2 ‰ between cracked H_2S (lighter) and residual sulphurous bitumens (heavier) (Orr, 1974). Assuming that Proterozoic organic-matter diagenetic processes were similar to modern sediments, sulphur sourcing from organic phases is incompatible with the distribution of isotopic values at Century. If Proterozoic seawater had $\delta^{34}S$ between +15 and +20 ‰ (Muir et al., 1985; section 6.7.4), $\delta^{34}S$ of 5-10‰ from the main-stage sulphide mineralisation is too light. The progression to $\delta^{34}S$ of +20-30‰ late in the mineralisation and lode paragenesis is inexplicable.

In summary, the concepts developed in section 6.7.4 for an oxidised, sulphate- and metal- bearing hydrothermal fluid at Century are interpreted to represent the best model alternative.

7.5 Sources of Zinc and Lead

This section discusses general mechanisms by which sedimentary basin fluids may evolve and acquire metals. Specifically, the following theoretical mechanisms are reviewed before developing an interpretation for the Century system.

- Mechanisms of brine development
- Metal sourcing by dissolution of oxide mineral phases
- Metal sourcing by hydration of basic volcanic rocks
- Metal sourcing from clay transformation reactions

7.5.1 Mechanisms of Brine Development

Past workers have invoked sources of metals for shale-hosted base-metal deposits to range from volcanogenic to deep metamorphic and plutonic origins (Stanton, 1972). Over time, models for derivation of metals from sedimentary basinal fluids have gained currency (e.g. Badham, 1981). Most current ideas favour metal transport by brines analogous to the modest temperature (<250^{0}C) metal-carrying oil-field brines originally documented by the pioneering work of Carpenter and co-workers (Carpenter et al., 1974; Carpenter, 1978; Carpenter and Trout, 1978). Large at al. (1998) mount cogent arguments for the high metal-carrying capacity of oxidised, sulphate-bearing, brines relative to reduced, H_2S-bearing brines of the type championed by Ohmoto et al. (1990). There have been many ideas proposed for source regions, mobility and interactions of metal-carrying brines (e.g. Carpenter et al., 1974; Carpenter and Trout, 1978; Bischoff et al., 1981; Garven and Freeze, 1984; Lydon, 1986; Russell, 1986; Sverjensky, 1986; Hanor, 1987; Cooke et al., 1998). Most of these models involve fluids scavenging soluble constituents over a substantial source volume. They give a range of metal concentrations from around one to several thousands of ppm.

Lydon (1986) conducted a critical review of models of ore fluid derivation for large zinc-lead deposits. He concluded that high concentrations of metals in low temperature (<250^{0}C) hydrothermal fluids are most realistically attainable only if irreversible mineral reactions are taking place in the fluid source area. Development of high concentrations of metals in fluids is thought to be promoted if at least one of the following mineralogical criteria is met in the fluid source area:

- presence of oxide phases or soluble coatings on mineral grains which have high background content of the appropriate metals.

- a large proportion of a primary mineral assemblage that may be converted to a secondary mineral assemblage by hydration alone (e.g. basaltic or ultramafic rocks).

- a large proportion of a mineral assemblage that is susceptible to non-equilibrium reactions at the temperatures and pressures of the fluid reservoir. Prograde transformations of disordered clays, such as smectite, to more ordered assemblages such as illite, are a likely example at the temperatures typical of many shale-hosted ore fluids. [As a speculative aside, partly reduced green smectite-rich sediments could comprise better quality source rocks for metals. Partial submarine oxidation of organic material and early formed sulphides during the sub-oxic diagenetic processes responsible for greensands gives anomalously high contents of reactive cations adsorbed to diagenetic clays (Aller et al., 1986).]

A complexing agent must be present to effectively hold metals in solution. High chloride contents are effective for lead and zinc. Water:sediment ratios must be as low as possible, consistent with acceptable permeability. If the fluid:rock ratio is too high, equilibrium conditions are quickly established between pore fluids and surrounding mineral phases and only a fraction of the total available metal is dissolved. If new undersaturated fluid is continually being introduced to the system and saturated fluids are continuously removed, a large proportion of the available metal will be leached. However, because of the high fluid throughput, fluids will probably be too dilute to form a large ore deposit without substantial recirculation or very large amounts of fluid.

The following discussion attempts to use these simple criteria to develop plausible scenarios for the sources of metals to the Century system. These are compared to the ideas developed from discussion of the lead isotope data (section 6.7.5), which propose that at least some metals in the Lawn Hill region were sourced independently of the main sulphate-rich (section 7.4) fluid reservoir.

7.5.2 Dissolution of Oxide Mineral Phases

It seems improbable that metals could have been sourced from the shale-dominated, relatively reduced strata of the Lawn Hill Formation, Termite Range Formation and Riversleigh Siltstone by the dissolution of oxide mineral phases. Evaporites of the Lady Loretta Formation were likely to have been sufficiently oxidised to have

preserved oxide mineral phases (section 7.4). However, the Lady Loretta Formation has very low clastic content (Sweet and Hutton, 1982). It is therefore intrinsically low in oxide mineral phases and would be a dubious quality source for base metals. More clastic-rich oxidised fluvial and evaporitic facies of the Lower McNamara Group, beneath the Lady Loretta Formation, may have had sufficient content of oxidised mineral species to constitute potential source facies. As a possible analogy, Large et al. (1998) persuasively argue that metal sourcing for the HYC deposit was from the lower McArthur and Tawallah Groups. In some respects, these have lithologically similar facies to the Lower McNamara Group and are disposed at similar relative depths to the HYC host shale.

7.5.3 Hydration of Basic Volcanic Rocks

The only basalts known in the Lawn Hill region (Fiery Creek Volcanics; see Sweet and Hutton, 1982) lie stratigraphically beneath the Lower McNamara Group, which places them at least 8-10,000m stratigraphically below Century. It is possible that fluids derived by leaching or dehydration reactions of basalts at such depth could have supplied the metals for the Century mineralisation. However, in this context, the low abundance of copper (<100ppm; Waltho and Andrews, 1993) at Century may be problematic.

Studies by Cooke et al. (1998) on interaction of relatively low temperature (<200^{0}C) oxidised fluids with Cu and Zn-rich dolerites in the McArthur basin, indicate that copper zinc and lead were very effectively leached from these rocks. Large et al. (1998) invoke similar fluids to be responsible for the formation of the giant HYC deposit. HYC does indeed have significant copper content of around 0.3% (Eldridge et al., 1993). Other things being equal, intuitively, zinc-rich fluids derived from copper-rich source rocks should have high copper content relative to zinc-rich fluids with low copper provenance. The low copper content at Century may be indicative of metal derivation from source regions with relatively low amounts of basic volcanic rocks. If volcanic rocks were present in the source region, they were likely at deep basinal depths, beneath fluvial sequences of the Lower McNamara Group.

7.5.4 Clay Transformation Reactions

Smectite-illite transformations are mentioned in the context of iron mobility in section 7.2 (Fig. 7.1). The reaction is a complex process, dependant on the original starting composition of the smectite and rates of burial, temperature change and fluid flux in the sedimentary sequence (Boles and Franks, 1979; Colten-Bradley, 1987; Freed and Peacor, 1989; Primmer and Shaw, 1991). The process commences at temperatures of 80-100^0 C and continues through to almost 200^{0}C, with an early stage of removal of one of the two inter-layers water in smectite at the low end of the temperature range and loss of the remaining water from about 170^{0}C to 190^{0}C (Colten-Bradley, 1987). These intervals correspond to the 2nd dehydration and 3rd dehydration stages of Lydon (1986; after Burst, 1969), in relation to large-scale mineral transformation reactions and windows of metal solubility (Fig. 7.2).

An interesting aspect of the smectite:illite transformation is its relationship to overpressure. Interestingly, the progress of smectite:illite transformations appears to be retarded in environments with high pore fluid pressures and low rates of fluid throughput (Colten-Bradley, 1987). This phenomenon is poorly understood but appears to occur either because the high fluid pressure retards desorption of water from clay interlayers, or because the low-salinity pore fluids produced by dehydration reactions easily become saturated in liberated cation species. In conditions of pore fluid saturation, smectite can no longer dissolve, so illite can no longer precipitate (Primmer and Shaw, 1991; Freed and Peacor, 1992). This may have important implications for the sourcing of metals. If high pore-fluid pressures are achieved and then maintained in a potential source rock lithofacies, source rocks can be buried to greater than expected depths and experience higher than expected temperatures before appreciable metal release occurs. Any major changes in conditions (loss of pressure, influx of high salinity fluids, etc) in such a reservoir may lead to very rapid progression of smectite:illite reactions, with a corresponding sudden release of metals.

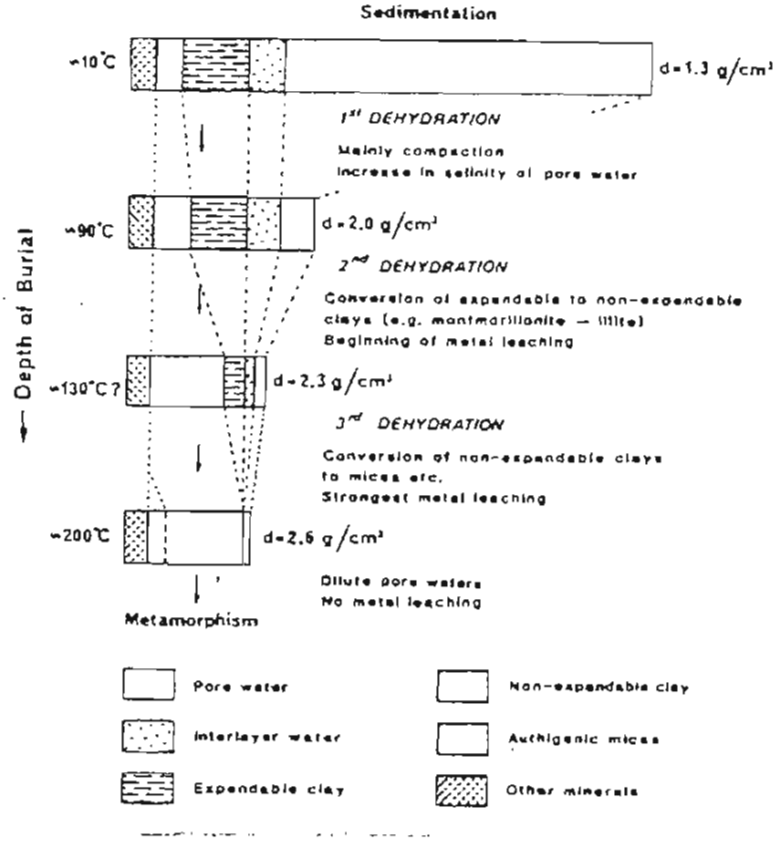

Figure 7-2 Schematic of dehydration events involved in metal derivation (from Lydon, 1986).

The low salinity fluids produced by loss of interlayer water have low capacity to transport base metals (Lydon, 1986). To effectively enhance the concentrations of cations such as Fe, Mn, Zn, Pb, Ca to potential ore fluid levels, high fluid salinities are required (Bischoff et al., 1981; Lydon, 1986). The most realistic way of doing this is to introduce a high salinity fluid from elsewhere, by large-scale fluid migration.

7.5.5 Metal Sourcing for Century

The following scenario for derivation of metals by clay transformation reactions may be applicable to the Century fluid system.

Beneath Century, units Pmh2/3 of the Lawn Hill Formation and the turbidites of the Termite Range Formation comprise substantial partly reduced sedimentary units with an abundance of clays and disordered mineral phases (Sweet and Hutton, 1981; Wright, 1992; Andrews, 1998). Field observations indicate that these rocks have relatively low content of sulphate and organic material, so possible metal-fixative sulphide precipitation reactions are unlikely to have occurred during burial diagenesis. The Pmh2 unit, in particular, has suffered regional hydrothermal carbonate alteration and has low trace-metal content (Andrews, 1998b).

Evidence for regional migration of hot fluids at various stratigraphic levels in the Century region is discussed in section 6.7.1. High temperature fluids from deep in the basin stratigraphy would most likely have high salinity (Carpenter et al., 1974). Local aquifer sands (Pmh3; Termite Range sands) would enable lateral access of brines. The thick shale sections of the lower Pmh4, Pmh1 and Riversleigh Formation would also confine fluids and force them to flow laterally within sand-rich units. Migration of high temperature and salinity fluids would conceivably accelerate the release of trace metals from clays, with good potential to produce high metal concentrations in the resultant mixed fluids. Local fluid compositions would be influenced by the amount and distribution of minerals containing radiogenic lead in aquifer sands (e.g. felspars). Individual fluid compartments could thus develop individual lead isotope signatures (section 6.7.5).

This combination of factors makes thicker portions of the Pmh2/3 horizon or the Termite Range Formation potential candidates for being the source facies for the metals of the Century deposit, provided they were accessed by high salinity fluids at the right time. Insufficient detailed geochemical data are available to make quantitative mass balance calculations. Collectively, the two formations appear to

have an adequate volume (>200km^3) at extraction efficiencies of a few tens of ppm Zn and Pb to account for the known base metals in the Lawn Hill district.

Otherwise, metals were sourced from deep in the basin section, most likely from the oxidised clastic rocks and evaporites of the Lower McNamara Group. Potential fluid pathways and transport mechanisms are discussed in section 7.8.

7.6 Mineralisation Chemistry and Processes

Possible reaction paths for derivation of acetate-rich sediment pore fluids and subsequent reactions with hydrothermal fluids (section 7.2) are summarised on Figure 7.4.

Previous sections (7.4 and 6.7) discuss the likely existence of thermochemical sulphate reduction processes (TSR) in the Century mineralisation, mostly based on trends and relationships in sulphur, carbon and oxygen isotopes. Section 5.4 interprets systematic relationships between various mineral species and textural variants and metal zoning patterns to be related to a hydrocarbon *source-reservoir* trap. This section consolidates these into a single process model for the main stage Century mineralisation.

7.6.1 Thermochemical Sulphate Reduction in the Century System

Many studies have postulated thermochemical reduction of sulphate by kerogen or hydrocarbons as a mechanism of producing reduced sulphur for metal precipitation (e.g. Williams, 1978; Leventhal, 1990; Anderson, 1991; Arne et al., 1991; Davidson and Dixon, 1992; Large et al., 1998). A review paper by Machel et al. (1995) gives a useful summary of possible reactions for TSR (Fig. 7.3). Figure 7.3 illustrates considerable variety of potential TSR reactions, with activity of various species and the likelihood of a given reaction to occur within any given system related to variation in composition and maturity of organic phases, relative proportions of oxygen, H_2S, carbonate, alkalinity, etc. However, for the purposes of this discussion, this potential complexity may be reduced in a simple way. Although there may be many alternative

possibilities for reaction schemes, there is an irreversible convergence to simple end-products of bicarbonate, H_2S, CO_2, residual bitumens and heat. The net reaction is comparable in form to the simple methane-sulphate reduction reaction proposed in section 3.7.3 in the context of diagenetic silica mobility.

Reaction 1:	paraffinic hydrocarbons	→	biodegraded hydrocarbons
Reaction 2:	crude oil	→	light crude oil + H_2S + CH_4
Reaction 3 a:	$4R\text{-}CH_3 + 3SO_4^{2-} + 6H^+$	→	$4R\text{-}COOH + 4H_2O + 3H_2S$
b:	$R\text{-}CH_3 + 2R{=}CH_2 + CH_4 + 3SO_4^{2-} + 5H^+$	→	$3R\text{-}COOH + HCO_3^- + 3H_2O + 3H_2S$
c:	$2CH_2O + SO_4^{2-}$	→	$2HCO_3^- + H_2S$
Reaction 4 a:	$2H_2S + O_2$	→	$2S^\circ + 2H_2O$
b-1:	$3H_2S + SO_4^{2-} + 2H^+$	→	$4S^\circ + 4H_2O$
b-2:	$H_2S + SO_4^{2-} + 2H^+$	→	$S^\circ + 2H_2O + SO_2$
c:	H_2S + hydrocarbons	→	S° + altered hydrocarbons
d:	S^{2-}	→	S°
Reaction 5:	$4S^\circ + 1.33(-CH_2-) + 2.66\ H_2O + 1.33\ OH^-$	→	$4H_2S + 1.33\ HCO_3^-$
Net Reaction:	hydrocarbons + SO_4^{2-}	⟹	altered hydrocarbons + bitumen HCO_3^- + H_2S (+CO_2?) + heat

Figure 7-3 Reactions important for thermochemical sulphate reduction. R = complex hydrocarbons (from Machel, 1987).

A conceptually simple reaction-scheme integrating metal- and carbonate-fixing reactions with methane-catalysed sulphate reduction and silica dissolution (see section 3.7.3) is therefore proposed as representative of the general kinds of reactions within the Century sulphide system. This consolidation is the starting point for a detailed discussion of likely process operation and timing.

$$CH_4 + SO_4^{2-} \rightarrow H_2S + HCO_3^- + OH^- \text{ (section 3.7.3)}$$

$$SiO_2 + OH^- + H_2O \leftrightarrow H_3SiO_4^- \text{ (section 3.7.3)}$$

$$HCO_3^- + Me^{2+} \rightarrow MeCO_3 + H^+$$

$$H_2S + Me^{2+} \rightarrow MeS + 2H^+$$

These reactions would form an intricate feedback system for solution and deposition of various mineral phases, depending on local conditions of reactant supply, carbonate buffering, silica saturation and H_2S loss. Once started, several factors could have encouraged self-generating positive feedback behaviour of the total system, accounting for much of the textural complexity and overprinting relationships within the deposit. Increased generation of hydrocarbons, especially methane, would be favoured by rising temperatures, driven by continual supply of hydrothermal fluid and the exothermic nature of the sulphate reduction reaction. Methane would be sufficiently soluble to directly interact with dissolved sulphate in hydrothermal fluids, with dissolved metals stripping the resultant H_2S directly from solution. Mineral precipitation reactions around the lower temperature periphery of the system could continually reinforce seal integrity, thereby retarding release of volatile reactive species from the system.

The concept of two fluid interaction of an oxidised (sulphate + metals) and a reduced (hydrocarbon-rich) fluid is central to the concept of TSR as a process. Relationships at Century are consistent with a process model for such two-fluid interaction. This simple scenario for chemical reactions within the system allows logical projections of timing of the onset of sulphate reduction and physico-chemical evolutionary paths of the system.

It could be argued that H_2S should have been produced very early in the Century paragenesis. Release of methane from acetate by either thermocatalytic processes or hydrolysis (Sürdam et al., 1989), before the main maturation of reduced hydrocarbons, could in theory have induced non-biological reduction of hydrothermal sulphate. There appears to be elevated pyrite in the vicinity of siderite-rich zones in the mineralisation shale (sections 5.3.2; 5.3.12), some of which could be derived by this mechanism. Zinc was certainly present, because it substitutes into early siderite. However, petrographically there seems to be very little to almost no sulphide co-precipitated with early siderite, apart from very minor euhedral pyrite (section 5.3.2).

Apart from the probable time required to heat the rock mass and build up hydrocarbon abundance, a simple explanation for the time lag between introduction of hydrothermal fluid and sulphide precipitation is that there appears to be a kinetic barrier to the onset

of TSR. TSR is thought to be possible between 80 and 120°C (Krouse et al., 1988) although this threshold is debated by Worden et al. (1995) who postulate a minimum temperature of 140°C for gas- (methane-) catalysed TSR. However it probably proceeds most efficiently from about 120 to 140^{0}C (vitrinite reflectances >1.5%R_0), up to temperatures around 200-300^{0}C (Kiyosu, 1980; Machel, 1987). It seems probable that the presence of free H_2S is required as an autocatalyst to initiate TSR at low temperatures (Orr, 1974, Machel et al., 1995).

If the main phase of (zinc-rich) siderite was deposited at relatively low temperature, in the prograding stages of the hydrothermal system (section 7.2), this kinetic barrier to TSR potentially explains the initial low sulphide content of the system. As time went on, the progressive occlusion of porosity by siderite deposition and the rapid rise in temperature from hydrothermal fluids irreversibly drove the system towards hydrocarbon generation and past the kinetic barrier to the onset of TSR. The precise trigger for the initiation of TSR is uncertain. Simple enrichment of volatiles within the system could have led to a gradual build up of sufficient H_2S concentration in the fluid to catalyse self-sustaining TSR and sulphide deposition (see Orr, 1974, Machel, 1987). More speculatively, a small pulse of reduced H_2S-rich fluid from an external source could have entered the system and triggered TSR.

Figure 7.4 integrates the conceptual metal precipitation scheme with the paleo-reservoir geometry developed in section 5.4.5. Methane-dominated TSR occurred in the upper portion of the reservoir (with complete conversion of CH_4 to CO_2), or perhaps even a H_2S rich gas cap evolved from underlying TSR reactions with liquid hydrocarbons. This catalysed direct replacement of silica and some siderite to produce non-porous sphalerite. Continuing consumption of methane and deposition of sulphides by reactions in the gas rich zone (and eventually breach of the reservoir seal) would ultimately leave few traces of organic material in this zone apart from refractory traces of solid pyrobitumen. Simultaneously, oil-mediated sulphate reduction catalysed the deposition of pyrobitumen-rich porous sphalerite. The zone of most intense mineralisation, where the highest zinc grades and both porous and non-porous sphalerite are present, is interpreted to represent a broad gas:oil interface in the paleo-reservoir system (Fig. 7.4). This hypothesis explains the cross-stratigraphic migration

in the grade of mineralisation and the pattern of distribution of the porous and non-porous sphalerite types (e.g. Figs 5.3; 5.4, 5.5 and 5.7).

The high purity of the sphalerite (section 5.2) suggests that the fS_2 of the system was relatively high (Scott and Kissin, 1973), and possibly that SO_4^{2-} and H_2S concentrations at any given time were relatively high. The dominance of siderite over pyrite in the system, with siderite seemingly co-precipitated with sphalerite, is problematic. Contradictory opinions are expressed in the literature as to the feasibility of co-precipitation of a carbonate with sulphides (c.f. Anderson & Garven, 1987; Plumlee et al., 1994). Further chemical modelling is required to resolve this issue. The coexistence of siderite and sphalerite below 250°C probably indicates high CO_2 pressures and high fS_2 (Holland, 1959). These are plausible outcomes of TSR in the confined, overpressured, conditions envisioned for the Century reservoir during main stage mineralisation.

Passage of large volumes of hydrothermal fluid through a sealed or semi-sealed hydrocarbon reservoir is a potentially problematic aspect of the model. It could have occurred by exchange of fluids from siltstone aquifer facies below the lower hydrocarbon:water contact, or perhaps the silt-rich facies within the immediate host sequence functioned as fluid conduits. Oscillating hydrothermal fluid pressures could have episodically forced hydrocarbons out to the periphery of the reservoir, which would then have returned as fluid pressures dropped (valved?). There would have been a continual drive to replenish hydrocarbons by the very *source-reservoir* nature of the trap. Hydrocarbons have different wetting properties to water (Tissot and Welte, 1978), and could have adhered to mineral surfaces with sufficient tenacity to permit reactions with hydrothermal fluids. Such physically-bound hydrocarbons could have continually liberated more-soluble methane to hydrothermal fluid as they decayed, thus facilitating hydrocarbon-fluid interaction.

Regardless of internal fluid transfer mechanisms, the hanging-wall sedimentary sequences (especially the chlorite-cemented massive sandstone of Pmh_5 and the siderite-silica-cemented siltstone of upper Pmh_4) acted as an overall regional seal to the fluid system for an extended period of time.

Solution and deposition of various mineral phases in such a delicate feedback type of chemical system will depend on local conditions of reactant supply, carbonate buffering, silica saturation and H_2S loss. Because of the dynamic and complementary nature of the various reactions, conditions would have continuously changed within the system over small distances. For example, liberation of H_2S and CO_2 could have locally increased gas pressure to the point where hydrothermal fluid was temporarily displaced from shifting microenvironments. As larger-scale pressures fluctuated, such gas phases could have migrated elsewhere within the system and created local fluxes that temporarily changed or reversed other local reactions. Fixation of metals by interaction with hydrogen sulphide is an acid generating reaction; increased acidity as sulphides were precipitated would enable local dissolution of siderite, explaining petrographic observations (section 5.3.2). Such micro-environmental variation could help to explain the high degree of textural complexity and local overprinting relationships within the deposit. The essentially simple, self-organising, nature of the underlying processes is consistent with the overall simple mineralogy of the system and the variations on a theme observations of relationships between the various mineral phases and textures.

The relatively narrow range of temperature between 150 to 200^{0}C for Century mineralisation and the regional lodes (section 6.7.1) indicates the likely importance of TSR as an ongoing mineralising process during the entire life span of the regional fluid system. Bresser (1992) postulated TSR as the major process for sulphide derivation in the regional lode mineralisation.

This scenario for the processes inside the Century system could be further investigated by hydrothermal geochemical modelling, but such an exercise will not be easy because of the likely complexity of kinetic effects within the system. It is considered beyond the scope of this study.

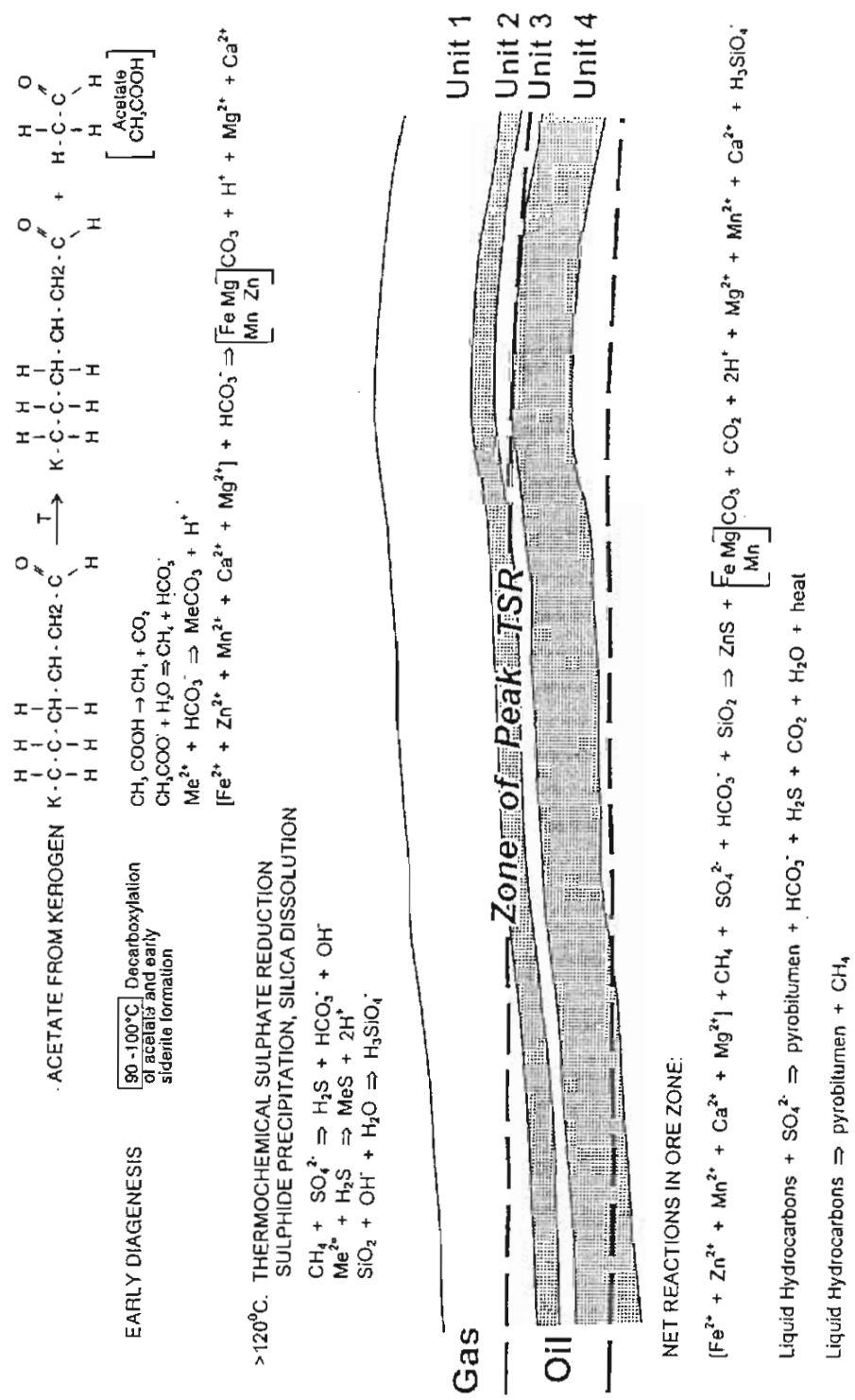

Figure 7-4 Summary of organic-inorganic reactions and TSR for the Century deposit, superimposed on the schematic hydrocarbon reservoir geometry developed in chapter 5 (Fig. 5.9). Mechanism for acetate liberation from kerogen adapted from Surdam et al., 1986. Other reactions discussed in text.

7.7 Hydrocarbon Generation and Overpressuring

The interconnected relationships of siderite precipitation, consequent permeability reduction and potential seal development (sections 7.3 and 7.6) require further discussion in the context of possible overpressure development within the Century system. Relationships of overpressured fluids to a variety of mineralisation styles is becoming increasingly identified (e.g. Fowler, 1994). However, most described systems involve high temperature fluids in deep level brittle:ductile regimes that are not really appropriate to the early Century conditions.

7.7.1 Mechanisms of Overpressure Development

Overpressure development is a common feature in sedimentary basins all over the world, at an average depth of ~3000m (Hunt, 1990). This burial depth corresponds to temperatures around 80-100^{0}C, coinciding with the zone of intense diagenesis and peak acetate production (Surdam et al., 1989). Volume-expansive pore fluid reactions associated with organic acid release and the release of water from smectite:illite transformations may increase the volume of pore fluid by 1-3% (Hunt, 1990). This may only seem like a small amount of fluid, but if a well-developed top seal is present, this small increase in volume is sufficient to hydraulically fracture the host-rock (Palciauskis and Domenico, 1980) and create thin laterally extensive zones with substantial permeability and porosity.

A predominance of layer-parallel horizontal fractures would be implied by this flat geometry of overpressure zones. Few detailed descriptions of textural characteristics of hydraulic fracture networks in sedimentary basins are available (e.g. Kulander et al., 1990). Textural similarities of the mineralised fracture networks at Century to dolomite- and hydrocarbon-filled fracture networks within *source-reservoir* hydrocarbon reservoirs are discussed in section 4.7. Many papers on the origin and orientations of reservoir fractures are available which implicate the role of high fluid pressures in the development of stratabound fracture networks (Gorham et al., 1979; Woodward, 1984; Do Rosario, 1991; Lorenz and Finley, 1991; Lorenz et al., 1991).

As the internal pressures rise within a given zone and the limiting strength of the rock is approached, there is a corresponding increase in differential stress, moving the system away from a hydrostatic scenario. The directed nature of far-field stresses creates a resultant systematic alignment of fractures preferentially in the overpressured zones, generally parallel or conjugate to the maximum principal stress (Lorenz et al., 1991). Many recent studies of fault and shear arrays are now tacitly acknowledging the influence of high internal fluid pressures on the geometry of shear zones (Segall and Simpson, 1986; Butler, 1991; Byerlee, 1992; Moore and Byerlee, 1992).

Overpressuring has been interpreted by many recent workers to be integral to the process of hydrocarbon maturation and migration. There is a growing school of thought that, without the presence of a top seal, economic hydrocarbon accumulations will not develop (Hunt, 1990; J Cartwright, pers. comm., 1992). It seems that, without a seal, the generated hydrocarbons migrate almost as fast as they are formed and are degraded before an economic accumulation can be preserved. If the seal is present, hydrocarbon generative reactions, together with lithostatic loading and porosity occlusion by diagenetic minerals, build up fluid pressure until it exceeds the minimum principal compressive stress and the confining strength of the rock. Rapid migration of the concentrated hydrocarbon phases from beneath the seal then takes place (Spencer, 1987; Buhrig, 1989; Barker, 1990, Hunt, 1990; Luo and Vasseur, 1992). Interestingly, in some circumstances, a feedback relationship may arise between oil and the seal. Carbonate is one of the characteristic mineral assemblages in seal facies capping hydrocarbon-rich overpressured zones (Hunt, 1990; see also discussion of source-reservoir traps in section 5.3.3). It seems that, in these systems, sealing diagenetic carbonate is most likely derived from relatively slow degradation of initial (acetate-rich?) maturation products. The developing hydrocarbon accumulation may in fact be responsible for its own seal in some circumstances, thus accelerating maturation, etc.

The real question in overpressure development is that of seal integrity. If the top seal remains intact, fluid pressure will build up until the lithostatic pressure and seal strength are exceeded. If the top seal re-establishes itself, fluid will build up again until the seal is breached. The cycle will continue until either the top seal fails irreversibly or the reaction mass, which drives fluid generation, is exhausted.

This scenario has fascinating resonance with the pulsing of hydrothermal fluids invoked for many mineralised systems, in particular the valving concepts of Sibson (1994). What the oil industry has learned is that overpressure development may be associated with dramatic changes in fluid fluxes over very short distances and equally dramatic changes in sediment properties and mechanical state. Overpressuring is basically driven by processes intrinsic to the sediment pile (Hunt, 1990). No particularly unusual basinal conditions need to be invoked, although, if present, they would exacerbate some features of the process.

In traditional metalliferous economic geology, several difficulties have always bedevilled subsurface emplacement/replacement concepts of ore genesis (e.g. critique by Goodfellow et al., 1993). One has always been the remarkably selective nature of fluid ingress to a few individual horizons, and the lack of mineral and isotopic zonation along individual mineralised lamallae. Another is explanation of zones with puzzling deformation textures such as apparent soft-sediment folding, injection breccias, nodules, boudins and the like, which are enclosed within apparently normally textured, compacted sediments. Yet another is the basic problem of passing sufficient fluid through a previously coherent rock mass to satisfactorily reconcile mass transport requirements with metal solubility considerations. Finally, there is the problem of removing spent fluid and waste products, without destroying the integrity of the fluid system.

Normal overpressure development within basin sequences appears to illuminate some aspects of these traditional problems. Further study of mechanisms of overpressure development and textures in burial diagenetic environments may not provide any definitive answers, but it may provide some insights into enigmatic systems like Century.

7.7.2 Overpressure Development in the Century System

Speculatively, the upper Pmh4 sediment sequence beneath the impermeable Pmh5 sandstone cap may have been intrinsically under-compacted and overpressured (section 3.7.4), conditions which allowed focussed ingress of hydrothermal fluid in the first place (section 5.4.2). Regardless of the truth of this speculation, the implied acetate-rich nature of diagenetic pore fluids at the onset of the Century hydrothermal system (section 7.2) may justifiably be interpreted to have a genetic link to early-stage overpressure development.

In the Century context, ingress of hydrothermal fluid itself would likely have added to the internal fluid pressure of the mineralisation zone, as it must have been derived from deeper, higher pressure, portions of the basin.

The (hydrothermally-promoted) maturation of hydrocarbons in the source-reservoir shale of the mineralised zone would have added to build up of internal fluid pressure, as hydrocarbon generation is associated with a further increase of fluid volumes (Tissot and Welte, 1978; Hunt, 1990). Decay of liquid hydrocarbons to gas with increasing temperature further increases pressures.

In this context, the significance of the fracture patterns described in section 4.6 is more readily appreciated. The confinement of early stylolitic fractures and layer parallel stylolites (section 3.4.1) to the mineralised zone is consistent with development of substantial overpressure in early time, most likely progressively accompanying deposition of seal-enhancing siderite in the hanging wall siltstone sequence. Gundu Rao (1979) consider texturally-similar late-diagenetic flasers in carbonate oil reservoirs to have contributed considerably to reservoir permeability. Hydrocarbon generation within the source-reservoir facies of the mineralisation sequence would have further contributed to internal pressure. Stylolites and layer-parallel fractures were likely then have repeatedly reactivated and jacked open by pulses of hydrothermal fluid or ongoing generation of fluid and gas phases within the system. In mechanically weak reactive lithologies, widespread diffusion of fluids along sediment layers away from fracture surfaces would be a viable process in the early stages of such a system,

accounting for the layer-parallel replacement of shale. Occlusion of pore space by sulphide deposition during initial diffusive fluid-transport may not have been a major issue in the weak ore shale, but would have progressively contributed over time to blockage of internal fluid pathways. Extensive along-layer mobility of material within discrete overpressure zones is indicated by the work of Vandenbroucke and Durand (1981).

Episodic release of high internal pressures by hydraulic fracturing and valve type venting (Sibson, 1994), probably triggered in part by incremental shifts in contemporaneous tectonic stresses, is envisioned as a major mechanism for removal of volatiles and spent hydrothermal fluid. Periodic fluid pumping could simultaneously have removed waste products from the system and allowed replenishment of new reaction mass (fluid) from the deeper fluid reservoir. A self-organising kind of system is envisioned, with reactions inside the system acting to delicately modulate ingress and removal of fluid over a long time frame.

In the early stages of the model, fluid supply was relatively abundant and there was plenty of reaction mass, permeability and porosity. As the thermal regime prograded to more gas-prone conditions, mineral precipitates built up and the supply of reaction mass and fluid declined. The general trend was to progressively more brittle conditions with time, with higher internal fluid (gas) pressure. The increasing proportion of transgressive, but still stratabound, fracture-filling mineralisation (Plate 19) within Century is interpreted to represent the products of increasing internal overpressure with time. As deformation proceeded, the stratabound mineralisation at Century was terminated and fluid activity was diverted into the district-scale faults that host the transgressive lode mineralisation. It is not known whether this transition was gradual or abrupt. Speculatively, the correlation of closed-system sulphur isotopic behaviour with brittle fracture textures (section 6.7.4) suggests that the transition may have been rather abrupt. This question is discussed further in section 7.8. Figure 7.5 presents a speculative cartoon diagram of alternatives for possible fluid pressure cycling and evolution of the system, linked to valve concepts of fluid transmission of Sibson (1992, 1994).

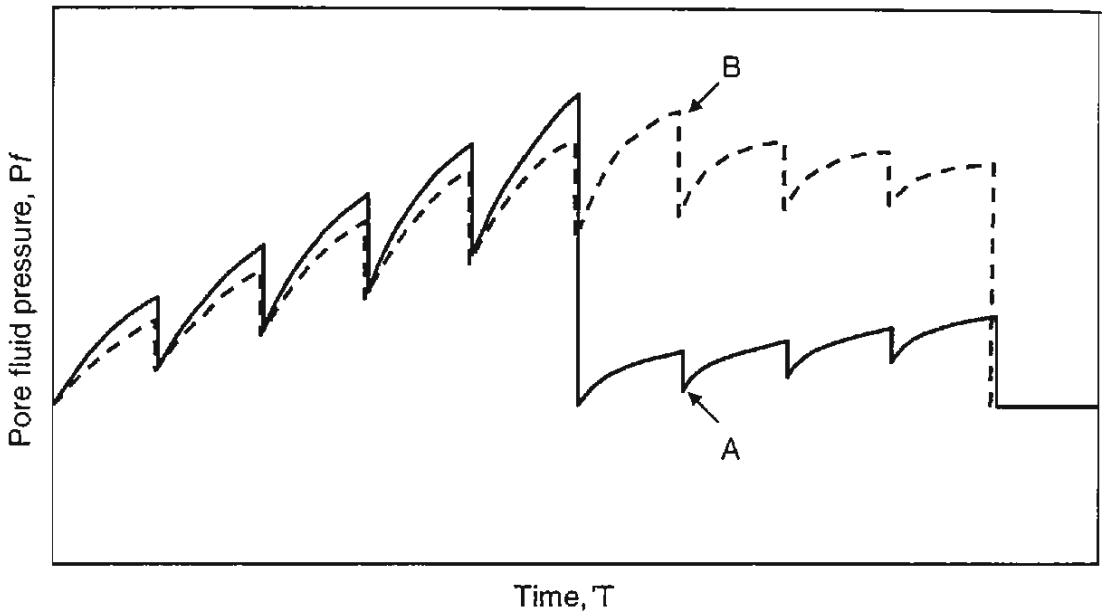

Figure 7.5 Speculative fluid pressure cycling and evolutionary paths for the Century system, adapted from concepts developed by Sibson (1994, 1992). Individual cycles represent valve type increases in pore fluid pressures that periodically exceed combined lithostatic pressure and the strength of the overlying top seal. The changing amplitude of cycles refers to the combined effect on pore fluid pressures of deposition of within-system sealing phases, increasing lithification and rock strength and changing internally generated fluid (gas) pressures. Path A superimposes these within-system factors on a prograding regional fluid pressure regime which suffers catastrophic top seal failure and is re-established at a lower level, with reduced regional fluid drive. This model envisions an abrupt switch between a fluid system originally focussed into the Century deposit to more dispersed, district fault-focussed, flow with lowered top seal integrity and low recharge capacity. Path B relates to a scenario of longer-sustained regional fluid drive with reducing recharge capacity and higher influence of within-system processes. Amplitude of within-system cycles initially increases, then decreases as overall regional fluid supply declines and successive breach events incrementally disrupt integrity of top seal before final failure. See also discussion in section 7.8.

Implicit in these speculations is the notion of the mineralising processes being of essentially closed system character at some scales and partly open at others. First, the regional top seal to the district-scale fluid system (Pmh5) is envisioned as having maintained its overall integrity for a long time. In this respect, the regional-scale system can be thought of as being closed. Second, the internal seals to the orebody itself likewise maintained integrity for long periods (of time), but required to be periodically breached so the system could be resupplied with reaction mass and would not have choked on its own waste products. In this respect, the ore system had open system character. The relationship between closed and open system behaviour can be viewed conceptually as being related to the actual internal dynamics of feedback relationships between processes inside the system.

Most features of Century are compatible with its formation in an essentially deeply buried, sealed or semi-sealed environment. Closed-system circulation of fluids, supply of reaction mass and the removal of waste products remain formidable unsolved conceptual problems. The final section of this chapter discusses fluid movement concepts in basin systems and develops a conceptual model for fluid transport in the Century region.

7.8 Fluid Sources and Migration Concepts

7.8.1 Overview of Mechanisms for Fluid Movement

Most current hypotheses of sediment-hosted base-metal ore genesis invoke solution leaching of ore metals from a large volume of source rocks (Goodfellow et al., 1993). This process requires a mechanism to drive large-scale fluid migration. To form orebodies, such fluid flow requires to be focussed into a very small area relative to the original source volume. It is useful here to discriminate between three interdependant scales of fluid activity. Regional fluid migration involves movement of fluid at a scale appropriate to major tectonic units or entire sedimentary basin systems. Fluid mobilisation at a smaller, but still possibly semi-regional scale, appropriate to the development of ore districts is termed district-scale fluid migration. Within a district fluid system, a great variety of smaller-scale fluid pathways, circulation mechanisms and fluid:rock interactions is possible, appropriate to the scale of mass transfer involved in orebody formation, giving the concept of an identifiable ore fluid system. In ore fluid systems, it is useful to differentiate between system dynamics which act to supply fluid to the orebody environment, those which remove waste fluid and those which precipitate metals and gangue. This latter is an extrapolation of the familiar source-transport-deposition paradigm.

Figure 7.6 shows three alternative model concepts for regional-scale mechanisms for brine migration, from important papers by Garven and Freeze (1984), Lydon (1986),

and Oliver (1986). These examples have been chosen because they represent generic major alternatives for geodynamic settings of ore genesis.

Gravity-driven fluid flow (Figure 7.6a), with continued supply of meteoric fluid that evolves in composition as it traverses subsurface aquifer (source) facies has been invoked to explain very large provinces such as the Mississippi Valley Pb-Zn mineralisation (Cathles and Smith, 1983; Garven and Freeze, 1984).

Compactive expulsion of basin fluids by the "squeegee" effect associated with major prograding orogenic fronts (Oliver, 1986; Fig. 7.6b) is another important hypothesis. Tectonic loading by advancing thrust fronts pushes high temperature fluids from deep basin sections outward and upward into lower temperature regimes.

In rifting environments, Lydon (1986; Fig. 7.6c) argues that there are fundamental deficiencies in the amount of fluid available from deep-seated basin-compartments. He argues for convective circulation of deep basinal fluids to resolve mass balance and metal concentration problems in hydrothermal fluids. Many similar models invoke notions of convective fluid recirculation or advective recharge to reconcile large-scale mass transfer with realistic pore space-controlled fluid volumes in source rocks (e.g Russell et al., 1981; Jowett, 1986; Russell, 1986).

Within any given geodynamic regime, fluid dynamics modelling studies indicate that significant ore fluid systems require a regional system to be focussed by up to several orders of magnitude (Deming et al., 1990; Deming and Nunn, 1991). The most important influences on processes and directions of focussed fluid migration are permeability contrasts. Basin and sub-basin controls on sedimentary facies architecture and mineralogy exert profound influence on permeability (Lawrence and Cornford, 1995). Sedimentary architecture varies over much shorter distances than the scale of the geodynamic regime that provides the overall fluid drive. Fluid discharge zones will tend to be focussed and guided along tectonic fault zones (e.g. Cathles and Smith, 1983; Deming et al., 1990; Deming and Nunn, 1991; Goldhaber and Reynolds, 1991; Deming, 1992;).

Garven & Freeze, 1984.

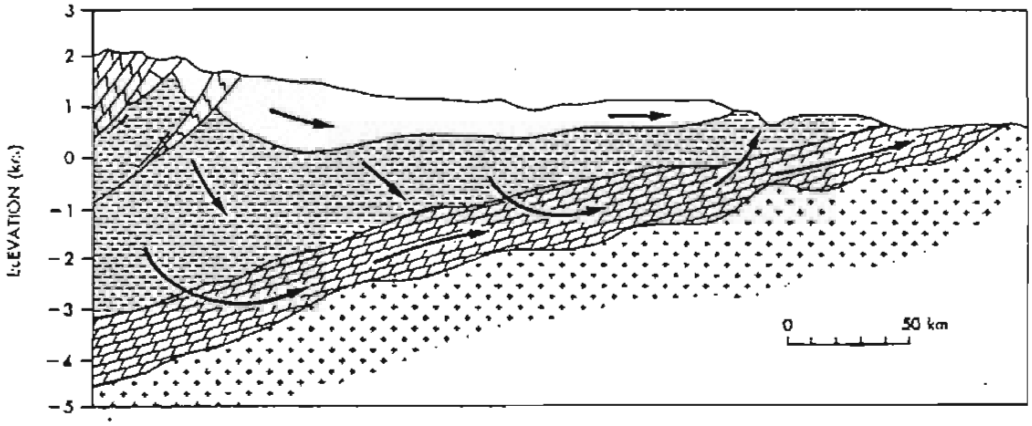

Oliver, 1986.

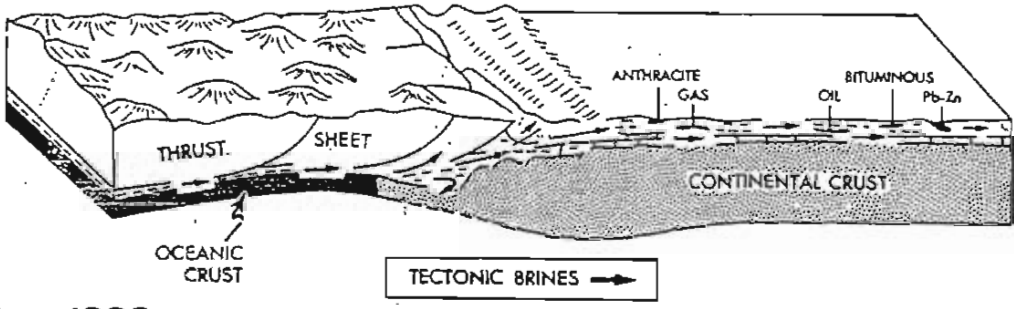

Lydon, 1986.

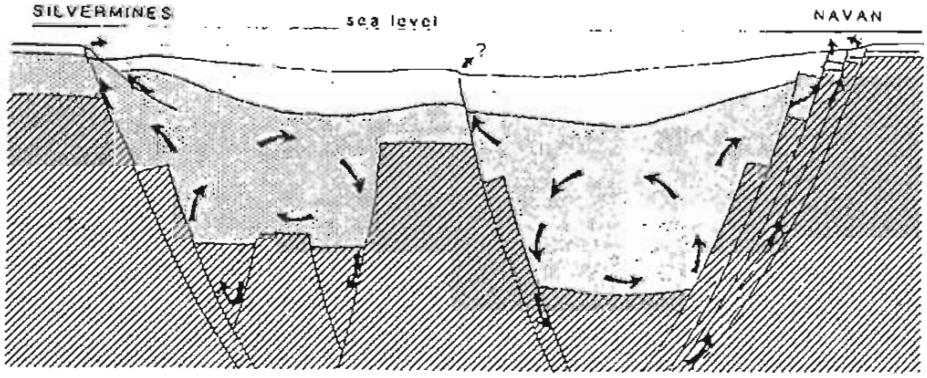

Figure 7.6 Generic brine movement concepts. Figure 7.6a (taken from Garven and Freeze, 1984) illustrates a model for topographically driven meteoric water recharge, with progressive evolution of brine compositions as waters traverse sub-surface aquifers. Figure 7.6b (taken from Oliver, 1986) illustrates a simple concept for expulsion of fluids from deep basinal sources ahead of an advancing orogenic front. Topographic relief in the orogen behind the thrust front will likely create hybrid flow regimes somewhat between 7.6a and 7.6b model concepts. Figure 7.6c (taken from Lydon, 1986) illustrates the postulated convective recycling concepts required in shallow rift environments to reconcile constraints imposed by requirements for reasonable pore fluid volumes and high metals solubilities required for mass transfer. Many aspects of these generic smaller-scale fluid recycling concepts (whether convective or advective) are applicable to lesser-scale fluid kitchens in individual basin compartments nested within the larger-scale environment illustrated by Fig. 7.6b.

The fault valving and seismic pumping concepts of Sibson (1994) offer conceptually elegant mechanisms for focussed transmission and episodic release of fluids during basin inversion in contractional tectonic regimes. Convective (Jowett, 1986) or advective (Bickle and McKenzie, 1987) fluid flow regimes may become established around local thermal perturbations.

Within a given tectonic regime, such factors combine to establish a network of independent, but interdependant, fluid compartments, with discrete subsurface fluid reservoirs confined by major faults and stratigraphic seals. Fluid movement paths and locations of possible mixing zones within individual basin compartments are inherently complex. Individual fluid compartments may coexist for extensive periods without appreciable lateral communication until external events (e.g. faulting or pressure rupture) force a connection between them. If an overall seal is maintained to a very large-scale subsurface fluid-system, subsidiary fluid cells may be repeatedly established and broken up at smaller scales beneath the top seal.

In summary, ore fluid derivation can be viewed as the product of semi-independent evolution of isolated orebody-sized fluid cells with different permutations of chemistry, heat flow, fluid supply and degrees of fluid confinement. Such fluid cells evolve in parallel in response to larger-scale geodynamic processes. They will resemble each other in the way that members of an extended family resemble each other, with general similarities but many differences in detail.

7.8.2 Model for Century and the Lawn Hill Region

In section 7.5, two alternative metal-sourcing scenarios are developed, involving supply from either deep in the basin section (Lower McNamara Group), or from higher level clastic units, such as the Termite Range Formation or Pmh2/3. A constraint that could be applied to fluid supply from more deeply buried sequences than the Lady Loretta Formation is the evidence for relatively low (150-200^{0}C) temperature of hydrothermal fluids (section 6.7.1). A simple temperature-depth diagram for the Century area (Fig 7.7) illustrates this point. Minimum to average stratigraphic thicknesses and a geothermal gradient of 30^{0}C/km have been assumed. The 30^{0}C/km

geothermal gradient has been chosen to best reconcile the interpreted ~80-100^{0}C temperature of the mineralisation sequence at the commencement of mineralisation (section 7.1) with a thickness of ~2000-2500m of upper McNamara Group rocks above Pmh5 (section 6.7.1). This scenario indicates the Lady Loretta Formation to lie between the 200^{0}C and 250^{0}C isotherms. Decreasing the geothermal gradient to 25^{0}C/km changes the mineralisation sequence temperature to ~70-80^{0}C, with the Lady Loretta Formation from ~150-200^{0}C. Geothermal gradients lower than 25^{0}C/km become increasingly more difficult to reconcile with the interpreted pre-mineralisation temperature of the Century host sequence in the context of reasonable depths of cover. Increasing the thickness of individual formations will simply increase the temperature estimate for lower formations. There are many uncertainties at this level of speculation, but issues of temperature of source aquifers are high amongst those that will have to be addressed in any future fluid modelling. Regional organic reflectance studies to better constrain any assumed geothermal gradient are a priority for future work.

The speculative reservoir temperatures for the Lady Loretta Formation at the lower range of plausible geothermal gradients are reasonably compatible with the interpreted 150-200^{0}C range of Century district hydrothermal fluids (section 6.7.1). However, the Lower McNamara Group section would consistently have been at higher temperatures, >200-300^{0}C. Some evidence for higher fluid temperatures in the mineralisation might be expected if fluids from these depths were rapidly carried to the site of ore deposition with minimal conductive heat loss. High temperature fluids sourced from deeper in the basin section could of course have interacted or mixed with higher level, cooler temperature, aquifers (e.g Goldhaber, 1991) and reduced their overall temperature whilst retaining or even gaining metal content. Glikson et al. (1998) have demonstrated the likelihood of substantial episodes of high-temperature fluid migration localised within some units of the Upper McNamara Group (section 6.7.1).

Mixing of deep, hotter, fluids and higher level, cooler, fluids is integral to the scenario developed in section 7.5 for metal sourcing from the Termite Range Formation or

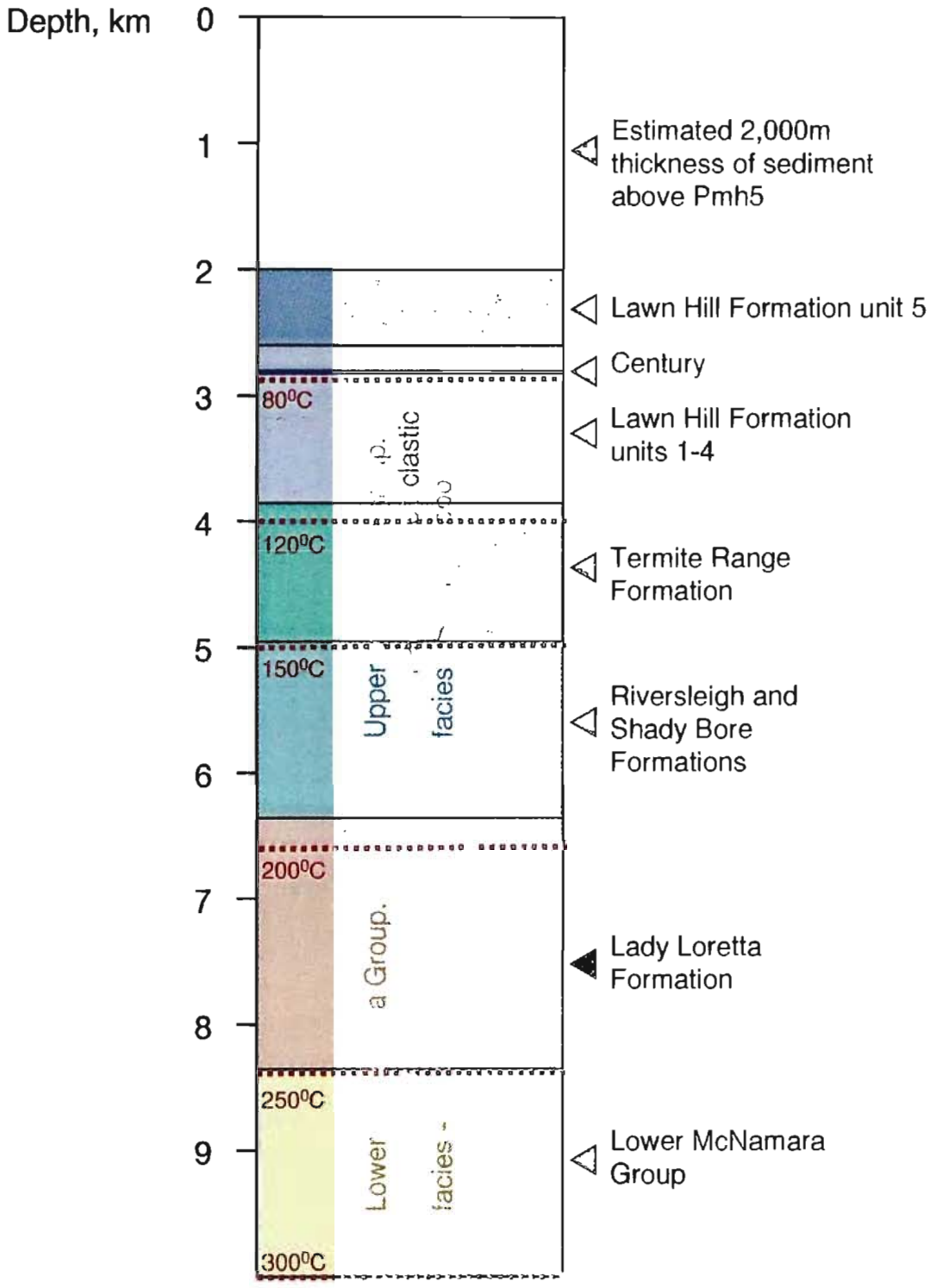

Figure 7.7 Schematic temperatures with depth under the Century deposit. Assumed stratigraphic thicknesses: Lower McNamara Group 1700m; Lady Loretta Formation 2000m; Riversleigh/Shady Bore Formations 1400m; Termite Range Formation 1100m; Lawn Hill Formation units 1-4 1500m; Pmh5 600m; Upper McNamara group above Pmh5 estimated at 2000m. Thickness estimates compiled from from Waltho & Andrews, (1993); Hutton and Sweet, (1982); McConachie et al, (1993). Assumed geothermal gradient 30°C/km (discussed in text).

Pmh2. Metal supply from high-level clastic units of the McNamara Group and sulphate sourcing from the Lady Loretta Formation or deeper evaporites is the preferred scenario for reasons of simplicity and the very limited evidence for local metal supply provided by the lead isotope data (section 6.7.5). Conceptual alternatives for flow paths for this scenario are summarised in Figure 7.8.

Mixing of high salinity, sulphate-rich, low base-metal fluids with moderate to low salinity, metal-carrying fluids sourced by clay dehydration reactions could be expected to have left some thermal or alteration signature if it occurred within an aquifer system (Fig. 7.8, scenario A). It is however possible that mixing took place within fluid conduits as separate basin compartments dewatered independently (Fig. 7.8, scenario B). Metal depletion of source facies would be one obvious effect. Insufficient data presently exist to enable determination of source vectors for the Century mineralisation. Andrews (1998b) has documented widespread hydrothermal siderite alteration of several units in the Lawn Hill Formation. He interprets this to be related to influx of hydrothermal fluid in a major fluid cell centred in the general area of the Century deposit. Siderite from this alteration is generally low in metals but has many similarities to late stage Century siderite (Andrews, 1998b), so this is perhaps not unexpected. Systematic comparison of trace element analyses of Pmh2 hostrock facies with the extent of regional alteration may give some insights into metal sourcing. Questions of metal depletion and hydrothermal alteration in the Termite Range Formation likewise need geochemical and petrographic investigation.

In summary, with present data there is no way of discriminating between the options for supply of metals from deep basinal sources or the scenario adopted in this study (Fig. 7.8) for higher level metal-sourcing. Comparative isotopic and petrographic studies of the Termite Range Formation and the exposed Lower McNamara Group rocks to the south of Century could yield insights into this fundamental question.

CENTURY DEPOSIT
EVOLUTION OF PRESSURE BARRIERS AND FLUID CELLS

EXPLANATORY NOTES - STAGE 1

1. Dewatering slows progressively in Pmh5 as pore cementation progresses.
2. Differential compaction at thick end of mudrock wedge sets up overpressure regime at lateral flow restriction.
3. High internal clay content of turbidites in TR Fm causes natural internal overpressure due to diagenetic cementation.
4. Good permeability of sand bodies in Riversleigh Siltsone makes this unit normally compacted, normally pressured - shale facies seal underlying formations.
5. Modest overpressure beneath lowermost Riversleigh seal facies confines deep pore fluids in sulphate rich evaporitic carbonates (Lady Loretta Fm and Shady Bore Quartzite aquifer).

EXPLANATORY NOTES - STAGE 2

Pmh5 top seal complete by diagenetic cementation -maintains overall seal to the basin fluid system for a long time.

SCENARIO A

1. Lowermost portion of Termite Range Fault guides regional fluid flow beneath Riversleigh shales .
2. Fluid ascends along fault, then moves laterally into thick updip wedge of TR Fm. Top seal is hydraulically fractured by increase in total fluid pressure at 3.
3. Saline fluid mixes with metal producing pore fluids, passes into Pmh3 sands, and back to main fault channel Delivered to orebody pressure compartment, closed system maintained by regional Pmhs top seal.

SCENARIO B

1. Termite Range Fault breaches Loretta carbonate/sulphate reservoir as in Scenario A.
2. Metal bearing fluids simultaneously being generated in TR Fm and volcaniclastic wedge in LH Fm move laterally and mix in fault conduit at 3 to form ore fluid.

To enable sufficient metal transport, sufficient salinity must be present in these fluids to complex metals. Scenario A is preferred at present, to better explain mineralisation distribution, the sulphur isotope evolution, and the lead isotope distribution in regional lodes. Position of "valve" fluid discharge points (4) unknown.

EXPLANATORY NOTES - STAGE 3

Basin sediments almost fully dewatered, folded and being actively faulted as basin inversion progresses.

1. Deep hot SO_4 rich fluids are much more confined to fault conduits. Permeability progressively confined to fracture systems (themselves partly hydraulic fractures).
2. Stratabound fracture network and lode filled mineralisation overprints earlier more permeable fabrics still confined in part to this stratabound zone in Pmh2/3.
3. Big faults like TR fault breach seal integrity, fluids escape up these and terminally breach overpressure compartments associated with stratabound mineralisation.

Lawn Hill Formation
- Unit 6
- Unit 5
- Upper Unit 4 mud facies
- Unit 4/2/1 mud facies
- Unit 3 tuff facies
- Unit 3 sand facies
- Unit 2 tuff facies

Termite Range Formation
- Turbidite sand and mud facies

Riversleigh Siltstone
- Sand facies
- Mud facies

Shady Bore Quartzite
- Sand facies

Lady Loretta Formation
- Evaporative carbonates

FLUID PATHWAYS

- Early dewatering flow path
- Metal prone fluids from clay dehydration reactions
- Hot, saline, sulphate bearing fluids ex evaporites
- Ore fluid cell -mixture of fluids trapped beneath top seal
- Pressure barriers/seals
- Century orebody position
- Regional Lode mineralistion

STAGE 1 - EARLY BURIAL (PRE-MINERALISATION)

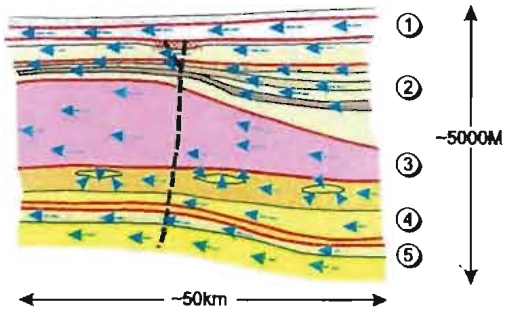

STAGE 2 - ALTERNATIVE SCENARIOS FOR EARLY TECTONIC/THERMAL LOADING AND FLUID MIGRATION (SYN MINERALISATION)

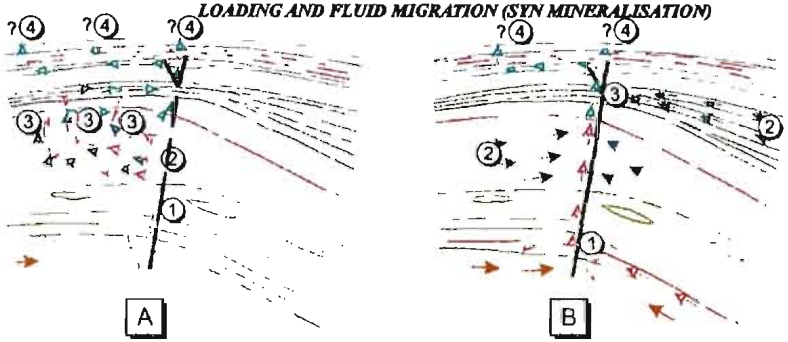

STAGE 3 - ADVANCED TECTONISM (LATE STAGE VEINS + REGIONAL LODES TO POST MINERALISATION)

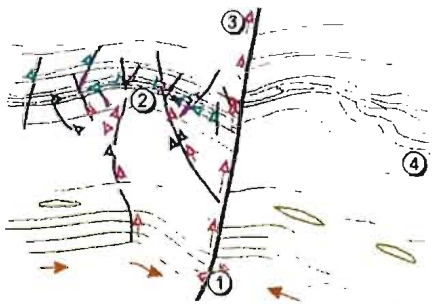

Figure 7.8 Lawn Hill Region. Conceptual fluid movement pathways in relation to pressure barriers, sedimentary units and fault architecture.

7.8.3 Regional Geodynamic Setting

This section concludes with some speculations on the geodynamic setting and driving mechanisms for the Century regional fluid system. The three generic geodynamic model alternatives outlined above (Fig. 7.6) are used as a starting point for discussion. In the Mt Isa-McArthur basin context, HYC is interpreted to be the result of a classic SEDEX-style episode of rift-related sediment/basin/basement dewatering (e.g. Large et al., 1998; see discussion in section 2.3). At the other extreme, direct involvement of syn-metamorphic fluids associated with the Isan Orogeny has been interpreted by some workers to be responsible for Pb-Zn mineralisation (e.g. Perkins, 1997). Few workers have tried to integrate local deposit models with conceptual models for distal fluid expulsion driven by far-field orogenic events (e.g. Oliver, 1986) or topographically-driven regional brine migration (Garven and Freeze, 1984).

The Century regional setting (Chapter 2) has little evidence for many of the geological attributes associated with the classic SEDEX model for mineralisation, for example, rifting and high heat flow (e.g. Goodfellow et al., 1993). Rather, the Century deposit is interpreted by the present study to represent a shale-hosted mineralisation style formed during regional migration of deep basin fluids into an overpressured/undercompacted shale sequence. The temporal linkages between mineralisation and local deformation events developed in section 4.7 are relevant here. Initiation of the hydrothermal fluid system responsible for main stage mineralisation at Century appears to be synchronous with the first south-east to north-west stage of basin inversion (local D1; Fig. 4.6). Fluid mobilisation continued into later east-west stages of inversion in the Lawn Hill region (local D2; Fig. 4.6). This phase of the regional fluid system was largely responsible for the regional lode mineralisation. There was probably a progressive overall decline in fluid volumes through the life span of the regional fluid system (section 6.7.4).

Local D2 east-west folding and faulting events in the Lawn Hill region, including folding of main-stage mineralisation at Century, are correlated with the main stage of regional D2 (after Bell, 1983) compression of the Isan Orogeny (Fig. 4.6). The southeast-northwest local Century D1, which is interpreted to be synchronous with

main-stage mineralisation (Fig. 4.6), is indirectly correlated with the final stages of the north-south D1 (after Bell, 1983) event of the Isan Orogeny. This correlation is based on the premise that regional D1 represents the final contractional stages of the basin, with long-continued activity from about 1600Ma to 1570Ma (section 2.2).

Tectonic loading associated with the initial phases of development of the Isan Orogen several hundred kilometres to the south-east is therefore postulated to have provided the initial stimulus for regional fluid mobilisation. The tectonic squeegee hypothesis of Oliver (1986) appears to be a viable geodynamic model for triggering the development of regional fluid flow.

7.8.4 The Rise and Fall of the Century Fluid System

The overall decline in hydrothermal fluid abundance and relatively closed-system behaviour of the fluid system in late time (section 6.7.4) is interpreted to be the consequence of declining fluid-supply capacity of more locally-controlled deep-fluid reservoirs.

Maintenance of large-scale fluid pressure gradients is viewed as critical for the potential longevity of lesser-scale deep basin aquifer systems at the scale envisioned in Figure 7.8. Even if the metal content of hydrothermal fluids was very high (say, 1%Zn; see Large et al., 1998, Fig 18), district fluid systems of the ~400km^2-size appropriate to the scale of the Century deposit and Lawn Hill lode system are probably too small to meet the mass-transfer constraints imposed by a single episode of pore fluid expulsion (Lydon, 1986). Without the push of new water supplied by convective, tectonically-driven or topographically-driven pressure gradients there is no drive for deep basin aquifers to discharge fluid into lower pressure-temperature regimes as envisioned in the model for the Century system (Fig. 7.8).

It can therefore be postulated that there was appreciable recharge of fluid to the deep Lady Loretta aquifer during deposition of the early stages of Century mineralisation, driven by an unknown mechanism. Large fluid throughput in the early stages of the Century system is supported by the narrow range in $\delta^{34}S$ of ~5-10‰ of the early

sulphide species, before the fluid reservoir became closed and enriched in heavy sulphur (section 6.7.4). Fluid throughput must have been sufficiently rapid to sustain fluid supply to the Century environment and ongoing dissolution of sulphate in the deep Lady Loretta aquifer system, but slow enough to not exceed the pressure required to catastrophically breach the top seal to the hydrocarbon reservoir system.

The interpreted constancy of temperature of the Century fluids through time (section 7.2) argues for recharge of fluid to the district-scale system from a relatively fixed and uniform hydrodynamic level of the regional-scale fluid system. Fluid convection beneath the regional top seal could be a possible mechanism for deep brine recharge, but it is difficult to see how this would work given the low permeability of the shale-dominated facies of the Pmh4, Pmh1 and Riversleigh Formations (Fig 2.2). These units have an aggregate thickness of over 2000m and show little textural evidence for large scale fluid migration (Andrews, 1998b). Downward-descending fluids would have to be channeled by fault structures, and it is difficult to see how a sustainable flow regime could develop.

Speculatively, the implied overall closure of the district-scale system in late time imposes some constraints on possible mechanisms for brine recharge. It may be argued that, by analogy to modern orogens, the developing Mt Isa Orogen to the south and east of Century probably had sufficient topographic relief to allow topographically-driven recharge of meteoric water and maintenance of regional hydrodynamic gradients. Partial gravity-driven recharge as modelled by Garven and Freeze (Fig. 7.6b) can be envisioned to have developed on orogenic topography at the scale modelled by Olivers' (1986) "squeegee" hypothesis (Fig. 7.6a). A hybrid model incorporating both mechanisms could simultaneously encompass the requirement for brine recharge early in the system whilst still allowing flexibility for modification of fluid paths as orogenic forces and structural kinematics changed with time. The requirement for closure of the fluid system may therefore be satisfied at the overall regional scale whilst still allowing a sufficient supply of fluid to the district-scale system.

A modified tectonic "squeegee" type model concept (Oliver, 1986) has therefore been adopted to relate overall geodynamic architecture to driving mechanisms for the

regional-scale fluid regime (Figure 7.9). Progressive regional deformation of deeply buried Lower McNamara Group aquifer facies during progressive tectonic loading imposed by the ongoing development of the Isa Orogen to the south and east, is the preferred geodynamic mechanism for triggering a long-lived regime of pore fluid expulsion from deep basin aquifers. A component of gravity-driven recharge and meteoric water influx to maintain hydrodynamic head and along-stratal flow within deep aquifer system is postulated, to maintain fluid throughput in the early stages of the total Century system.

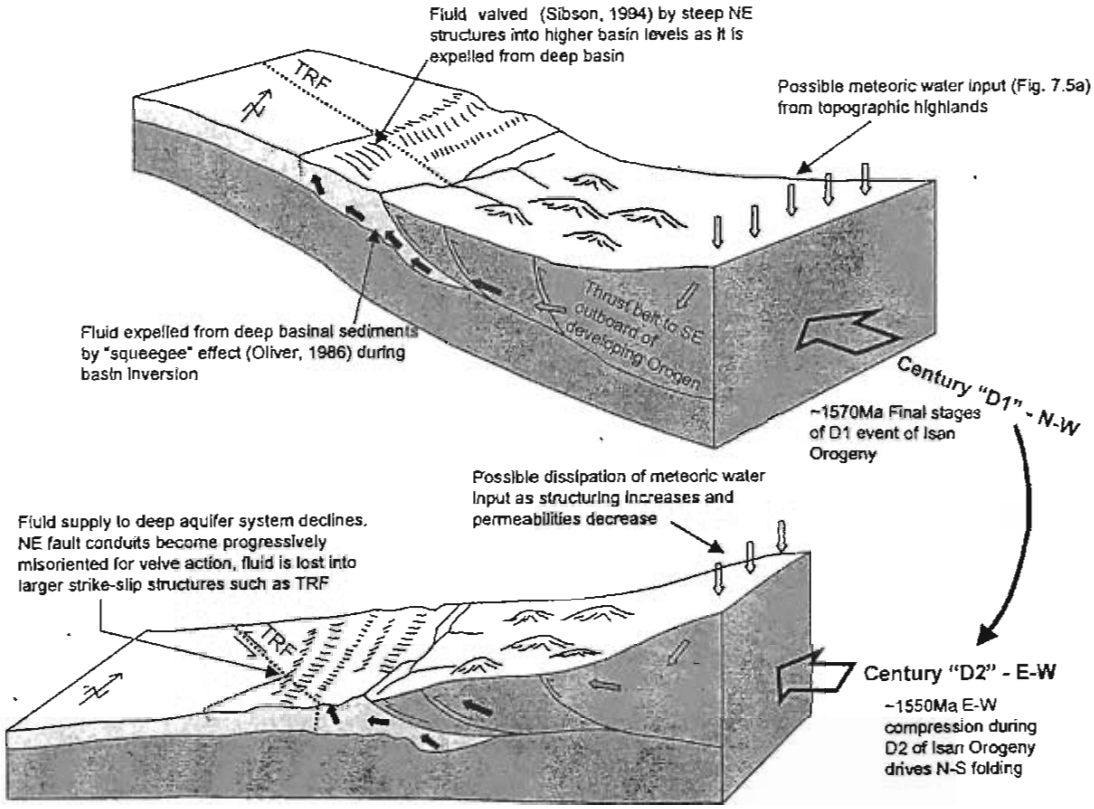

Figure 7.9 Speculative geodynamic model for regional fluid movement during the time span of Century mineralisation. Inspired by Oliver (1986) and Garven and Freeze, (1984)

This study does not purport to examine questions of overall mass balance or the total fluid budget in detail, as there is too little information available to even make an assumption of the metal concentration in the Century fluids. However, some speculations may be made about the relationships and evolution of kinematically suitable regional- and district-scale fluid pathways over time by considering them in this geodynamic context.

It is approximately 200km from Century to the margins of the Eastern Fold Belt of the Mt Isa Inlier (Fig. 1.1). The fold belt is interpreted to represent part of the developing Mt Isa Orogen at the time Century was being emplaced (Chapter 2). It is assumed that major regional faults could be expected to play a prominent role in shaping the internal dynamics of a regional fluid-flow regime outward from the developing orogen. Any such fault could perhaps also be assumed to provide a controlling asymmetry to pressure distribution and ultimate connectivity of a regional hydrodynamic regime. The north-west striking Termite Range Fault is a likely candidate for such a role. The fault is in excess of 100km long (as mapped by Blake, 1987) and exists at deep basinal levels, as evidenced by its long-lived control on sedimentation (Andrews, 1998). In the context of the initial southeast to northwest stage of the regional compressive regime (Fig. 7.9a), the Termite Range Fault is favourably oriented to function as a major regional conduit for fluid transmission away from the orogen. Steep parasitic northeast-trending faults in the Lawn Hill region (section 4.7) are kinematically well oriented to focus district-scale fluid transmission by fluid valving (Sibson, 1994).

Declining fluid volumes in the later stages of the Century system are temporally associated with increasing lithification and east-west shortening of the enclosing rocks (sections 7.6.1, 7.7). A potential explanation is that subsurface fluid-recharge pathways to the deep sulphate reservoir were progressively occluded by kinematic changes in regional-scale structural conduits as the regional stress regime changed, although decreasing permeability of regional aquifers could also have contributed to the decline. The shift in district tectonism, which correlates with the decline of the district fluid system, is genetically connected to the change within the Isan Orogen to east-west compression (Fig. 7.9b; section 4.7). The Termite Range Fault became progressively misoriented as a regional fluid conduit through time. Developing north-south folds and other structures commenced to modify smaller scale fluid transmission pathways, acting to progressively isolate individual district-scale fluid compartments. There was also a likely concurrent decline in valve behaviour of the local northeast fluid conduits at Century as they became progressively misoriented with respect to district scale stress. Once connectivity in the regional fluid system was interrupted (e.g. path A of Fig. 7.5), fluid capacity of the district subsurface aquifer system at Century went into steep decline, as evidenced by the sulphur isotope fractionation (Fig. 6.9).

7.9 Summary

It is proposed that the deep footwall siderites at Century were precipitated during relatively deep burial and are likely to be diagenetic siderites unrelated to mineralisation. They are interpreted to indicate the existence of soluble organic acids, such as acetate, derived from pre-mineralisation abiotic diagenesis of organic matter at temperatures around 80-100^{0}C. Deep footwall siderite is postulated to be precipitated as a consequence of reaction of these soluble organic acids with iron liberated from clay mineral transformations (smectite:illite reactions) proceeding synchronously with acetate production.

Deposition of the abundant pre-sulphide hydrothermal siderite in the hanging wall sequence and within the mineralisation may have been the result of massive re-equilibration of acetate-rich sediment pore-fluid and hydrothermal fluid. The heat from the hydrothermal fluid may have catalysed irreversible thermal-decarboxylation reactions in acetate-type species over a relatively narrow temperature window between 80 and 120^{0}C. Resultant carbonate saturation in mixed iron, manganese, magnesium and zinc-rich fluids caused dumping of siderite into available sediment pore space. This hypothesis is consistent with well-established principles of diagenetic carbonate derivation discussed in the literature and the mixing trend range of organic carbon isotope values from 0-2‰ and oxygen isotope values from 25 to 14‰ discussed in Chapter 6 (sections 6.3 and 6.7.3).

The initial top seal to the fluid system was provided by the overlying chlorite-cemented Pmh5 sandstone (section 3.7.4). Further reduction of porosity in the hanging-wall sequence by siderite cementation had the effect of progressively confining the fluid system to a relatively narrow interval with higher mechanically weak shale content.

The mineralising system subsequently increased in temperature, probably for the most part because of continuing addition of heat from the hydrothermal fluid. This temperature increase drove organic phases in the host sediments through the onset of oil generation, creating a *source-reservoir* hydrocarbon accumulation. The availability of

highly reduced hydrocarbon species initiated widespread thermochemical reduction of sulphate (TSR) in the hydrothermal fluid. TSR probably commenced after the internal temperature regime had exceeded ~120^{0}C and H_2S abundance had increased sufficiently to autocatalyse reactions. There were linkages of cross-stratigraphic metal migration and zoning of sulphide mineral species to internal zoning of the paleo-hydrocarbon reservoir (section 5.4). In process terms, the zone of peak mineralisation intensity is interpreted be the consequence of more intense sulphate reduction reactions along the interpreted paleo-gas:oil contact in the reservoir.

The Century deposit appears to represent a shale-hosted mineralisation style formed during tectonically-driven migration of basin fluids into an overpressured and possibly undercompacted shale sequence. Tectonic loading, associated with the initial phases of development of the Isan Orogen several hundred kilometres to the south-east, is envisioned to have provided the stimulus for regional fluid mobilisation, in accordance with the tectonic squeegee hypothesis of Oliver (1986). Initiation of the hydrothermal fluid system responsible for main stage mineralisation at Century appears to be synchronous with the first south-east to north-west stage of basin inversion (local D1). This correlates with the early geodynamic regime for the Isan Orogeny as deduced regional studies. Fluid mobilisation at declining intensity continued into later east-west stages of inversion in the Lawn Hill region (local D2), in sympathy with the change of major stress directions during the Isan Orogeny. This phase of the regional fluid system was largely responsible for the regional lode mineralisation. Through time, regional water-recharge pathways were interrupted by structuring and decreasing permeability of aquifers consequent upon progressive misorientation of local and regional fluid transmission structures. Once connectivity in the regional fluid system was interrupted, fluid capacity of the district-scale subsurface aquifer system at Century went into steep decline.

Chapter 8
Summary and Conclusions

8.1 Geology

The Century deposit represents an important new genetic variation of the style of sediment-hosted zinc-lead-silver rich mineralisation which is so well represented in the Proterozoic sedimentary sequences of the Mount Isa Inlier and McArthur Basin. The deposit differs from the well documented HYC and Mount Isa orebodies in that it is hosted by deeper water siliciclastic deposits rather than shallow water carbonate-rich lithologies. Mineralisation is sphalerite dominated. Diagenetic pyrite regarded as characteristic of other shale-hosted deposits in the region, is much less abundant and appears to be distributed as a halo around the main zinc and lead mineralisation. Ferroan carbonate (approx. 70% iron) is the principal iron-bearing gangue phase. Sphalerite in the deposit is unusually pure (62% zinc) and is associated with significant quantities of pyrobitumen.

The deposit occurs as several blocks which represent parts of an originally continuous body of mineralisation, disrupted by later faulting and tectonism. The Termite Range Fault, a major north west striking regional fault structure, trends parallel to the north east boundary of the deposit. However, this north eastern margin now consists of a pre-Cambrian erosional boundary and is not known to intersect this fault. Smaller east-west striking faults, named the Magazine Hill, Pandora's and Nikki's, form the boundaries of the main deposit blocks, in combination with erosional terminations associated with a Cambrian age unconformity or the present land surface.

Economic grade mineralisation consists of fine-grained sphalerite, galena and minor pyrite which mostly occurs as delicate bedding-parallel lamellae in black shale units up to 5 metres thick. These are separated by less mineralised, but more siderite-rich, siltstone marker horizons. The 40-50m thick mineralised envelope of stratigraphy that hosts the ore is similar in sedimentological character to unmineralised siltstone and

shale facies in the immediate host sediment sequence. The important differences are the development of characteristic stylolitic bedding surfaces in siltstone beds within the ore envelope and that the black shale beds are thicker and more abundant in the mineralised sequence. The stylolites appear to be the result of silicate dissolution from the matrix of the siltstone beds, and, in many instances, are infilled with trace sphalerite and pyrobitumen. Their development is intimately linked to mineralising processes.

Although in detail most of the sulphide mineralisation occurs as bedding parallel lamellae, overall the mineralisation transgresses stratigraphy, with the position of the most intense mineralisation moving upward within the mineralised sequence from south east to north west. This manifests itself as systematic grade variation within each mineralised shale unit along this vector. In addition, there appears to be a general increase in grade across the deposit from southwest to northeast, with grade in all units generally increasing towards the Termite Range Fault. Significantly, this grade variation occurs without appreciable changes in thickness of the host shale beds. Additionally, the host shale beds show no lateral chemical or textural changes suggestive of exhalative facies within the preserved portions of the deposit.

The timing of mineralisation relative to the compaction of the sediments is constrained by the development of nodular patches of silica cement in the siltstone beds, which predate the deposition of the earliest siderite generations. The deformation of bedding around these patches indicates that a significant amount of compaction took place after the silica cementation but before the deposition of the siderite. In turn, it is clear that compaction continued after the formation of nodular siderite cements within the mineralised sequence. As discussed below, the deposition of siderite and sphalerite are closely linked processes.

Two principal textural varieties of stratabound sphalerite are recognised: - porous, which has a high pyrobitumen content, and non-porous, which has a relatively low pyrobitumen content. These varieties appear to be co-genetic and almost co-abundant. Petrographically, both varieties appear highly replacive, the porous variety having a preference for organic-rich micro-laminae and the non-porous for siliceous microlaminae. The silica replacement is interpreted to be linked in genetic process

terms to the silica dissolution related to stylolite development. In general terms, the non-porous textural variety of sphalerite appears more abundant stratigraphically higher in the ore sequence than the porous variety of sphalerite, although both may coexist in the same hand specimen, and porous-sphalerite-rich bands may occur high in the ore zone stratigraphy. Collectively, these two types of sphalerite account for more than 90% of the total sphalerite in the deposit. The remainder of the sphalerite is present as progressively coarser grained and more discordant fracture filling forms, stratabound within the overall ore sequence.

Siderite is the main iron-bearing phase in the mineralisation. Petrographically the siderite appears to postdate much of the compaction in the host siltstone and is in part synchronous with stylolite development and sphalerite deposition. Microprobe analysis of the siderite reveals very marked changes in the siderite composition with time. The earliest siderites have a significant manganese and zinc content (up to 20% manganese and 5% zinc) while later generations are more iron- and magnesium-rich with correspondingly less manganese and no zinc. Petrographically, this chemical change appears to coincide with the introduction of mobile carbon phases (now pyrobitumen, interpreted to have been liquid hydrocarbon) and the onset of major sulphide deposition.

Carbon and oxygen isotope data for the siderites indicate systematic trends to lighter oxygen and carbon with time. These changes occur in sympathy with the above-mentioned changes in carbonate composition. The trend to lighter oxygen is interpreted to be best explained by mixing or exchange between ^{18}O-enriched hydrothermal fluids and sediment pore fluids with lower ^{18}O and slightly heavy to neutral (0-2‰PDB) carbon. The trend to lighter carbon is interpreted to reflect progressive incorporation of ^{12}C from either hydrocarbons or the host shales.

It seems probable that the early ore zone and hanging wall siderites were deposited from, or heavily exchanged with, an ^{18}O-enriched fluid with neutral carbon isotope values, which travelled laterally through the ore zone and the hanging wall sequence. The most likely source of such a fluid is from deep in the basin, with a strong possibility of a deep marine-carbonate influence. The marine carbonates of the Lady Loretta Formation and underlying evaporative carbonate sequences are a plausible

source region, with a strong corollary that the hydrothermal fluid would also have been relatively oxidised and sulphate-rich. Metal sourcing could either have been from the deep, sulphate-rich evaporitic lower Mcnamara Group or from clastic sequences rich in disordered clay species such as the Termite Range Formation or thicker portions of the tuffaceous Pmh2 sequence of the Lawn Hill Formation. The latter alternative is preferred on conceptual grounds and some evidence for local metal sourcing provided by limited lead-isotope data from the regional lodes

The sulphur isotopic composition of the sphalerite in the Century deposit appears to evolve with time to progressively heavier values. The earliest porous and non-porous forms have $\delta^{34}S$ values of between 5-10 ‰ CDT, while the later fracture filling styles evolve to $\delta^{34}S$ values of between 10 and 20 ‰CDT. This isotopic evolution appears to follow through into more widespread syn-deformational vein-style lodes in the 50-100 km^2 area surrounding the deposit. In the regional lodes, early sphalerite has a sulphur composition of 20-25 ‰CDT while later sphalerite generations have progressively heavier values, reaching a maximum of 25-30 ‰CDT in the final stages of vein mineralisation (Bresser, 1992).

8.2 The Century Genetic Model

At Century, conventional exhalative (SEDEX) or near-surface diagenetic emplacement models for ore genesis are considered inadequate to explain:

- The overall mineral zoning and the deposit-scale transgressive geometry of the mineralisation.

- The stylolites and abundant petrographic evidence for silica dissolution and mobility associated with sulphide deposition.

- The consistent stratigraphic thickness of ore host shale horizons, regardless of total sulphide content or ore grade.

- The intimate association of sulphides, siderite and pyrobitumen and timing relationships of sulphides and siderite to compactional features.

An origin by deep-subsurface late-diagenetic to early syn-tectonic replacement is proposed for the Century mineralisation. Events are summarised as follows:

- The Lawn Hill Formation was invaded sometime during moderate to deep burial of the Century sedimentary host sequence by a sulphate-bearing hydrothermal fluid driven out of the deeper parts of the basin. Depth of burial could have ranged from 800 to 3000 metres, based on regional stratigraphic relationships. The main conduit for the fluid delivery to the deposit area was the regional north-west striking Termite Range Fault system. Fluid was possibly focussed to the immediate area of the orebody by valve activity on north-east striking minor cross-faults.

- The hydrothermal fluid interacted with acetate-rich sediment pore-fluids in the hangingwall siltstone and organic-rich shale beds. The heat from the hydrothermal fluid may have catalysed irreversible thermal decarboxylation reactions in acetate-type species over a relatively narrow temperature window between 80 and 120^{0}C. Resultant carbonate saturation in mixed iron, manganese, magnesium and zinc-rich fluids caused dumping of siderite into available sediment pore space. This cementation progressively restricted circulation of the fluid system until it was confined to an overpressured zone at the level of the orebody stratigraphy. The stylolites characteristic of the mineralisation sequence result from dissolution of material adjacent to fluid pathways that developed as a result of hydraulic jacking along bedding.

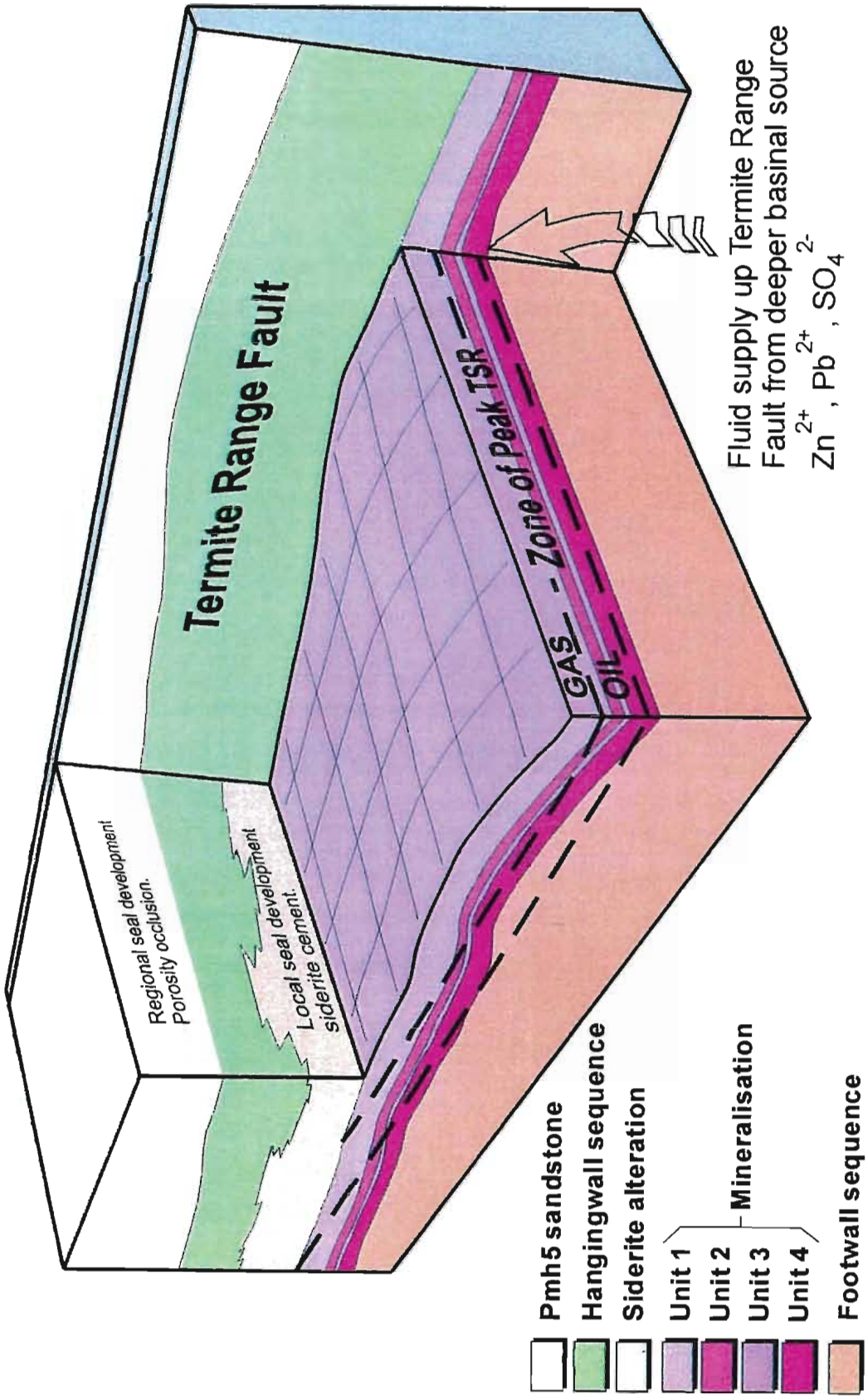

Figure. 8.1. Schematic block diagram of deposit geometry during main stage of mineralisation at Century. Zinc mineralisation was catalyzed by thermochemical sulphate reduction (TSR) of the deeper, basinal metal-bearing fluid, which peaks along the oil:gas contact of the hydrocarbon reservoir (see text and Fig. 24).

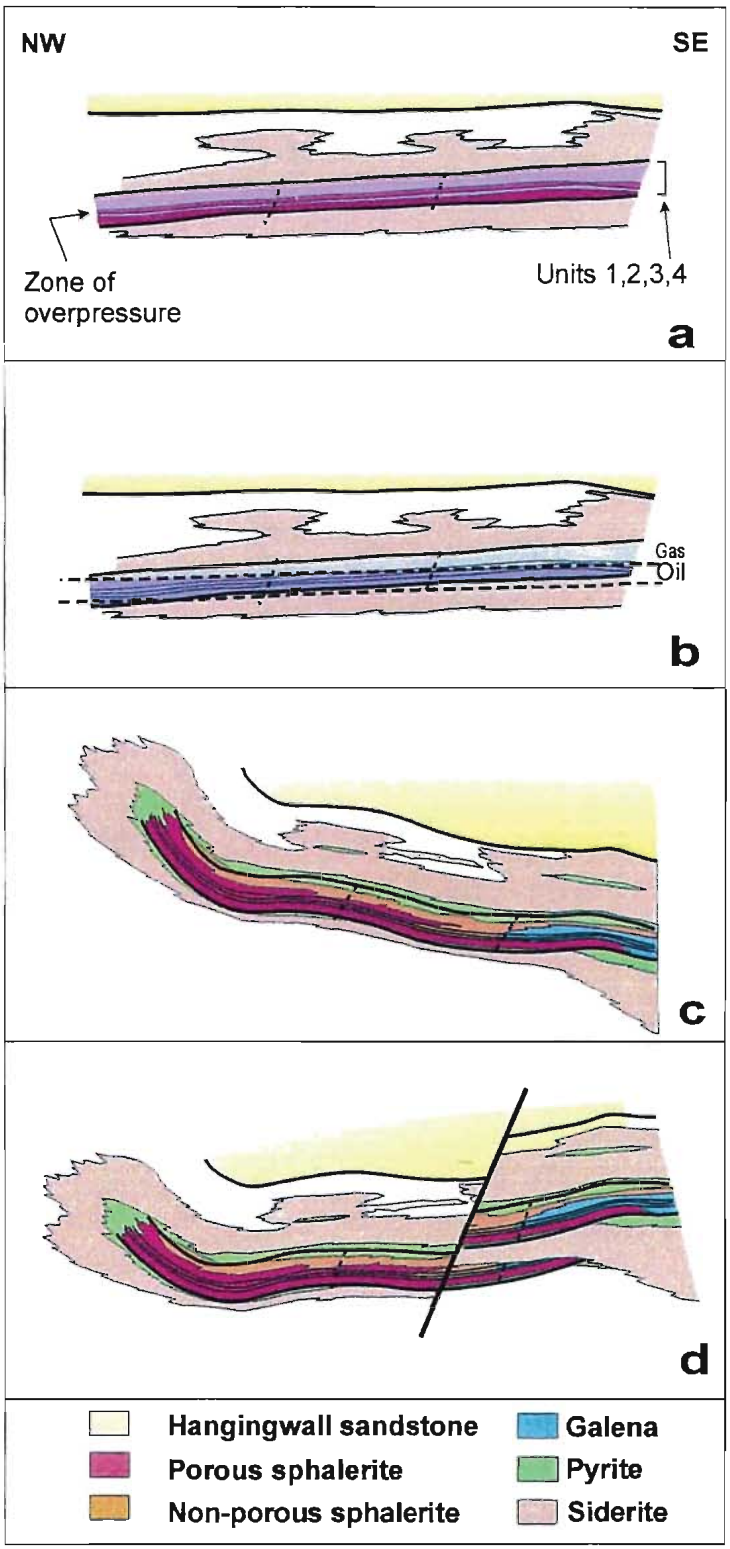

Figure 8.2. Schematic northwest to southeast cross-sections showing evolution of the Century deposit from initial development of early stage siderite cements, through hydrocarbon reservoir development and into final stages of folding and faulting: a. Initial fluid ingress and siderite (Mn/Zn-rich) cementation. Porosity occlusion in hanging wall sequence progressively confines fluid to orebody stratigraphy. Intense stylolite development in siltstone facies; shale beds are under-compacted. b. Hydrocarbons matured from organic-rich shale facies to form "source-reservoir" hydrocarbon trap. Thermochemical sulphate reduction initiated and main stage mineralisation commences. c. Main stage mineralisation after completion of N-S folding phase. d. Present geometry - post faulting. Regional lode mineralisation was emplaced between stages c and d.

- The ingress of hot metal-bearing fluid into the ore-envelope organic-rich shale resulted in the onset of gas (CO_2 and CH_4) and liquid hydrocarbon generation. These phases migrated within the host sequence to form a source-reservoir type hydrocarbon reservoir (c.f. Woodward, 1984) in the locally overpressured zone.

- The availability of highly reducing hydrocarbon phases led to the initiation of thermochemical sulphate reduction in the ore fluid. This coincides with a change in the siderite composition from zinc-rich to zinc-free and the onset of sphalerite precipitation. The unusually high purity of the sphalerite suggests relatively high fS_2 once TSR was initiated.

- Gas (methane?)-mediated sulphate reduction triggered direct replacement of silica and some siderite to produce the non-porous sphalerite type. Oil-mediated sulphate reduction simultaneously catalysed the deposition of the porous pyrobitumen-rich sphalerite type. The zone of most intense mineralisation, where the highest grades and both porous and non-porous sphalerite are present, is interpreted to represent the gas/oil interface in the paleo-reservoir system. This model is used to explain the cross-stratigraphic migration of the mineralisation and the pattern of distribution of the porous and non-porous sphalerite types.

- Deposition of the Century orebody was terminated by the loss of local overpressure within the orebody environment, which prevented fluid access for further along-layer replacement. The changes in the fluid pressure regime were manifested initially by the development of a stratabound network of hairline fractures throughout the Century orebody. Both the hairline fractures and larger breccia zones are mineralised with progressively more discordant sphalerite, galena and siderite at the deposit scale. At the district scale, large vein-style lode deposits, such as Silver King and Watson's, were deposited as the fluid system became progressively confined to a district-scale network of small faults active in the last stages of the deformation.

- The culmination of east-west tectonism was manifested by sinistral wrench reactivation of major north-west striking regional structures such as the Termite

Range Fault. Major faults that disrupt the Century deposit are interpreted to post-date the regional lode mineralisation and to have formed as an extensional duplex parasitic to the Termite Range Fault. They preserve the folded ore sequence in a small east-west graben complex bounded by the Magazine Hill and Nikki's fault trends.

- At least one episode of uplift and erosion in early Cambrian time and significant post-Cambrian fault reactivation and structuring has occurred. The combined effect of these factors has substantially modified the perimeter of the orebody to the point where no primary terminations of the mineralisation are known to be preserved. Many questions of the orebody's original geometric relationships will therefore remain speculative.

The apparent systematic evolution of sulphur isotopic compositions from the stratiform sphalerite through the stratabound replacement and hairline fracture mineralisation and finally to the regional-scale lode style mineralisation is very interesting. It suggests that the mineralising fluid reservoir became closed and experienced progressive incremental sulphate reduction, loss of ^{32}S and enrichment in ^{34}S of residual sulphate.

Migration of the mineralising fluids was triggered by south-east to north-west basin inversion and regional deformation asssociated with the early stages of the Isan Orogeny. Fluid migration continued through into the development of gentle north-south trending dome and basin folds. In the early stages of the fluid flow system, gravity-driven recharge from the developing Mt Isa Orogen possibly helped maintain the regional hydrodynamic regime. As regional deformation proceeded, faults were progressively developed or differentially reactivated, modifying fluid flow and redistributing it into different structural conduits. The closure of the district-scale fluid system is attributed to this progressive tectonically-driven fragmentation of the regional-scale fluid system.

8.3 Conclusions

The proposed genetic model differs in many respects from conventional models for the genesis of shale-hosted base-metal deposits. The orebody can be considered as the product of the coincidence of several, partly interdependant, geological processes which have interacted to produce a complex orebody geometry and chemistry. These processes have operated over a long interval of geological time, commencing with sedimentation at ~1600 Ma and concluding with final stages of basin inversion and regional deformation as much as 100 million years later.

The links between shale-hosted lead-zinc mineralisation and classical Mississippi Valley-type deposits have often been alluded to (e.g. Goodfellow et al., 1993) but comparisons have to a large extent been obscured by the specific geological attributes assigned to the respective mineralisation models. The Century deposit appears to represent an example of shale-hosted mineralisation which has formed during orogenically driven migration of fluids into an overpressured/undercompacted shale sequence. Regional migration of hotter metal-bearing, deeper basinal brines was impeded by local sedimentary facies and fault architecture to create a local trap environment. This resulted in rapid maturation of organic material in the trap, which in turn led to sulphate reduction and base-metal sulphide deposition. This scenario is much more reminiscent to some models of Mississippi Valley style mineralisation than those traditionally associated with SEDEX processes, although the utility of the established SEDEX model is still acknowledged to be valid for many (perhaps the majority) of other deposits. The recognition of this style of mineralisation greatly expands the framework in which to explore for shale-hosted zinc and lead, particularly in the Proterozoic Mt Isa Inlier and McArthur Basin.

References

Aller, R. C., Mackin, J. E., and Cox, R. T., 1986, Diagenesis of Fe and S in Amazon Inner Shelf muds: apparent dominance of Fe reduction and implications for the genesis of ironstones: Journal of Continental Shelf Research, v. 6, No 1/2, p. 263-289.

Anderson, G. M., and Garven, G., 1987, Sulfate-sulfide-carbonate associations in Mississippi Valley-type lead-zinc deposits: Economic Geology, v. 82 p. 482–488.

Anderson, G. M., 1991, Organic Maturation and ore precipitation in Southeast Missouri: Economic Geology, v. 86, p. 909-925.

Andrews, S. and Stolz, N., 1991, The Century zinc-lead deposit, Northwest Queensland: RTE unpublished report No 17693.

Andrews, S., 1998, Stratigraphy and depositional setting of the Upper McNamara Group, Lawn Hill Region: Economic Geology, v. 93, p. 1132-1152.

Andrews, S., 1998b, The regional setting of base metal mineralisation in the mid-Proterozoic Upper McNamara Group Lawn Hill Region. Unpublished PhD thesis, University of Queensland, Brisbane.

Arne, D. C., Curtis, L. W., and Kissin, S. A., 1991, Internal Zonation in a carbonate hosted Zn-Pb-Ag deposit, Nanisivik, Baffin Island, Canada: Economic. Geology, v. 86, p. 699-717.

Badham, J. P. N., 1981, Shale hosted Pb-Zn deposits: products of exhalation of formation waters?: Transactions of the. Institute of. Mining Metallurgy Section B, p. 70-76.

Baines, S. J., Burley, S. D., and Gize, A. P., 1991, Sulphide mineralization and hydrocarbon migration in North Sea oilfields: *in*: Pagel, M., and Leroy, J., eds., Source, Transport and Deposition of Metals, Proceedings, 25th Anniversary Mineral Deposits Meeting, Nancy, France, p. 87-91.

Barker, C., 1990, Calculated volume and pressure changes during the thermal cracking of oil to gas in reservoirs: American Association of Petroleum Geologists Bulletin, v. 74, No 8, p. 1254-1261.

Baskin, D. K., and Peters, K. E., 1992, Early generation characteristics of a sulfur-rich Monterey kerogen: American Association of Petroleum Geologists Bulletin, v. 76, No 1, p. 1-13.

Beardsmore, T. J., Newbury, S. P. and Laing, W. P., 1988, The Maronan Supergroup: An inferred early volcanosedimentary rift sequence in the Mount Isa Inlier, and its implications for ensialic rifting in the Middle Proterozoic of northwest Queensland: Precambrian Research, v. 40/41, p. 487-507.

Bell, T. H., 1983, Thrusting and duplex formation at Mount Isa, Queensland, Australia: Nature, v. 304, p. 493-497.

Bell, T. H., 1991, The role of thrusting in the structural development of the Mt Isa mine and its relevance to exploration in the surrounding region: Economic Geology, v. 86, p. 1602-1625.

Bell, T. H., Perkins, W. G., and Swager, C. P., 1988, Structural controls on development and localization of syntectonic copper mineralisation at Mount Isa, Queensland: Economic Geology, v. 83, p. 69-85.

Bickle, M. J., and McKenzie, D., 1987, Transport of heat and matter by fluids during metamorphism. Contributions to mineralogy and petrology v. 95, p. 384-392.

Bischoff, J. L., Radtke, A. S., and Rosenbauer, R. J., 1981, Hydrothermal alteration of graywacke by brine and seawater: Roles of alteration and chloride complexing on metal solubilisation at 200 and 350 C: Economic Geology, v. 76, p. 659-676.

Blake, D. H.,1987, Geology of the Mount Isa Inlier and environs, Queensland and Northern Territory: Australian Bureau of Mineral Resources Bulletin 225, 83 pp.

Blake, D. H., Etheridge, M. A., Page, R. W., Stewart, A. J., Williams, P. R., and Wyborn, L. A., 1990, Mount Isa Inlier - Regional Geology and Mineralisation: *in*: Hughes, F. E., ed., Geology of the mineral deposits of Australia and Papua New Guinea: Australian Institute of Mining and Metallurgy Monograph 14, p. 914-925.

Blake, D. H., and Stewart, A. J., 1992, Stratigraphic and tectonic framework, Mount Isa Inlier: *in*: Stewart, A. J., and Blake, D. H., eds., Detailed Studies of the Mount Isa Inlier, AGSO Bulletin 243, p. 1-12.

Bodon, S., 1996, Paragenetic relationships at the Cannongton Ag-Pb-Zn deposit, Mount Isa Inlier,. NW Queensland: Economic Geology Resource Unit Contribution 55, James Cook University of North Queensland, p. 15-19.

Boles, J. R. and Franks, S. G., 1979, Clay diagenesis in Wilcox sandstones of south west Texas: Implications of smectite diagenesis on sandstone cementation: Journal of Sedimentary Petrology, v. 49, No1, p. 55-70.

Braithwaite, C. J. R., 1989, Stylolites as open fluid conduits: Journal of Marine and Petroleum Geology, v. 6, p. 93-96.

Bresser, H. A., 1992, Origin of Base Metal Vein Mineralisation in the Lawn Hill Mineral Field, North Western Queensland: Unpublished BSc. Hons. Thesis, James Cook University, Townsville.

Bresser, H. A., and Myers, R. E., 1993, Timing of brine migration in the Lawn Hill Platform: Evidence from the Lawn Hill Mineral Field, Geological Society of Australia Abstracts, v. 34, p. 10.

Broadbent, G. C., 1995, The Century Discovery, North west Queensland - Is Exploration ever Complete? Pacific Rim Congress 95, Auckland, N.Z., Proceedings, p. 81-86.

Broadbent, G. C., and McKnight, S., 1993, Microstructures of ore minerals from the Century Deposit, Northern Queensland [abs.]: Geological Society of Australia Abstracts, v. 34, p. 11.

Buhrig, C.,1989, Geopressured Jurassic reservoirs in the Viking Graben: Modelling and geological significance: Journal of Marine and Petroleum Geology, v. 6, p. 31-48.

Burley, S. D., and MacQuaker, J. H. S., 1992, Authigenic clays, diagenetic sequences and conceptual diagenetic models in contrasting basin-margin and basin-center North Sea Jurassic sandstones and mudstones: *in*: Origin, Diagenesis and Petrophysics of Clay Minerals in Sandstones. SEPM Special Publication 47, p. 81-110.

Butler, R. W. H., 1991, Hydrocarbon maturation, migration and tectonic loading in the Western Alpine foreland thrust belt: *in*: England and Fleet,(1991), p. 227-244.

Byerlee, J., 1992, The change in orientation of subsidiary shears near faults containing pore fluid under high pressure: Tectonophysics, v. 211, p. 295-303.

Carpenter, A. B., 1978, Origin and chemical evolution of brines in sedimentary basins: Oklahoma Geological Survey Circular No 79, p. 60-77.

Carpenter, A. B., and Trout, M. L., 1978, Geochemistry of bromide-rich brines of the Dead Sea and southern Arkansas: Oklahoma Geology Survey Circular No 79, p. 78-87.

Carpenter, A. B., Trout, M. L., and Pickett, E. E., 1974, Preliminary report on the origin and chemical evolution of lead and zinc rich oil field brines in central Mississippi: Economic Geology, v. 69, p. 1191-1206.

Carr, G. L. 1992, Report on lead isotopic analysis of samples from the Century deposit: Unpublished report to CRA Exploration Pty Ltd.

Carr, G. L., and Smith, J. W., 1977, A comparative isotopic study of the Lady Loretta Zinc-Lead-Silver deposit: Mineralium Deposita, v. 12, p. 105-110.

Cartwright, J. A., 1987, Transverse structural zones in continental rifts – an example from the Danish sector of the North Sea: *In*: Brooks, J. and Glennie, K. W. (eds) Petroleum geology of north west Europe. Graham and Trotman, London, p. 441-452.

Cartwright, J. A., 1994, Episodic basin-wide fluid expulsior. from geopressured shale sequences in the North Sea basin. Geology, v. 22, p. 447-450.

Cathles, L. M., and Smith, A. T., 1983, Thermal constraints on the formation of Mississippi Valley type lead-zinc deposits and their implications for episodic basin dewatering and deposit genesis: Economic Geology, v. 78, p. 983-1002.

Chough, S. K., and Chun, S. S., 1988, Intrastratal rip-down clasts, Late Cretaceous Uhangri Formation, southwest Korea: Journal of Sedimentary Petrology, v. 58, No 3, p. 530-533.

Colton, G. W., 1967, Orientation of carbonate concretions in the Upper Devonian of New York: US Geological Survey Professional Paper 575-B, p. B57-B59.

Colten-Bradley,, V. A., 1987, Role of pressure in smectite dehydration - effects on geopressure and smectite-to-illite transformation: American Association of Petroleum Geologists Bulletin, v. 71, No 11, p. 1414-1427.

Connors, K. A., and Page, R. W., 1995, Relationships' between magmatism, metamorphism and deformation in the western Mount Isa Inlier, Australia: Precambrian Research, v. 71, p. 131-153.

Connors, K. A., Proffet, J. M., Lister, G. S., Scott, R. J., Oliver, N. H. S., and Young, D. J., 1992, Geology of the Mount Novitt ranges, Southwest of Mount Isa Mine. *in* Stewart, A. J. and Blake, D. H., Detailed studies of the Mt Isa Inlier: Australian Bureau Mineral of Research Bulletin No 243., p. 137-161.

Cooke, D. R., Bull, S. W., Donovan, S., and Rogers, J. R., 1998, K-metasomatism and base metal depletion in volcanic rocks from the McArthur Basin, Northern Territory – Implications for base metal mineralization. Economic Geology, v. 93, p. 1237-1263.

Corselli, C., and Aghib, F. S., 1987, Brine formation and gypsum precipitation in the Bannock Basin, eastern Mediterranean: Marine Geology, v. 75, p. 185-199.

Crick, I. H., Boreham, C. J., Cook, A. C., and Powell, T. G., 1988, Petroleum Geology and geochemistry of Middle Proterozoic McArthur Basin, Northern Australia II: Assessment of source rock potential: American Association of Petroleum Geologists Bulletin, v. 72, No 12, p. 1495-1514.

Croxford, N. J. W., and Jephcott, S., 1972, The McArthur lead-zinc-silver deposit, N. T: Australian Institute of Mining and Metallurgy Proceedings, v. 243, p. 1-26.

Curtis, C. D., 1978, Possible links between sandstone diagenesis and depth related geochemical reactions occurring in enclosing mudstones: Journal of Geological Society of London, v. 135, p. 107-117.

Curtis, C. D., and Coleman, M. L. 1986, Controls on the precipitation of early diagenetic calcite, dolomite and siderite concretions in complex depositional sequences: Journal of Sedimentary Petrology, p. 23-33.

Curtis, C. D., Coleman, M. L., and Love, L. G., 1986, Pore water evolution during sediment burial from isotopic and mineral chemistry of calcite, dolomite and siderite concretions: Geochimica et Cosmochimica Acta, v. 50, p. 2321-2334.

Cutler, H., 1992, The origin and timing of the sub-Cambrian alteration profile on the Century Zinc-lead deposit, Lawn Hill, Far North Queensland: Unpublished BSc. Hons thesis, James Cook University, Townsville.

D'Aigle, L., 1996, Geological mapping of the Lawn Hill Formation near the Century Deposit and lode mineralisation of the Zinc Hills. Rio Tinto Exploration Pty Ltd Unpublished Report No 21890.

Davidson, G. J., and Dixon, G. H., 1992, Two sulfur isotope provinces deduced from ores in the Mt Isa Eastern Succession, Australia: Mineralium Deposita, v. 27, p. 30-41.

Deming, D., 1992, Catastrophic release of heat and fluid flow in the continental crust: Geology, v. 20, p. 83-86.

Deming, D. and Nunn, J. A., 1991, Numerical simulations of brine migration by topographically driven recharge: Journal of Geophysical Research, v. 96, No B2, p. 2485-2499.

Deming, D., Nunn, J. A. and Evans, D. G., 1990, Thermal effects of compaction-driven groundwater flow from overthrust belts: Journal of Geophysical Research, v. 95, No B5, p. 6669-6683.

Do Rosario, R. F., 1991, Palm Valley Gas Field – Australia. Amadeus Basin, Northern Territory: *in*: Beaumont, E. A. and Foster, N. H., eds., Treatise of Petroleum Geology. Atlas of Oil and Gas Fields, v. 4, p. 255-272. American Association of Petroleum Geologists Special Publication.

Dooley, T., and McClay, K., 1997, Analog modelling of pull-apart basins. American Association of Petroleum Geologists Bulletin. v. 81, p. 1804-1826.

Dove, P. M., and Rimstidt, J. D., 1994, Silica-Water Interactions: *in:* Heaney, P. J., Prewitt, C. T. and Gibbs, G. V., Silica. Physical behaviour, geochemistry and materials applications: Reviews in Mineralogy v. 29. Mineralogical Society of America. Washington D.C. p. 259-308.

Eldridge, C. S., Williams, N., and Walshe, J. L., 1993, Sulfur isotopic variability in sediment-hosted massive sulfide deposits as determined using the ion microprobe SHRIMP II. A study of the H.Y.C. deposit at McArthur River, Northern Territory, Australia: Economic Geology, v. 88 , p. 1-26.

Elliot, C. G., and Williams, P. F., 1988, Sediment slump structures: A review of diagnostic criteria and application to an example from Newfoundland: Journal of Structural Geology, v. 10, No 2, p. 171 182.

Eriksson, K. A. and Simpson, E. L., 1990, Recognition of high frequency sea level fluctuations in Proterozoic siliciclastic tidal deposits, Mount Isa, Australia: Geology, v. 18, p. 474-477.

Eslinger, E., Highsmith, P., Albers, D., and deMayo, B., 1979, Role of iron reduction in the conversion of smectite to illite in bentonites in the disturbed belt, Montana: Clays and Clay Minerals, v. 27, No 5, p. 327-338.

Faure, G, 1986, Principles of Isotope Geology: Wiley and sons, New York. 2nd ed.

Flottmann, T., 1996, Aspects of the regional structure and tectonic setting of the Century orebody, Lawn Hill, Queensland. Rio Tinto Exploration unpublished Report No 21892.

Forrestal, P. J., 1990, Mount Isa and Hilton silver-lead-zinc deposits, *in* Hughes, F. E., ed., Geology of the mineral deposits of Australia and Papua New Guinea: Australian Institute of Mining and Metallurgy Monograph 14, p. 927-934.

Fowler, A. D., 1994, The role of geopressure zones in the formation of hydrothermal Pb-Zn Mississippi Valley type mineralisation in sedimentary basins: *In*: Parnell, J. (ed) Geofluids: Origin, migration and Evolution of fluids in sedimentary basins. Geological society special publication No 78, p. 293-300.

Freed, R. L. and Peacor, D. R., 1989, Geopressured shale and sealing effect of smectite to illite transition: American Association of Petroleum Geologists Bulletin, v. 73, No 10, p. 1223-1232.

Freed, R. L. and Peacor, D. R., 1992, Diagenesis and the formation of authigenic illite-rich I/S crystals in Gulf Coast shales: TEM study of clay separates: Journal of Sedimentary Petrology, v. 62, No 2, p. 220-234.

Garven, G., 1984, The role of regional fluid flow in the genesis of the Pine Point deposit, Western Canada Sedimentary Basin: Economic Geology, v. 80, p. 307-324.

Garven, G., and Freeze, R. A., 1984a, Theoretical analysis of the role of groundwater flow in the genesis of stratabound ore deposits I: Mathematical and numerical model: American Journal of Science, v. 284, p. 1085-1124.

Garven, G., and Freeze, R. A., 1984b, Theoretical analysis of the role of groundwater flow in the genesis of stratabound ore deposits II: Quantitative Results: American Journal of Science, v. 284, p. 1125-1174.

Gautier, D. L., 1982, Siderite concretions: indicators of early diagenesis in the Gammon Shale (Cretaceous): Journal of Sedimentary Petrology, v. 52, p. 859-871.

Gautier, D. L., 1987, Isotopic composition of pyrite: Relationship to organic matter type and iron availability in some North American Cretaceous shales: Chemical Geology, v. 65, p. 293-303

Ghazban, F., Schwarcz, H. P., and Ford, D. C., 1990, Carbon and sulfur isotopic evidence for in situ reduction of sulfate, Nanisivik lead-zinc deposits, Northwest Territories, Baffin Island, Canada: Economic Geology, v. 85, p. 360-375.

Ghibaudo, G., 1992, Subaqueous sediment gravity flow deposits: practical criteria for their field description and classification: Sedimentology, v. 39, p. 423-454.

Gize, A. P., 1985, The development of a thermal mesophase in bitumens from high temperature ore deposits, *in*: Dean, W. D., ed., Denver Region Exploration Geologists Society Symposium. Organics and Ore deposits. Proceedings: Denver Region Exploration Geologists Society, p. 137-150.

Glikson, M., Mastalerz, M., Golding, S. D., and McConachie, B. A., 1998, The role of organic matter in sub-ore and ore-grade mineralisation in Proterozoic sediments of the western Mount Isa Basin, Australia. In press.

Goldhaber, M. B., and Reynolds, R. L., 1991, Relations among hydrocarbon reservoirs, epigenetic sulfidization, and rock magnetization: Examples from the South Texas coastal plain: Geophysics, v. 56, No. 6, p. 748-757.

Goodfellow, W. D., Lydon, J. W., and Turner, R. J. W., 1993, Geology and genesis of stratiform sediment-hosted (SEDEX) zinc-lead-silver sulphide deposits. *In*: Kirkham, R. V., Sinclair, W. D., Thorpe, R. I., and Duke, J. M., (eds) Mineral Deposit modelling: Geological Association of Canada Special Paper 40, p. 201-251.

Gorham, F. D., Woodward, L. A., Callender, J. F., and Greer, A. R., 1979, Fractures in Cretaceous rocks from selected areas of San Juan Basin, New Mexico - Exploration Implications: American Association of Petroleum Geologists Bulletin, v. 63, No. 4, p. 598-607.

Greer, A. R., and Ellis, R. K., 1991, West Puerto Chiquito - USA San Juan Basin, New Mexico: *in*: Beaumont, E. A. and Foster, N. H., eds., American Association of Petroleum Geologists. Treatise of Petroleum Geology - Atlas of Oil and Gas Fields, v. 5, p. 59-78:

Gulson, B. L., 1985, Shale hosted lead-zinc deposits in Northern Australia: lead isotope variations: Economic Geology, v. 80, p. 2001-2012.

Gundu Rao, C., 1979, Late diagenetic solution seams and flaser structures in the carbonate reservoir rocks of Bombay Offshore, India. Journal of the Geological Society of India, v. 20, p.128-131.

Gwosdz, W., and Krebs, W., 1976, Manganese halo surrounding Meggen ore deposit, Germany: Transactions of the Institute of Mining and Metallurgy, Section B, p. 73-77.

Hanor, J. S., 1987, Origin and migration of subsurface sedimentary brines: Society of Economic Paleontologists and Mineralogists special publication.

Hashimi, N. H., and Ambre, N. V., 1979, Gypsum crystals in the inner shelf sediments off Maharashtra, India. Journal Geological Society of India, v. 20, p. 190-192.

Hinman, M., 1996 Constraints, timing and processes of stratiform base metal mineralisation at the HYC Ag-Pb-Zn deposit, McArthur River [abs.]: Economic Geology Resource Unit Contribution 55, James Cook University of North Queensland, p. 56-59.

Hitchon, B., 1984, Geothermal Gradients, Hydrodynamics, and Hydrocarbon occurrences, Alberta, Canada: American Association of Petroleum Geologists Bulletin, v. 68, No 6, p. 713-743.

Holland, H. D., 1959, Some applications of thermochemical data to problems of ore deposits. I. Stability relations among the oxides, sulfides, sulfates and carbonates of ore and gangue metals: Economic Geology, v.54, p. 184–233.

Hunt, J. M., 1990, Generation and migration of petroleum from abnormally pressured fluid compartments: American Association of Petroleum Geologists Bulletin, v. 74, No1, p. 1-12.

Hunt, J. M., 1991, Generation and migration of petroleum from abnormally pressured fluid compartments: reply to discussion by Waples: American Association of Petroleum Geologists Bulletin, v. 75, No 2, p. 326-327.

Hutton, L. J., Cavaney, R. J., and Sweet, I. P., 1981, New and revised stratigraphic units, Lawn Hill Platform, Northwest Queensland: Queensland Government. Mining Journal, p. 423-434.

Hutton, L. J., and Sweet, I. P., 1982, Geological evolution, tectonic style, and economic potential of the Lawn Hill Platform cover, Northwest Queensland: Journal of Australian Geology and Geophysics, v. 7, p. 125-134.

Huyck, H. O., 1991, When is a metalliferous black shale not a black shale? *in*: Metalliferous Black Shales and Related Ore Deposits, p. 42-56.

Idnurm, M., Giddings, J. W., and Plumb, K. A., 1995, Apparent polar wander and reversal stratigraphy of the Paleo- Mesoproterozoic southeastern McArthur Basin, Australia. Precambrian Research, v. 72, p. 1-41.

Idnurm, M., and Wyborn, L. A., 1998, Paleomagnetism and mineral exploration related studies in Australia: a brief overview of Proterozoic applications. AGSO Journal of Australian Geology and Geophysics, v. 17, p. 277-284.

Imam, M. B., and Shaw, H. F., 1986, Diagenetic controls on the reservoir properties of gas bearing Neogene Surma Group sandstones in the Bengal Basin, Bangladesh: Journal of Marine and Petroleum Geology, v. 4, p. 103-111.

Irwin, H., 1980, Early diagenetic carbonate precipitation and pore fluid migration in the Kimmeridge Clay of Dorset, England: Sedimentology, v. 27, p. 577-591.

Irwin, H., and Curtis, C., 1977, Isotopic evidence for the source of diagenetic carbonates formed during burial of organic rich sediments: Nature, v. 269, p. 209-213.

Jackson, M. J. and Raiswell, R., 1991, Sedimentology and Carbon-sulphur geochemistry of the Velkerri Formation, a Mid-Proterozoic potential oil source in northern Australia: Precambrian Research, v. 54, p. 81-108.

Jackson, M. J., Simpson, E. L., and Eriksson, K. A., 1990, Facies and sequence stratigraphic analysis in an intracratonic, thermal relaxation basin: the Early Proterozoic, Lower Quilalar Formation and Ballara Quartzite, Mount Isa Inlier, Australia: Sedimentology, v. 37, p. 1053-1078.

Jensenius, J., and Burrus, R. C., 1990, Hydrocarbon-water interactions during brine migration: evidence from hydrocarbon inclusions in calcite cements from Danish North Sea oilfields: Geochimica et Cosmochimica Acta., v. 54, p. 705-713.

Jowett, E. C., 1986, Genesis of Kupferschiefer Cu-Ag deposits by convective flow of Rotliegende brines during Triassic Rifting: Economic Geology, v. 81, p. 1823-1837.

Kiyosu, Y., 1980, Chemical reduction and sulfur-isotope effects of sulfate by organic matter under hydrothermal conditions: Chemical Geology, v. 30, p. 47-56.

Krouse, H. R., Ueda, A., and Campbell, F. A., 1990, Sulphur isotope abundances in coexisting sulphate and sulphide: kinetic isotope effects versus exchange phenomena: *in*: Herbert, H. K., and Ho, S. E.,1990., eds., Stable isotopes and fluid processes in mineralisation. University of Western Australia Extension Publication, 23, p. 226-243.

Krouse, H. R., Viau, C. A., Eliuk, L. S., Ueda, A., and Halas, S., 1988, Chemical and isotopic evidence of thermochemical sulphate reduction by light hydrocarbon gases in deep carbonate reservoirs: Nature, v. 333, p. 415-419.

Kulander, B. R., Dean, S. L. and Ward, B. J., 1990, Fractured core analysis: Interpretation, Logging and Use of Natural and Induced Fractures in Core: American Association of Petroleum Geologists Methods in Exploration Series, No 8, 88pp.

Lambert, I. B., and Scott, K. M., 1973, Implications of geochemical investigations of sedimentary rocks within and around the McArthur zinc-lead-silver deposit, Northern Territory: Journal of Geochemical Exploration, v. 2, p. 307-330.

Large, D. E., 1980, Geological parameters associated with sediment-hosted, submarine exhalative Pb-Zn deposits: An empirical model for mineral exploration: Geol. Jb. p. 59-129.

Large, R. R., Bull, S. W., Cooke, D. R., and McGoldrick, P. J., 1998, A genetic model for the HYC Deposit, Australia: based on regional sedimentology, geochemistry and sulfide-sediment relationships. Economic Geology, v. 93, p. 1345-1368.

Lawrence, S. R., and Cornford, C., 1995, Basin Geofluids: Basin Research v. 7, p. 1-7.

Leeder, J. F., 1992, High temperature pyrolysis GC/MS of samples from the Century Deposit: Applied Environmental Services Unpublished analytical report 926607 to CRA Exploration Pty Ltd.

LeHuray, A. P., Caulfield, J. B. D., Rye, D. M., and Dixon, P. R., 1987, Basement Controls on Sediment_Hosted Zn-Pb: A Pb Isotope Study of Carboniferous Mineralisation in Central Ireland: Economic Geology, v. 82, p. 1695-1709.

Lerbekmo, J. F., and Platt, R. L., 1962, Promotion of pressure solution of silica in sandstones: Journal of Sedimentary Petrology, v. 32, no3, p. 514-519.

Leventhal, J. S., 1990, Organic matter and thermochemical sulphate reduction in the Viburnum Trend, Southeast Missouri: Economic Geology, v. 85, p. 622 - 632.

Lister, G. S., 1990, The interaction of brittle and ductile processes in the mid-crust during Proterozoic wrenching in the Mount Isa Inlier [abs]: *in*: Monash University Geology Department Mount Isa Inlier Geology Conference abstracts, November, 1990. 78pp.

Logan, R. G., Murray, W. J., and Williams, N., 1990, HYC Silver-lead-zinc deposit, McArthur River: *in*: Hughes, F. E., ed., Geology of the mineral deposits of Australia and Papua New Guinea: Australian Institute of Mining and Metallurgy Monograph 14, p. 907-911.

London, W. W., 1972, Dolomite in flexure-fractured petroleum reservoirs in New Mexico and Colorado: American Association of Petroleum Geologists Bulletin, v. 56, p. 815-826.

Longstaffe, F. J., 1989, Stable isotopes as tracers in clastic diagenesis: *In*: Hutcheon, I. E., ed., Short Course in Burial Diagenesis: Mineralogical Association of Canada shortcourse volume 15, p. 201-257.

Loosveld, R. J. H., 1989, The intra-cratonic evolution of the central eastern Mount Isa Inlier, Northwest Queensland, Australia: Precambrian Research, v. 44, p. 243-276.

Loosveld, R. J. H., and Schreurs, G. M. M. F., 1987, Discovery of thrust klippen, northwest of Mary Kathleen, Mount Isa Inlier, Australia: Australian Journal of Earth Sciences, v. 34, p. 387-402.

Lorenz, J. C. and Finley, S. J., 1991, Regional fractures II: Fracturing of Mesaverde Reservoirs in the Piceance Basin, Colorado: American Association of Petroleum Geologists Bulletin, v. 75, No 11, p. 1738-1757.

Lorenz, J. C., Teufel, L. W., and Warpinski, N. R.,1991, Regional fractures I: A mechanism for the formation of regional fractures at depth in flat lying reservoirs: American Association of Petroleum Geologists Bulletin, v. 75, No 11, p. 1714-1737.

Loutit, T. S., Wyborn, L. A. I., Hinman, M. C., and Idnurm, M., 1994, Paleomagnetic, tectonic, magmatic and mineralisation events in the Proterozoic of northern Australia. Proceedings of Australasian Institute of Mining and Metallurgy Annual Conference, Darwin, p. 123-128.

Luo, X., and Vasseur, G., 1992, Contributions of compaction and aquathermal pressuring to geopressure and the influence of environmental conditions: American Association of Petroleum Geologists Bulletin, v. 76, No 10, p. 1550-1559.

Lydon, J. W., 1986, Models for the generation of metalliferous hydrothermal systems within sedimentary rocks and their applicability to the Irish Carboniferous Zn-Pb deposits: *in*: Andrew et al, Geology and genesis of mineral deposits in Ireland, p. 555-577.

McConachie, B. A., Barlow, M. G., Dunster, J. N:, Meaney, R. A., and Schaap, A. D., 1993, The Mount Isa Basin - Definition, Structure and Petroleum geology: Australian Petroleum Exploration Association Journal, v. 33, p. 237-257.

McGoldrick, P. J., Keays, R. R., 1989, Mount Isa copper and lead-zinc-silver ores - coincidence or cogenesis? Economic Geology, v. 85, p. 641-650.

Machel, H. G., Krouse, H. R., and Sassen, R., 1995, Products and distinguishing criteria of bacterial and thermochemical sulfate reduction. Applied Geochemistry, v. 10, p. 373-389.

Machel, H. G., 1987, Some aspects of diagenetic sulphate-hydrocarbon redox reactions: *in*: Marshall, J. D., ed., Diagenesis of Sedimentary Sequences. Geological Society Special Publication No 36, p. 15-28.

McKnight, S., and Broadbent, G. C., 1993, Transmission electron microscopy study of bitumens occurring in the Century zinc deposit, north Queensland: *in*: Proceedings of International Congress on Applied Mineralogy, Perth, 1993, p. 61: International Council for Applied Mineralogy.

McClay, K. R., and Carlile, D. G., 1978, Mid-Proterozoic evaporites at Mt Isa mine, Queensland, Australia: Nature, v. 274, p. 240-241.

McCracken, S. R., 1997, Stratigraphic, diagenetic, and structural controls of the Admiral Bay carbonate-hosted Zn-Pb-Ag deposit, Canning Basin, Western Australia: Unpublished PhD thesis, University of Western Australia, Perth, Western Australia.

McMahon, P. B., Chapelle, F. H., Falls, W. F., and Bradley, P. M., 1992, Role of microbial processes in linking sandstone diagenesis with organic rich clays: Journal of Sedimentary Petrology, v. 62, No 1, p. 1-10.

Maltman, A. J., 1984, On the term 'soft sediment deformation': Journal of Structural Geology, v. 6, No 5, p. 589-592.

Maltman, A. J., 1988, The importance of shear zones in naturally deformed wet sediments: Tectonophysics, v. 145, p. 163-175.

Masuzawa, T., Handa, N., Kitagawa, H., and Kusakabe, M., 1992, Sulfate reduction using methane in sediments beneath a bathyal "cold seep" giant clam community off Hatsushima Island, Sagami Bay, Japan: Earth and Planetary Science Letters, v. 110, p. 39-50.

Maynard, J. B., and Klein, G. D., 1995, Tectonic subsidence analysis in the characterisation of sedimentary ore deposits: Examples from the Witswatersrand (Au), White Pine (Cu) and Molango (Mn). Economic Geology v. 90, p. 37-50.

Miall, A. D., 1990, Principles of Sedimentary Basin Analysis: Springer-Verlag, New York, 2nd ed., 668pp.

Minenco, 1990, Metallurgical aspects of Century mineralogy: Minenco unpublished report R2605, CRA Limited, Melbourne.

Miyata, T., 1990, Slump strain indicative of paleoslope in Cretaceous Izumi sedimentary basin along median tectonic line, southwestern Japan: Geology, v. 18, p. 392-394.

Moore, D. E., and Byerlee, J., 1992, Relationships between sliding behavoiur and internal geometry of laboratory fault zones and some creeping and locked strike-slip faults of California: Tectonophysics, v. 211, p. 305-316.

Mozley, P. S., and Carothers, W. W., 1992, Elemental and isotopic composition of siderite in the Kuparuk formation, Alaska: effect of microbial activity and water/sediment interaction on early pore-water chemistry: Journal of Sedimentary Petrology, v. 62, p. 681-692.

Mozley, P. S., and Wersin, P., 1992, Isotopic composition of siderite as an indicator of depositional environment: Geology, v. 20, p. 817-820.

Muir, M. D., 1985, Depositional environments of host rocks to Northern Australian lead-zinc deposits, with special reference to McArthur River: *in*: Sangster, D. F., ed., Sediment hosted stratiform lead-zinc deposits: Mineralogical Association of Canada Short Course Handbook, p. 141-174.

Muir, M. D., Donnelly, T. H., Wilkins, R. W. T., and Armstrong, K. J., 1985, Stable isotope, petrological and fluid inclusion studies of minor mineral deposits from the McArthur Basin: implications for the genesis of some sediment-hosted base metal mineralisation from the Northern Territory: Australian Journal of Earth Science, v. 32, p. 239-260.

Myrow, P. M. and Hiscott, R. N., 1991, Shallow water gravity flow deposits, Chapel Island formation, Southeast Newfoundland, Canada: Sedimentology, v. 38, p. 935-959.

Myrow, P. M., 1992, Bypass-zone tempestite facies model and proximality trends for an ancient muddy shoreline and shelf: Journal of Sedimentary Petrology, v. 62, No 1, p. 99-115.

Neudert, M. K., 1983, A depositional model for the upper Mt Isa Group and its implications for ore genesis: Unpublished PhD thesis. Australian National University, Canberra.

Neudert, M. K. and Russell, R. E., 1981, Shallow water and hypersaline features from the middle Proterozoic Mt Isa sequence: Nature, v. 293, p. 284-286.

Ohmoto, H., Kaiser, C. J., and Geer, K. A.,1990, Systematics of sulphur isotopes in recent marine sediments and ancient sediment- hosted basemetal deposits: *in*: Herbert, H. K., and Ho, S. E., eds., Stable isotopes and fluid processes in mineralisation: University of Western Australia Extension Publication 23, p. 70-120.

Okita, P. M., 1992, Manganese Carbonate Mineralisation in the Molango District, Mexico: Economic Geology, v. 87, p. 1345-1366.

Okita, P. M., and Shanks, W. C. III., 1992, Origin of stratiform sediment-hosted manganese carbonate deposits: examples from Molango, Mexico, and TaoJiang, China: Chemical Geology, v. 99, p. 139-164.

Oliver, J., 1986, Fluids expelled tectonically from orogenic belts: Their role in hydrocarbon migration and other geologic phenomena: Geology, v. 14, p. 99-102.

Orr, W. L., 1974, Changes in sulfur content and isotopic ratios of sulfur during petroleum maturation- study of Big Horn Basin Paleozoic oils: American Association of Petroleum Geologists Bulletin, v. 58, No 11, p. 2295-2318.

Page, R. W., 1981, Depositional ages of the stratiform base metal deposits at Mount Isa and McArthur River, based on U-Pb dating of concordant tuff horizons: Economic Geology, v. 76, p. 648-658.

Page, R. W., 1993, Geochronological results from the Eastern Fold Belt, Mount Isa Inlier: new depositional and metamorphic ages: Australian Geological Survey Organisation Research Newsletter, v. 19, p. 4-5.

Page, R. W., and Bell, T. H., 1986, Isotopic and structural responses of granite to successive deformation and metamorphism: Journal of Geology, v. 94, p. 365-379.

Page, R. W., Sun, S., and Carr, G., 1994, Proterozoic sediment-hosted lead-zinc-silver deposits in Northern Australia - U-Pb zircon and Pb isotope studies [abs.]: Geological Society of Australia Abstracts, v. 37, p. 334-335.

Page, R. W. and Sweet, I. P., 1998, Geochronology of basin phases in the Mount Isa Inlier, and correlation with McArthur Basin: Australian Journal of Earth Sciences v. 45, p. 219-232.

Palciauskas, V. V., and Domenico, P. A., 1980, Microfracture development in compacting sediments: Relation to hydrocarbon-maturation kinetics: American Association of Petroleum Geologists Bulletin, v. 64, No 6, p. 927-937.

Passchier, C. W., 1986, Evidence for early extensional tectonics in the Mt Isa Inlier, Australia: Geology, v. 14, p. 1008-1011.

Passchier, C. W., and Williams, P. R., 1989, Proterozoic extensional deformation in the Mount Isa Inlier, Queensland, Australia: Geology Magazine, v. 126, No 1, p. 43-53.

Perkins, W. G., 1984, Mount Isa silica-dolomite and copper orebodies: the result of a syntectonic hydrothermal alteration system: Economic Geology, v. 79, p. 601-637.

Perkins, W. G., 1990, Mount Isa Copper Orebodies: *in*: Hughes, F. E., ed., Geology of the mineral deposits of Australia and Papua New Guinea: Australian Institute of Mining and Metallurgy Monograph 14, p. 935-941.

Perkins, W. G., 1997, Mount Isa lead-zinc orebodies: Replacement lodes in a zoned syndeformational copper-lead-zinc system?: Ore Geology Reviews, v. 12, p. 61-110.

Plumlee, G. S., Leach, D. L., Hofstra, A. H., Landis, G. P., Rowan, E. L., and Viets, J. G., 1994, Chemical reaction path modeling of ore deposition in Mississippi Valley type Pb-Zn deposits of the Ozark Region, U.S. midcontinent: Economic Geology, v.89, p. 1361–1383.

Potter, R. W., 1977, Pressure corrections for fluid inclusion homogenisation temperatures based on the volumetric properties of the system $NaCl-H_2O$: US Geological Survey Journal of Research, v. 5, p. 603-608.

Primmer, T. J. and Shaw, H., 1991, Variations in the delD and del18O compositions of illite-smectites in a partly overpressured Tertiary sequence from an offshore well, Texas Gulf Coast, USA: Journal of Marine and Petroleum Geology, v. 8, p. 225-231.

Prokopovich, N., 1952, The origin of Stylolites: Journal of Sedimentary Petrology, v. 22, No 4, p. 212-220.

Quinby-Hunt, M. S., and Wilde, P., 1991, The provenance of low-calcic black shales: Mineralium Deposita, v. 26, p. 113-121.

Rahe, B., Ferrill, D. A., and Morris, A. P., 1998, Physical analog modelling of pull-apart basin evolution. Tectonophysics, v. 285, p. 21-40.

Ramsay, J. G. and Huber, M. I., 1987, The Techniques of Modern Structural Geology: Academic Press, inc.

Redwine, L., 1981, Hypothesis combining dilation, natural hydraulic fracturing, and dolomitization to explain petroleum reservoirs in Monterey Shale, Santa Maria area, California: *in*: Garrison, R. E., and Douglas, R. G., eds., The Monterey Formation

and related siliceous rocks of California: Society of Economic Paleontologists and Mineralogists (Pacific Section) Publication 15, p. 221-248.

Reed, C. L., and Hajash, A., 1992, Dissolution of granitic sand by pH-buffered carboxylic acids: A flow-through experimental study at 100 C and 345 bars: American Association of Petroleum Geologists Bulletin, v. 76, No 9, p. 1402-1416.

Richards, J. R., 1975, Lead isotope data on three north Australian galena localities: Mineralium Deposita, v. 10, p. 287-301.

Richmond, J. M., Chapman, L. H., and Williams, P. J., 1996, Two phases of garnet alteration at the Cannington Ag-Pb-Zn deposit, NW Queensland. Economic Geology Resource Unit Contribution 55, James Cook University of North Queensland, p. 113-117.

Roehl, P. O., 1981, Dilation brecciation - a proposed mechanism of fracturing, petroleum expulsion and dolomitisation in the Monterey Formation, California: *in*: Garrison, R. E., and Douglas, R. G., eds., The Monterey Formation and related siliceous rocks of California: Society of Economic Paleontologists and Mineralogists (Pacific Section) Publication 15, p. 285-315.

Russell, M. J., 1986, Extension and convection: a genetic model for the Irish Carboniferous base metal and barite deposits: *in*: Andrew et al, Geology and Genesis of Mineral Deposits in Ireland, p. 545-554.

Russell, M. J., Solomon, M. and Walshe, J. L., 1981, The genesis of sediment-hosted, exhalative zinc + lead deposits: Mineralium Deposita, v. 16, p. 113-127.

Rye, D. M., and Williams, N., 1981, Studies of the base metal sulfide deposits at McArthur River, Northern Territory, Australia; III. The stable isotope geochemistry of the H.Y.C., Ridge, and Cooley deposits: Economic Geology, v. 76, No 1, p. 1-26.

Sami, T and Desrochers, A., 1992, Episodic sedimentation on an early Silurian, storm dominated ramp, Becscie and Merrimack formations, Anticosti Island, Canada: Sedimentology, v. 39, p. 355-381.

Sawkins, F. J., 1984, Ore genesis by episodic dewatering of sedimentary basins: application to giant Proterozoic lead-zinc deposits. Geology, v. 12, p. 451-454.

Saxby, J. D., 1970, Technique for the isolation of kerogen from sulfide ores: Geochimica et Cosmochimica Acta, v. 34, p. 1317-1326.

Saxby, J. D., and Stephens, J. F., 1973, Carbonaceous matter in sulphide ores from Mount Isa and McArthur River: an investigation using the electronprobe and the electron microscope: Mineralium Deposita, v. 8, p. 127-137.

Scheiber, J., 1986, The possible role of benthic microbial mats during the formation of carbonaceous shales in shallow Mid-Proterozoic basins: Sedimentology, v. 33, p. 521-536.

Scheiber, J., 1989, Facies and origin of shales from the Mid-Proterozoic Newland Formation, Belt Basin, Montana, USA: Sedimentology, v. 36, p. 203-219.

Scheiber, J., 1991, The origin and economic potential of sandstone-hosted disseminated Pb-Zn mineralisation in pyritic shale horizons of the Mid-Proterozoic Newland Formation, Montana, USA: Mineralium Deposita, v. 26, p. 290-297.

Scott, S. D., and Kissin, S. A., 1973, Sphalerite composition in the Zn-Fe-S system below 300°C. Economic Geology, v. 68, p. 475-479.

Segall, P., and Simpson, C., 1986, Nucleation of ductile shear zones on dilatant fractures: Geology, v. 14, p. 56-59.

Shanks, W. C. III, Woodruff, L. G., Jilson, G. A., Jennings, D. S., Modene, J. S., and Ryan, B. D., 1987, Sulfur and lead isotope studies of stratiform Zn-Pb-Ag deposits, Anvil Range, Yukon: Basinal brine exhalation and anoxic botton-water mixing: Economic Geology, v. 82, p. 600-634.

Sibson, R. H., 1992, Implications of fault-valve behaviour for rupture nucleation and recurrence: Tectonophysics, v. 211, p. 283-293.

Sibson, R. H., 1994, Crustal stress, faulting and fluid flow: *In* Parnell, J. (ed), Geofluids: Origin, migration and evolution of fluids in sedimentary basins. Geological Society Special Publication No 78, p. 69-84.

Siesser, W. G., and Rogers, J., 1976, Authigenic pyrite and gypsum in South West African continental slope sediments: Sedimentology, v. 23, p. 567-577.

Simpson, J., 1985, Stylolite-controlled layering in an homogeneous limestone: pseudo-bedding produced by burial diagenesis: Sedimentology, v. 32, p. 495-505.

Smith, J. W., and Croxford, N. J. W., 1975, An isotopic investigation of the environment of deposition of the McArthur mineralisation: Mineralium Deposita, v. 10, p. 269-276.

Smith, J. W., and Burns, M. S., 1978, Stable Isotope studies of the origins of mineralisation at Mount Isa: Mineralium Deposita, v. 13, p. 369-381.

Smith, W. D., 1991, Major factors of relevance to ore localisation at Mount Isa: RTE Confidential Report No 17565.

Solomon, M., and Heinrich, C. A., 1991, Are high heat producing granites essential to the origin of giant lead-zinc deposits at Mount Isa and McArthur River, Australia? Australian Bureau of Mineral Resources record 1991/17, 25pp.

Solomon, P. J., 1965, Investigations into sulfide mineralisation at Mount Isa, Queensland: Economic Geology, v. 60, p. 737-765.

Spencer, C. W., 1987, Hydrocarbon generation as a mechanism for overpressuring in the Rocky Mountain Region: American Association of Petroleum Geologists Bulletin, v. 71, No 4, p. 368-388.

Stanley, D. J., 1981, Unifites: Structureless muds of gravity flow origin in Mediterranean basins: Geo-Marine Letters, v. 1, p. 77-83.

Stanton, R. L., 1972, Ore Petrology: McGraw-Hill, Sydney, 713pp.

Stewart, A. J., 1989, Extensional faulting as the explanation for the Deighton 'klippe' and other Mount Albert Group outliers, Mount Isa Inlier, northwestern Queensland: Australian Journal of Earth Science, v. 36, p. 405-421.

Stewart, A. J. and Blake, D. H., 1992, Detailed studies of the Mt Isa Inlier: Australian Bureau Mineral of Research Bulletin No 243, 374pp.

Sullivan, K. B., and McBride, E. F., 1991, Diagenesis of sandstones at shale contacts and diagenetic heterogeneity, Frio Formation, Texas: American Association of Petroleum Geologists Bulletin, v.75, No 1, p. 121-138.

Summons, R. E., Powell, T. G., and Boreham, C. J., 1988, Petroleum geology and geochemistry of the Middle Proterozoic McArthur Basin, Northern Australia III: Composition of extractable hydrocarbons: Geochimica et Cosmochimica Acta, v. 52, p. 1747-1763.

Sun, Shen-su, Carr, G. R., and Page, R. W., 1996, A continued effort to improve lead-isotope model ages. AGSO research newsletter v. 24, p. 19-20.

Surdam, R. C., Crossey, L. J., Hagen, E. S. and Heasler, H. P., 1989, Organic-Inorganic interactions and sandstone diagenesis: American Association of Petroleum Geologists Bulletin, v. 73, No1, p. 1-23.

Sverjensky, D. A., 1984, Oil field brines as ore forming solutions: Economic Geology, v. 79, p. 23-37.

Swager, C. P., 1985, Syndeformational carbonate replacement model for the copper mineralisation at Mount Isa, northwest Queensland: a microstructural study: Economic Geology, v. 80, p. 107-125.

Swager, C. P., Perkins, W. G., and Knights, J. G., 1987, Stratabound phyllosilicate zones associated with syntectonic copper orebodies at Mt Isa, Queensland: Australian Journal of Earth Science, v. 34, p. 463-476.

Sweet, I. P., 1985, Relationship of the Maloney Creek Inlier to other elements of the western Lawn Hill Platform Cover, Northern Australia: Australian Bureau of Mineral Resources Journal of Australian Geology and Geophysics, v. 9, p. 329-338.

Sweet, I. P., and Hutton, L. J., 1982, 1:100,000 geological map commentary Lawn Hill Region, Queensland: Australian Bureau of Mineral Resources/Geological Survey of Queensland joint publication. Australian Govt publishing service, 36pp.

Szulc, S. A., 1992, The stratigraphic reconstruction of a mega-breccia; a sedimentological study of the south-western corner of the Lawn Hill Outlier: Unpublished BSc. Hons. Thesis, James Cook University, Townsville.

Tissot, B. P., and Welte, D. H., 1978, Petroleum Formation and Occurrence: Springer-Verlag, Berlin-Heidelberg, 578pp.

Tompkins, L. A., Rayner, M. J., Groves, D. I., and Roche, M. T., 1994, Evaporites: In situ sulfur source for rhythmically banded ore in the Cadjebut Mississippi Valley-type Zn-Pb deposit, Western Australia: Economic Geology, v. 89, p. 467–492.

Valenta, R. K., 1989, Vein geometry in the Hilton area, Mt Isa, Queensland: implications for fluid behaviour during deformation: Tectonophysics, v. 158. p. 191-207.

Valenta, R., 1994a, Deformation of host rocks and stratiform mineralisation in the Hilton Mine area, Mt Isa. Australian Journal of Earth Sciences, v. 41, p. 429-443.

Valenta, R., 1994b, Syntectonic discordant copper mineralisation in the Hilton Mine, Mount Isa. Economic Geology, v. 89, p. 1031-1052.

Vandenbroucke, M., and Durand, B, 1981, Detecting migration phenomena in a geological series by means of C_1 - C_{35} hydrocarbon amounts and distributions: *in*: Advances in Organic Geochemistry. Wiley and Sons, New York, p. 147-155.

Waltho, A. E., Allnutt, S. L., and Radojkovic, A. M., 1993, Geology of the Century Zinc Deposit, Northwest Queensland: Australian Institute of Mining and Metallurgy World Zinc'93 Conference Proceedings, p. 111-129.

Waltho, A.E., and Andrews, S.J., 1993, The Century Zinc-lead Deposit, Northwest Queensland: Australian Institute of Mining and Metallurgy Centenary Conference Proceedings, p. 41-61.

Wanless, H. R., 1979, Limestone response to stress: pressure solution and dolomitization: Journal of Sedimentary Petrology, v. 49, No 2, p. 437-462.

Weedman, S. D., Brantley, S. L., Shiraki, R., and Poulson, S., R., 1996, Diagenesis, compaction, and fluid chemistry modelling near a pressure seal: lower Tuscaloosa Formation, Gulf Coast: American Association of Petroleum Geologists Bulletin, v. 80, No 7, p. 1045-1064.

Williams, N., 1978a, Studies of the base metal sulfide deposits at McArthur River, Northern Territory, Australia: I. The Cooley and Ridge deposits: Economic Geology, v. 73, p. 1005-1035.

Williams, N., 1978b, Studies of the base metal sulfide deposits at McArthur River, Northern Territory, Australia: II. The sulfide-S and organic-C relationships of the concordant deposits and their significance: Economic Geology, v. 73, p. 1036-1056.

Williams, N, and Logan, R. G., 1986, Geology and evolution of the HYC stratiform Pb-Zn orebodies, Australia [abs]: *In* Turner, R. J. W., and Einaudi, M. T., eds, The genesis of stratiform sediment-hosted lead and zinc deposits: Conference Proceedings, Stanford University Publication Geological Sciences, v. 20, p. 57-60.

Williams, P. R., 1989, Nature and timing of early extensional structures in the Mitakoodi Quartzite, Mount Isa Inlier, northwest Queensland: Australian Journal of Earth Science, v. 36, p. 283-296.

Woodward, L. A., 1984, Potential for significant oil and gas fracture reservoirs in Cretaceous rocks of Raton Basin, New Mexico: American Association of Petroleum Geologists Bulletin, v. 68, No 5, p. 626-636.

Worden, R. H., Smalley, P. C., and Oxtoby, N. H., 1995, Gas souring by thermochemical sulfate reduction at 140^{0}C: American Association of Petroleum Geologists Bulletin, v. 79, p. 854-863.

Wright, J. V., 1987, Sedimentary model for the giant Broken Hill Pb-Zn deposit, Australia: Geology, v. 15, p. 598-602.

Wright, J. V., 1992, Preliminary sedimentological investigation of the Century Zinc-lead Deposit, with recommendations for future research: Rio Tinto Exploration Pty. Ltd. unpublished report No 18067.

Wright, J. V., Haydon, R. C., and McConachy, G. W., 1993, Sedimentary analysis and implications for Pb-Zn mineralisation at Broken Hill, Australia: Economic Geology Resource Unit Contribution 48, James Cook University of North Queensland, 91pp.

Wright, T. O., and Platt, L. B., 1982, Pressure dissolution and cleavage in the Martinsburg shale: American Journal of Science, v. 282, p. 122-135.

Wyborn, L. A. I., 1992, The Williams and Naraku batholiths, Mt Isa Inlier: An analogue of the Olympic Dam Granites? Australian Bureau of Mineral Resources Research Newsletter, v. 16, p. 13-16.

Xiao, H., and Suppe, J., 1992, Origin of rollover: American Association of Petroleum Geologists Bulletin, v. 76, No 4, p. 509-529.

Zaback, D. A., and Pratt, L. M., 1992, Isotopic composition and speciation of sulfur in the Miocene Monterey Formation: Reevaluation of sulfur reactions during early diagenesis in marine environments: Geochimica et Cosmochimica Acta, v. 56, p. 763-774.